UNDERSTANDING THE NOVEL GENETIC MECHANISMS OF CONGENITAL HYPERINSULINAEMIC HYPOGLYCAEMIA

A thesis submitted by

Dr Ved Bhushan Arya

For the degree of Doctor of Philosophy in University College London

Genetics and Genomic Medicine

Institute of Child Health

University College London

February 2015

ACKNOWLEDGMENTS

My sincere thanks to

Professor Khalid Hussain for his excellent supervision, expert guidance and motivation throughout my PhD. Your enthusiasm, optimism and passion for work have been my inspiration and guiding light.

Dr Rakesh Amin for his encouragement and support.

Professor Sian Ellard and Dr Sarah Flanagan at the Exeter Medical School, for their valuable expertise and help throughout my studies.

Professor Andrew Tinker at Queen Mary University London for giving me an opportunity to conduct functional work in his laboratory and his guidance in planning my experiments. I am also indebted to his team, in particular Dr Qadeer Aziz Hussain, for his supervision and advice during my work at the QMUL.

Dr Azizun Nessa for teaching me various molecular biology techniques. Dr James Turton for his guidance and help with molecular cloning. Dr Sofia Rahman for conducting and teaching Western blotting. My sincere thanks to Azizun and Sofia for help with compiling the thesis together.

Dr Senthil Senniappan, Ms Sophia Tahir, Dr Maha Sherif, Dr Pratik Shah and Dr Maria Guemes for their friendship, encouragement and lovely time at the Institute of Child Health.

Medical Research Council for funding my PhD.

My parents for their love and blessings.

My lovely wife, Gunjeet, for her support and encouragement. Thank you for your love and perseverance.

My kids Arjun, Angad and Amar for their patience and sparing me the time to accomplish this endeavor.

DECLARATION OF WORK

I, Dr Ved Bhushan Arya, confirm that the work presented in this thesis is my own. Where information has been derived from other sources, I confirm that this has been indicated in the thesis.

ABSTRACT

Background: Hyperinsulinaemic hypoglycaemia (HH) is characterized by unregulated secretion of insulin in the presence of hypoglycaemia. Mutations in nine different genes (*ABCC8, KCNJ11*, *GLUD1, HNF4A, HNF1A, GCK, HADH, SLC16A1* and *UCP2)* have so far been identified as a cause of HH. Mutations in *ABCC8* and *KCNJ11*, which encode the sulfonylurea receptor 1 (SUR1) and potassium inward-rectifying 6.2 (Kir6.2) subunits of ATP-sensitive potassium channel (K_{ATP} channel), are the most common cause of HH. At least two (possibly more) well-described histological subtypes are associated with HH: a focal form and a diffuse form. Diffuse HH are most commonly due to recessive and dominant mutations in *ABCC8* and *KCNJ11*. Focal HH results due to somatic loss of the maternal 11p allele (11p15.1 to 11p15.5) involving the *ABCC8* and *KCNJ11* region in patients with paternally inherited mutation in *ABCC8* or *KCNJ11*. HH can be transient and resolve within few weeks. Transient HH is seen in association with intrauterine growth restriction, maternal diabetes mellitus, perinatal asphyxia, erythroblastosis fetalis, maternal administration of sulfonylureas, and intravenous glucose infusions during labour. In large series of HH patients, the underlying genetic cause was not identified in approximately 50% of the patients. Whole-exome sequencing is a powerful and cost-effective tool for identifying genetic basis of diseases. It involves sequencing the protein coding regions of the human genome.

Aim: To identify novel genetic mechanisms of HH. To functionally characterize two novel K_{ATP} channel mutations associated with a unique clinical phenotype.

Patients: Four patients had protein-sensitive HH with normal serum ammonia. Two families (one consanguineous and one non-consanguineous) had two affected siblings with HH. All these patients had negative molecular genetics for *ABCC8, KCNJ11, GLUD1* and *HADH.* One patient had a unique phenotype of HH and cardiac arrhythmias. In addition, three patients had two novel K_{ATP} channel mutations associated with a unique clinical phenotype (transient HH and combined focal/diffuse HH).

Methods: Whole-exome sequencing (WES) was performed on nine patients (from seven families), their parents and unaffected siblings to identify novel, deleterious gene variants. Based on the available biological information, two novel gene variants (p.F108del $K_{2P}17$ and p.A422V $K_v6.2$) were considered potential disease causing. The mutations were created in plasmid constructs containing the WT cDNA sequence for *KCNK17* ($K_{2P}17$) and *KCNG2* ($K_v6.2$) using site-directed mutagenesis. These constructs were transfected into HEK293 cells, which were studied by whole-cell patch clamping. Two novel K_{ATP} channel mutations (p.T1516M SUR1 and p.*391Rext*94 Kir6.2) were also studied. For studying the p.*391Rext*94 Kir6.2 mutation, the WT human cDNA and 3′UTR sequence of *KCNJ11* was cloned into pcDNA 3.1 vector. The K_{ATP} channel mutations were created in plasmid construct containing the WT cDNA sequence for *ABCC8/KCNJ11* using site-directed mutagenesis. These constructs were transfected into HEK293 cells, which were then studied by whole-cell patch clamping. The p.*391Rext*94 Kir6.2 is a non-stop mutation and the transcripts can undergo degradation by non-stop decay phenomenon. The presence of p. *391Rext*94 Kir6.2 mutant transcript in the pancreatic tissue of the affected patient was studied by cDNA sequencing and Western blotting on the patient's pancreatic tissue extracted RNA and protein fraction respectively.

Results: WES identified two potential disease-causing heterozygous gene variants (p.F108del $K_{2P}17$ and p.A422V $K_v6.2$) in a family with a phenotype of HH and cardiac arrhythmia, which were confirmed by Sanger sequencing. Whole-cell patch clamping experiments on HEK293 cells proved both variants to be pathogenic under heterozygous

expression. Whole-cell patch clamping experiments on the two novel K_{ATP} channel mutations (p.T1516M SUR1 and p.*391Rext*94 Kir6.2) was indicative of pathogenic nature of the mutation. Analysis of the pancreatic tissue, obtained at surgery from the patient with non-stop *KCNJ11* mutation (p.*391Rext*94 Kir6.2), by cDNA sequencing and Western blotting established the presence of transcript and protein with non-stop mutation.

Conclusions: Mutations in *KCNK17* ($K_{2P}17$) and *KCNG2* ($K_v6.2$) are potential novel genetic mechanisms for HH and cardiac arrhythmias. More patients with similar phenotype need to be screened for mutations in these two genes. A novel mechanism for HH (combined focal and diffuse HH phenotype) and molecular basis for a transient type of HH was identified.

TABLE OF CONTENTS

CHAPTER 9

CHAPTER 10

APPENDIX

LIST OF FIGURES

CHAPTER 1

CHAPTER 2

CHAPTER 3

CHAPTER 4

CHAPTER 5

CHAPTER 6

CHAPTER 7

LIST OF TABLES

CHAPTER 1

CHAPTER 2

CHAPTER 3

CHAPTER 4

CHAPTER 5

CHAPTER 6

ABBREVIATIONS

$^{86}Rb^{+}$	^{86}Rubidium
$140K^{+}$	140 mM Potassium
$5\ K^{+}$	5 mM Potassium
ABCC8	ATP binding cassette, subfamily C, member 8
ADP	Adenine diphosphate
ATP	Adenine triphosphate
BCA	Bicinchoninic acid
BSA	Bovine serum albumin
BWS	Beckwith-Wiedemann syndrome
Ca^{2+}	Calcium
CDG	Congenital disorder of glycosylation
cDNA	Complementary deoxyribonucleic acid
CFTR	Cystic fibrosis transmembrane conductance regulator
CHI	Congenital hyperinsulinism
C_m	Membrane capacitance
CO_2	Carbon dioxide
CSF	Cerebrospinal fluid
Cu^{+}	Cuprous ions
ddH20	Double distilled water
DNA	Deoxyribonucleic acid
dNTP	Deoxy nucleotide triphosphate
DZX	Diazoxide
ECL	Enhanced chemiluminescent

ECS	Extracellular solution
eGFP	Enhanced green fluorescent protein
EIHI	Exercise-induced hyperinsulinism
ER	Endoplasmic reticulum
E_K	Equilibrium potential of potassium
FBPase	Fructose-2,6-bisphosphatase
FBPase-1	Fructose-1,6-bisphosphatase
FISH	Fluorescence in situ hybridization
F(2,6)P2	Fructose-2,6-bisphosphate
GABA	γ-aminobutyric acid
G6Pase	Glucose-6-phosphatase
GCK	Glucokinase
GDH	Glutamate dehydrogenase
GFP	Green fluorescent protein
GLP-1	Glucagon like peptide 1
GLUT	Glucose transport facilitator
GTP	Guanine triphosphate
GΩ	Giga Ohm
HEK293	Human embryonic kidney cells 293
HEPES	4-(2-Hydroxyethyl) piperazine-1-ethanesulfonic acid
HH	Hyperinsulinaemic hypoglycaemia
HIHA	Hyperinsulinism Hyperammonaemia
HNF1A	Hepatocyte nuclear factor 1α
HNF4A	Hepatocyte nuclear factor 4α
HRP	Horse radish peroxidase

HZM	Homozygosity mapping
ICS	Intracellular solution
IGFBP1	Insulin-like growth factor-binding protein 1
IRS-1	Insulin receptor substrate 1
IUGR	Intrauterine growth restriction
K^+	Potassium
K_{ATP}	ATP sensitive potassium channel
KCNB1	Potassium voltage-gated channel, Shab-related subfamily, member 1
KCNG2	Potassium voltage-gated channel, subfamily G, member 2
KCNJ11	Potassium inwardly rectifying channel, subfamily J, member 11
KCNK17	Potassium channel subfamily K member 17
$K_{ir}6.2$	Inwardly rectifying potassium channel 6.2
KO	Knock out
K_v	Voltage-gated potassium channels
KΩ	Kilo Ohm
K_{2P}	Two-pore domain potassium channels
LB	Luria broth
LGA	Large for gestational age
LOH	Loss of Heterozygosity
MAF	Minor allele frequency
MCT1	Monocarboxylate transporter 1
MODY	Maturity onset diabetes of young
Mg^{2+}	Magnesium
mRNA	Messenger RNA

mTOR	Mammalian target of Rapamycin
MΩ	Mega Ohm
Na^+	Sodium
NBD1	Nucleotide binding domain 1
NBD2	Nucleotide binding domain 2
PBS	Phosphate buffered saline
PBST	Phosphate buffered saline Tween
pcDNA3	Plasmid vector 5.4kB
pcDNA3.1/Zeo	Plasmid vector 5Kb
PEPCK	Phosphoenol pyruvate carboxykinase
PFK-2	6-phosphofructo-2-kinase
PIP2	Phosphoinositol-4,5-biphosphate
PIP3	Phosphoinositol-1,4,5 triphosphate
PKA	Protein kinase A
PMA	Phorbol 12-myristate 13-acetate
R_a	Access resistance
RER	Rough endoplasmic reticulum
RIPA	Radioimmunoprecipitation assay
R_m	Membrane resistance
rpm	Revolutions per minute
RT	Representative trace
RT-PCR	Reverse transcriptase-Polymerase Chain Reaction
SCHAD	Short chain L-3-hydroxyacyl-CoA dehydrogenase
SDM	Site directed mutagenesis
SDS	Sodium dodecyl sulphate

SDS-PAGE	Sodium dodecyl sulphate – Polyacrylamide gel electrophoresis
SEM	Standard error of mean
SGLT	Sodium-coupled glucose transporter
SLC16A1	Solute carrier family 16, member 1
SNP	Single nucleotide polymorphism
SUR1	Sulphonylurea receptor type 1
TALK	TWIK-Related Alkaline pH-Activated K^+ Channel
TASK	TWIK-Related Acid-Sensitive K^+ Channel
TMD0	Transmembrane domain 0
TMD1	Transmembrane domain 1
TMD2	Transmembrane domain 2
UTR	Untranslated region
WC	Whole-cell
WT	Wild-type

CHAPTER 1

GLUCOSE PHYSIOLOGY, REGULATION OF INSULIN SECRETION AND HYPERINSULINAEMIC HYPOGLYCAEMIA

1.1 SUMMARY OF CHAPTER 1

Chapter 1 provides an introduction to glucose physiology, regulation of insulin secretion, ATP-sensitive potassium channels (K_{ATP}), and hyperinsulinaemic hypoglycaemia (HH). This chapter opens with a brief description of the physiological mechanisms of glucose regulation, followed by introduction to K_{ATP} channels. This then leads into detailed description of the clinical condition "hyperinsulinaemic hypoglycaemia", its causes, clinical presentation, diagnosis, histological subtypes and management.

1.2 GLUCOSE PHYSIOLOGY

1.2.1 Introduction

Glucose is one of the principal energy substrates and provides about one-half of the total energy requirements of the human body. It is the predominant metabolic fuel for the brain. As the brain can neither store more than a few minutes supply of glucose nor synthesize glucose, its function is solely dependent on maintenance of normal glucose level in the circulation. To avoid problems from impairment of brain function due to diminished supply of glucose (seizures, unconsciousness, and permanent brain damage or [rarely] death), physiological mechanisms have evolved to maintain blood glucose level in the normal range. An abnormally reduced level of glucose in the blood is referred to as hypoglycaemia. It is a medical emergency and can produce symptoms due to neuroglycopenia.

1.2.2 Physiological Mechanisms Regulating Blood Glucose Concentration

Blood glucose concentration is tightly regulated by maintaining a balance between the rate of glucose entry into the circulation and the rate of glucose removal from the circulation. This equilibrium is maintained by a complex interplay of glucose, insulin and counter-regulatory hormones that include glucagon, catecholamines, growth hormone and cortisol.

1.2.2.1 Glucose Production and Utilization

There are three sources of glucose flux in to the circulation:

- Absorption from intestine following digestion of dietary carbohydrates,
- Breakdown of stored glycogen into glucose in liver (glycogenolysis) and

- Formation of glucose from non-carbohydrate sources in liver and kidney (gluconeogenesis).

Glycogenolysis occurs in liver and muscle in response to glucagon and/or adrenaline secretion. Glycogenolysis in the muscles provides glucose to be utilized by the muscles only whereas liver glycogenolysis maintains the blood glucose concentration in the first few hours after the meal and provides the brain with a ready source of glucose.

Gluconeogenesis, which mainly occurs in the liver and to some extent in the kidneys, is responsible for maintaining blood glucose concentrations during prolonged fasting. The rate of gluconeogenesis is controlled by the concentrations of the available glucogenic substrates (alanine, lactate, glycerol etc.) and the activities of certain unidirectional enzymes, such as phosphoenolpyruvate carboxykinase (PEPCK), fructose-1,6-bisphosphatase and glucose-6-phosphatase (G6Pase). The activity of the key gluconeogenic enzymes is regulated by transcriptional and non-transcriptional mechanisms by key hormones, particularly insulin, glucagon and glucocorticoids (Beale et al., 1984, Christ et al., 1988).

In the fasted state, insulin levels decrease while glucagon secretion increases resulting in increased gluconeogenesis. Glucagon treatment has been shown to result in increased PEPCK mRNA levels in the liver or hepatocytes (Beale et al., 1984, Christ et al., 1988, Iynedjian et al., 1985). In the fed state, insulin concentration increases, which suppresses gluconeogenesis.

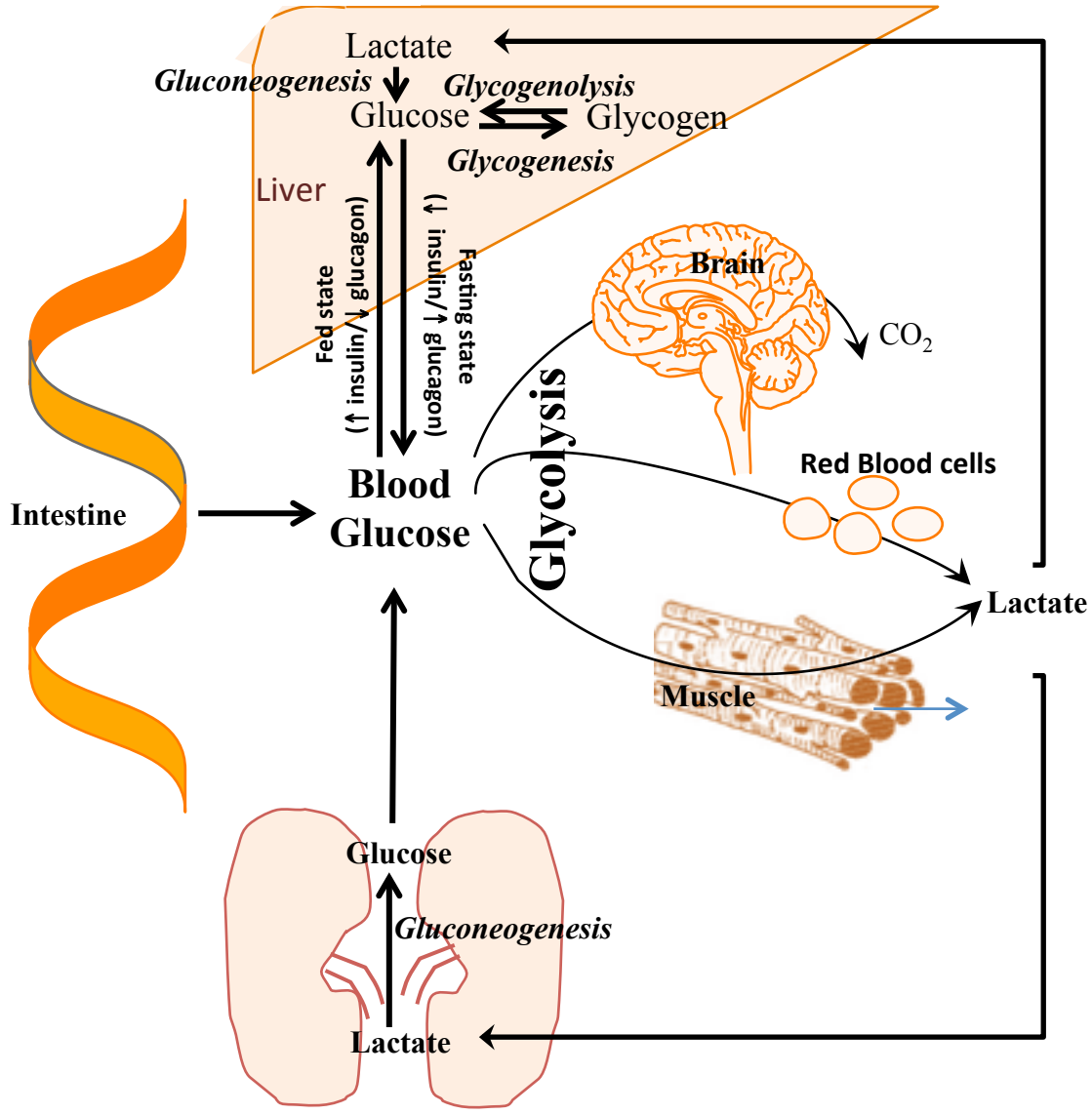

Figure 1.1: Schematic showing glucose production by glycogenolysis (liver) and gluconeogenesis (liver and kidney) and peripheral glucose utilisation

In contrast to glucose production (which occurs only in liver and kidneys), glucose utilisation is by nearly all peripheral tissues. Glucose enters the cells in these tissues via two different types of carrier proteins in the cell membrane, the sodium-coupled glucose transporters (SGLT) and glucose transport facilitators (GLUT) (Mueckler, 1990). The distribution of these transporters varies in different tissues depending upon the requirement of the tissues (Mueckler, 1990). After entry into the cells, glucose can undergo three metabolic fates:

1. Glycolysis – catabolism of glucose in the cells to produce adenosine triphosphate (ATP).
2. Glycogenesis – conversion of glucose into glycogen for storage (in the liver and muscle).
3. Conversion to fatty acids and storage as triglycerides (in adipose tissue).

These fates are dependent upon the blood glucose concentration, length of fasting and the hormonal milieu. Among the various hormones that play a role, the principal hormone is insulin.

1.2.2.2 Insulin

Insulin is a 51 amino acids long polypeptide hormone produced in the β-cells of the pancreatic islets of Langerhans. It is encoded by the *INS* gene on chromosome 11. It consists of two chains (A & B) that are connected by disulfide bridges and has a molecular weight of 5.8kDa. When first synthesized, insulin is a single polypeptide called preproinsulin. A 24 amino acid signal peptide is cleaved off preproinsulin as it is translocated into the lumen of rough endoplasmic reticulum (RER), forming proinsulin. In the RER, proinsulin is folded into the correct conformation before transported to the Golgi apparatus. Proinsulin undergoes further maturation through the action of peptidases. The peptidases cleave proinsulin at 2

positions, releasing a fragment (C-peptide). The 2-peptide chains (the B- and A- chains) linked by 2 disulfide bonds form the active insulin. The resulting active insulin is packaged inside mature granules in the β-cells.

Insulin receptor is a tyrosine kinase transmembrane receptor and is composed of two α and β subunits. Insulin binds to the extracellular portion of the α-subunits of the insulin receptor. The ligand binding causes a conformation change and activates the kinase domain on the intracellular portion of the β-subunits. The activated kinase domain autophosphorylates tyrosine residues on the c-terminus of the receptor as well as tyrosine residues in the IRS-1 (insulin receptor substrate-1), IRS-2 and IRS-3 proteins. This activates protein kinase B through the intermediate steps of activation of phosphoinositol-3-kinase and production of phosphoinositol 1,4,5-triphosphate (PIP3) (Combettes-Souverain and Issad, 1998, Houslay and Siddle, 1989, Rhodes and White, 2002). Activation of protein kinase B results in activation of glycogen synthase and increase in GLUT4 transporters in the plasma membrane. Insulin action is terminated by endocytosis and degradation of the receptor bound to insulin as well as dephosphorylation of the tyrosine residues by tyrosine phosphatases (Combettes-Souverain and Issad, 1998, Rhodes and White, 2002).

In addition to β-cells, the islets of Langerhans have α-, δ-, ε- and pancreatic polypeptide (PP) cells as well. The average size of a human islet is between 50 to 400 μm in diameter and there are approximately one million such islets in a human pancreas interspersed between pancreatic exocrine tissue (Nam et al., 2010, Permutt et al., 1984). The β-cells comprise around 50-80% of the islet and are situated in the centre of the human islets. They are surrounded by α-cells, which secrete glucagon. The δ-cells and PP cells secrete somatostatin and pancreatic polypeptide respectively.

The α-, β-, δ- and PP cells are able to communicate with each other through the extracellular spaces and gap junctions. This enables them to influence the action of each other. For example, the secretion of insulin by the β-cells suppresses the secretion of glucagon from the α-cells.

1.2.2.2.1 Regulation of Insulin Secretion

The main regulator of insulin secretion is the blood glucose concentration, although it is modified by other nutrients (amino acids and fatty acids), circulating hormones and the autonomic nervous system, as well as local paracrine and autocrine signals (Ahren, 2000, Li et al., 2002, Redmon et al., 1994).

Under normal physiological conditions the metabolism of glucose is intricately translated into signals regulating insulin secretion in pancreatic β-cells (Dunne et al., 2004).

Glucose enters the pancreatic β-cells through facilitative glucose transporters, especially the glucose transporter 2 (GLUT 2) and is converted to glucose-6-phosphate by an islet specific enzyme glucokinase (Johnson et al., 1990). In addition to pancreatic β-cells, glucokinase is also expressed in liver, gut and brain. GLUT2 has high K_m for glucose (approximately 40 mmol/l) which allows glucose transport across pancreatic β-cell membrane in proportion to the blood glucose concentrations (Gould et al., 1991). Glucokinase itself also plays a unique role in acting as a glucose sensor providing a link between the extracellular glucose concentration and the metabolism of glucose in the β-cell (Matschinsky, 1996). When the blood glucose concentration is high, the activity of glucokinase increases thereby increasing the signal regulating the insulin production from the β-cell. Similarly as the blood glucose

concentration decreases, less glucose transports across GLUT2 transporter and the activity of glucokinase is reduced. These events decrease the signal for insulin production and hence serum insulin becomes undetectable in adults at plasma glucose concentrations below 3mmol/l (Cryer, 1993, Cryer et al., 2009).

The pancreatic β-cell possesses a unique signal transduction system, which links the metabolism of the fuel stimulus to initiate insulin secretion, the so called "stimulus-response coupling"(Malaisse et al., 1979). Glucose is the most important fuel involved in the stimulus-response coupling mechanism. This stimulus response-coupling event is controlled by ATP-sensitive potassium channels (K_{ATP}) located in the pancreatic β-cell membrane, which are discussed later in this chapter.

1.2.2.3 Glucagon

Glucagon is a 29- amino acid peptide hormone processed from proglucagon. It plays a critical role in maintaining glucose homeostasis. Released from pancreatic α-cells in response to low circulating blood glucose, it acts via a seven-transmembrane G protein-coupled receptor consisting of 485 amino acids. The binding of glucagon activates $G_s\alpha$, which leads to activation of adenylate cyclase, increase in intracellular cAMP levels, and subsequent activation of protein kinase A (PKA) (Jiang and Zhang, 2003). Activated PKA phosphorylates and activates glycogen phosphorylase kinase which in turn phosphorylates and activates glycogen phosphorylase (Jiang and Zhang, 2003). The activated glycogen phosphorylase results in increased glycogen breakdown (glycogenolysis) and production of glucose 6-phosphate (G-6-P). Additionally, glucagon has been shown to upregulate the transcription of glucose-6-phosphatase (G-6-Pase) gene and increase G-6-Pase activity (Striffler et al., 1984). Through these mechanisms, glucagon potentiates glycogenolysis.

By inducing the phosphorylation of glycogen synthase, a key enzyme in glycogenesis, glucagon inhibits its activity (Ciudad et al., 1984, Ramachandran et al., 1983). Inactivation of glycogen synthase reduces glycogen synthesis and accordingly, increases the pool of glucose for hepatic output into blood.

Glucagon regulates blood glucose by also affecting glucose metabolism (increasing gluconeogenesis and decreasing glycolysis). Glucagon has been noticed to increase the PEPCK mRNA level in the liver (Beale et al., 1984, Christ et al., 1988, Iynedjian et al., 1985). PEPCK catalyzes the rate-limiting step of conversion of oxaloacetate into phosphoenol pyruvate in the pathway of hepatic gluconeogenesis.

Through phosphorylation of the bifunctional enzyme 6-phosphofructo-2-kinase (PFK-2)/ fructose-2,6-bisphosphatase (FBPase) by PKA, glucagon results in simultaneous inhibition PFK-2 and activation of FBPase (Kurland and Pilkis, 1995, Okar and Lange, 1999). These events reduce the intracellular levels of fructose-2,6-bisphosphate [F(2,6)P2]. As F(2,6)P2 is an allosteric inhibitor of fructose-1,6-bisphosphatase (FBPase-1), glucagon relieves the inhibition of FBPase-1, which catalyzes an important step in gluconeogenesis.

Glucagon inhibits glycolysis by inhibiting pyruvate kinase and phosphofructokinase-1 (PFK-1) (Castano et al., 1979, Veneziale et al., 1976). Glucagon inhibits the transcription of the pyruvate kinase gene and augments the degradation of pyruvate kinase mRNA.

1.2.3 K_{ATP} Channels

Dean and Matthews were the first to record electrical activity in the pancreatic β-cells (Dean et al., 1975). They found that the membrane potential of β-cells was glucose dependent. In the absence of glucose, the β-cells were hyperpolarized or silent. On exposure to high concentration of glucose, these cells depolarized. With the advent of patch clamp technique, the K^+ channel responsible for this electrical activity was identified in isolated rat pancreatic β-cells. This channel was found to be active at the resting potential and was inhibited by glucose (Ashcroft et al., 1984). This glucose sensitive K+ channel was shown to be identical to the K^+ channel identified in cardiac myocytes that was blocked by elevation of intracellular ATP (Rorsman and Trube, 1985).

1.2.3.1 Structure of K_{ATP} channel

K_{ATP} channels are expressed in many tissues (such as cardiomyocytes, pancreatic beta cells, skeletal muscles, vascular smooth muscles, adipose tissue, glial cells, and neurons). Functional K_{ATP} channels are now known to be octameric protein structures composed of four Kir6.x subunits that form the channel pore, surrounded by four sulfonylurea receptors (SURs) that regulate the channel pore activity (Figure 1.2).

Kir6.2 was identified by screening a human genomic library and the MIN6 cDNA library by using Kir6.1 cDNA as a probe (Inagaki et al., 1995). However no significant K_{ATP} channel currents were noticed when mouse Kir6.2 alone was expressed alone in COS-1 cells, HEK239 cells or Xenopus laevis oocytes. When co-expressed with SUR1, weakly inward rectifying K^+ currents were elicited. This channel activity could be inhibited by ATP and glibenclamide. This indicated that the pancreatic β-cell K_{ATP} channel comprises of two

subunits, SUR1 and Kir6.2. The 4:4 subunit stoichiometry of K_{ATP} channel was suggested by Inagaki and colleagues on the basis of optimum activity of K_{ATP} channels when SUR1 and Kir6.2 subunits were co expressed with-a molar ratio of 1:1 (Inagaki et al., 1995).

The Kir6.x subunits (either Kir6.1 or Kir6.2) belong to the superfamily of weak inwardly rectifying, voltage independent potassium (K^+) channels. These channels allow large K^+ flux at potentials negative to the equilibrium potential of potassium (E_K), but permit less current flow at more positive potentials (Lopatin et al., 1994). This characteristic, along with their voltage independence, makes Kir channels one of the major regulators of resting membrane potential. Furthermore, as K_{ATP} channels have the unique capability to respond to ATP/ADP levels, they are well suited to be the ideal cell metabolic sensors. Hence, K_{ATP} channels are able to regulate the membrane excitability in response to the metabolic status of the cell. This allows K_{ATP} channels to regulate many cellular functions, such as insulin secretion, excitability and cytoprotection.

Each Kir6.2 subunit has two transmembrane (TM) domains (TM1 and TM2), which are linked by a pore-forming region (H5) on the extracellular side (Figure 1.3) (Martin et al., 2013). The four TM2 domains of the four Kir6.2 subunits form the channel pore and the H5 region serves as the potassium selectivity filter. The amino and carboxyl terminals are both found cytoplasmically, and join together to form the cytoplasmic domain that is responsible for channel gating and ATP binding (Martin et al., 2013). Unlike other Kir subunits, it lacks the S4 voltage sensor region that is critical for gating in all voltage dependent calcium (Ca^{2+}), sodium (Na^+) and potassium (K^+) channels. Therefore, K_{ATP} channels are constitutively active if other regulatory mechanisms, such as SUR subunits, or ATP are absent.

SUR was first cloned from rat insulinoma (RINm5F) and hamster insulin-secreting tumor cell (HIT T15) λ phage libraries (Aguilar-Bryan et al., 1995). The open reading frame of hamster and rat SUR cDNA was found to encode proteins of 1582 amino acids. Northern (RNA) blot analysis of polyadenylated mRNA isolated from K_{ATP} channel expressing cell lines showed the presence of an approximately 5000-nucleotide transcript. A Blast search with nucleotide and amino acid sequence identified SUR sequence to be similar to cystic fibrosis transmembrane conductance regulator (CFTR) and multidrug resistance (MDR) proteins. This indicated that the SUR1 regulatory subunit belongs to the ATP-binding cassette (ABC) family (Aguilar-Bryan et al., 1995). The search also revealed two putative nucleotide-binding domains. These two domains had strong similarity to the 230- to 240- amino acid nucleotide-binding folds (NBFs) found in other members of the ABC superfamily. The sequence of two NBFs extended beyond the Walker "A" and "B" consensus sequences identified in ATP or ADP binding enzymes (Walker et al., 1982).

Each SUR1 subunit is now known to have 17 transmembrane regions, grouped into three transmembrane domains (TMDs) (Figure 1.3) (Martin et al., 2013). TMD1 (TM6-11) and TMD2 (TM12-17) are conserved among members of the ABC family. TMD0 (TM1-5) is unique to SUR, and is essential for trafficking Kir6.2 subunits to the membrane surface.

The two NBFs are present on the cytoplasmic side. The NBF-1 is present between TMD1 and TMD2, and NBF-2 is present after TMD2. As crystal structure of NBFs from bacterial ABC proteins proved NBFs as dimers, it was thought that the nucleotide-binding site of SUR is formed where NBF-1 and NBF-2 interacts (Hung et al., 1998). Matsuo *et al.* demonstrated that both NBFs are involved in nucleotide binding (Matsuo et al., 1999). The authors demonstrated that NBF-1 of SUR1 binds 8-azido-ATP strongly and the binding is

magnesium-independent, and NBF-2 binds 8-azido-ATP weakly and the binding is magnesium-dependent. They also suggested that NBF-2 might have ATPase activity.

In euglycaemic conditions, K_{ATP} channels are open which allows potassium efflux from the pancreatic β-cell. This keeps the β-cell membrane at a negative potential at which the voltage gated calcium (Ca^{2+}) channels are closed. An increase in the blood glucose concentration leads to production of ATP. The increase in the ATP/ADP ratio triggers closure of the K_{ATP} channels leading to the depolarization of the β-cell membrane. This in turn leads to the opening of the voltage gated Ca^{2+} channels and Ca^{2+} ions influx. The entry of calcium ions triggers exocytosis of insulin (Dunne and Petersen, 1991) (Figure 1.4) .

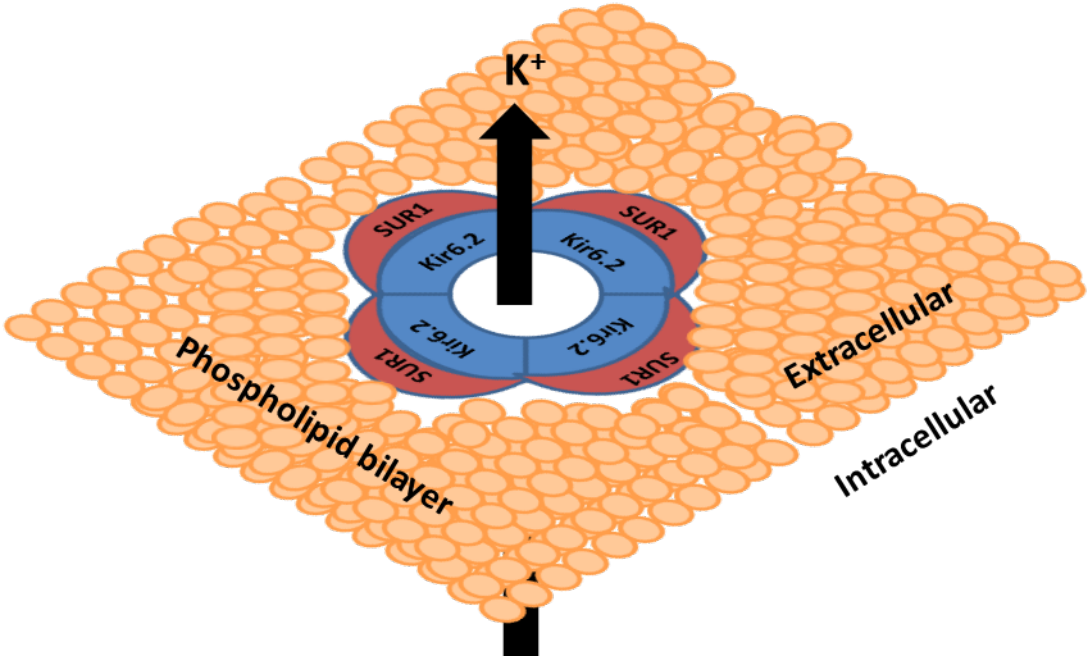

Figure 1.2: Schematic of K_{ATP} channel. Each K_{ATP} channel has four Kir6.2 subunits in the centre, which form the pore of the channel, and four regulatory SUR1 subunits.

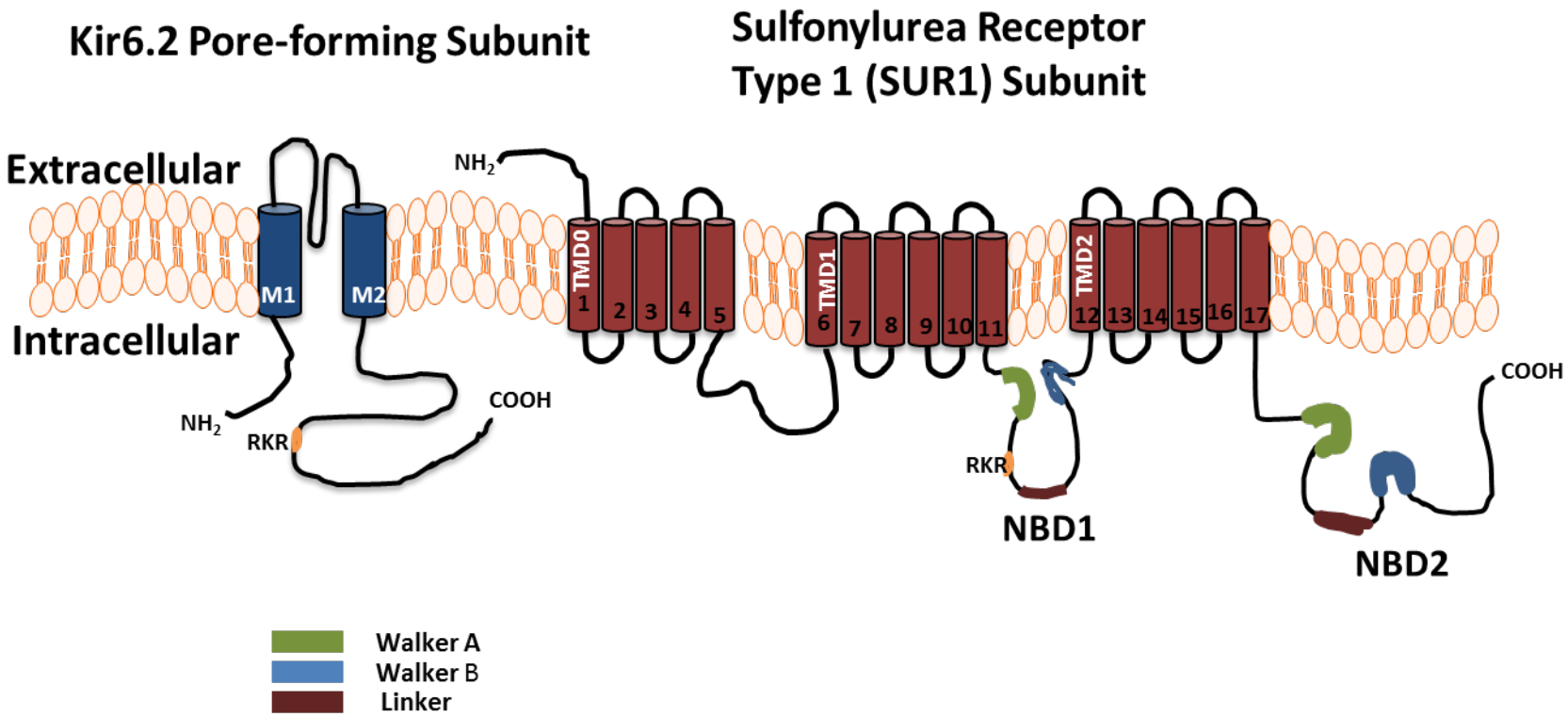

Figure 1.3: Schematic of Kir6.2 and Sulfonylurea Receptor Type 1 (SUR1) subunits of K_{ATP} channel. Kir6.2, the pore-forming subunit has two transmembrane (TM) domains (M1 and M2), which are linked by a pore-forming region (H5) on the extracellular side. SUR1 subunit has 17 transmembrane regions, grouped into three transmembrane domains (TMDs) – TMD0 (TM1-5), TMD1 (TM6-11) and TMD2 (TM12-17). SUR1 subunit has two cytosolic nucleotide-binding domains (NBD) which has conserved sequences including the Walker A and Walker B motifs. Both Kir6.2 and SUR1 subunits have an endoplasmic reticulum retaining recognition sequence (RKR).

Figure 1.4: Physiology of Insulin Secretion – In proportion to blood glucose concentration, glucose enters the pancreatic β-cell through GLUT2 transporter. ATP is produced by glucose metabolism, which is sensed by K_{ATP} channels leading to channel closure. The closure of K_{ATP} channels results in membrane depolarization that opens the voltage gated Ca^{2+} channels. Entry of Ca^{2+} ions leads to insulin exocytosis, which reduces the blood glucose concentration.

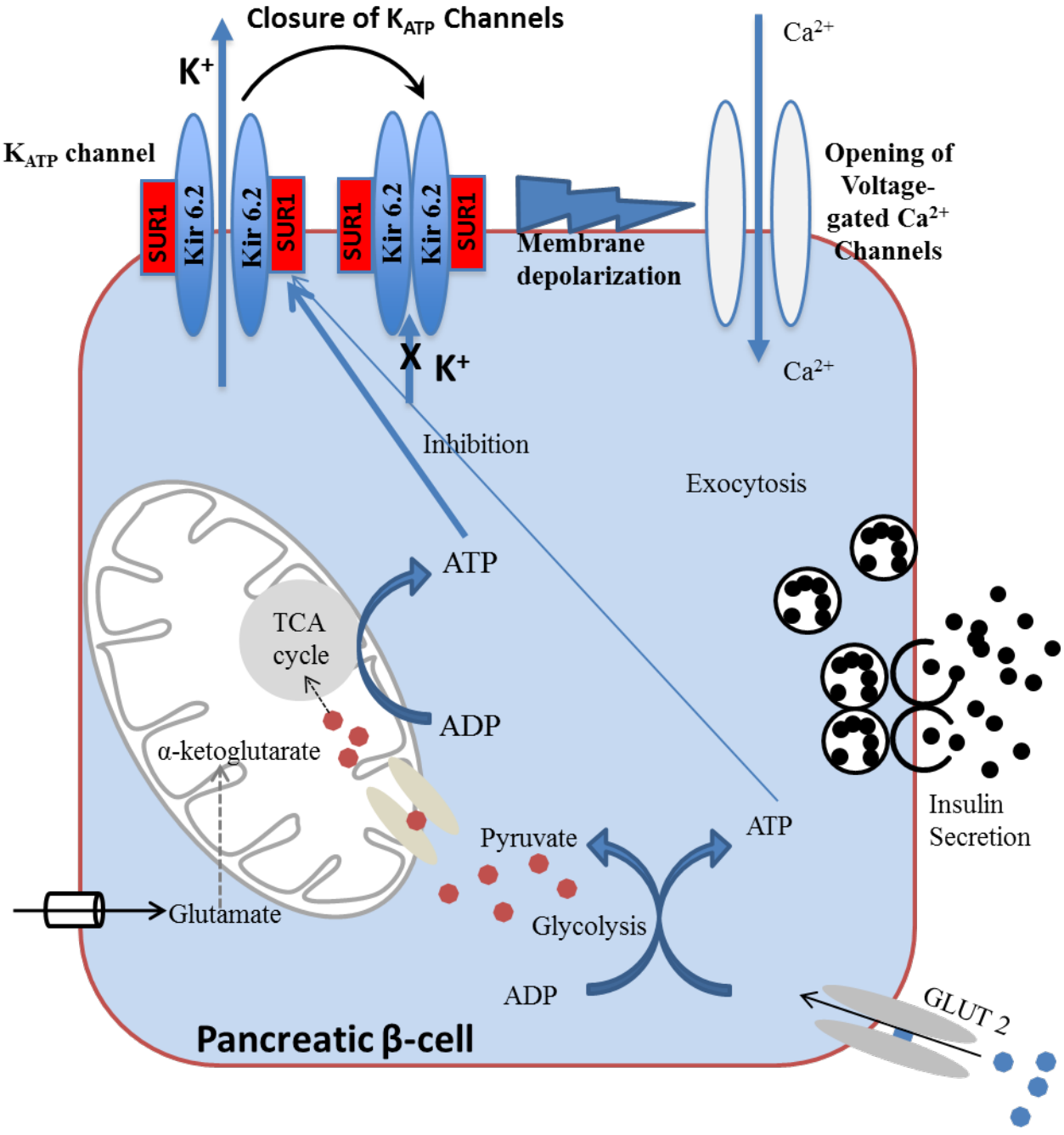

1.2.3.2 K_{ATP} Channel Gates

There is evidence for two independent types of gates in the K_{ATP} channel. One is a fast, ligand independent gate, which confers selectivity to particular ions (Proks et al., 2001). The second is a slow, ligand-dependent gate. The widely accepted hypothesis is that this gate involves a hinged motion of M2 (second transmembrane domain of Kir6.2) (Nichols, 2006).

1.2.3.3 Regulation of K_{ATP} Channels by ATP

The open state probability of the K_{ATP} channel was reduced by the application of ATP to the intracellular surface of excised membrane patches to such an extent that 10-50μM ATP produced half-maximal inhibition and millimolar concentrations caused complete block (Cook and Hales, 1984). With this high ATP sensitivity, it was expected that K_{ATP} channel would always be closed unless there are additional channel regulators present in the β-cells as well. A number of nucleotides were reported which influenced channel activity in the presence of ATP. Most interest was focused on the actions of ADP as concentrations of ATP and ADP change reciprocally as glucose is metabolized. In inside-out patch experiments where physiological concentrations of both ATP and ADP were used, K_{ATP} channel activity could be recorded even in the presence of millimolar concentrations of ATP, which had previously shown complete inhibition of K_{ATP} channel activity (Dunne and Petersen, 1986, Kakei et al., 1986). These findings suggested that ATP/ADP ratio may be more important than ATP alone in K_{ATP} channel activity regulation.

1.2.3.4 Regulation of K_{ATP} Channels by Phospholipids

In 1996, Fan and Makielski reported that anionic phospholipids activated K_{ATP} channels in pancreatic β-cells, cardiac myocytes, skeletal muscle cells and a cloned K_{ATP} composed of SUR/Kir6.2 stably expressed in a mammalian cell line (Fan and Makielski, 1997). Polyvalent cations and enzymatic treatment with phospholipases that reduced the negative charge on phospholipids antagonized the effect on K_{ATP} channel activation. The authors also demonstrated that mutation of two positively charged amino acid residues at the C-terminus of Kir6.2 reduced the activating effects of phospholipids. It was proposed that metabolism of anionic phospholipids in the membrane may be novel mechanism of regulation of K_{ATP} channels.

Shyng and Nichols subsequently demonstrated in inside out patch clamp experiments in COSm6 cells expressing Kir6.2/SUR1 that phosphatidylinositol decreased ATP sensitivity of the K_{ATP} channels (Shyng and Nichols, 1998).

1.2.3.5 Mechanism of K_{ATP} Channel Regulation by ATP and Phosphatidylinositol phosphates (PIPs)

The cytoplasmic domains of Kir6.2 subunit provide the binding sites for ATP and phosphatidylinositol 4,5-bisphosphate (PIP2) (Baukrowitz et al., 1998, Shyng and Nichols, 1998). Molecular modeling predicts four ATP-binding sites on K_{ATP} channel; one on each Kir6.2 subunit. Unliganded subunits are relatively unstable and at any time, Kir6.2 subunit can either bind to ATP or PIP2. In the absence of ATP, wild-type Kir6.2 subunits are bound to membrane PIP2 and are in the open state. Binding of ATP to the Kir6.2 subunit will trap it in the close state. The ATP concentration in energized cells is two to three orders of

magnitude higher than the association constant of wild-type Kir6.2 subunit (~10μM). Hence the expected open probability of wild-type Kir6.2 subunit for most cells would be negligible without the stimulatory effects of Mg-nucleotides at the SUR subunit.

Mutagenesis studies have suggested candidate residues in Kir6.2 subunit for the ATP-binding site. John *et al*. reported that mutations of three positively charged residues, R50, K185 and R201, impair the ability of ATP to close the K_{ATP} channel (John et al., 2003). The mutations did not affect the open probability in the absence of ATP, suggesting the role of these residues in ATP binding.

The amino acid residues (Arg54, Arg176, Arg177 and Arg206), which potentially interact with PIP2, are near the ATP binding site and appropriately located to interact with PIP2 (John et al., 2003). Close location of ATP and PIP2 location sites are consistent with the proposed 'negative heterotropic' interaction of the two ligands in channel regulation.

Although Kir6.2 subunit provides the inhibitory binding site for ATP, the site for activation of K_{ATP} channel is on NBFs of SUR. It is hypothesized that the nucleotide-bound NBF-1 and NBF-2 dimer is the catalytically active species. ATP labeling studies revealed high magnesium dependence for nucleotide binding of NBF-2, providing indirect evidence that SUR NBF hydrolyze ATP and this hydrolysis overcome the inhibitory effect of ATP on Kir6.2 (Matsuo et al., 2000a).

Evidence of activation of K_{ATP} channels by orthovandate and inhibition of K_{ATP} channels by beryllium fluoride gives weight to the hypothesis that ATP hydrolysis underlies channel activation. Orthovandate and beryllium fluoride are γ-phosphate analogs that stabilize the

ATPase cycle in distinct conformations. Orthovandate stabilized NBD2 ATPase cycle in a post hydrolytic conformation whereas beryllium fluoride in prehydrolytic conformation (Zingman et al., 2001).

However decreased MgADP stimulation of K_{ATP} channels in mutations affecting residues that have drastic effects on ATP hydrolysis suggests that ATP hydrolysis is an epiphenomenon and that preferential binding of MgADP at nucleotide-binding site of SUR1 is the activator of the channel.

1.2.3.6 K_{ATP} Channel Independent Insulin Secretion

Although K_{ATP} channels have an essential role in linking the metabolism of glucose to the secretion of insulin, there is now evidence that there may well be other mechanisms of insulin secretion, the so-called K_{ATP} channel independent pathways of insulin secretion (Gembal et al., 1993, Aizawa et al., 1994, Straub et al., 2001).

In a study on mouse islets, depolarisation of the membrane by increasing the concentration of extracellular K^+ from 4.8 to 30 mM could induce Ca^{2+} influx and insulin release even in the presence of diazoxide. This K^+-induced insulin release was dose-dependently increased by glucose. Based on these observations, the authors concluded the existence of K_{ATP} channel independent mechanism by which glucose can control insulin release (Gembal et al., 1993).

In a study on islets isolated from pancreas of a patient with K_{ATP} channel mutation, although understandably tolbutamide (K_{ATP} channel blocker) failed to cause insulin secretion, glucose

readily promoted insulin release. No rise in intracellular free calcium concentration over basal values was noticed either with glucose or tolbutamide (Straub et al., 2001).

Komatsu *et al*. demonstrated the insulinotropic action of glucose, in the presence of a phorbol ester (phorbol 12-myristate 13-acetate; PMA) and forskolin (adenylate cyclase activator), in Ca^{2+} depleted rat pancreatic islets. This action could be blocked by norepinephrine, a physiological inhibitor of insulin secretion, suggesting presence of K_{ATP}- and Ca^{2+}-independent pathway (Komatsu et al., 1995). Based on these observations, it can be concluded that either there are two different K_{ATP}-independent pathways or elevated intracellular free calcium concentration and activated protein kinase A and C lead to a common K_{ATP}-independent pathway (Komatsu et al., 1995).

1.3 HYPERINSULINAEMIC HYPOGLYCAEMIA (HH)

Hyperinsulinaemic hypoglycaemia (HH) is characterized by unregulated secretion of insulin in the presence of hypoglycaemia. HH occurs in all age groups (neonates, children and adults) but due to different mechanisms. In the newborn and infancy periods it is a major cause of persistent and recurrent hypoglycaemia associated with hypoglycaemic brain injury (Aynsley-Green et al., 2000).

Under normal physiological state, the pancreatic β-cells secrete the appropriate amount of insulin to maintain normoglycaemia. The unregulated insulin secretion in HH drives glucose into the insulin sensitive tissues especially skeletal muscle, adipose tissue and liver causing profound hypoglycaemia. This is compounded by the fact that insulin simultaneously inhibits glycogenolysis (glycogen breakdown), gluconeogenesis (glucose production from non-carbohydrate sources), lipolysis and ketogenesis. In view of the inhibitory insulin action on lipolysis and ketogenesis, the brain glucopaenia is accompanied by the lack of alternative substrates such as ketone bodies and lactate. It is under these conditions that the risk of brain damage is highest.

1.3.1 Causes Of HH (Table 1.1)

1.3.1.1 Transient HH:

HH, which resolves within few weeks, has been reported in association with intrauterine growth restriction, maternal diabetes mellitus (gestational or insulin-dependent), perinatal asphyxia, erythroblastosis fetalis, maternal administration of sulfonylureas, and intravenous glucose infusions during labour. Occasionally, no known risk factors are present in transient

HH cases (Yap et al., 2004). Transient HH can be protracted in some patients, requiring treatment with diazoxide for months (Fafoula et al., 2006, Arya et al., 2013).

1.3.1.2 HH due to defects in pancreatic β-cell K_{ATP} channels

1.3.1.2.1 Recessive K_{ATP} Channel Mutations

Given the key role of pancreatic β-cell K_{ATP} channels in regulating insulin secretion it is no surprise that genetic defects in the genes regulating the function of these channels lead to severe forms of HH. Glaser et al first suggested the link between HH and K_{ATP} channels. With linkage analysis in 15 families (12 Ashkenazi Jewish, 2 consanguineous Arab and 1 non-Jewish Caucasian), Glaser *et al.* mapped familial hyperinsulinism to chromosome 11p14-15.1 (Glaser et al., 1994).

With the cloning of sulfonylurea receptor (*SUR*) gene in 1995, a regulator of insulin secretion, Thomas et al mapped this gene to 11p15.1 by fluorescence in situ hybridization (FISH) (Thomas et al., 1995). They identified two separate *SUR* gene splice site mutations in HH affected individuals from nine different families. Both mutations resulted in disruption of the putative NBD2 of the SUR protein (Thomas et al., 1995).

A homozygous point mutation in Kir6.2 (L147P) was subsequently reported in a child severely affected with HH (Thomas et al., 1996).

Recessive inactivating mutations in K_{ATP} channel subunits are now the most common cause of HH. In a study of genotype-phenotype correlation of 300 patients with congenital hyperinsulinism, Kapoor *et al.* reported recessively inherited K_{ATP} channel mutations in 63 patients (Kapoor et al., 2013). In another recent study of 417 patients with congenital

hyperinsulinism, 84 patients had recessively inherited K_{ATP} mutations (Snider et al., 2013). As mentioned earlier, K_{ATP} channel is a heteromultimeric complex of at least two proteins designated SUR1 (*ABCC8* gene) and Kir6.2 (*KCNJ11* gene). So far, over 150 mutations have been identified in the *ABCC8* and 25 in *KCNJ11*. These include missense, frame shift, nonsense, insertions/deletions, splice site and regulatory mutations, either present in homozygous or compound heterozygous state. In the Ashkenazi Jewish population, two common (F1388del and c.3992-9G4A) mutations account for 90% of all cases of congenital HH (Nestorowicz et al., 1996, Thomas et al., 1995).

The molecular basis of recessive inactivating *ABCC8* and *KCNJ11* mutations involves multiple defects in K_{ATP} channel biogenesis and turnover, in channel trafficking from the endoplasmic reticulum and Golgi apparatus to the plasma membrane and alterations of channels in response to both nucleotide regulation and open state frequency (Cartier et al., 2001a, Partridge et al., 2001a, Shyng et al., 1998, Dunne et al., 1997). There are two different classes of these loss-of-function mutations. In class I, all K_{ATP} channels are absent from the β-cell plasma membrane, resulting in no K_{ATP} current. The most common class I mutations are those leading to defects in trafficking. In class II mutations, K_{ATP} channels are present in the membrane (although less than normal) but show reduced sensitivity to Mg-nucleotide activation or reduced intrinsic channel open probability (Dunne et al., 2004).

Table 1.1: Causes of HH

Common Perinatal Risk factors for HH (Likely to be transient)
Maternal diabetes mellitus (gestational and insulin dependent) IUGR Perinatal asphyxia Rhesus isoimmunisation
Congenital Hyperinsulinism (Identified Gene mutations)
ABCC8 *KCNJ11* *GLUD1* *GCK* *HADH* *HNF4A* *HNF1A* *SLC16A1* *UCP2*
Metabolic Causes
Congenital disorders of glycosylation (CDG), Type 1a/b/d Tyrosinaemia type I.
Syndromic Causes
Beckwith-Wiedemann Kabuki Trisomy 13 Central Hypoventilation Syndrome Leprechaunism (insulin resistance syndrome) Mosaic Turner Soto Usher Timothy Costello
Miscellaneous causes
Noninsulinoma pancreatogenous hypoglycaemia (Adults) Factitious Hypoglycaemia Insulinoma Insulin autoimmune syndrome Post Prandial HH after Post gastric bypass surgery for obesity (Adults) Non Islet cells tumor hypoglycemia (NICTH) (Adults) Dumping syndrome Drug induced (Oral antidiabetic drug (sulfonylurea, glinides, biguanides), Beta Blockers. Antiarrhythmic drugs (quinine).

1.3.1.2.1.1 Defect in Biogenesis and Turnover

Crane and Aguilar-Bryan determined the lifetimes of SUR1 and Kir6.2 with pulse-labeling methods (Crane and Aguilar-Bryan, 2004). They estimated the half-life of SUR1 (expressed alone) to be approximately 25.5 hours. On the other hand, Kir6.2 turnover was biphasic. Approximately 60% was lost with t1/2 of 36 minutes. The remaining converted to a long-lived species (t1/2 ~26 hours). When Kir6.2 and SUR1 were co-expressed, the fast-degradation of Kir6.2 was not noticed. The half-life of K_{ATP} channels was estimated to be ~7.3 hours.

Some mutations in K_{ATP} channel subunits affect the association with their partners resulting in rapid degradation. Two examples of such mutations are Kir6.2 W91R and SUR1ΔF1388.

1.3.1.2.1.2 Defect in Channel Trafficking

Correct trafficking and cell surface expression of K_{ATP} channels requires the tripeptide endoplasmic reticulum (ER) retention signal sequence (RKR; Arg-Lys-Arg), present in both the SUR1 and Kir6.2 subunits, to be shielded. When expressed alone, the two proteins (SUR1 and Kir6.2) are retained in the ER because of exposure of the RKR signal. When SUR1 and Kir6.2 coexpress and associate to form an octameric channel complex, the ER-retention signal in both subunits is shielded and the channel complex is able to traffic to the cell surface.

The RKR motif in SUR1 is in a cytoplasmic segment right before the first nucleotide-binding fold (NBF-1). The RKR motif in Kir6.2 is near the C-terminus. The discovery that when expressed alone, c-terminal truncated Kir6.2 allowed potassium currents allowed the mapping of RKR motif in Kir6.2 sequence (Tucker et al., 1997, Zerangue et al., 1999).

Mutations in K_{ATP} channels can cause HI by affecting the trafficking of the channels to the cell surface. Cartier *et al.* demonstrated that F1388 in SUR1 is critical for normal trafficking and function of K_{ATP} channels by uncovering the defective trafficking as the underlying molecular mechanism of PHHI in SUR1ΔF1388 (Cartier et al., 2001b).

Other mutations that affect trafficking include SUR1 L1544P and SUR1 R1394H (Partridge et al., 2001b, Taschenberger et al., 2002). Conti *et al.* mutated the two N-glycosylation residues (Asn10 and Asn1050) and noticed ER retention of the mutant channels (Conti et al., 2002). The authors suggested that SUR1 glycosylation is a key element for correct trafficking of K_{ATP} channels.

1.3.1.2.1.3 Defects of Channel Regulation

SUR1 regulates the conductance of Kir6.2 through interaction with intracellular nucleotides. SUR1 has two nucleotide-binding folds (NBF-1 and NBF-2). Several mutations affect the sensitivity to changes in the ATP/ADP ratio and result in loss of ADP dependent activation of K_{ATP} channels (Shyng et al., 1998, Matsuo et al., 2000b). Loss of ADP dependent gating results in the constitutive closure of the K_{ATP} channel and persistent membrane depolarization of the β-cell. Examples of mutations that result in defective channel regulation are R1420C, T1139M and R1215Q.

Overall, these mutations result in a loss-of-function of K_{ATP} channels in the pancreatic β-cell, leading to constitutive exocytosis of insulin-containing secretory vesicles.

Recessive inactivating mutations in *ABCC8* and *KCNJ11* usually cause severe HH, which in the vast majority of patients is unresponsive to medical treatment with diazoxide. However, some compound heterozygote mutations may be milder and may respond to treatment with diazoxide (Dekel et al., 2002).

1.3.1.2.2 Dominant acting K_{ATP} channel mutations

The first description of dominant acting K_{ATP} channel mutation was from Huopio *et al* (Huopio et al., 2000). The authors identified a heterozygous E1506K (E1507K based on the 1582 amino acid transcript NM_000352.3) in seven related patients with congenital hyperinsulinism (CHI) and their mothers. All the patients were successfully managed with diazoxide.

Linkage and haplotype analysis was suggestive of a dominant pattern of inheritance in this large multi-generation pedigree. Using an allele frequency of 0.03 (corresponding to the frequency of the conserved haplotype), the two-point linkage analysis yielded LOD scores of 6.00 at $\theta = 0$ and 3.83 at $\theta = 0.045$ for the dominant and recessive models respectively.

Experiments in oocytes injected with Kir6.2/SUR1-WT and Kir6.2/SUR1-E1507K revealed that SUR1-E1507K could form functional channels with Kir6.2. However these channels were insensitive to metabolic inhibition (equivalent to hypoglycaemia in the clinical setting) but could be opened by diazoxide. Experiments with injecting 1:1 mixture of WT and E1507K mutant indicated that this mutation does not have a dominant negative effect.

Thornton *et al.* reported a heterozygous SUR1 mutation (delSer1387) in a family with dominantly inherited hyperinsulinism affecting five individuals in three generations

(Thornton et al., 2003). With surface immunofluorescence studies, it was shown that delSer1387 SUR1 mutant protein could form K_{ATP} channels with Kir6.2 protein but exhibited no rubidium efflux in response to metabolic inhibition and diazoxide. However when equimolar mixture of delSer1387 and wild-type SUR1 cDNA was used, surface expression and rubidium efflux was similar to control.

Pinney *et al.* characterized 14 dominantly inherited K_{ATP} channel mutations with surface expression and inside-out patch clamping (Pinney et al., 2008). All of the mutations were single amino acid changes: 13 were amino acid substitutions and 1 was a single amino acid deletion. Eleven were *ABCC8* mutations and 3 were *KCNJ11* mutations. The authors noticed that these mutations (SUR1 as well as Kir6.2) had no or only mild effects on biogenesis and expression of the channel. However, the SUR1 mutant channels had significantly diminished or completely abolished response to MgADP and diazoxide. Kir6.2 mutants had dramatically reduced channel open probability or were non-conducting. Under simulated heterozygous conditions, presence of the WT *ABCC8* or *KCNJ11* allele resulted in partial channel response to changes in ATP/ADP ratio and to diazoxide. There data suggested dominant inactivating mutations to result in much milder phenotype than that of patients with recessive inactivating mutations (Huopio et al., 2000).

In 2011, dominant acting K_{ATP} mutations resulting in diazoxide-unresponsive disease were reported. Flanagan *et al.* reported three *ABCC8* mutations (D1506E, G1485E, and M1544K) in five patients (Flanagan et al., 2011a). The mutation arose either de novo or one of the parents who carried the mutation was also affected. All five patients had severe hyperinsulinaemic hypoglycaemia and were unresponsive to maximum doses of diazoxide.

Histological analysis of the pancreatic material from four patients showed similar changes to that seen in recessive acting *ABCC8* mutations.

In the same year, MacMullen *et al.* reported 13 different monoallelic missense *ABCC8* mutations associated with diazoxide-unresponsive disease (Macmullen et al., 2011). Expression of these mutations in COSm6 cells revealed normal trafficking of channels but severely impaired responses to MgADP or diazoxide. The responses were significantly lower than the *ABCC8* mutations studied by their group that caused diazoxide-responsive disease.

To summarize, dominant acting K_{ATP} channel mutations can cause diazoxide-responsive or diazoxide-unresponsive disease depending on the responses of the channel subunits to MgADP or diazoxide. The normal trafficking of channel subunits is retained.

1.3.1.3 HH due to gain of function mutation in the *GLUD1* gene

Zammarchi *et al.* and Weinzimer *et al.* reported a group of patients with hyperinsulinism and concomitant hyperammonaemia (Weinzimer et al., 1997, Zammarchi et al., 1996). Stanley *et al.* studied eight such patients and noticed increased activity of glutamate dehydrogenase (GDH) enzyme in lymphoblasts prepared from peripheral blood lymphocytes from these patients (Stanley et al., 1998a). All these eight patients had heterozygous mutation in the proposed allosteric domain of the glutamate dehydrogenase enzyme.

GDH is an intramitochondrial enzyme that is encoded by *GLUD1* gene on the chromosome 10q23.3. It catalyzes the oxidative deamination of glutamate to α-ketoglutarate, which enters Krebs's cycle and results in ATP production. The enzyme is allosterically inhibited by ATP and GTP, and allosterically activated by leucine (Fahien et al., 1988). Mutations in *GLUD1*

reduce the sensitivity of GDH to allosteric inhibition by GTP and ATP (Stanley et al., 1998a). This results in increased activity of GDH.

GDH is widely distributed at high levels in the pancreas, liver, brain, kidney, heart and lungs. In pancreatic β-cells, the resulting increased ATP/ADP ratio due to increased GDH activity consequently activates K_{ATP} channels, with subsequent cell depolarization and insulin release (Stanley, 2004).

Increased GDH activity in liver may lead to hyperammonaemia because of excessive ammonia production and impaired urea cycle activity. Reduced concentrations of glutamate will reduce the synthesis of N-acetylglutamate, an essential activator of carbamoyl-phosphate synthetase, the first step in the conversion of ammonia to urea. Recent animal model studies suggest the role of renal ammoniagenesis due to activation of GDH as a source of hyperammonaemia in these patients (Treberg et al., 2010).

Mutations in *GLUD1* gene are the second most common congenital form of HH (HI/HA syndrome)(Stanley et al., 1998b).

The *GLUD1* gene mapped to the 10q23.3 region contains 13 exons encoding a 505 amino acid mature enzyme. Mutations causing HI/HA syndrome have been identified in the GTP allosteric region of the enzyme encoded by exons 11 and 12 of the *GLUD1* gene, as well as in the GTP binding site encoded by exons 6 and 7 (MacMullen et al., 2001, Stanley et al., 2000).

The major clinical feature of children with HI/HA syndrome is recurrent episodes of symptomatic HH. These may occur with fasting or can be provoked by protein feeding, as leucine is an allosteric activator of GDH. Some carriers can be asymptomatic, resulting from incomplete expression of enzyme abnormality (Palladino and Stanley, 2010).

Hyperammonaemia, a characteristic biochemical marker of HI/HA syndrome, is typically mild to moderate (up to 3-5 times the upper limit of normal). It is resistant to detoxification compounds (sodium benzoate, sodium phenylbutyrate, N-carbamylglutamate) or protein-restricted diet (Palladino and Stanley, 2010).

Children with HI/HA syndrome appear to have epilepsy more frequently as compared to other congenital forms of HH (Raizen et al., 2005, Kapoor et al., 2009a, Bahi-Buisson et al., 2008). The increased frequency of epilepsy is thought to be either the result of a) hypoglycaemic brain injury due to recurrent hypoglycaemia or b) chronic hyperammonaemia or c) decreased concentrations of glutamine and the neurotransmitter γ-aminobutyric acid (GABA) in the brain due to raised GDH activity. Over activity of GDH in the brain may lead to a decrease in glutamate availability for glutamate decarboxylase and GABA synthesis, which results, in turn, in altered GABA concentration (Bahi-Buisson et al., 2008). However, measurements of GABA and other neurotransmitters in CSF of these patients have been normal (Bahi-Buisson et al., 2008). Finally, mutations in the GTP binding site tend to be more frequently associated with epilepsy than those in the allosteric domain (Bahi-Buisson et al., 2008, Kapoor et al., 2009a).

1.3.1.4 HH due to gain of function mutation in the *GCK* gene

Glucokinase (GCK) is a key regulatory enzyme in the pancreatic β-cells. It plays a crucial role in the regulation of insulin secretion and is referred to as the pancreatic β-cell sensor (Matschinsky, 1996). Its unique kinetics of low affinity for glucose (high Km) and no inhibition by its end product glucose-6-phosphate helps in modulation of its activity in relation to the concentration of glucose over a range of physiological glucose concentrations (4-15mmol/L). Hence pancreatic β-cells are able to increase their rate of glucose metabolism in response to a rise in the extracellular glucose concentration.

Activating (or gain of function) mutations in GCK increase the affinity of GCK for glucose and alter the threshold for glucose stimulated insulin secretion (Davis et al., 1999). Thus insulin continues to be produced at lower blood glucose concentrations. All reported activated mutations cluster in the allosteric activator site of the enzyme. There is no evidence of increased gene expression as a likely cause HH.

GCK mutations can lead to a variable phenotype, ranging from asymptomatic hypoglycaemia to medically unresponsive HH, with majority causing mild diazoxide responsive HH (Cuesta-Munoz et al., 2004, Christesen et al., 2002, Dullaart et al., 2004, Thornton et al., 1998). In a large study, activating GCK mutations accounted for ~ 7% of medically responsive HH (Christesen et al., 2008).

1.3.1.5 Transcription factors and HH

The hepatocyte nuclear factor 4α (HNF-4α), encoded by *HNF4A*, is a member of the nuclear receptor (NR) family of transcription factors. The *HNF4A* gene is highly expressed in the liver, kidney, gut, and pancreatic islets and is thought to play an important role in the

development and function of these organs (Sladek et al., 1990). Other transcription factors important for the development of the pancreas include HNF-1α and HNF-1β (Xanthopoulos et al., 1991). These along with HNF-4α are thought to play a crucial role in expression of several genes involved in glucose stimulated insulin secretion.

Heterozygous mutations in *HNF4A* have been reported to lead to a dominantly inherited condition with a dual phenotype of HH in the neonatal period and MODY1 in the adult life (Kapoor et al., 2008, Pearson et al., 2007). Pearson et al generated a mouse model with β-cell specific *HNF4A* deletion. By studying these β-*HNF4A*-KO mice, they identified significantly elevated insulin concentrations in late gestation β-*HNF4A*-KO embryos and significantly higher insulin/glucose ratios in β-*HNF4A*-KO versus control mice in the neonatal period. They did not find any difference in the expression of genes implicated in human hyperinsulinaemic hypoglycaemia (*ABCC8*, *KCNJ11*, *SCHAD*, *GCK* and *GLUD1*) in β-*HNF4A*-KO mice.

The exact mechanism behind HH in *HNF4A* mutations is unclear. Gupta and colleagues, in a conditional knockout of HNF4A mouse model, noticed 60% reduction in the expression of the potassium channel subunit Kir6.2. They also demonstrated that the *KCNJ11* gene is a transcriptional target of *HNF4A* (Gupta et al., 2005). The other possible mechanism is HNF-4α deficiency leads to lower levels of PPARα (peroxisomal proliferator-activated receptor alpha), which is important for insulin regulation (Gremlich et al., 2005).

Clinically *HNF4A* mutations are characterized by an early neonatal presentation of HH and macrosomia. The severity may range from mild transient hypoglycaemia not needing medication to persistent HH requiring treatment with diazoxide for up to 8 years (Kapoor et

al., 2008). In all reported cases, the HH improved with age and responded to diazoxide. A variable penetrance is often observed within families, demonstrated by absence of neonatal HH in some *HNF4A* mutation carriers. A family history of diabetes is a useful indicator of an *HNF4A* gene mutation, however its absence should not preclude *HNF4A* sequencing in patients with diazoxide responsive HH (Kapoor et al., 2008). The reason for the differences in clinical presentations is not currently understood; though, it is likely that other genetic and environmental factors may influence the severity of the disease. The *HNF4A* mutation phenotype may extend beyond β-cells of pancreas and include liver glycogenosis and renal Fanconi tubulopathy (Stanescu et al., 2012).

A recent report described two cases with diazoxide responsive HH associated with mutations in *HNF1A* (Stanescu et al., 2012). The phenotype described is very similar to *HNF4A* mutations – macrosomia, early neonatal presentation and diazoxide responsiveness.

1.3.1.6 HH and defects in the mitochondrial oxidation enzyme Short chain 3 Hydroxyacyl-coenzyme A dehydrogenase (SC*HAD*)

Short chain L-3-hydroxyacyl-CoA dehydrogenase (SCHAD) catalyzes the penultimate step in fatty acid β-oxidation in the mitochondria. It is encoded by *HADH*, which is highly expressed in the pancreatic β-cells. Short chain 3-hydroxyacyl-CoA dehydrogenase (SCHAD) deficiency is a recently described disorder of mitochondrial fatty acid β-oxidation (Clayton et al., 2001, Hussain et al., 2005b, Molven et al., 2004). Unlike other inherited defects of fatty acid β-oxidation, the main clinical feature of this metabolic disease is HH.

A number of studies have demonstrated that *HADH* has a pivotal role in regulating insulin secretion (Hardy et al., 2007b, Martens et al., 2007). Recently, the mechanism behind unregulated insulin secretion in SCHAD deficiency is becoming clear. These patients were noticed to be severely protein sensitive, suggesting an amino acid triggered unknown pathway of insulin release (Kapoor et al., 2009b). Subsequently hadh -/- knockout mice studies demonstrated protein-protein interactions between HADH and glutamate dehydrogenase (GDH) (Li et al., 2010). Similar interactions have been reported in human control lymphoblast, which are lost in patients with *HADH* mutations (Heslegrave et al., 2012). Studies on isolated islets showed an increase in the affinity of GDH for its substrate α-ketoglutarate. It is therefore likely that *HADH* mutations cause HH by activation of GDH via loss of inhibitory regulation of GDH by HADH.

Metabolic profile in affected individuals may reveal a raised plasma hydroxyl-butyryl-carnitine and urinary 3-hydroxyglutarate levels. However, the reason why not all patients show abnormal organic acid profiles or defects in acylcarnitine metabolism is unclear. Most cases reported to date are from consanguineous families (Flanagan et al., 2011b). Hence sequencing of *HADH* is recommended in patients with diazoxide responsive CHI who come from consanguineous families and do not have an identifiable mutation in the *ABCC8/KCNJ11* genes.

1.3.1.7 Exercise-induced hyperinsulinism (EIHI)

Exercise-induced hyperinsulinism (EIHI) is an autosomal dominant disorder in which strenuous physical exercise causes inappropriate insulin secretion in affected individuals, leading to hypoglycemia. Heterozygous gain-of-function mutations in the solute carrier

family 16, member 1 (*SLC16A1*) that encodes monocarboxylate transporter 1 (MCT1; required for trans-membrane transport of pyruvate and lactate) causes exercise induced hyperinsulinism (Meissner et al., 2005, Ishihara et al., 1999, Otonkoski et al., 2003).

In normal individuals, expression of the pyruvate transporter (MCT1) is specifically silenced in pancreatic β-cells, despite nearly universal expression across other tissues (Ishihara et al., 1999). Affected patients have symptoms due to activating mutations in the *SLC16A1* promoter in β-cells. Increased expression of MCT1 thus renders the plasma membrane permeable to lactate and pyruvate, allowing the latter to inappropriately stimulate insulin secretion (Ishihara et al., 1999). Affected patients do not normally experience fasting hypoglycemia. During exercise pyruvate is generated along with lactate by muscle, thereby stimulating inappropriate insulin secretion from the pancreatic β-cell despite low blood glucose levels. The mechanism highlights the importance of MCT1 absence from these cells for the normal control of insulin secretion. Although the HH is usually quite severe in these patients, specific treatment is not usually needed as avoiding strenuous exercise may prevent hypoglycaemic episodes.

1.3.2 Clinical Presentation Of HH

Most common and severe presentation of HH is during the neonatal period. The presenting symptoms of hypoglycaemia may be very non-specific (irritability, poor feeding and lethargy) and severe (seizures and coma). Typically these infants are macrosomic and require very high dextrose infusion rate to maintain normoglycaemia (blood glucose > 3.5mmol/l). Transient forms of HH are observed in in infants born to mothers with diabetes mellitus

(insulin dependent or gestational), those who have sustained perinatal asphyxia or those with intrauterine growth restriction (IUGR). In these groups of infants the HH tends to resolve after few weeks or months.

HH may also be the presenting feature in some developmental syndromes such as Beckwith-Wiedemann syndrome (BWS), Soto's syndrome and rare metabolic conditions such as congenital disorder of glycosylation (CDG). Of these, the commonest is BWS. HH in the vast majority of patients with BWS is transient and resolves spontaneously. The other clinical features of BWS include prenatal and/or postnatal overgrowth, macroglossia, anterior abdominal wall defects, organomegaly, hemihypertrophy, ear lobe creases, helical pits, and renal tract abnormalities (Choufani et al., 2010).

During infancy and childhood, the presentation of HH may be very subtle and difficult to diagnose. The presenting symptoms before 1 year of age are seizures, episodes of drowsiness or excitability. After 1 year, the symptoms are typical of hypoglycaemia; pallor, faint, tachycardia and sweating, seizures.

Patients with HH due to *GLUD1* mutations (HI/HA syndrome) demonstrate two characteristic features. Firstly, they show marked sensitivity to dietary protein (leucine), and symptoms of hypoglycaemia become manifest or aggravated following a protein-rich meal, rather than a fast (Kapoor et al., 2009a). Secondly, they typically show mild to moderate asymptomatic hyperammonaemia. Hypoglycaemia is usually not as severe as that seen in HH due to K_{ATP} channels defects. Children with HI/HA syndrome show good response to therapy with diazoxide and in some cases protein restricted diet. In addition, these children usually

are not macrosomic at birth and their hypoglycaemia is often not recognized before several months of age.

HH may be observed postprandially, for example, in the dumping syndrome. The “dumping syndrome” is classically observed in infants following gastro-esophageal surgery (Veit et al., 1994). In exercise induced HH symptoms of hypoglycaemia occur within the 30 minutes following a short period of anaerobic exercise.

1.3.3 Diagnosis And Investigations (Table 1.2)

The diagnosis of HH is based on clinical presentation and detection of characteristic biochemical profile of hypoketonaemic, hypofattyacidaemic hypoglycaemia arising from the anabolic effects of excessive insulin action at the time of hypoglycaemia. Certain clinical clues for diagnosis of HH include macrosomia or severe IUGR, and high glucose requirement (>8 mg/kg min, normal range 4-6 mg/kg min) to maintain normoglycaemia.

Characteristic metabolic profile can either be identified during spontaneous hypoglycaemia or hypoglycaemia induced by provocation tests (controlled fast/ exercise/protein ingestion). However, provocation test should only be done within a controlled environment with appropriate monitoring as this can be potentially life threatening. Laboratory findings at time of hypoglycaemia would unveil inappropriately elevated insulin and inappropriately low beta-hydroxybutyrate and free fatty acids. Plasma insulin levels may not be dramatically elevated (Al-Otaibi et al., 2013). Under normal physiological conditions, insulin production is switched off during hypoglycaemic state. As insulin release is pulsatile and has a short half- life, measurement of C-peptide (which has a longer half-life and reflects the endogenous insulin production) can prove to be more helpful when the diagnosis is in doubt.

Additional supportive evidence can be provided by a positive glycaemic response to intramuscular/ intravenous glucagon at the time of hypoglycaemia (a clear increment in blood glucose of >1.5mmol/L despite severe hypoglycaemia), a positive glycaemic response to octreotide and a decreased serum levels of insulin-like growth factor-binding protein 1 (IGFBP-1) (as insulin suppresses the transcription of *IGFBP-1* gene (Hussain et al., 2005a, Finegold et al., 1980, Levitt Katz et al., 1997).

Table 1.2: Diagnostic Findings of HH

Blood glucose < 3mmol/l on Glucose infusion rate of >8mg/kg/min		
	Factor	**Result in HH**
Blood Samples	Insulin	Detectable or elevated
	C-peptide	Detectable or elevated
	Free fatty acids	Inappropriately low
	β-hydroxybutyrate	Inappropriately low
	Acetoacetate	Inappropriately low
	Lactic acid	Normal
	Hydroxybutyryl Carnitine	Elevated in *HADH* deficiency.
	Amino acids	Low
	Ammonia	Elevated in HI/HA syndrome
	Cortisol	Elevated due to hypoglycaemia
	IGFBP-1	Low
Urine Samples	Ketone bodies	Negative
	Reducing substances	Negative
	C-peptide	Elevated
	3-hydroxyglutarate	Elevated in *HADH* deficiency.

A low serum cortisol and/or growth hormone levels at the time of hypoglycaemia is not diagnostic of cortisol or growth hormone deficiency (Hussain et al., 2003). Appropriate stimulation tests are required to confirm cortisol or growth hormone deficiency.

In the persistent rare forms of CHI, certain specific diagnostic findings can suggest likely underlying genetic diagnosis. Elevated serum ammonia and HH imply HI/HA syndrome (GDH-HH) (Stanley, 2004). However, normal ammonia concentrations do not necessarily exclude GDH-HH. In these patients with "activating" *GLUD1* mutations, hypoglycaemia may occur after ingestion of leucine- or protein-rich meal and can be provoked by performing a protein/leucine provocation test (Hsu et al., 2001, MacMullen et al., 2001).

Abnormal plasma acylcarnitine profile (elevated 3-hydroxtbutyryl-carnitine) and urine organic acids (3-hydroxyglutarate in urine) characterize HADH-HH (Clayton et al., 2001). If HH is related to exercise, consider performing an exercise provocation test or pyruvate load test (Otonkoski et al., 2003). An exercise test with submaximal to maximal exercise over 10 minutes is diagnostic.

In patients with mutations in *HNF4A* and *UCP2*, there are no specific laboratory findings. *HNF4A* mutations are associated with a considerable increase in birth weight, macrosomia and family history of MODY (Kapoor et al., 2008, Pearson et al., 2007). However, prenatal hyperinsulinism due to other genetic causes may also increase the birth weight. Family history of MODY and postprandial HH may denote GCK-HH.

1.3.4 Histological Subtypes And Underlying Molecular Basis of HH

Despite identical clinical presentation, at least two (possibly more) well described histological types are associated with HH: a focal form and a diffuse form (Figure 1.5) (Rahier et al., 2000). In diffuse form, all of the islets of Langerhans throughout the pancreas are enlarged and contain distinctly hypertrophied insulin producing cells. Focal form is characterized by nodular hyperplasia of islet-like cell clusters, including ductuloinsular complexes and giant β-cell nuclei surrounded by a histologically and functionally normal pancreatic tissue.

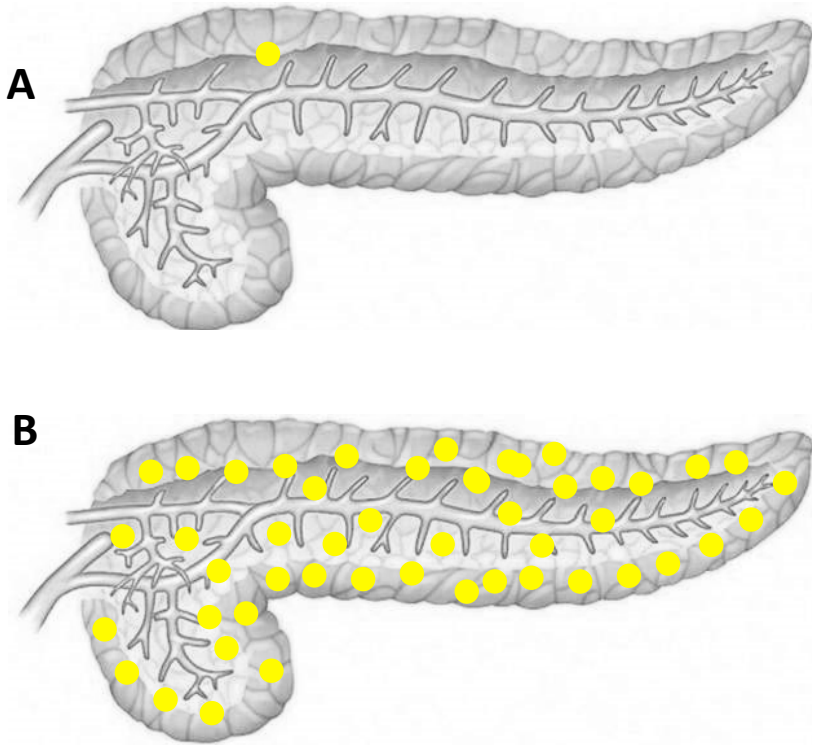

Figure 1.5: Schematic of focal and diffuse hyperinsulinism. **A** Focal lesion at the junction of head and body of pancreas **B** Diffuse disease affecting the islets throughout the pancreas

These two subtypes have different underlying genetic mechanisms. The most common causes of diffuse HH are recessive and dominant mutations in *ABCC8* and *KCNJ11*. The focal form has a unique genetic aetiology and involves two independent events – the inheritance of a paternal mutation in *ABCC8* or *KCNJ11*, and somatic loss of the maternal 11p allele (11p15.1 to 11p15.5) involving the *ABCC8* and *KCNJ11* region within the focal lesion (Verkarre et al., 1998). This region includes two clusters of genes. The first cluster corresponds to 11p15.5 region that contains an imprinted domain. The maternal LOH leads to an imbalance between the maternally expressed tumor suppressor genes *H19* and *CDKN1C*, and the paternally expressed growth factor *IGF2* (Fournet et al., 2001). The second cluster of genes in 11p15.1 region includes the *ABCC8* and *KCNJ11* genes. Hence maternal LOH of the 11p15 region will lead to paternal uniparental disomy unmasking the paternally inherited K_{ATP} channel mutation. These events form the basis of unregulated insulin secretion and focal increased proliferation of β-cells evolving into a focal adenomatous hyperplasia. The focal disease is mostly sporadic in origin; however a familial case has been reported in literature (Ismail et al., 2011).

Sempoux *et al.* recently described a novel histological form of PHHI (Sempoux et al., 2011). This particular form was characterized by the presence of two types of islets: large islets with β-cells with large cytoplasm and enlarged nuclei, and shrunken islets with β-cells with little cytoplasm and small nuclei. Large islets had hyperactive β-cells, characterized by large proinsulin antibody-labeled Golgi, strong labeling for insulin mRNA by insitu hybridization (ISH) and faint labeling of the antiinsulin antibody. Shrunken islets had resting β-cells, characterized by punctate proinsulin antibody-stained Golgi and strong antiinsulin antibody staining. This morphological entity was not associated with genomic mutations in *ABCC8*,

KCNJ11 and *GCK*, or 11p15 deletion. The abnormal hyperfunctional islets were most often confined to few adjacent lobules.

Recently, the same authors studied the insulin secretion by pancreatic fragments from six of the 14 patients described with a novel histopathological form (Henquin et al., 2013). The authors showed that β-cells of the hyperfunctional islets have functionally normal K_{ATP} channels. The β-cells were noticed to be inappropriately sensitive to glucose in in vitro studies of pancreatic fragments. Addition of only 1mmol/L glucose consistently induced a large peak in insulin secretion, with no or little further effect with subsequent increase in glucose. Subsequent studies with immunohistochemistry and genetic analysis identified undue expression of low-K_m hexokinase I (HK-I) or to an activating mutation in glucokinase in hyperfunctional islets only.

1.3.4.1 Differentiation Between Diffuse And Focal Hyperinsulinism

The outcome in children with congenital HH is dependent on distinguishing between diffuse and focal hyperinsulinism. Medically unresponsive diffuse hyperinsulinism requires near-total pancreatectomy with a very high risk of iatrogenic diabetes mellitus later in life. Focal hyperinsulinism can be treated with partial pancreatectomy if the region of focal adenomatous islet-cell hyperplasia can be identified.

De Lonlay-Debeney *et al.* studied 52 neonates with hyperinsulinism referred for pancreatic surgery with transhepatic catheterization of the portal vein and selective catheterization of the pancreatic vein to locate the sites of insulin hypersecretion (de Lonlay-Debeney et al., 1999). The authors collected samples of venous blood from the head, the isthmus, the body and the tail of the pancreas for measurements of plasma glucose, insulin and c-peptide. Focal hyperinsulinism patients had high plasma insulin and c-peptide concentration in one or several samples from contiguous areas, with low concentrations from the remaining samples. Diffuse hyperinsulinism patients had high plasma insulin and c-peptide concentration in all samples. Pancreatic catheterization successfully localized the focal lesion in 17 out of 19 neonates with histologically confirmed focal adenomatous hyperplasia. Among the 26 neonates with diffuse hyperinsulinism who underwent pancreatic catheterization, the diagnosis was correctly established in 17 patients. In 7 patients with diffuse hyperinsulinism, the result of pancreatic catheterization was suspected of localized hyperinsulinism; however the intraoperative histologic testing revealed diffuse β-cell hyperfunction.

Although pancreatic venous sampling was found useful in some centres, it was not widely accepted because of being invasive and technically demanding. In 2006, Otonkoski *et al.* described a non-invasive technique ^{18}F-DOPA Positron Emission Tomography for diagnosis

of focal hyperinsulinism of infancy (Otonkoski et al., 2006). Any patient with a visually clear [^{18}F] hot spot in the pancreas with maximum uptake (standardized uptake values) measuring ≥ 1.5 times the maximum pancreatic tracer concentration elsewhere was defined as having focal disease. Based on this cut-off, ^{18}F-DOPA PET correctly identified focal disease in five patients.

The principle of this imaging technique is based on the fact that pancreatic islets take up L-DOPA and convert it into dopamine using the enzyme DOPA decarboxylase, which is expressed in islet cells. ^{18}F-DOPA is an analogue of DOPA and thus the positron-emitting compound is useful for tracking the uptake of this dopamine precursor. Both diffuse and focal diseases have a high DOPA decarboxylase activity.

Apart from differentiating diffuse and focal disease, 18F-DOPA PET/CT simultaneously permits precise preoperative localization of the lesion (Hardy et al., 2007a, Laje et al., 2013, Ribeiro et al., 2007). A recent meta-analysis reported the pooled sensitivity and specificity of ^{18}F-DOPA PET/CT in differentiating between focal and diffuse HH as 89% (95% CI: 81–95%) and 98% (95% CI: 89–100%), respectively (Treglia et al., 2012). The pooled accuracy in localizing focal HH was 80% (95% CI: 71–88%).

1.3.5 Management

1.3.5.1 Medical management

The goal of treatment in patients with HH is to maintain normoglycaemia (blood glucose levels between 3.5–6 mmol/L). Intravenous dextrose infusion of up to 15–25 mg/kg/min through an established central venous access may be required to maintain normoglycaemia in neonates with severe forms of HH. This should be supported with enteral feeding to maintain orality. It is important to note that orality is often affected possibly due to disturbed feeding pattern and gastro-esophageal reflux, often inducing feeding refusal behavior. Frequent monitoring of blood glucose levels is required.

Diazoxide

Once the diagnosis of HH has been confirmed, medical therapy with diazoxide should be initiated, and within the first week of diagnosis, the response to diazoxide would give an indication of the need for further evaluation and surgical intervention.

In all newborns and infants diagnosed with HH, diazoxide (K_{ATP} channel opener) is the first-line medical therapy. Diazoxide is administered orally at a starting dose of 5 mg/kg/day in 3 divided doses. The dose can be increased by 5 mg/kg/day every 48 h to an effective and tolerated dose (the maximal dose rate is 15 mg/kg/d). The responsiveness to diazoxide is determined by a) appropriate fasting tolerance for age; b) feed volume and frequency normal for age; c) normal blood glucose levels at the end of the fast.

The use of diazoxide is often limited by its side effects. The most common side effects of diazoxide are hypertrichosis and fluid retention (especially in the newborn), followed by hyperuricaemia, tachycardia, leukopenia, and feeding problems. In newborns, the drug is

given in conjunction with the thiazide diuretic chlorothiazide (5–10 mg/kg per day in 2 divided doses), which reduces water retention. If the dose of diazoxide falls below 5 mg/kg/day, a trial off diazoxide should be considered under medical observation in the hospital setting. In those with less severe HH (HH associated with perinatal stress or IUGR), it may be preferable to start at a lower dose (2–3 mg/kg/day) of diazoxide.

Diazoxide is an agonist of the K_{ATP} channel and a dose range of (5–15 mg/kg/day) is usually effective in all forms of congenital HH, except those caused by autosomal recessive mutations in the *ABCC8* and *KCNJ11* genes (Aynsley-Green et al., 2000). A functional K_{ATP} channel is required for diazoxide to exert an effect. Hence patients with focal or diffuse K_{ATP} HH do not respond to therapy with diazoxide. Patients with GDH-HH, SCHAD-HH, HNF4A and transient HH typically respond well to diazoxide. Patients with GCK-HH have a variable response to diazoxide and some may require surgery (Cuesta-Munoz et al., 2004).

Patients unresponsive to maximum doses of diazoxide need urgent genetic analysis to identify those who should undergo ^{18}F-DOPA-PET/CT in search of a focal lesion. Those with a paternally inherited *ABCC8*/*KCNJ11* mutation are likely to have a focal lesion. While these investigations are carried out, normoglycaemia should be achieved with second-line medications.

Octreotide

Octreotide is the second line of medical therapy for HH. Octreotide inhibits insulin secretion by activation of somatostatin receptor-2 and -5 and inhibition of calcium mobilization in β-cells (De Leon and Stanley, 2007). Octreotide is administered subcutaneously every 6–8 h, beginning at a low dose (5 μg/kg/day) and titrating up to a maximum of 30 μg/kg/day. Necrotizing enterocolitis is a rare but potentially life-threatening adverse effect of octreotide and therefore, it must be used with caution in neonates (Laje et al., 2010). In most patients,

there is transient hyperglycaemic response to the initial doses of octreotide. However desensitization can occur after 2–3 doses, requiring increasing doses (tachyphylaxis) that in some patients makes this drug unsuitable for long-term use. There are reports suggesting that continuous subcutaneous octreotide infusion can overcome tachyphylaxis and lead to reduction in the dosage required as compared to when given by multiple daily injections (Vezzosi et al., 2005, Yorifuji et al., 2013).

Newer Medical Therapies

Treatment with long acting preparations of octreotide has been reported to be successful in older children and needs more research to prove efficacy in younger group of patients (Le Quan Sang et al., 2012, Modan-Moses et al., 2011). In combination with frequent feeding, it may be a long-term treatment option either alone or in conjunction with diazoxide (Le Quan Sang et al., 2012). In diazoxide unresponsive patients, glucagon can be given along with octreotide, as a continuous intravenous infusion as a rescue therapy to help maintain normoglycaemia (Mohnike et al., 2008).

GLP-1 receptor may be a new therapeutic target in future for children with K_{ATP} HH. In a mouse model of K_{ATP} HH (SUR-$1^{-/-}$), treatment with exendin-(9–39) (GLP-1 receptor antagonist) had been shown to result in improved fasting blood glucose levels (De Leon et al., 2008). The authors' findings suggested cAMP may have a role in K_{ATP} HH as cAMP content in SUR-$1^{-/-}$ was reduced by exendin-(9–39) both basally and when stimulated by the amino acids (De Leon et al., 2008). More recently, in a randomized, open-labeled, 2-period crossover pilot clinical study involving 9 human subjects with K_{ATP} HH, it was shown that significantly higher nadir blood glucose levels were observed with exendin-(9–39) as compared to placebo. These findings propose that GLP-1 and its receptor may play a role in the regulation of fasting glycaemia in K_{AT}P HH (Calabria et al., 2012).

Senniappan *et al* recently described the successful use of mTOR inhibitor sirolimus in the management of diazoxide and octreotide unresponsive HH (Senniappan et al., 2014). The authors treated four consecutive HH patients, who were unresponsive to the maximum doses of diazoxide and octreotide, with sirolimus and noticed improved glycaemia. A possible underlying mechanism of β-cell hyperplasia and HH is constitutive activation of mTOR pathway. Inhibitors of mTOR and mTOR kinase have also been shown to improve glycaemia in insulinoma patients, who have a similar pathophysiology (Bourcier et al., 2009, Kulke et al., 2009).

1.3.5.2. Surgical management

The indications for surgery in HH patients include medically unresponsive diffuse disease and confirmed focal disease on ^{18}F-DOPA-PET/CT scan. Despite the huge advances in diagnosing and accurately localizing focal lesions preoperatively with novel imaging techniques such as ^{18}F-DOPA-PET/CT there is still a potential for ambiguity. Therefore, it is very important to have an experienced surgeon, endocrinologist, as well as pathologists trained in evaluating intraoperative frozen sections to confirm the focal lesions, which aid in guiding the extent of the surgery.

Infants with diffuse disease require a near-total pancreatectomy (95–98% removal) to control the HH. They might require additional therapy post-operatively with diazoxide, octreotide, and/or frequent feedings to maintain normoglycaemia. Laparoscopic pancreatectomy is a new approach to the diagnosis and management of patients with congenital HH associated with less operative trauma and faster recovery than traditional laparotomy (Al-Shanafey, 2009, Pierro and Nah, 2011).

1.4 AIMS OF THE PROJECT

Previous research under Prof Khalid Hussain at Great Ormond Street Hospital, London has recruited 300 patients with CHI (Figure 1.6). Depending upon responsiveness to diazoxide treatment, the patients were broadly classified into diazoxide responsive (183) and diazoxide unresponsive (105). Molecular genetic analysis performed at University of Exeter Medical School confirmed the underlying genetic aetiology in 51 (27.8%) diazoxide responsive and 92 (87.6%) diazoxide unresponsive patients.

Within this large cohort of patients, there are some patients with unique complex phenotypes (protein sensitive HH with normal ammonia, HH and renal cysts, HH and cerebellar dysfunction with normal imaging) and no identified genetic aetiology. Additionally, there are consanguineous and non-consanguineous families with two affected siblings with no identified genetic aetiology.

The aims of this project were:

1. To recruit patients with complex forms of HH with no identified genetic aetiology for detailed clinical and biochemical phenotyping of these patients.

2. To study these patients with homozygosity mapping and whole-exome sequencing techniques to identify potential novel genetic mechanisms of HH based on the available biological information.

3. Based on the function of the gene, functionally characterize the mutation by appropriate laboratory techniques.

4. To functionally characterize two novel K_{ATP} mutations associated with unique clinical phenotypes (transient HH; combined focal and diffuse HH phenotype).

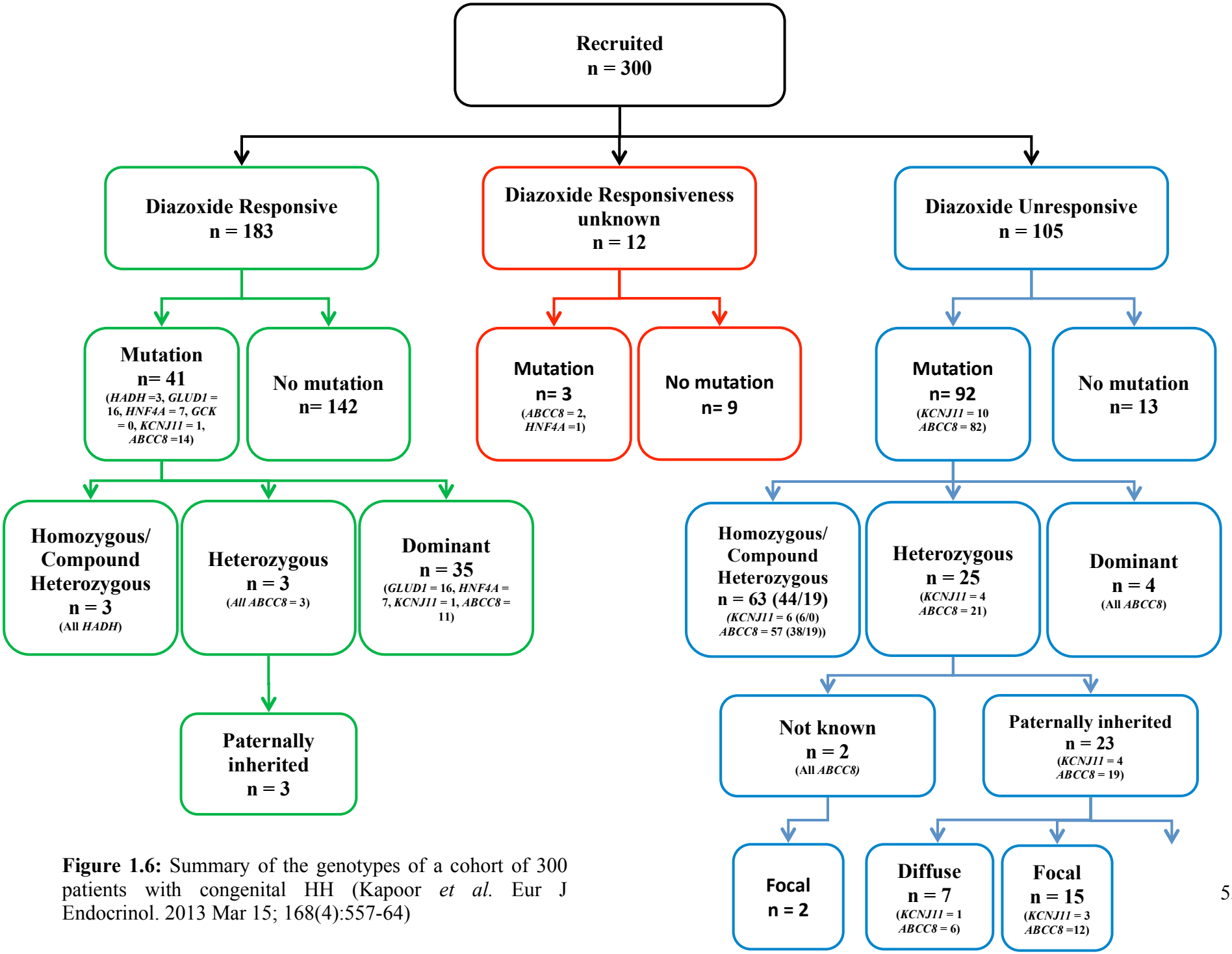

Figure 1.6: Summary of the genotypes of a cohort of 300 patients with congenital HH (Kapoor *et al.* Eur J Endocrinol. 2013 Mar 15; 168(4):557-64)

Chapter 2

GENERAL METHODS

2.1 SUMMARY OF CHAPTER 2

In chapter 2, various molecular biology techniques used in this project such as homozygosity mapping, whole-exome sequencing, site-directed mutagenesis, molecular cloning, RNA and protein extraction from the pancreatic tissue, Western blotting etc., are discussed. Dr Kerra Pearce from UCL Genomics Department performed the homozygosity mapping. Oxford Gene Technology carried out the whole-exome sequencing of the patients recruited in this project. Dr Sofia Rahman, post-doctoral fellow in Professor Khalid Hussain's laboratory, performed Western blotting.

2.2 HOMOZYGOSITY MAPPING

A genomic region is considered to be homozygous when the nucleotide (A, C, G or T) present at corresponding positions on the homologous chromosomes are identical. There are numerous positions in the genomic sequence, which differ in the single nucleotide sequence between corresponding positions on the paired chromosomes. These are referred as single nucleotide polymorphisms (SNPs).

Individuals born of consanguineous marriages show long stretches where the nucleotides at SNP sites are identical on the homologous chromosomes (homozygous regions). The size of the homozygous region will depend on the degree of inbreeding. If the parents are first cousins, then 1/16 of their offspring's genome will be homozygous. If they were second cousins then the homozygous genome amongst their offspring would be 1/64. More outbred populations have shorter shared homozygous regions.

Homozygosity mapping (HZM) is a powerful technique for identifying the genes underlying rare autosomal recessive diseases in consanguineous families. The technique was first suggested by Lander and Botstein in 1987 (Lander and Botstein, 1987). This technique is based on identifying the regions of homozygosity and searching these regions for the causative gene. The homozygous regions in the affected individual can be identified by SNP arrays. Homozygous regions in the affected siblings can then be compared and overlapping regions are likely to carry the causal gene.

The fundamental principle underlying HZM is that in children born to consanguineous marriages, and affected with an autosomal recessive condition, a common homozygous

region spanning the disease locus will be inherited in all affected individuals; and this region will be "identical by descent".

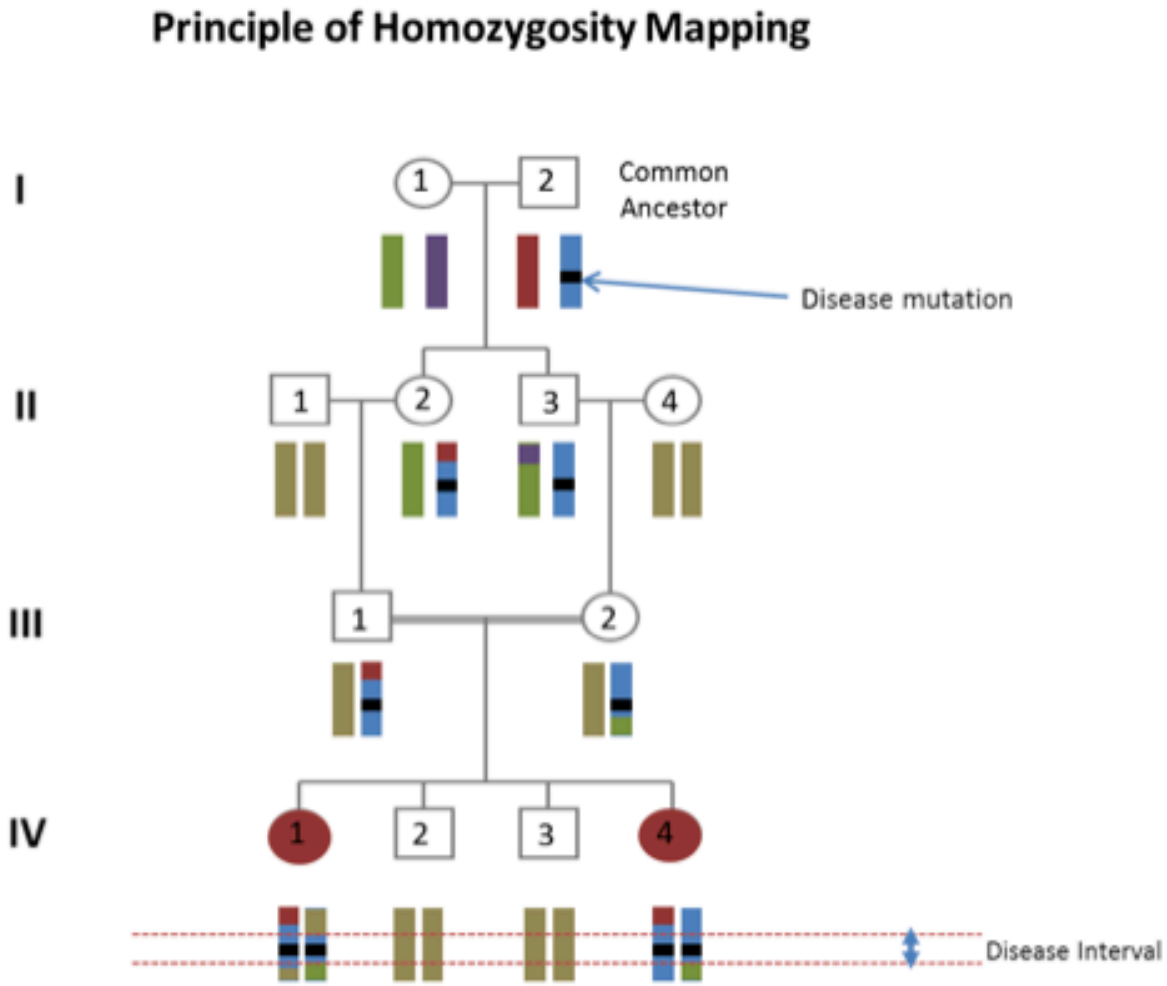

Figure 2.1 Principle of Homozygosity Mapping: In children born to consanguineous marriages, and affected with an autosomal recessive condition, a common homozygous region spanning the disease locus will be inherited in all affected individuals.

2.3 EXOME SEQUENCING

Exome sequencing involves sequencing the protein coding regions of the human genome. It is a powerful and cost-effective tool for identifying genetic basis of diseases. There are several reasons to choose exome sequencing above genome sequencing in search of rare alleles underlying Mendelian diseases. First, positional cloning studies that have focused on protein-coding sequences have, when adequately powered, identified disease-causing variants for a number of monogenic diseases (Antonarakis and Beckmann, 2006). Second, most alleles that are known to underlie Mendelian disorders disrupt protein-coding sequences. Third, a significant percentage of rare, protein-altering variants, such as missense or nonsense single-base substitutions or small insertion-deletions, are predicted to have functional consequences and/or to be deleterious (Kryukov et al., 2007). In view of the above reasons, exome sequencing is likely to identify variants that are deleterious for the function of the protein.

One particular challenge for exome sequencing has been how best to define the regions of the genome that constitutes the exome (Bamshad et al., 2011). Considerable uncertainty remains regarding which sequences of the human genome truly are protein coding. Nevertheless, all existing targets have limitations.

1. Our knowledge of all truly protein-coding exons in the genome is still incomplete, so current capture probes are designed to target known exons and will not capture genomic regions which have not been identified to be protein coding so far.
2. The efficiency of capture probes varies considerably, and some exonic sequences are not captured by the probes altogether.
3. All templates are not sequenced with equal efficiency, and not all sequences can be aligned to the reference genome so as to allow base calling.

4. Finally, whether important genomic sequences other than exons should be targeted in the capture probe design (for example, microRNAs (miRNAs), promoters and ultra-conserved elements).

Despite these caveats, exome sequencing is rapidly proving to be a powerful new strategy for finding the cause of known or suspected Mendelian disorders for which the genetic basis has yet to be discovered (Johnson et al., 2010, Bilguvar et al., 2010, Walsh et al., 2010).

2.3.1 Workflow for exome sequencing

The basic steps for exome sequencing are shown in the figures 2.2 and 2.3. The steps include sample preparation, hybridization, sequencing and alignment to the human reference genome.

2.3.1.1 Sample preparation:

The samples were prepared according to Agilent's SureSelect Protocol Version 1.2. The genomic DNA was sheared with the target peak for base pair size of 200, which was then confirmed using a DNA 1000 Bioanalyzer assay. The ends of the sheared DNA were repaired with T4 DNA Polymerase and Klenow enzyme. This was followed by addition of 'A' bases to the 3′ ends of the DNA fragments. The DNA fragments with 3′ overhanging 'A' bases were ligated with adapters with 3′ overhanging 'T' bases. The sample was then run on an agarose gel and the region of the gel that contained fragments in the 200 to 300 bp range was excised. The DNA was purified from the gel and amplified with two primers that annealed to the ends of the adaptors. Following PCR, the genomic DNA purity and quantity was checked on the spectrophotometer. A minimum of 500 ng is required for the next step of hybridization. The quality was assessed with Agilent 2100 Bioanalyzer to verify a single peak in the size range of 200 to 300 nucleotides.

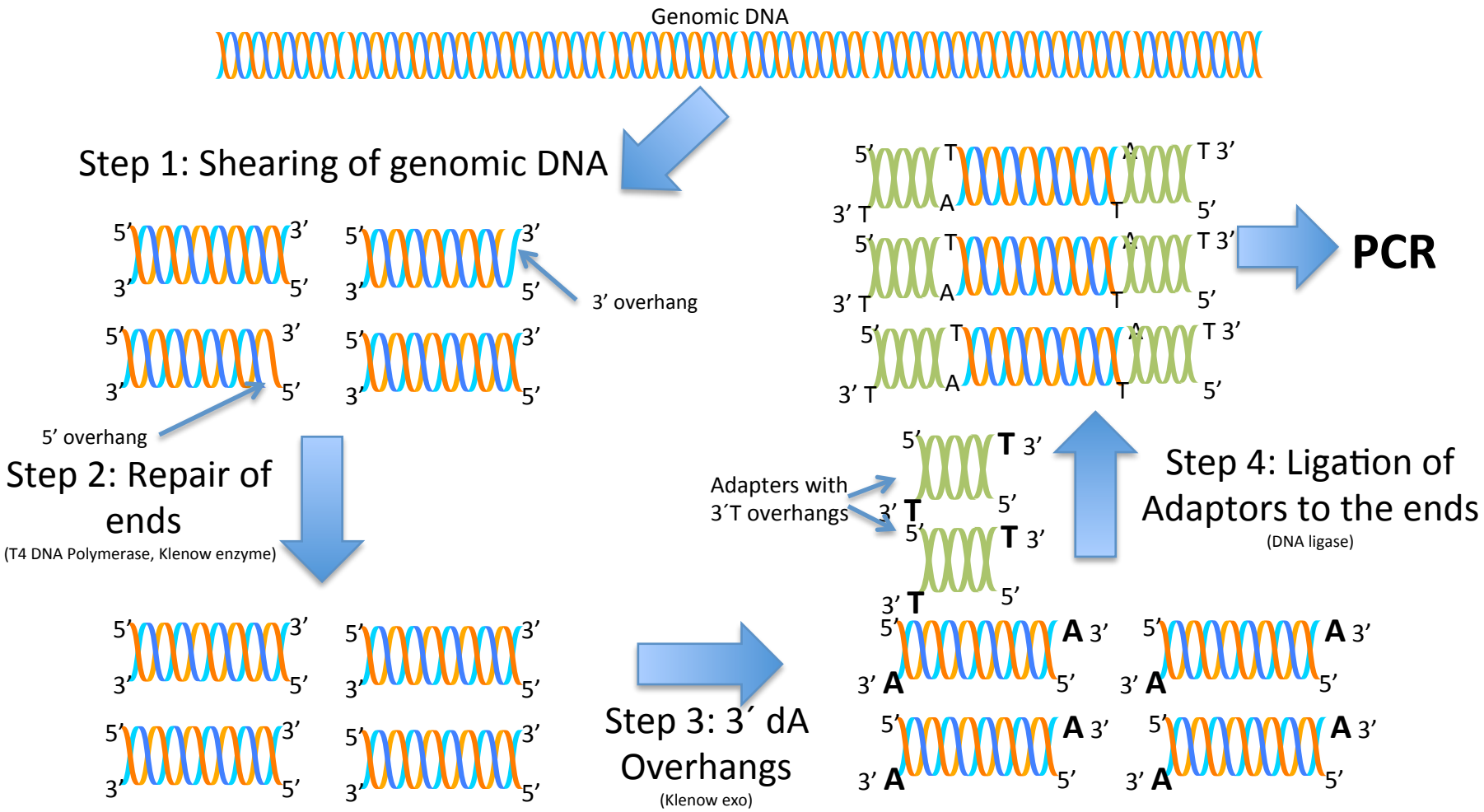

Figure 2.2: Sample preparation for Exome sequencing showing genomic DNA shearing, repair of the ends of the DNA fragments, addition of 3´ A overhangs, ligation with adapters and PCR amplification with primers complementary to adapters

2.3.1.2 Hybridization:

SureSelect Oligo Capture Library Mix (Biotinylated RNA Library Baits) is mixed with the genomic DNA sample (prepared in the previous step) in the presence of hybridization buffers. RNA Baits will hybridize with the complementary DNA fragments present in the prepared genomic sample. The hybridization mixture is then added to the solution containing Streptavidin coated magnetic beads. Streptavidin has an extraordinarily high affinity for biotin. With the use of a magnet, DNA fragments, which hybridized with the Biotinylated RNA library baits, can be separated from the rest of the DNA fragments on the magnetic beads. The beads are then washed and RNA is digested. The DNA is amplified and then sequenced.

2.3.1.3 Sequencing:

Sequencing was performed on the Illumina HiSeq2000 platform. The read files (Fastq) were generated from the sequencing platform via the manufacturer's proprietary software. The reads were mapped to their location in the most recent build of the human genome (hg19/b37) using the Burrows-Wheeler Aligner (BWA) package.

Local realignment of the mapped reads around potential insertion/deletion (indel) sites was carried out with the Genome Analysis Tool Kit (GATK) version 1.6 This algorithm ensures that the alignment has the minimum number of mismatching bases across the reads, the biggest effect of this is to reduce false-positive SNP calls around indels, and accurately determine indel length.

Duplicate reads were marked using Picard version 1.83. This removes reads likely to be the result of PCR bias. Such PCR artifacts can introduce false positive SNP calls. Reads are not removed from the alignment but are not considered further in the analysis.

Base quality (Phred scale) scores were recalibrated using GATK's covariance recalibration. This improves the accuracy of the base quality metrics, which in turn improves the quality of variant calls. SNP and indel variants were called using the GATK Unified Genotyper for each sample. SNP novelty is determined against dbSNP release 135.

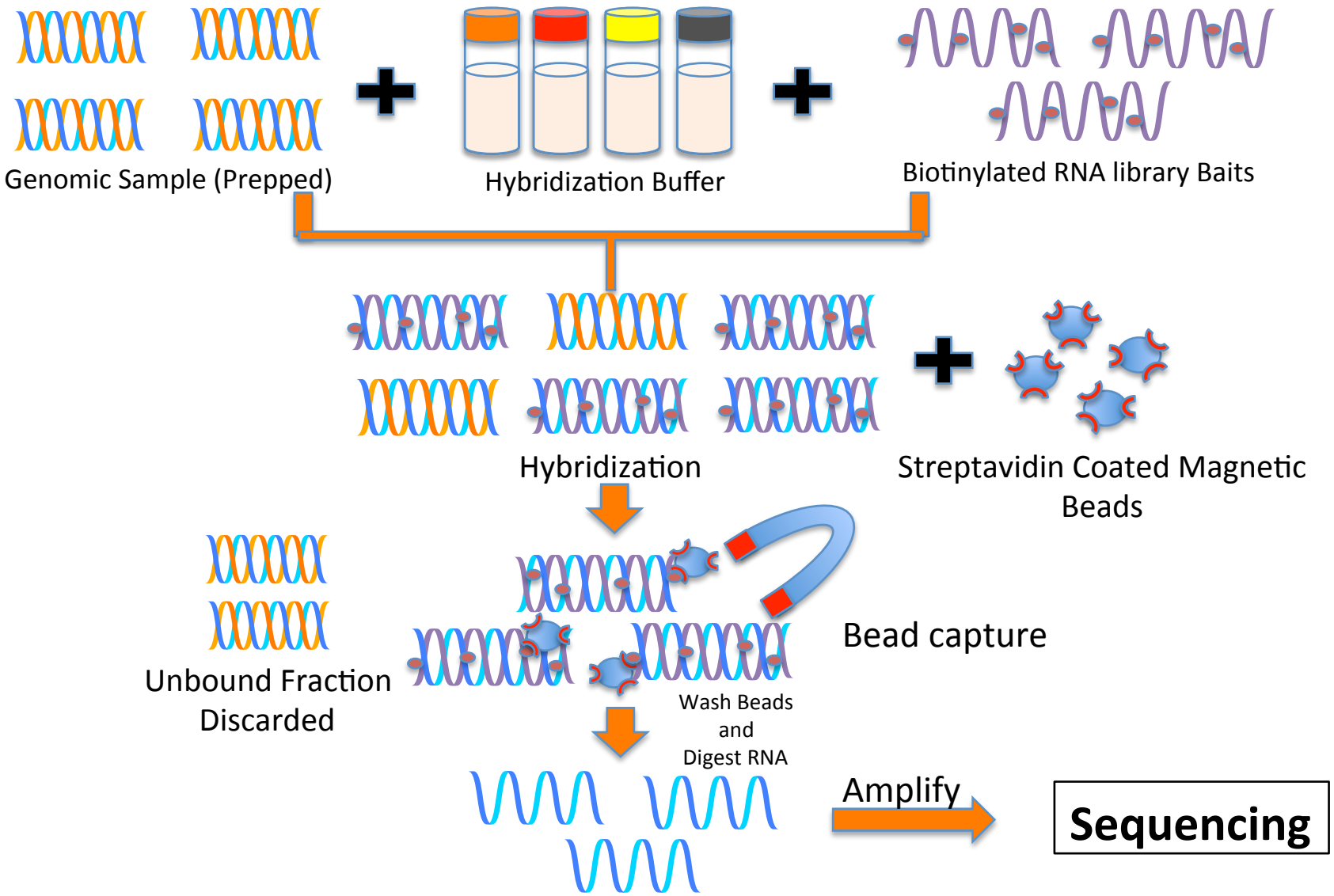

Figure 2.3: SureSelect Target Enrichment

2.3.2 Identifying causal alleles

One of the demanding aspects of using exome sequencing to find novel disease genes for either Mendelian or complex traits is identifying disease-related alleles among the background of non-pathogenic polymorphism and sequencing errors. On average, exome sequencing identifies ~24,000 single nucleotide variants (SNVs) in African American samples and ~20,000 in European American samples. More than 95% of these variants are already known as polymorphisms in human populations (Bamshad et al., 2011).

Factors which govern strategies to be used in finding causal alleles against this background of non-pathogenic polymorphism include: the mode of inheritance of a trait; the pedigree or population structure; whether a phenotype arises owing to de novo or inherited variants; and the extent of locus heterogeneity for a trait. Such factors also influence both the sample size needed to provide adequate power to detect trait-associated alleles and the selection of the most successful analytical framework.

The main approaches for identifying causal variants in exome-sequencing data are below:

2.3.2.1 Discrete filtering: This approach relies on identifying rare alleles or novel alleles in the same gene shared among a small number of unrelated or closely related affected individuals. The identified shared variants among affected individuals are filtered for novelty against a set of polymorphisms that are available in public databases (dbSNP and 1000 Genome Project) and/or those found in a set of unaffected individuals (i.e. controls). This 'discrete filtering' step is used to reduce the

number of candidate genes by assuming that any allele found in the 'filter set' cannot be causative. This approach reduces the number of candidate genes drastically because only a small fraction (~ 2% on average) of the single nucleotide variants (SNVs) identified in an individual by exome sequencing is novel.

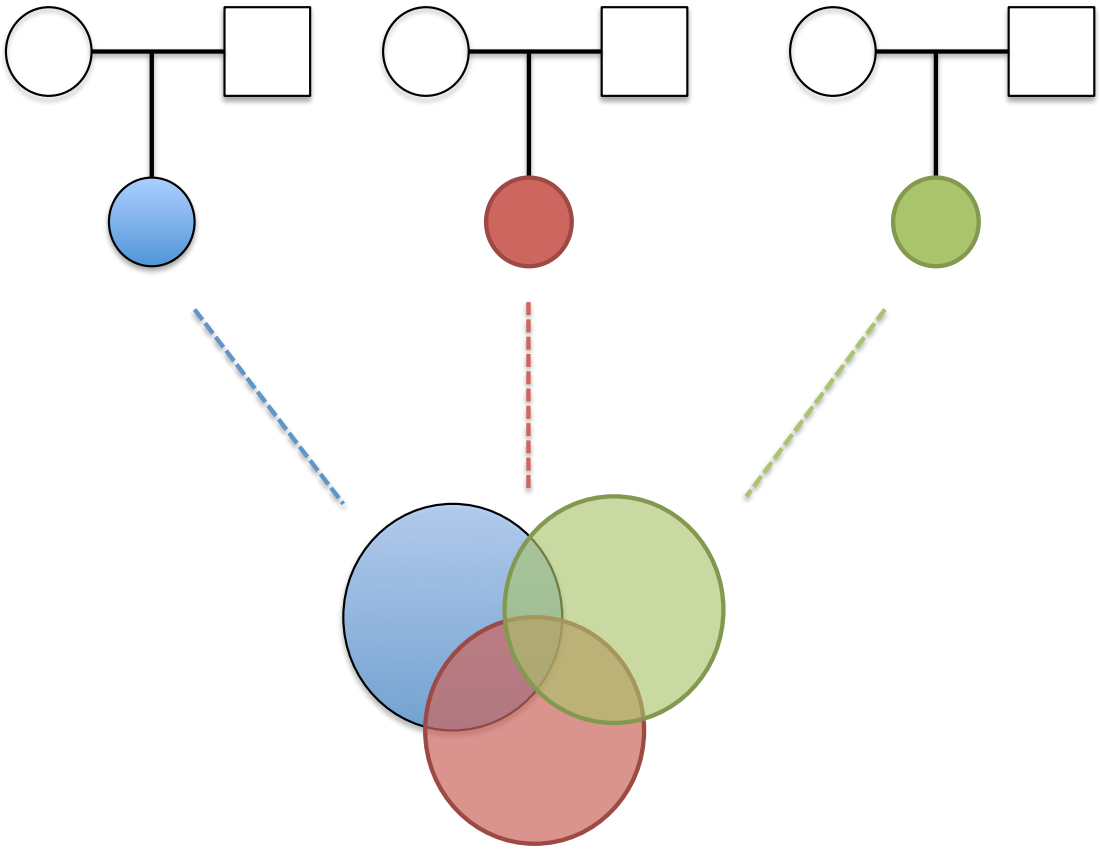

Figure 2.4: Sequencing and filtering across multiple unrelated, affected individuals (indicated by the three colored circles)

This assumption that the filter set contains no alleles from individuals with the phenotype can be problematic for two reasons. First, dbSNP is 'contaminated' with a small but appreciable number of pathogenic alleles. Second, as the number of sequenced exomes and genomes increases, the filtering of observed alleles in dbSNP

should take into account the minor allele frequency (MAF) as otherwise truly pathogenic alleles that are segregating in the general population at low but appreciable frequencies will be eliminated. This risk is especially relevant for recessive disorders, in which carrier status (heterozygous) will not result in a phenotype but will be present in the control population at a low frequency. Analysis of recessive disorders in which the maximum MAF is set at 1% is still well powered. Alternatively, discrete filtering with a maximum MAF >1% can be carried out using a substantially larger sample size and/or in conjunction with pedigree-based approaches.

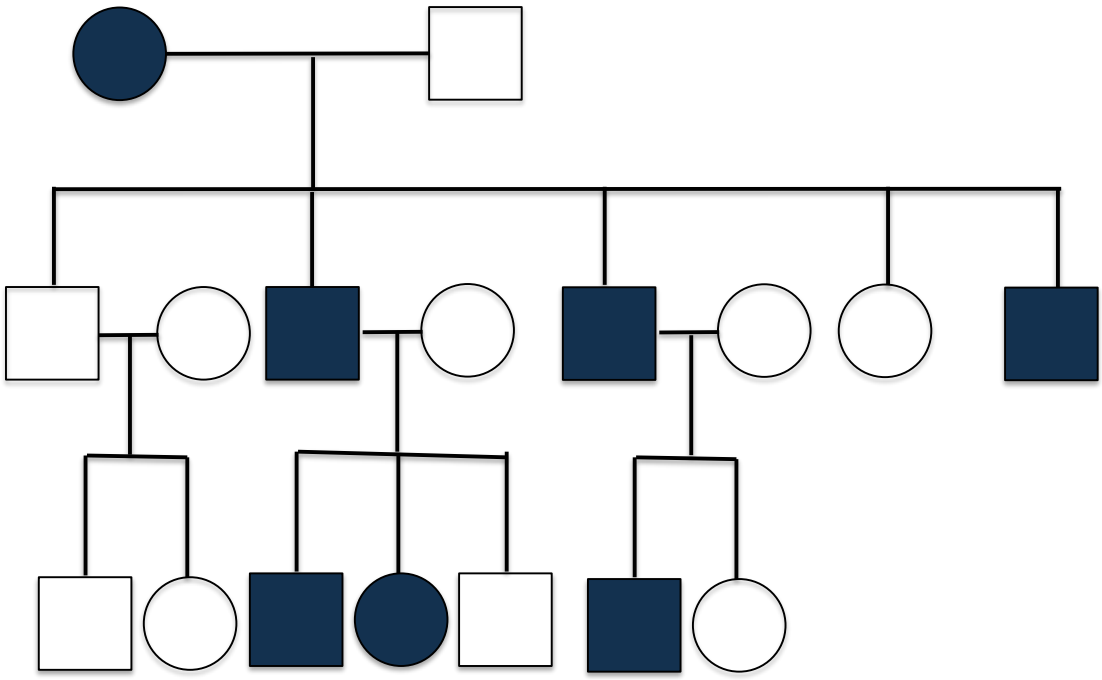

Figure 2.5 Sequencing and filtering among multiple affected individuals from within a pedigree (shaded circles and squares) to identify a gene with a novel variant in a shared region of the genome

A lower MAF cutoff of 0.1% is helpful for dominant disorders, as the estimated prevalence of the disorder (generally well below 0.1%) provides an upper bound on the MAF. However, if the number of novel variants with lower MAFs in a sample population is high, it will be difficult to identify the causal gene. This limitation highlights the importance of having control SNP data from the same populations as the one from which cases were sampled.

2.3.2.2 Stratifying candidates after discrete filtering: To reduce the number of potential variants to a sizeable number, candidate alleles after filtering against SNP databases can be further stratified on the basis of their predicted impact or deleteriousness.

Alleles can be stratified by their functional class. Frameshift mutations, nonsense mutations and mutations which disrupt the canonical splice sites are more likely to be causal as compared to missense variants. However, this is an oversimplification that is insensitive to causal alleles that do not directly alter protein-coding sequences or canonical splice sites.

Additionally, candidate alleles can be stratified by existing biological or functional information about a gene; for example, alleles with a predicted role in a biological pathway which can explain the phenotype or alleles which are known to interact with genes or proteins that are known to cause a similar phenotype.

Another approach for stratifying candidate alleles is to use quantitative estimates that have functional impact. There are sequences that show high conservation among

different species and mutations in these are likely to be pathogenic. Sites that have experienced purifying selection can be identified by quantifying rates of mammalian evolution at the nucleotide level.

Approaches that stratify non-synonymous alleles [for example SIFT, Polymorphism Phenotyping (PolyPhen2) and Multivariate Analysis of Protein polymorphism (MAPP)] also explore the predicted changes in proteins caused by specific amino acid substitutions.

All of the above strategies enrich for functional sites at which observed variants are more likely to affect phenotype.

Use of pedigree Information: For Mendelian phenotypes, the pedigree information can be used to substantially narrow the genomic search space for candidate causal alleles. However, exome sequencing may not need to be performed on every individual in a pedigree. Depending on the frequency of a disease-causing allele and the nature of the relationship between the individuals, the most informative individuals can be chosen for exome sequencing. For very rare alleles, the probability of identity-by-descent given identity-by-state is high even among distantly related individuals.

The mapping data are also helpful in deciding the individuals who should be exome-sequenced from a pedigree. In the absence of mapping data, the two most distantly related individuals with the phenotype of interest should be sequenced to substantially restrict the number of shared candidate alleles.

When mapping data are available, the most efficient strategy is to sequence those affected individuals whose overlapping haplotype produces the smallest shared genomic region. If the haplotype shared by all affected individuals is sufficiently short, then sequencing a single individual may be enough. For consanguineous pedigrees with suspected recessive node of inheritance, sequencing the individual with the smallest region (or regions) of homozygosity, as determined by the genome-wide genotyping data, should be sufficient. In each of these instances, exome sequencing is merely used as a replacement for Sanger sequencing of all the genes in a crucial interval.

For identifying de novo coding mutations, an approach that involves sequencing of parent-child trios is extremely efficient as it is highly unlikely that the proband will have multiple de novo events occurring within a specific gene (or within a gene family or pathway) (Nachman and Crowell, 2000, Vissers et al., 2010). This study design may be especially relevant to gene discovery in disorders where most cases are sporadic (that is, the parents are unaffected) and when a dominant mode of inheritance is likely (for example, when there are few instances of parent-to-child transmission) or substantial locus heterogeneity is expected. Despite the fact that identifying Mendelian inconsistencies in which the proband has a variant that is not called in either parent is unequivocal, more than 70% of these inconsistencies turn out to be false negatives that result from failure to call the corresponding germline variants in one or the other parent. This is likely to become less of an issue as the variant callers improve.

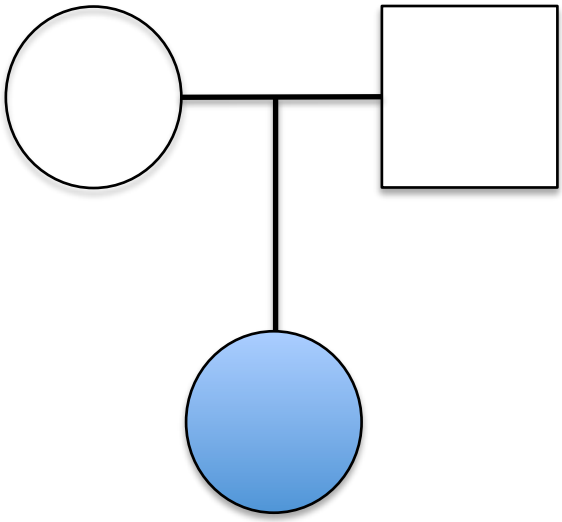

Figure 2.6: Sequencing parent-child trios for identifying de novo mutations

2.3.3 Technical and analytical limitations: Exome sequencing followed by discrete filtering has been the most rewarding strategy for establishing a novel disease gene, often with the aid of mapping data (Gilissen et al., 2010, Lalonde et al., 2010, Simpson et al., 2011, Hoischen et al., 2010). However, how often this approach has been unsuccessful is challenging to work out, as negative results are rarely reported. Failure can result for many reasons, most of which can be broadly considered as either technical or analytical.

Technical failure can occur because: part or all of the causative gene is not included in the target definition and capture is not designed for this region; there may be inadequate depth of sequencing of the region that contains a causal variant (for example, because of poor capture or poor sequencing); the causal variant may have been covered but not accurately called due to the presence of a small but complex indel (Bamshad et al., 2011). Mismapping of the sequence reads or errors in alignment to the reference sequence may result in false variants in a gene.

Analytical failures may result from the limitations and assumptions of discrete filtering. Genetic heterogeneity limits the power of discrete filtering. For example, if the disease is caused by mutations in a number of different genes (genetic heterogeneity), more than one gene in the sample population will have disease-causing alleles (Bamshad et al., 2011). Several other genes may also carry neutral mutations in as many cases, depending on the sample size. Hence it may become extremely difficult to separate the causal alleles from the non-causal alleles unless a large number of cases are sequenced.

No variant calling due to the presence of disease-causing alleles in the comparative set, and reduced penetrance will result in a reduced signal-to-noise ratio. This problem is very similar to genetic heterogeneity. False-positive calls (true variant in the genes but not responsible for the phenotype) will result in detection of candidate genes that cannot logically be eliminated by filtering alone.

2.4 RNA EXTRACTION

A small section of the pancreatic tissue removed during surgery of the patient with heterozygous non-stop *KCNJ11* mutation had been stored at -80ºC in RNA*later*. RNA*later* is an RNA stabilization reagent that stabilizes RNA in tissue samples and preserves the gene expression profile. RNA was extracted from the stored pancreatic tissue according to the following steps:

1. The pancreatic tissue was thawed on ice and rinsed with ice-cold phosphate buffer saline. The tissue was then homogenized in 1 ml trizol reagent in a sterilium and was incubated at room temperature for 5 minutes.
2. The homogenized mixture was transferred in a 1.5 ml microcentrifuge tube and mixed with chloroform (200 µL). The microcentrifuge tube was vortexed to ensure complete mixing. The mixture was incubated for another 5 minutes at room temperature.
3. The sample was centrifuged at 12,000 rpm for 15 minutes at 4ºC. At the end of centrifuge step, the sample was separated into different layers.
4. The superficial aqueous layer was carefully transferred to a new 1.5ml microcentrifuge tube.
5. Isopropanol (ice cold; 500 µL) was added to the microcentrifuge tube containing the aqueous layer and mixed by vortexing. The mixture was centrifuged at 12,000 rpm for 30 minutes at 4ºC. This resulted in pellet formation.
6. The supernatant was discarded and the pellet was washed with 70% ethanol twice.
7. After the second ethanol wash, the pellet was air-dried.

8. Nuclease free water (NFW; 30 μL) was added to the pellet and gently mixed. The mixture was incubated at 55ºC for 10 minutes.
9. The sample was immediately transferred to ice and the concentration of RNA and its quality determined by NanoDrop ^{TM} 1000 Spectrophotometer (Thermo Scientific).
10. The RNA concentration obtained was 3736 ng/μL and $OD_{260/280}$ of the RNA sample was 1.81. The ratio of absorbance at 260 and 280 nm is used to assess the purity of the sample.

2.5 REVERSE TRANSCRIPTASE – POLYMERASE CHAIN REACTION (RT-PCR)

RT-PCR is a technique to detect RNA expression in the tissue. To ensure the transcript encoded by the *KCNJ11* allele with a non-stop mutation is not degraded by non-stop decay phenomenon, RT-PCR was performed on the RNA extracted from the pancreatic tissue. The synthesized cDNA was sequenced to confirm the presence of both *KCNJ11*transcripts in the pancreatic tissue.

SuperScript® III First-Strand Synthesis System (Invitrogen) was used for RT-PCR. SuperScript III reverse transcriptase is a thermostable variant of MMLV (Moloney Murine Leukaemia Virus) reverse transcriptase and also has reduced RNaseH activity, which increased the yield of first-strand cDNA.

The steps for RT-PCR technique were as follows:

1. The following mixture (RNA/primer) was prepared in a 0.5mL tube

Table 2.1: RNA/Primer mixture for RT-PCR technique

Component	Amount
Total RNA (3736 ng/µL)	0.27 µL (1 µg)
Random Hexamers (50ng/µL)	1 µL
10 mM dNTP mix	1 µL
Double distilled water	7.73 µL (to make total volume of 10 µL)

2. The RNA/primer mixture tube was incubated at 65ºC for 5 minutes, and then on ice for at least 1 minute.

3. The cDNA Synthesis Mix was prepared as shown below:

Table 2.2: cDNA Synthesis Mix Reaction

Component	Amount
10X RT buffer	2 µL
25 mM MgCl2	4 µL
0.1 M DTT	2 µL
RNaseOUT (40 U/µL)	1 µL
SuperScript III RT (200U/µL)	1 µL

4. The cDNA Synthesis Mix (10 µL) and RNA/primer Mix (10 µL) were gently mixed in a 0.5 µL tube, followed by a brief centrifugation.
5. The mixture was then cycled in a thermocycler according to the following settings:

Table 2.3: Thermocycler Settings for RT-PCR technique

Temperature	Duration
25 ºC	10 minutes
50 ºC	50 minutes
85ºC	5 minutes

6. The cDNA synthesis reaction was then used for PCR using the following primers to amplify the region around the stop codon position of *KCNJ11*.

Table 2.4: Primers sequence for *KCNJ11* sequencing

Primer	Sequence
Forward	TACTGGAAGCTCTGACCCTC
Reverse	TGCCTTGTAACACCCTGGAT

7. The PCR products were sequenced to detect the presence of both *KCNJ11* alleles.

2.6 PROTEIN EXTRACTION FROM PANCREATIC TISSUE

For Western blotting to confirm the presence of larger Kir6.2 protein translated from *KCNJ11* allele carrying the non-stop mutation, protein was extracted from the pancreatic tissue according to the following steps:

1. Tissue lysis buffer was prepared in a 1.5 mL microcentrifuge tube as follows:

Table 2.5: Preparation of Tissue Lysis Buffer

Component	Amount
10X RIPA Buffer	100 µL
Protease inhibitor	100 µL
Double distilled water	800 µL

RIPA buffer is a lysis buffer used to lyse cells and tissue for Radioimmunoprecipitation assay. It contains the ionic detergents SDS and sodium deoxycholate.

2. The pancreatic tissue sample was washed with ice-cold phosphate buffer saline.
3. The pancreatic tissue was placed in 300 µL of tissue lysis buffer (prepared above) in a small container and homogenized.

4. The homogenized tissue was placed on ice for 30 minutes and then transferred into a 1.5 mL microcentrifuge tube.
5. The tissue sample was centrifuged at 10,000g for 10 minutes at 4ºC.
6. After centrifugation, the supernatant layer was carefully transferred to a new 1.5 mL microcentrifuge tube. This layer contained the protein fraction of the tissue.

2.7 PROTEIN QUANTIFICATION

The Thermo Scientific Pierce BCA Protein Assay was used for protein quantification in the sample extracted from the pancreatic tissue.

2.7.1 Principle:

This assay utilizes the property of protein to reduce Cu^{2+} to Cu^{+} in an alkaline medium (the biuret reaction). The cuprous cation (Cu^{+}) is then detected calorimetrically using a reagent contained bicinchoninic acid (BCA). Two molecules of BCA chelate one cuprous ion to form a purple-colored reaction product. This reaction product exhibits a strong absorbance at 562nm that is nearly linear with increasing protein concentrations over a broad range (20-2000µg/mL).

As the extent of color formation is not merely proportional to sum of individual color-producing functional groups, the protein concentrations are reported with reference to standards of a common protein such as bovine serum albumin (BSA).

2.7.2 Method:

1. The BCA working reagent (WR) was prepared by mixing Reagent A and Reagent B in the ratio 50:1 (50 parts of Reagent A with 1 part of Reagent B). The following formula was used to determine the total volume of WR required:

   (# Standards + # unknowns) × (# replicates) × (Volume of WR per sample) = total volume WR required.

2. The diluted albumin (BSA) standards were prepared as shown below:

Table 2.6: Preparation of diluted albumin standards for protein quantitation

Vial	Volume of BSA (µL)	Volume of Diluent (µL)	Final BSA Concentration (µg/mL)
A	300	0	2000
B	210	70	1500
C	140	140	1000
D	70 of vial B dilution	70	750
E	140 of vial C dilution	140	500
F	140 of vial E dilution	140	250
G	0	200	0 = Blank

3. 10 µL of each prepared BSA standards and 4 different dilutions (1:1, 1:2, 1:4 and 1:8) of protein sample extracted from pancreatic tissue was pipetted into a microplate well in triplicates.
4. 200 µL of BCA WR prepared above was added to each well.
5. The microplate was thoroughly mixed on a plate shaker for 30 seconds.
6. The plate was covered and incubated at 37ºC for 30 minutes.
7. The plate was then cooled to room temperature and the absorbance was measured at 584nm.
8. The average 584nm absorbance measurement of the blank standard replicates was subtracted from the measurements of all other individual standard and unknown sample replicates.

9. The average blank-corrected 584nm measurement of each BSA standard was plotted against its concentration in μg/mL to get a standard curve. This curve was used to determine the protein concentration in the sample extracted from the pancreatic tissue of the patient (15.22mg/mL).

2.8 WESTERN BLOTTING

Western blotting was performed to detect the presence of two different molecular weight Kir6.2 proteins in the pancreatic tissue of the patient with a non-stop *KCNJ11* mutation.

Technique:

Invitrogen's Xcell SureLock Mini-Cell Electrophoresis System was used for Western blotting.

Gel Electrophoresis: The inner chamber was filled with 200 mL 1× NuPAGE (Polyacrylamide) SDS running buffer with antioxidant and the outer chamber was filled with 600 mL 1× NuPAGE SDS running buffer. The pancreatic tissue sample (20 µg) was mixed in Laemmli buffer to a final protein concentration of 1 µg/µL and the mixture was loaded in the well of the pre-cast gel along with a control pancreatic tissue sample (20 µg) and molecular markers, and run at 150V for 1 hour at room temperature. The control pancreatic tissue sample was from a patient with HH with no mutation in *ABCC8/KCNJ11* who had undergone pancreatectomy at GOSH. This step resulted in separation of proteins based on their molecular weight.

Transfer by Electroblotting: After electrophoresis, the gel was removed from the cassette and a nitrocellulose membrane (pre-soaked with 1× NuPAGE Transfer Buffer with 10% methanol) was placed on top of the gel. The gel/membrane assembly was sandwiched between filter paper and blotting pads on either side. This was placed in the Xcell II Blot Module, with the gel closest to the cathode plate. During the assembly, any trapped air was removed. The blot module was filled with 1× NuPAGE Transfer Buffer and the outer buffer chamber was filled with deionized water. The

transfer was run at 30V for 2 hours. This step resulted in the transfer of proteins from the gel to the nitrocellulose membrane.

Ponceau S Staining: The nitrocellulose membrane was washed in 1× PBST (1× PBS in 0.1% Tween) and then placed in Ponceau S solution for few seconds to detect the successful transfer of polypeptide bands from the gel to the membrane. The membrane was then repeatedly washed with double distilled water until the stain of Ponceau S was removed.

Subsequent steps were performed after putting the nitrocellulose membrane in a 50 ml falcon.

Blocking: The nitrocellulose membrane was blocked using 5%milk/PBST solution on a roller for 1 hour. The proteins in the blocking solution attached to all places on the membrane where the target proteins have not attached during the transfer.

Detection: The membrane was incubated with the primary Kir6.2 antibody (raised in goat) in a concentration of 1:500, diluted in 10 ml of 5% milk/PBST solution, for 1 hour on a roller. After 1 hour, the membrane was washed three times with 1× PBST. Following wash steps, the membrane was incubated with the secondary antibody (conjugated to HRP [Horseradish Peroxidase] enzyme) in a concentration of 1:20,000, diluted in 10 ml of 5% milk/PBST solution. The membrane was repeatedly washed again to remove unbound antibody and incubated with ECL (enhanced chemiluminescent) substrate for 4 minutes. The excess ECL solution was blotted off and the membrane was wrapped in a clear plastic wrap.

The HRP enzyme catalyze the oxidation of luminol with emission of low intensity light at 428nm that is enhanced in the presence of enhancers in ECL solution. The

intensity of the light is proportional to the amount of HRP, which is proportional to the amount of protein in the blot.

By comparing polypeptide bands in the sample pancreatic tissue and control pancreatic tissue and estimating the size of polypeptides with the molecular weight markers, the presence of an additional higher molecular weight Kir6.2 polypeptide was determined.

2.9 MOLECULAR CLONING

The molecular cloning is a technique to assemble recombinant DNA molecules. In this project, human *KCNJ11* gene was inserted into pcDNA3.1 Zeo+ plasmid. The vector with mouse *KCNJ11* cDNA insert is commercially available. However the commercially available vector contains only the cDNA sequence of the *KCNJ11*. The patient studied had a heterozygous non-stop mutation, which resulted in insertion of an extra 94 amino acids into the Kir6.2 protein sequence. To replicate the gene sequence in in-vitro experiments, a plasmid construct with an insert of coding region and 3′ UTR sequence of *KCNJ11* in the multiple cloning site of pcDNA3.1 Zeo^{+} vector was prepared according to the following steps:

1. Designing primers with restriction enzyme sites on the ends
2. PCR amplification of the insert (cDNA of interest)
3. Gel purification
4. Double Restriction digest of the empty vector and PCR product
5. Phosphatase treatment of Recipient Plasmid Double Restriction Digest Reaction
6. PCR purification
7. Ligation
8. Transformation
9. Isolation of plasmid DNA from the bacterial cells
10. Confirmation of the cloning of the cDNA of interest in the plasmid by diagnostic restriction digest and sequencing

2.9.1 Primer Design for Cloning PCR reaction

The forward and reverse primers (oligonucleotides) were designed using the Primer3web version 4.0.0 (http://bioinfo.ut.ee/primer3/). The entire coding sequence of *KCNJ11* with flanking UTR (untranslated regulatory) sequences was pasted in the Primer3web software. The designed primers by the Prmer3web with no SNPs (single nucleotide polymorphisms) in their sequences were selected by using the SNPCheck3 software (https://secure.ngrl.org.uk/SNPCheck/snpcheck.htm;jsessionid=72BF23547E16DA70F16FDE86FE1124B3). The sequences of the forward and reverse primers are shown in table 2.7.

GCCGCCCAGGCTGCCCCACAGCAGTAGCAGGTGTTAAACTGTGCTCCTTTCCTGCCGAGG
CCTTTTTTTTTTTTTTTTTTTTTTTTTTTTTTAATGAGAGGGAGTCTGAGCTTCCATCAG
ATTGTCAAAGGATTCAAGACTAAGATTAAGAGCATCCCCCAAAGAGAAGCAGCTGCAGGT
TGAGAAGTCCTCGGACCGCCTAATTTCCGCCAGCCCTGGGATTGGTGGCGCCGCCTCTCA
GCGCCTCCTTTCCCGGGGAACCTGCAAACCTGGCGCGGCCGAGAGGCGGATTACTGACCC
AAATACGGATGGGGATATTGGGGGAGGGGAGCCAGGGCGACAGGGCGGCGGCCCCAGACT
GGGAGGGCGGGTCACAGATCCCTCCCAGCCCCCCACTTTCGTAGAGCGTGGGCAGGAGGA
ACCTCTGGGTTCCGCGGATCAGAAAAACTCCAAAGGCCGGGTTGTGAGTCCCGGGAGGGG
AGGTGGAGGGCGGGGGCGGGGAGGGGCGCGGGAGGGGCGGGGGCTTGCTCCGGCCCCGCC
CCCTGCGCTCCGGTGCAGGTCGGGCTCCCCCTGGCGGTCCCCGGCCCCGTTCCTCTCCTC
GTGCGCCCCCCTCCCGCCGTCCTAGACCCCTGCCTAGCCCAGGTCGGTCTCCGCGGACCC
ACGGACGGACAGACAGACGGGAGGACGGCCAGCCGCGAGCGCCCGGGCGGCGGGAGGGGG
CGGGGAGGCGACGGCCGTGGCGTGAGGAGCAGGAGCAGGTGCAGCGGCGGCGGCGGGCGG
GGCCGGGACCCGGCGCGGAGCGGGAGCCGCGGCGCGGGCGGGCGGCAGGGACCGGGAGGC
CGCGACTCGGAGTCAGCCCCGCCGGGTCGCGCGCAGGTCCGGGGAGCCGCGGTTGAGCCG
GGTGGGGTGGTGACTCCAGAGAACGCAGGATCCCAAGGAGACAGAGAGGACGAGAGCTGG
AGGGGGATCCGGAAAGCGGCGGGGGCGCTCCGGGAGGGGTGGAGTAGGACATAGGGGGCG
CACCTGGAGGAGAGACGGGGCGGGGGTGGCCAGGACCTGAGCTGGAGCCTGGGAGCCCGA
AGGCCAGACAGGTGAGGCGGGAGACCCGGAGGTGGGGGTGAGGTCCGGTTAGTGGGAGAG
ATCCGGAGGTGTTAAGTTCTGAGCTGGGCTGGGAAGGCAGGCTGGGCGGGGAGAAGGGCT
CTTAGCGGGAGGCCCAGGGGTGGTCAGCTGGTGGGGGAAGCTGGGGGAGGACGCAGGGCC
AGGTGGAGAGCCGGCAGGGTTGGGGGCTCCCTAGGCGCCAGGCAGGTGGGCTCAAGGGTG
AGGCTGTTTTTTTTGTTTTGTTTTTTGTTTTTGAGACGGAGTCTCGCTCTGTCGCCCAGG
CTGGAGTGCAGTGGCGTGATCTTGGCTCACTGCAACCTCCGCCTCTCGGGTTCAAGCGAT
TCTCCTGCCTCAGCTTCCTGAGTAGCTGGGATTACAGGTGCGCACCACCATGCCCGGCTA
ACTTTTGTATTTTTAGTAGAGATGGGGTTTCACCATGTTGGTCAGGCTGGTCTCGAACTC
CTGACCTAGTGATCTGCCCTCCTCAGCCTCCCAACGTACTGGGATTACAGGCGTGAGCCA
CCGCGCCCGGCCTGAGGCTGGTATTAAGAAGTGAAGTGGGACCCAGGTGGAGGTAAGGAA
GAGTCTGGTGGGGAGTTATCTCAGAAGTGAGGCCAGCACAGGCTGAGTGCAGCCCCAGGG
TGAGAAGGTGCCCACCGAGAGGACTCTGCAGTGAGGCCCTAGGCCACGTCCGAGGGGTGC
CTCCGATGGGGGAAGCCCCTCCCTGGGGGTCACCGGAGCCATGCTGTCCCGCAAGGGCAT
CATCCCCGAGGAATACGTGCTGACACGCCTGGCAGAGGACCCTGCCAAGCCCAGGTACCG
TGCCCGCCAGCGGAGGGCCCGCTTTGTGTCCAAGAAAGGCAACTGCAACGTGGCCCACAA
GAACATCCGGGAGCAGGGCCGCTTCCTGCAGGACGTGTTCACCACGCTGGTGGACCTCAA
GTGGCCACACACATTGCTCATCTTCACCATGTCCTTCCTGTGCAGCTGGCTGCTCTTCGC
CATGGCCTGGTGGCTCATCGCCTTCGCCCACGGTGACCTGGCCCCCAGCGAGGGCACTGC
TGAGCCCTGTGTCACCAGCATCCACTCCTTCTCGTCTGCCTTCCTTTTCTCCATTGAGGT
CCAAGTGACTATTGGCTTTGGGGGGCGCATGGTGACTGAGGAGTGCCCACTGGCCATCCT
GATCCTCATCGTGCAGAACATCGTGGGGCTCATGATCAACGCCATCATGCTTGGCTGCAT
CTTCATGAAGACTGCCCAAGCCCACCGCAGGGCTGAGACCCTCATCTTCAGCAAGCATGC
GGTGATCGCCCTGCGCCACGGCCGCCTCTGCTTCATGCTACGTGTGGGTGACCTCCGCAA
GAGCATGATCATCAGCGCCACCATCCACATGCAGGTGGTACGCAAGACCACCAGCCCCGA
GGGCGAGGTGGTGCCCCTCCACCAGGTGGACATCCCCATGGAGAACGGCGTGGGTGGCAA
CAGCATCTTCCTGGTGGCCCCGCTGATCATCTACCATGTCATTGATGCCAACAGCCCACT
CTACGACCTGGCACCCAGCGACCTGCACCACCACCAGGACCTCGAGATCATCGTCATCCT
GGAAGGCGTGGTGGAAACCACGGGCATCACCACCCAGGCCCGCACCTCCTACCTGGCCGA
TGAGATCCTGTGGGGCCAGCGCTTTGTGCCCATTGTAGCTGAGGAGGACGGACGTTACTC
TGTGGACTACTCCAAGTTTGGCAACACCGTCAAAGTGCCCACACCACTCTGCACGGCCCG
CCAGCTTGATGAGGACCACAGCCTACTGGAAGCTCTGACCCTCGCCTCAGCCCGCGGGCC
CCTGCGCAAGCGCAGCGTGCCCATGGCCAAGGCCAAGCCCAAGTTCAGCATCTCTCCAGA
TTCCCTGTCCTGAGCCATGGTCTCTCGGGCCCCCCACACGCGTGTGTACACACGGACCAT
GTGGTATGTAGCCCGGCCAGGGCCTGGTGTGAGGCTGGGCCAGCCTCAGCTCAGCCTCCC
CCTGCTGCTCATCCAGGGTGTTACAAGGCACTTGTCACTATGCTATTTCTGGCCTCAGCA
GGAACCTGTACTGGGTTATTTTTGTCCCTGCTCCTCCCAACCCAATTCAGGACTGGCTCA
CCCCTCTCCCCCGCCCAAGGCTGCAGAGGCTGTGGGAGGTACTGGGCCCTAGAGCTGTGC
GTCCAGCCAGTCCTGGGTCCCCACGATTGACCAGCCACACTCTGGGCCGGTGGCTGGGGA

AGAACAATCCCCGAGGGCTGCTGCTTTGCGTCTGTGGCTCCAAGAAGTGCCTGTGGTCAG
GCCCCAGCTCTACTTGGTCCCTGAAAAAGCACCTGGCTAAGGGCTGGGCCTGGCCAGCAG
GGAGGGCAGTTGATGAGAGAGGGTGTTCCCGCTGGAGGGTTGGTGCTGTGGAGCCTACAC
CGGCAGGGACAGCCTGGGGCTGACAGGGCTCCCCTCCGAGGGCCAGTTTCAGGTCTGGAA
GGGGAGGAAGCAGGGGAAGGTGACCTGAGGAGGCTCGGCTTTGTAGAGCCCCGCTCAGGC
ACAGGGAGGAGGAGATGCCAGGGCTCCTGCCTTTTGCCACATCGGCCTCGTGCAGTGAGG
GCTCTGTGGGCTGGGGCTGCTGCCCCTGCCTACCTCCTGCCTGTCCCCAGAGGCTGAGGA
GAGGGGGTACTGTGCCCACCACACATGATTAGGCCTCAGACCCAACTCTGGTCCTGGCTC
CACAACAGTGGCTGCCACTCACTTTGTCCAGAAGGTGGCTTGGGGGTGGATATCTTTGGG
TTGCTGGAAAAGGTGTGGGAAGGTTCAGGATGGTGGGAGGGACTGAGGTCCCTGAGGTGA
AGAGGCCCTTGGTCCTGACGGGTTTGACCCGTGCCTGGACCCTTGGAGCAGTGTTGTGTG
AACTTGCCTAGAACTCTGCCTTCTCCGTTGTCAATAAAGCCTCCCCCTCATGACCTAAAC
TCTGGGCTTTTCTTGCTGGGGAGGCAGCAAGCATGCTGGTGGGAAGGGAGGCAGGGACTG
GCAGCTGCCACCCCCTTCAAGAGGCGCCATAGACCCTAGCGGGGAGGGCAGGGGAGGGAC
GGAAGGCTGGCACCTCTTCCACCAGTTCAGGGGGACTTTCCCCTCTCCTGTCTCAGGTGG
CCCAGCCCTGTCAGCCTGTCTGGCCAACTCAGCCTTTGGGCACTCACCAGGCTTTGCAGC
CCTGGGCTCTGTCTCTACTCCCAGGGACCTGCTGGAAGGCTGGAGTGCCCAGGGAGAGGT
ATAGAGGTGTCATAGGCATTAGTGTAGTAATTGGAGCACTAACTCTCGAGCCAACTGCCT
GGGTTCGAATCCTGGCTCTAGCTGTATGACTTTTGTCAAGTAACTTAGCCTCTCTGTGTC
TCAGTTGCCTCTTCTATAACATGGATGCTAATAGTACCTACCTCATAGAATTGTTTTGGA
AGTAAATGAAAAATATGTAAAATGCTGAAGTGCCTGGTCTACAGTAAGTGCTCAATAAAT
GTTAACTATTGTGATTGCTGCTGAATCAGCTACATGCTGAGGAAACGGCCAAA

Figure 2.7: Sequence of human *KCNJ11* gene from Ensembl genome browser. The start and end of the coding sequence is shown by the grey highlighted sequence. The start and end of the sequence amplified with PCR for cloning into the vector is shown by red underlined sequence (included in the PCR insert). The normal stop codon is highlighted by the red font. The next stop codon in the sequence (TAG) is shown in the green font.

	Sequence
Forward Primer	TAGGATCCGCCGCCATGCTGTCCCGCAAGGGCAT
Reverse Primer	TAGAATTCCTAGGGCCCAGTACCTCCCA

Table 2.7: Sequences of the forward and reverse primers used to clone *KCNJ11* sequence into the vector pcDNA3.1 Zeo+. The recognition site sequences of type II restriction endonucleases BamH1 (from Bacillus amyloliquefaciens) and EcoR1 (from Escherichia coli) are underlined with red and green colour respectively. The sequence underlined with blue colour in the forward primer sequence is the Kozak sequence.

2.9.2 PCR Amplification Of The Region Of Interest

The coding sequence and 279 nucleotides in the 3'UTR sequence of *KCNJ11* was amplified by PCR using a high fidelity taq polymerase (Pfu Turbo DNA Polymerase). The reaction ingredients are shown in table 2.8. The reaction ingredients were mixed in 200µL PCR tubes on ice.

Ingredient	Amount per reaction (50 µL)
10X cloned Pfu reaction buffer	5.0 µL
dNTPs 10mM	1.25 µL
DNA template (100 ng/µL)	1.0 µL
Forward primer (100 ng/µL)	1.0 µL
Reverse primer (100 ng/µL)	1.0 µL
Pfu Turbo DNA Polymerase (2.5U/µL)	1.0 µL (2.5 U)
ddH_2O (Double distilled water)	39.75 µL

Table 2.8: Reaction Ingredients for Cloning PCR Reaction

Following the preparation of the reaction mixture, the DNA region of interest was amplified by running the PCR reaction. PCR is a widely used scientific technique for exponentially amplifying a small number of DNA copies by several magnitudes, ultimately producing millions of copies of a specific DNA region. PCR involves three stages described below, which are repeated in multiple cycles of heating and cooling of the DNA containing reaction mixture. With each cycle, the copies of DNA double from the previous stage. The PCR protocol used for cloning is shown in table 2.9.

Steps	Temperature	Duration	Number of cycles
Initial Denaturation	95ºC	2 minutes	1
Denaturation	95ºC	30 seconds	30
Primer Annealing	56ºC	30 seconds	
Extension	72 ºC	4 minutes	
Final Extension	72 ºC	10 minutes	1

Table 2.9: Thermocycler Settings for Cloning PCR Reaction

2.9.3 Gel Electrophoresis

Following PCR amplification, the reaction mixture was analyzed on a 1% agarose gel. The gel was made by mixing 1.5g of agarose powder with 150ml of 1X TBE (Tris Borate EDTA) in a 500 ml glass bottle. The solution was heated in a microwave till the agarose powder was completely dissolved. Ethidium bromide (3 µL) was added to the solution and the mixture is then poured into a gel tray. The gel was then allowed to solidify for 30 minutes. The gel was placed in the gel electrophoresis tank filled with TBE buffer. If required, more TBE buffer was added to ensure complete submersion of the gel in the TBE buffer. The wells in the gel were loaded with mixture of loading dye and PCR product (10 µL Loading dye and 50 µL PCR product). A DNA ladder was loaded in an adjacent well to allow identification of the size of the PCR product. A voltage of 80 volts was applied for 60 minutes to allow the

migration and separation of the DNA molecules according to their size. The gel was visualized under the UV light to identify the bands from PCR product.

2.9.4 Gel Purification of the PCR Insert

QIAquick gel extraction protocol was used for DNA extraction from the agarose gel according to the following steps:

1. The DNA fragment was excised from the agarose gel with a clean and sharp scalpel.
2. The agarose gel was weighed and three volumes of Buffer QG were added for 1 volume of gel.
3. The mixture was then incubated at 50ºC for 10 minutes to solubilize agarose completely. The colour of the mixture remained similar to the colour of Buffer QG without dissolved agarose.
4. The mixture was then transferred to QIAquick column and centrifuged at ≥10,000 × g (~13,000 rpm) for 1 minute.
5. The flow-through was discarded and QIAquick column was placed in the same collection tube and centrifuged for another 1 minute.
6. Buffer PE (750 µL) was added to the QIAquick column and centrifuged for 1 minute. The flow-through was discarded and QIAquick column was placed in the same collection tube and centrifuged for another 1 minute.
7. QIAquick column was then placed in a clean 1.5ml microcentrifuge tube. Double distilled water (ddH2O; 30 µL) was added to the center of the QIAquick membrane and allowed to stand for 1 minute before centrifuging for another 1 minute.
8. The DNA concentration in the eluate was 6ng/µL.

2.9.5 Double Restriction Enzyme Digest

Following the purification of the DNA region of insert, which had recognition sites for restriction enzymes at either ends, the next step in cloning is to set up the restriction digest of the PCR product as well as the recipient plasmid (pcDNA3.1 Zeo+). The double restriction digest was performed in a volume of 20 µL on 100ng of PCR product and 1 µg of recipient plasmid using 5 units of enzyme as shown in table 2.10.

Table 2.10: Restriction Digest Reaction

PCR product double restriction digest		**Recipient Plasmid (pcDNA3.1 Zeo+) double restriction digest**	
Reaction volume 20 µL		Reaction volume 20 µL	
Restriction Enzyme 10× Buffer	2.0 µL	Restriction Enzyme 10× Buffer	2.0 µL
Bovine Serum Albumin (BSA)	0.2 µL	Bovine Serum Albumin (BSA)	0.2 µL
EcoR1 Restriction Enzyme (10 u/ µL)	0.5 µL	EcoR1 Restriction Enzyme (10 u/ µL)	0.5 µL
BamH1 Restriction Enzyme (10 u/ µL)	0.5 µL	BamH1 Restriction Enzyme (10 u/ µL)	0.5 µL
PCR product (6ng/ µL)	16.8 µL (100ng)	Recipient Plasmid (1 µg/ µL)	1 µL (1 µg)
ddH_2O	-	ddH_2O	15.8 ddH_2O

After preparing the reactions as mentioned in the table, the reaction mixture was incubated at 37ºC for 1 hour.

2.9.6 Phosphatase treatment of Recipient Plasmid Double Restriction Digest Reaction

To avoid the problem of ligation of the ends of the recipient plasmid during the ligase reaction, the recipient plasmid restriction digest reaction was treated with Antarctic phosphatase. It catalyzes the removal of 5′ phosphate from DNA and RNA, which is required for ligation reaction. The reaction was prepared as shown in table 2.11.

Table 2.11: Antarctic Phosphatase Reaction Ingredients

Ingredient	Volume
Recipient plasmid double restriction digest reaction mixture	20 µL
Antarctic phosphatase 10× Buffer	2.5 µL
Antarctic phosphatase (5U/µL)	1 µL
ddH_2O	1.5 µL

The above reaction mixture was incubated at 37ºC for 15 minutes.

2.9.7 PCR Purification

The two reaction mixtures from the previous steps (phosphatase treatment of recipient plasmid double restriction digest and double restriction enzyme digest of PCR product) were subjected to purification to remove enzymes. The steps of the PCR purification step were as below:

1. Five volumes of Buffer PB were added to 1 volume of the reaction mixture and mixed. The colour of the mixture remained similar (yellow) to the colour of Buffer PB.
2. The above mixture was poured into the QIAquick column held in a 2ml collection tube and centrifuged at ≥10,000 × g (~13,000 rpm).
3. The flow-through was discarded and 0.75ml Buffer PE was added to the QIAquick column and centrifuged for another 1 minute.
4. After discarding the flow-through again, the QIAquick column was centrifuged once more to remove residual wash buffer (Buffer PE).
5. QIAquick column was then placed in a clean 1.5 ml microcentrifuge tube and 30 µL of ddH2O was added to the center of the QIAquick membrane. QIAquick column was centrifuged for another 1 minute after letting it stand for 1 minute.
6. The DNA concentration in the eluate from recipient plasmid reaction mixture was 23 ng/ µL and from the PCR reaction digest was 6ng/µL.

2.9.8 Ligation Reaction

The next step, after cutting the PCR product and recipient plasmid with restriction enzymes to generate the cohesive ends, is to ligate the two products together using T4 DNA Ligase. The molar ratio of recipient plasmid: PCR insert DNA in cloning can be 1:1, 1:3 or 3:1. I used 1:3 ratio of recipient plasmid: PCR insert during ligation. Typical ligation reactions use 100-200 ng of plasmid DNA and are 10µL reactions. The formula to calculate the mass of PCR insert DNA in a ligation reaction is

$$\frac{ng\ of\ plasmid \times kb\ size\ of\ insert}{kb\ size\ of\ plasmid} \times molar\ ratio\ of\ \frac{insert}{plasmid} = ng\ of\ insert$$

For 100ng of plasmid DNA, I had to use 77 ng of insert DNA according to the above formula (ng of plasmid = 100ng, kb size of insert = 1.4, kb size of the plasmid = 5.4).

$$\frac{100\ ng\ plasmid \times 1.4\ kb\ insert}{5.4\ kb\ plasmid} \times \frac{3}{1} = 77\ ng\ insert$$

However I would not have been able to fit this amount in a 10 µL reaction as the concentration of recipient plasmid and insert DNA was less. Hence I carried out the ligation reaction using 50 ng of recipient plasmid DNA.

$$\frac{50\ ng\ plasmid \times 1.4\ kb\ insert}{5.4\ kb\ plasmid} \times \frac{3}{1} = 38.5\ ng$$

The ligation reaction was prepared according to table 2.12.

Table 2.12: Ligation Reaction Ingredients

Ingredient	Volume (10 µL Reaction)
Recipient plasmid DNA (23ng/µL)	2.2 µL (50 ng)
PCR Insert DNA (6ng/ µL)	6.4 µL (38.5 µL)
Ligase 10× Buffer	1 µL
T4 DNA Ligase (3U/ µL)	0.4 µL (1.2U)

The ligation reaction mixture was incubated at room temperature for 3 hours and then chilled on ice. This was followed by transformation of 5 µL of the reaction mixture into competent cells.

2.9.9 Transformation

The ligation reaction mixture (5 μL) was transformed into AG1 competent cells. AG1 competent cells are high transformation efficiency derivatives of DH1 cells. The transformation protocol used is described below:

1. Two 14-ml BD Falcon polypropylene round-bottom tubes were pre-chilled on ice. SOC medium was kept on the heat block set at 42ºC.
2. AG1 cells were removed from -80ºC storage and thawed on ice. The cells (100 μL) were aliquoted into the pre-chilled round-bottom tubes.
3. The β-mercaptoethanol (β-ME) reagent (1.7 μL) was added to each aliquot of cells. β-ME increases the transformation efficiency.
4. The tubes were gently swirled every 2 minutes for a total of 10 minutes while on ice.
5. The ligation reaction mixture (5 μL) was added to one aliquot of cells. The pUC18 control plasmid (1 μL) was added to the other aliquot as a control for transformation efficacy.
6. The tubes were gently swirled and then incubated on ice for another 30 minutes.
7. The tubes were submerged in the 42ºC water bath for 45 seconds. The duration of this step is critical as optimal transformation efficiency is observed when cells are heat-pulsed for 45-50 seconds.
8. Following the heat-pulse, the tubes were immediately incubated on ice for 2 minutes.
9. Preheated SOC medium (0.9 ml; from step 1) was added to each tube. The tubes were then incubated at 37ºC for 1 hour with shaking at 225-250 rpm.

10. The transformation mixture was plated on LB-ampicillin agar plates. Different volumes (50 µL, 100 µL and 200 µL) of the transformation mixture were plated on each LB-ampicillin agar plate used. For the pUC18 control transformation, 5 µL of the transformation mixture was plated on the LB-ampicillin agar plate.
11. The plates were incubated overnight at 37ºC.
12. Approximately 100 colonies were noticed on the LB-ampicillin agar plate used for plating ligation reaction transformation mixture.

2.9.10 Starter Cultures and Miniprep

Eight colonies were picked from the ligation-reaction transformation mixture plated agar plate with sterile pipette tips. Each colony was transferred into a 15 ml falcon containing 3-5 ml of autoclaved LB media with ampicillin at a concentration of 50µg/mL. These starter cultures were incubated at 37ºC overnight with shaking at 225-250 rpm.

The following morning, a miniprep was carried out on all the successful overnight starter cultures (turbid looking LB media due to growth of bacteria containing plasmid for antibiotic resistance) using the QIAprep Spin Miniprep Kit (Qiagen). This technique purifies plasmid DNA and the procedure is based on alkaline lysis of bacterial cells followed by adsorption of DNA onto silica in the presence of high salt. Bacteria are lysed under alkaline conditions, and the lysate is subsequently neutralized and adjusted to high-salt binding conditions, ready for purification on the QIAprep silica-gel membrane. The optimized buffers in the lysis procedure combined

with the unique silica-gel membrane ensure that only DNA will be adsorbed, while RNA, cellular proteins, and metabolites are not retained on the membrane but are found in the flow-through. Salts are efficiently removed by a brief wash step with Buffer PE. High-quality plasmid DNA is then eluted from the QIAprep column with Buffer EB or water.

2.9.11 Diagnostic Restriction Digest

Following isolation of plasmid DNA, a diagnostic restriction digest was performed with an endonuclease EcoN1 (isolated from E.coli) to confirm the cloning of *KCNJ11* into pcDNA3.1 Zeo+ vector. EcoN1 is predicted to cut the plasmid, pcDNA3.1 Zeo+ with *KCNJ11* insert between BamH1 and EcoR1 recognition sites, at two positions and generate two fragments of sizes 648 bp and 6221 bp. The gel image of the diagnostic restriction digest is shown in figure.

2.9.12 Verification of Plasmid by Sequencing

As PCR based cloning carries the risk of insertion of mutations depending on the fidelity of DNA polymerase used, the entire *KCNJ11* insert in the vector pcDNA3.1 Zeo+ was sequenced to confirm no mutations have been inserted by error. The sequences of the oligonucleotides used to sequence the insert are shown in the table.

Table 2.13: Primers Sequence for Sequencing of *KCNJ11* insert in pcDNA3.1 vector

Oligonucleotide	Sequence
T7 Promoter	*TAATACGACTCACTATAGG*
***KCNJ11*_F**	*TACTGGAAGCTCTGACCCTC*
***KCNJ11*_R**	*TGCCTTGTAACACCCTGGAT*
BGH Reverse	*TAGAAGGCACAGTCGAGG*

2.10 SITE DIRECTED MUTAGENESIS

In vitro site-directed mutagenesis is an invaluable technique for carrying out vector modification. QuikChange Site-Directed Mutagenesis Kit allows site-specific mutagenesis in double-stranded DNA (dsDNA) plasmid. It can be used to make point mutations, deletions and insertions with greater than 80% efficiency.

Principle:

The basic principle of this technique is that two synthetic oligonucleotide primers containing the desired mutation are designed, which will anneal to the complementary strands of the double-stranded DNA (dsDNA) vector. These primers will then be extended by a high fidelity DNA polymerase (*PfuTurbo* DNA Polymerase) in a temperature cycler. This extension will result in incorporation of the oligonucleotide primers, which carried the mutation, in the dsDNA vector. Subsequent treatment with a specific endonuclease, *Dpn* I, will digest the parental DNA template and leave behind the mutated synthesized nicked DNA vector. The final step is transformation of the mutated DNA vector in the XL1-Blue supercompetent cells.

The steps are described in more details below:

2.10.1 Alignment of human and hamster *ABCC8* sequence

For studying *ABCC8* mutation, the plasmid pcDNA3.1 Zeo+ with inserted hamster *ABCC8* sequence was used. To identify the corresponding position of the mutation identified in my patient in the hamster SUR1 sequence, the human *ABCC8* cDNA sequence was aligned with the hamster SUR1 *ABCC8* sequence (*Cricetus cricetus*) using the Clustal programme.

For *KCNJ11* and *KCNK17* mutations identified in the patients studied in this thesis, the plasmids with human clone were used. The plasmid containing *KCNJ11* was constructed as explained above, whereas the *KCNK17* plasmid was purchased from Thermofisher Scientific Biosciences.

2.10.2 Mutagenic Primer Design

The mutagenic primers were designed according to the following guidelines from the QuikChange Site-Directed Mutagenesis Kit.

1. Both of the mutagenic primers must contained the desired mutation and anneal to the same sequence on opposite strands of the plasmid.
2. Primers should be between 25 and 45 bases in length.
3. Melting temperature (T_m) of the primers as estimated by the following formula should be ≥78ºC.

$$Tm = 81.5 + 0.41(\%GC) - \frac{675}{N} - \%\, mismatch$$

N is the primer length in bases

%GC and % mismatch must be whole numbers

4. For primers designed to introduce insertions or deletions, the following formula should be used.

$$Tm = 81.5 + 0.41(\%GC) - 675/N$$

N does not include the bases, which are being inserted or deleted

5. The desired mutation should be in the middle of the primer with ~10-15 bases of correct sequence on both sides
6. Optimally, the primers should have a minimum GC content of 40% and should terminate in one or more C or G bases.

The mutagenic primers were ordered from *Sigma Aldrich* and were supplied in a lyophilized form. The primers were dissolved in appropriate volume to ddH_2O to prepare a stock solution of 100 µM. The working primer solution (5 µM) was prepared by diluting 10 µL of the primer stock solution with 190 µL of ddH_2O. The stock solution was stored at -20ºC and the working solution at 4ºC.

The sequences of the mutagenic primers used to insert mutations are shown in table 2.14.

Mutagenic Primers	Primer Sequence
***KCNJ11*_Primer 1**	CTCTCCAGATTCCCTGTCCCGAGCCATGGTCTCTCGGG
***KCNJ11*_Primer 2**	CCCGAGAGACCATGGCTCGGGACAGGGAATCTGGAGAG
***KCNK17*_Primer 1**	GCTCGTGGGCTCCTTCTTTTCTGTGTCCACCATCAC
***KCNK17*_Primer 2**	GTGATGGTGGACACAGAAAAGAAGGAGCCCACGAGC
***KCNG2*_Primer 1**	CAAGGAGCAGCAGCAGCGCGTGGCCAGCCCCGAGCCGGC
***KCNG2*_Primer 2**	GCCGGCTCGGGGCTGGCCACGCGCTGCTGCTGCTCCTTG
***ABCC8*_Primer 1**	CCTCCATCGACATGGCTATGGAGAACATCCTCCAGAAG
***ABCC8*_Primer 2**	CTTCTGGAGGATGTTCTCCATAGCCATGTCGATGGAGG

Table 2.14: Mutagenic Primers used to insert mutations in the genes carried in the vector

2.10.3 Site-Directed Mutagenesis (SDM) Reaction

The SDM reaction was prepared on ice in thin-walled PCR tubes utilizing the designed mutagenic primers and the double-stranded DNA vector containing the wild-type gene as shown in table 2.15.

Table 2.15: SDM Reaction Preparation

Reagent	Amount
10× Reaction Buffer	5 µL
dsDNA template	50 ng (volume varied with the concentration)
Oligonucleotide Primer #1	125 ng
Oligonucleotide Primer #2	125 ng
dNTP mix	1 µL
ddH_2O	To a final volume of 50 µL
***PfuTurbo* DNA Polymerase (2.5 U/ µL)**	1 µL

After preparing the SDM reaction, it was cycled 16 times in a thermal cycler according to the settings shown in table 2.16.

Segment	Cycles	Temperature	Time
1	1	95ºC	30 seconds
2	16	95ºC	30 seconds
		55ºC	1 minute
		68ºC	1 minute/kb of plasmid length

Table 2.16: Thermocycler Settings for QuikChange SDM Method

2.10.4 Digestion

After the thermal cycling, the SDM reaction was placed on ice for 2 minutes. To the 50 μL of the reaction mixture, *Dpn* I restriction enzyme (1 μL; 10 u/μL) was added and mixed thoroughly first by pipetting and then spinning the mixture in a microcentrifuge for 1 minute. The reactions were then incubated at 37ºC for 1 hour. *Dpn* I restriction enzyme digests the methylated parental DNA and leaves behind the mutation-containing synthesized DNA.

2.10.5 Transformation

The next step is to transform the XL1-Blue Supercompetent cells with the *Dpn* I digested SDM reaction. The supercompetent cells are gently thawed on ice and aliquoted (50 μL) into prechilled 14-ml BD Falcon polypropylene round-bottom tubes. The *Dpn* I treated SDM reaction (1-4 μL) was transferred into an aliquot of supercompetent cells. The reaction mixture is gently swirled and incubated on ice for 30 minutes. After 30 minutes, the transformation reactions were heat-pulsed for 45 seconds by immersing the round-bottom tubes in 42ºC water bath. The reactions were then placed on ice for 2 minutes and 900 μL of preheated SOC medium (42ºC) was added. Afterwards, the reaction mixtures were incubated at 37ºC for 1 hour with shaking at 225-250 rpm.

2.10.6 Inoculating Agar Plates

The LB-ampicillin agar plates were plated with varying volumes of the transformation reaction mixture. The transformation mixture was pipetted on the LB-ampicillin agar plates and was spread with a sterile glass spreader. The plates were air-dried for 5-10 minutes and then incubated upside down in an incubator at 37ºC for >16 hours.

2.10.7 Starter Cultures and Mini Prep

Colonies were picked with sterile pipette tips and inoculated into 15 ml falcons containing 3-5 ml of autoclaved LB media with ampicillin at a concentration of 50µg/mL. These starter cultures were incubated at 37ºC overnight with shaking at 225-250 rpm. A mini prep was carried out on all the successful starter cultures as described above under the technique of molecular cloning.

2.10.8 Sequencing

After the isolation of plasmid DNA using the miniprep technique, sequencing was performed to confirm the insertion of the mutation in the plasmid as well as to ensure no mutations at other sites in the gene of interest have been generated during thermal cycling. The sequences of the primers used for sequencing the entire gene are shown in table 2.17.

Table 2.17: Primers Sequence for sequencing of the entire gene insert in the vector

Primers	**Sequence**
pCMV-SPORT6-*KCNK17* vector	
*KCNK17*_attB1	ACAAGTTTGTACAAAAAAGCAGG
*KCNK17*_T7 Promoter	AATACGACTCACTATAGGG
*KCNK17*_1F	CTTCCAGCGCGACAAGTG
*KCNK17*_1R	AAAGAAGAAGGAGCCCACGA
*KCNK17*_2F	CCGCCTCTTCTGCATCTTCT
*KCNK17*_2R	CTGGGAGGGGTTCATTCCAA

Primers	Sequence
pCMV-XL4-*KCNG2* vector	
*KCNG2*_VP1.5	GGACTTTCCAAAATGTCG
*KCNG2*_XL39	ATTAGGACAAGGCTGGTGGG
*KCNG2*_1F	GAGTTCTTCTTCGACCGCAG
*KCNG2*_1R	GGTCTCCAGCACGAACAGG
*KCNG2*_2F	CGTGTCCGTGTCCTTCGT
*KCNG2*_2R	AGGTGTGGAAGATGGAGGTG
*KCNG2*_Reverse	TCAGCGCCCTGCCCGCACCC
pcDNA3.1-*KCNJ11* vector	
*KCNJ11*_T7 Promoter	AATACGACTCACTATAGGG
*KCNJ11*_BGH reverse	TAGAAGGCACAGTCGAGG
*KCNJ11*_F	TACTGGAAGCTCTGACCCTC
*KCNJ11*_R	TGCCTTGTAACACCCTGGAT
pcDNA3.1-*ABCC8* vector	
ABCC8 cDNA_1F	ATGCCCTTGGCCTTCTGCGG
ABCC8 cDNA_1R	CACACAAGGACGAAGAGCAA
ABCC8 cDNA_1F′	CCTCAACAACGGCTGCTT
ABCC8 cDNA_1R′	ATGTTGCTGCTTGTGGAGGT
ABCC8 cDNA_2F	GGGCTTCTGGTGATCCTGTA
ABCC8 cDNA_2R	ATCCCAAAGATGCAGAGTGG
ABCC8 cDNA_3F	TGATCCTCAGCAGCACATTC
ABCC8 cDNA_3R	CACGCCCACAATGATCTGTA
ABCC8 cDNA_3.1F	CTTTCTGTGCCCAAACCTCT

Primers	Sequence
ABCC8 cDNA_3.1F	CTCCCACGCATACAGTTTGA
ABCC8 cDNA_4F	TGAAGCAGACCAACGAGATG
ABCC8 cDNA_4R	CCGATGATCTGGACACAGAA
Covers_G716D_F	GGTTGTGAACCGCAAACG
Covers_G716D_R	TGGTTTCTGAGATGCGTAGG
ABCC8 cDNA_5F	CAGGACCAAGAGCTGGAGAA
ABCC8 cDNA_5R	CACGGGTGTGACATAGGAGA
ABCC8 cDNA_6F	TCGGATATCAGGAGCAGAGG
ABCC8 cDNA_6R	TGAGATGGCTCTGAGGCTTT
ABCC8 cDNA_7F	ATGCCTTGATGGTCTCCAAC
ABCC8 cDNA_7R	GCAGATCCCGATCTTCTGC
ABCC8 cDNA_7F′	CCCCCATGAGGTTCTTTGA
ABCC8 cDNA_7R′	CAGGTTCCTCACCATCCAGT
ABCC8 cDNA_8F	CGTGAGGAAGACCAGCATCT
ABCC8 cDNA_8R	CTGTCCTTCTGGCTGAGGAG
ABCC8 cDNA_8F′	GAAGCATGTCAACACCCTCA
ABCC8 cDNA_8R′	CAGGATAGCACCCCTCTTGA

2.10.9 Transformation into AG1 Competent Cells

After the confirmation of the sequence of the insert in the vector, the plasmid DNA obtained after the mini prep step was transformed into AG1 competent cells according to the steps explained under the technique of molecular cloning.

2.10.10 Maxi-prep

Endo-Free Plasmid Maxi Kit (Qiagen) was used to perform maxi-preps after retransformation according to the manufacturer's instructions. This technique is based on the principle of alkaline lysis of the bacterial cells followed by binding of the plasmid DNA to Qiagen Anion-Exchange Resin under appropriate low salt and pH conditions. Plasmid DNA is eluted in a high-salt buffer and then concentrated and desalted by isopropanol precipitation. This technique can yield up to 500 μg of plasmid DNA ready for transfection.

Chapter 3

CLINICAL ASPECTS AND WHOLE-EXOME SEQUENCING RESULTS OF THE PATIENTS

3.1. RECRUITING PATIENTS WITH CONGENITAL HH

A cohort of 12 patients from 9 families was recruited into this project during the three years, based on their characteristic clinical phenotype. All patients were being managed by Professor Khalid Hussain at Great Ormond Street Hospital NHS Trust, London. Personal data (name, date of birth, gender and ethnic background) and detailed phenotypic data were collected on these patients. The phenotypic information included clinical information (age at presentation, birth weight, gestational age, presenting symptoms, family history of hypoglycaemia/diabetes mellitus, and consanguinity, and responsiveness to diazoxide) and biochemical information (results of controlled diagnostic fast and protein loading test). Information on histology was collected if the patient required pancreatectomy for management of HH. Eight patients have had molecular genetic testing done for *ABCC8*, *KCNJ11*, *HNF4A* and *GLUD1* at University of Exeter Medical School, Exeter and were negative for mutations in known genes associated with the clinical phenotype.

One patient had not undergone molecular genetic testing but had a unique phenotype. Another three patients recruited in this project were found to have novel heterozygous K_{ATP} channel mutations. Two second-degree cousins had an *ABCC8* mutation and one patient had a *KCNJ11* mutation.

3.2 ETHICS

Ethical approval was obtained for this study (R&D ID: 06BC06) from the ethical committee of Great Ormond Street Hospital and UCL Institute of Child Health.

FAMILY A

3.3 CLINICAL INFORMATION (FAMILY A)

This Caucasian non-consanguineous family had two maternal half-sisters with congenital HH. The pedigree of this family is shown in figure 3.1. The elder sister was born at term gestation with a birth weight of 4500g. She presented with hypoglycaemic seizures at 1 year of age and investigations confirmed HH. She was commenced on diazoxide to which she was unresponsive. Blood glucose profile and controlled fasting studies on diazoxide revealed persistent hypoglycaemia with inappropriately elevated serum insulin concentrations. Management with regular daytime feeds and continuous overnight feeds along with maximum doses of Octreotide (30 micrograms/kg/day in 4 divided doses) was unsuccessful. In view of suboptimal control with medical management, she underwent near-total pancreatectomy at the age of 4 years and 8 months. Histological examination of the pancreatic tissue confirmed diffuse disease.

The younger sister, aged 2 years, presented in the neonatal period with severe hypoglycaemia. She was born by emergency LSCS at 37^{+6} weeks of gestation with a birth weight of 4195 grams. She required high glucose infusion to maintain stable blood glucose (≥3.5mmol/l). Investigations confirmed HH. She showed a good response (defined as age appropriate fasting tolerance with no episodes of hypoglycaemia) to diazoxide (5 mg/kg/d) in the initial few months after diagnosis. However with increasing age, she required increased doses of diazoxide in view of recurrent hypoglycaemia on blood glucose profile.

The mother also suffered from hypoglycaemia in infancy and developed diabetes mellitus in her early 30's.

Figure 3.1: Pedigree of Family A. The two affected probands are maternal half-sisters

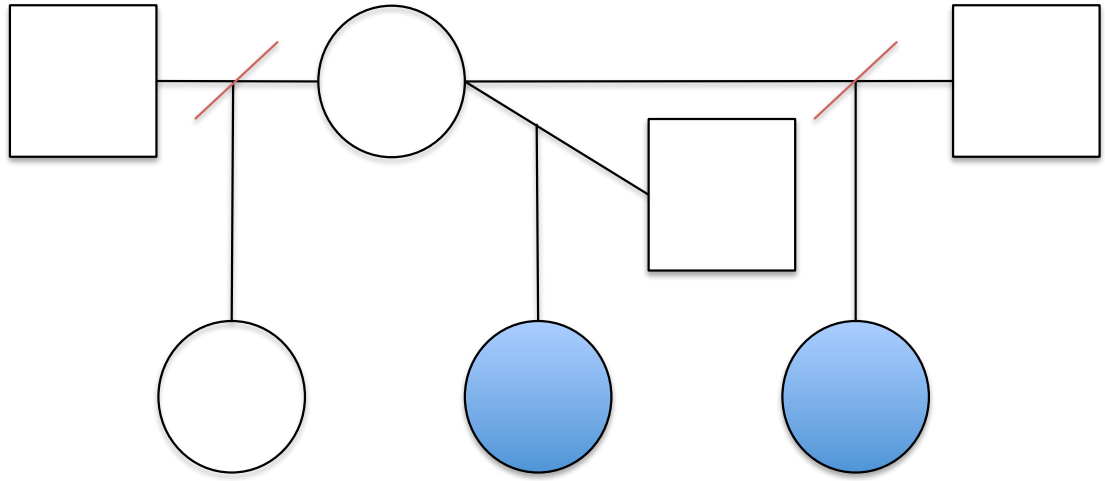

The results of the controlled diagnostic fast of the two affected siblings are shown in table 3.1.

Table 3.1: Controlled Diagnostic Fast of the affected patients (Family A)

Investigation	Patient 1	Patient 2	Normal Reference
Blood glucose (mmol/l)	3.1	2.7	3.5 – 5.5
Serum Insulin (mU/l)	2.9	19.4	< 2 mU/l in the presence of hypoglycaemia
C-peptide (pmol/l)		432	<94 pmol/l in the presence of hypoglycaemia
Non-esterified fatty acids (mmol/l)	0.9		0.84 – 2.74
β-hydroxybutyrate (mmol/l)	0.77		0.22 – 2.34
Ammonia (mmol/l)	27		< 40
Lactate (mmol/l)	1.05		0.7 – 2.1
Plasma Cortisol (nmol/l)	353	221	
Carnitine profile	Normal		
Plasma amino acids	Normal		
Urine organic acids	Normal		

3.4 WHOLE-EXOME SEQUENCING RESULTS (FAMILY A)

In this family, whole-exome sequencing was performed on the mother and her three children (two affected and one unaffected). Assuming a dominant inheritance pattern, filters were applied to whole-exome data as shown in figure 3.2.

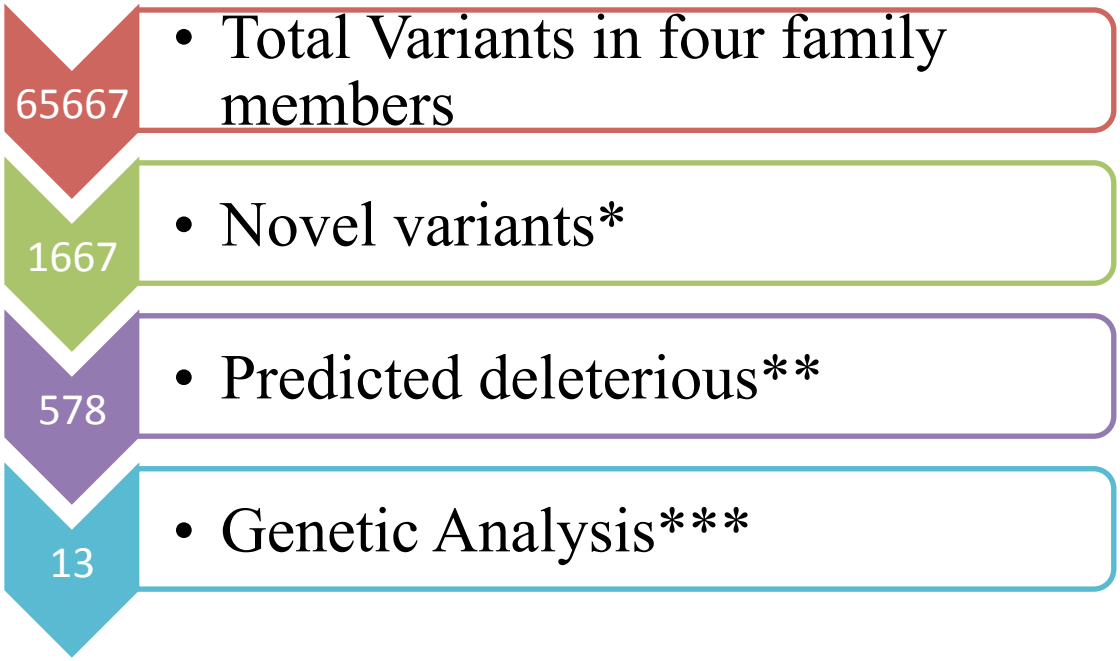

Figure 3.2: Dominant Variant Analysis of Whole-Exome Sequencing Data of Family A (*Novel variants include variants present in at least 1% minor allele frequency in 1000 Genomes Project, Complete Genomics genomes and NHLBI ESP exomes excluded; ** Predicted deleterious variants included variants which were non-synonymous coding, splice site, frameshift, stop gain; *** Variants present in heterozygous state in affected siblings and mother and not present in unaffected sibling)

The potential candidate gene variants and their locations in family A are shown in table 3.2

Table 3.2: List Of Genes With Novel, Predicted Deleterious Variants In Heterozygous State Shared Between Mother And Two Affected Siblings, And Not Present In Unaffected Sibling (Family A)

Gene	Chromosome	Position	Protein Variant
KCNN3	1	154842199	p.Q77_Q80dup
APOB	1	21229265	p.I3492T
PRSS56	2	233386683	p.P87Aa
SH3TC2	5	148389857	p.R1101fs*15
RABL6	9	139728262	p.G266R
ZEB1	10	31810733	p.P757S
CCDC33	15	74564056	p.G187R
EFTUD1	15	82532853	p.P141L
POLG	15	89876827	p.Q54_Q55dup
RNF135	17	29325810	p.Q301fs*34
TRIM25	17	54991137	p.N71K
WDR62	19	36558261	p.F206del
LMTK3	19	49001897	p.G839A

A brief description of these genes is presented next. From the available biological information about these genes, the phenotype of HH could not be explained with variations in these genes.

***KCNN3 (*Potassium channel, Calcium activated, intermediate/small conductance, subfamily N, member 3)**

These channels are responsible for afterhyperpolarization phase in vertebrate neurons (Kohler et al., 1996). In situ hybridization studies have shown wide expression of mRNA encoding these channels in rat brain. By experimental silencing of *KCNN3* gene, no overt phenotype was seen whereas overexpression induced abnormal respirations in response to hypoxia as well as compromised parturition (Bond et al., 2000).

***APOB* (Apolipoprotein B)**

Apolipoprotein B is the main lipoprotein on chylomicrons and low density lipoproteins (LDLs). Allelic variants in *APOB* have been associated with the phenotype of hypercholesterolemia and hypobetalipoproteinemia (Linton et al., 1993, Soria et al., 1989).

***PRSS56* (Protease, Serine, 56)**

Mutations in *PRSS56* gene have been associated with an autosomal recessive condition, isolated posterior micropthalmos (Gal et al., 2011).

***SH3TC2* (SH3 Domain and Tetratricopeptide Repeat Domain 2)**

Mutations in *SH3TC2* are linked with Charcot-Marie-Tooth disease, type 4C (Senderek et al., 2003).

***RABL6* (Partner of ARF)**

RABL6 encodes for a 729-amino acid human protein, which has an N-terminal GTP-binding domain, followed by a RAB-like domain, 2 proline-rich sequences, and a C-terminal nuclear localization signal (Tompkins et al., 2006). This has been shown to bind p19 (ARF) isoform of CDKN2A in in-vitro and in-vivo binding assays. The knockdown of *RABL6* function resulted in increased cell proliferation (Tompkins et al., 2006).

***ZEB1* (Zinc finger E box-binding homeobox 1)**

Heterozygous mutations in *ZEB1* have been reported in association with a phenotype of Fuch's endothelial corneal dystrophy (Krafchak et al., 2005).

***CCDC33* (Coiled-coil domain containing 33)**

CCDC33 protein contains 3 coiled-coil domains, a C2-domain, 2 ER membrane retention signal-like motifs and 2 putative peroxisomal targeting signals type 2 (Kaczmarek et al., 2009). Its expression was predominantly seen in the testis in mouse model (Kaczmarek et al., 2009).

***EFTUD1* (Elongation factor Tu GTP binding domain containing 1)**

The protein encoded by *EFTUD1* has a role in the biogenesis of the 60S ribosomal subunit as well as in the translational activation of the ribosomes (Finch et al., 2011).

***POLG* (Polymerase, DNA, Gamma)**

Mutations in *POLG* are associated with phenotypes of mitochondrial DNA depletion syndrome and progressive external ophthalmoplegia (Naviaux and Nguyen, 2004, Schulte et al., 2009).

***RNF135* (Ring finger protein 135)**

Mutations in *RNF135* have been reported in association with a phenotype of macrocephaly, macrosomia and facial dysmorphism syndrome (Douglas et al., 2007).

***TRIM25* (Tripartite Motif-containing protein 25)**

TRIM25 encodes a RING-finger dependent ubiquitin ligase (E3), also known as estrogen-responsive finger protein (EFP). EFP is essential for the normal estrogen-induced cell proliferation as evidenced by significant underdeveloped uterus in EFP-/- mice (Orimo et al., 1999). Loss of EFP function in mouse embryonic fibroblasts has been shown to lead to increased levels of a negative cell cycle regulator, 14-3-3-sigma explaining tumors generated by EFP-overexpressing breast cancer MCF7 cells in ovariectomized athymic mice in the absence of estrogen (Urano et al., 2002).

***WDR62* (WD Repeat-containing protein 62)**

Mutations in *WDR62* are associated with a phenotype of primary autosomal recessive microcephaly (Bilguvar et al., 2010).

***LMTK3* (Lemur tyrosine kinase 3)**

LMTK3, a member of LMTK family of protein kinases, is predominantly expressed in brain. *LMTK3(-/-)* mice display pronounced locomotor hyperactivity, reduced anxiety and decreased depression, along with increased dopamine turnover in the striata, as compared to the wild-type control mice (Inoue et al., 2014).

FAMILIES B, C, G and H

(PROTEIN SENSITIVE HH)

3.5 CLINICAL INFORMATION (FAMILY B)

Proband B presented at 1year and 7 months of age with 9 months history of vacant episodes associated with floppiness. Initial investigations performed in local hospital suggested HH. She was born at 41^{+4} weeks of gestation weighing 3430g. She is the second child of non-consanguineous parents, with an unaffected older brother aged 10 years. The pedigree of the family B is shown in figure 3.3.

On controlled diagnostic fast at initial presentation, she developed hypoglycaemia at ~10 hours. At the time of hypoglycaemia, she had appropriately suppressed serum insulin with appropriate mobilization of free fatty acids and β-hydroxybutyrate (Table 3.3). Investigations for other causes of hypoglycaemia (cortisol insufficiency, glycogen storage diseases) were non-contributory.

She was further investigated with oral protein loading test. Following a fast for 4 hours, oral protein load (1.5g/kg body weight) was given in the form of a standard protein powder (*Vitalopro*) dissolved in water. Serum insulin and blood glucose investigations were performed at -30, 0, +30 and +60 minutes. As is evident from table 3.4, she demonstrated HH at +60 minutes. She responded well to diazoxide treatment and did not have further vacant episodes.

Molecular genetic analysis for *ABCC8*, *KCNJ11* and *GLUD1* did not identify any mutation.

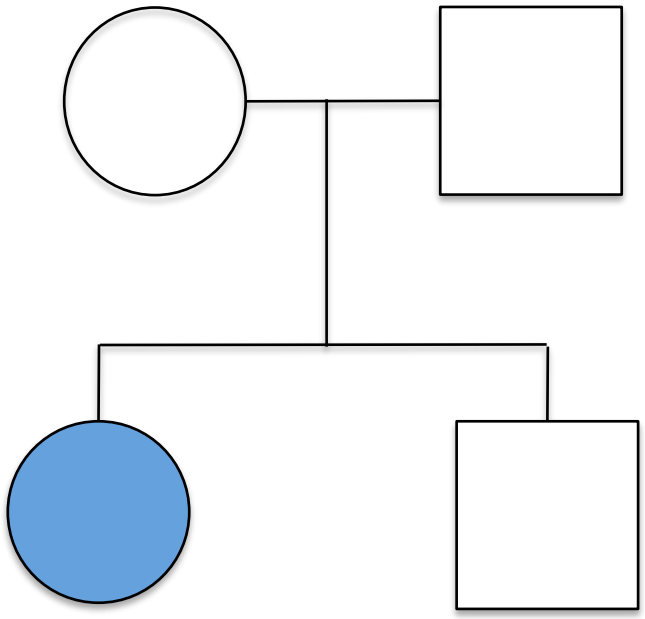

Figure 3.3: The pedigree chart of Family B

Table 3.3: Controlled Diagnostic Fast (Proband B)

Investigations	Start of Fast	End of Fast
Blood glucose (mmol/L)	3.2	2.2
Serum Insulin (mU/L)	4.7	<2.0
Non-esterified free fatty acids (mmol/L)	0.19	1.39
β-hydroxybutyrate (mmol/L)	<0.05	1.45
Lactate (mmol/L)	0.9	
Cortisol (nmol/L)	205	214
Growth hormone (µg/L)	0.2	0.8
Ammonia (mmol/L)	2	

Table 3.4: Protein Load Test (Family B)

	Before diazoxide		On diazoxide	
Time (min)	Glucose (mmol/l)	Insulin (mU/l)	Glucose (mmol/l)	Insulin (mU/l)
-30	3.0	<2.0		
0	2.7	<2.0	4.1	<2.0
+30	2.9	<2.0	3.8	<2.0
+60	2.1	3.8	3.1	<2.0

3.6 CLINICAL INFORMATION (FAMILY C)

Proband C presented with recurrent episodes of vacant staring and floppiness at 4 months of age. She was born to non-consanguineous parents after normal pregnancy and delivery (Figure 3.4). Her development was normal. MRI brain and EEG were normal. Antiepileptic treatment with sodium valproate showed no response. Further investigations confirmed the diagnosis of HH (Table 3.5). Her glucagon stimulation test evidently shows presence of stored liver glycogen, which was not released because of hyperinsulinism despite development of hypoglycaemia. Her serum ammonia repeated was normal. Molecular genetic testing for *ABCC8*, *KCNJ11*, *GLUD1* and *GCK* was negative.

Table 3.5: Controlled Diagnostic Fast and Glucagon stimulation test (Proband C)

Investigation	Results
Blood glucose	1.4 mmol/L
Serum Insulin	10.8 mU/L
Non-esterified fatty acids	0.14 mmol/L
Beta-hydroxybutyrate	<0.05 mmol/L
Glucagon stimulation test	
Blood glucose before Glucagon	1 mmol/L
Blood glucose after 30 minutes	4 mmol/L

Protein load test confirmed protein sensitive HH. The results of the protein load test are shown in table 3.6.

Table 3.6: Protein Load Test (Proband C)

Time (min)	Blood glucose (mmol/l)	Serum Insulin (mU/l)
0	4.3	4.6
30	3.4	44.2
60	2.8	31.8
90	2.9	30.9
120	3.1	30.4

Figure 3.4: The pedigree chart of Family C:

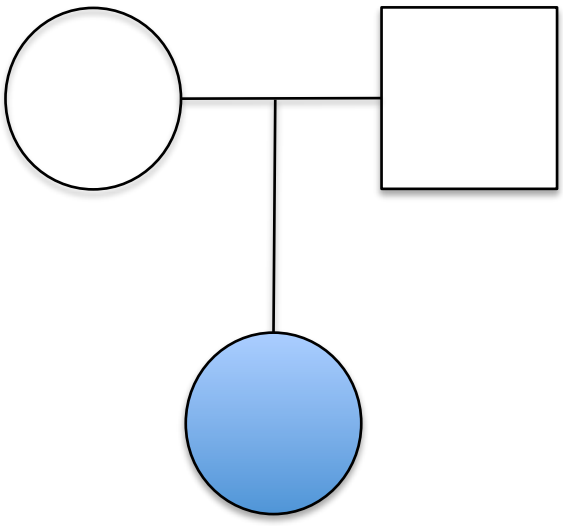

3.7 CLINICAL INFORMATION (FAMILY G)

Proband G was born at a gestational age of 38 weeks with a birth weight of 2800 grams to non-consanguineous Caucasian parents. There was no documented history of hypoglycaemia in the neonatal period. He presented at the age of 8 months with generalized tonic-clonic convulsion associated with hypoglycaemia. Investigations revealed a varying fasting tolerance. The results of one of the controlled diagnostic fast are shown in table 3.7.

Table 3.7: Controlled diagnostic Fast (Proband G)

Investigation	Result
Blood Glucose (mmol/L)	1.8
Serum Insulin (mU/L)	<2.0
C-peptide (pmol/L)	<94
Serum Cortisol (nmol/L)	212
Serum Growth hormone (ng/mL)	0.3
Non-esterified fatty acids (mmol/L)	1.26
Beta-hydroxybutyrate (mmol/L)	0.11
Serum Ammonia (mmol/L)	23
Serum Lactate (mmol/L)	1.1
Plasma Amino acids	Normal
Urine Organic acids	Normal
Serum Carnitine profile	Normal

The results of Protein load test with 1.5g/kg of *Maxipro* are shown in table 3.8.

Table 3.8: Protein Load test (Proband G)

Time (minutes)	Blood Glucose (mmol/L)	Serum Insulin (mU/L)
-30	3.4	2.6
0	4.2	2.4
+30	3.4	12.5
+60	3.0	14.2
+90	2.8	14.8

He was commenced on Diazoxide (5mg/kg/day). Following the commencement of diazoxide, he was able to fast appropriately for his age with no episodes of random hypoglycaemia. Sequencing of *ABCC8, KCNJ11, GLUD1* and *HADH* genes was normal. At the age of 4 ½ years, the proband continues to show protein sensitive HH and is being successfully managed with a small dose of diazoxide.

3.8 CLINICAL INFORMATION (FAMILY H)

The proband in family H was born at term gestation to Caucasian non-consanguineous parents with a birth weight of 3600g. He presented with history of recurrent episodes of floppiness, unresponsiveness, jerking of limbs and sweating. During one of these episodes, his blood glucose was recorded as low (1.1mmol/L). On controlled provocation fast, there was no obvious cause for hypoglycaemia. The results of controlled provocation fast are shown in table 3.9.

Table 3.9: Controlled Diagnostic Fast (Proband H)

Investigation	Result
Blood Glucose (mmol/L)	2.4
Serum Insulin (mU/L)	<2.0
C-peptide (pmol/L)	<94
Serum Cortisol (nmol/L)	469
Serum Growth hormone (ng/mL)	0.3
Non-esterified fatty acids (mmol/L)	1.96
Beta-hydroxybutyrate (mmol/L)	0.66
Serum Ammonia (mmol/L)	23
Serum Lactate (mmol/L)	1.1
Plasma Amino acids	Normal
Urine Organic acids	Normal
Serum Carnitine profile	Normal

Further investigations with protein loading test confirmed the diagnosis of protein sensitive HH. The results of protein loading test are shown in table 3.10

Table 3.10: Protein Load Test (Proband H)

Time (minutes)	Blood Glucose (mmol/L)	Serum Insulin (mU/L)
-30	3.5	<2.0
0	3.7	4.3
+30	3.2	56.5
+60	1.5	53.5

He showed remarkable clinical improvement with diazoxide (10mg/kg/day). Sequencing of *ABCC8, KCNJ11, GLUD1* and *HADH* genes was normal.

3.9 WHOLE-EXOME SEQUENCING RESULTS FAMILIES B, C, G AND H (PROTEIN SENSITIVE HH)

Whole-Exome sequencing was performed on the probands (4), their unaffected parents (8) and siblings (1).

3.9.1 Recessive Inheritance Analysis

Assuming a recessive inheritance, the filtering strategy applied to whole-exome sequencing data on four probands with protein sensitive HH is shown in figure 3.5.

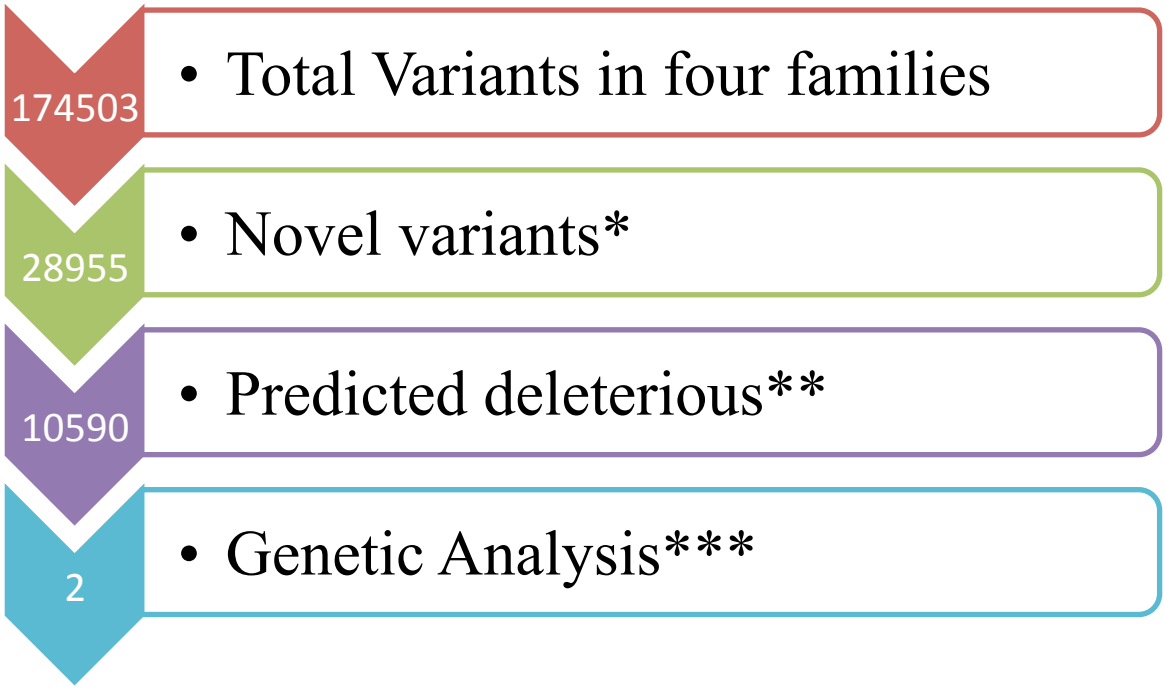

Figure 3.5: Recessive Variant Analysis Of Four Probands With Protein Sensitive HH (*Novel variants include variants present in at least 3% minor allele frequency in 1000 Genomes Project, Complete Genomics genomes and NHLBI ESP exomes excluded; ** Predicted deleterious variants included non-synonymous coding, splice site, frameshift, stop gain variants; *** Variants present in homozygous/compound heterozygous state in at least 2 of the four case samples and none of the controls [parents and unaffected siblings])

The two genes with variants identified through autosomal recessive analysis are shown in table 3.11.

Table 3.11: Novel Recessive Predicted Deleterious Variants In At Least 2 Of The Four Probands With Protein Sensitive HH And None Of The Unaffected Parents And Siblings

Gene	Chromosome	Position	Protein Variant
NOTCH4	6	32191658	p.L16dup
HLA-DRB5	6	32489766/32489856	p.F96L/p.D66N

***NOTCH4* (Notch [Drosophila] homolog 4)**

The *NOTCH4* gene encodes a member of Notch family. The members of this family are transmembrane proteins with an extracellular domain consisting of multiple epidermal growth factor-like (EGF) repeats, and an intracellular domain of various different types (Li et al., 1998). In Drosophilia, the members of Notch family interacts with its cell-bound ligands (delta, serrate) and this interaction plays a key role in development. In humans, Notch4 functions as a receptor for membrane bound ligands Jagged 1, Jagged 2 and Delta 1 (Gray et al., 1999). Upon binding with its ligand, the intracellular domain (NICD) is released from the transmembrane domain. The NICD activates the transcription of genes downstream and affects the differentiation, proliferation and apoptosis (Jarriault et al., 1995). In situ hybridization has revealed that primarily endothelial cells express Notch4 transcripts in embryonic and adult life (Uyttendaele et al., 1996).

By studying the Notch-4 deficienct mouse, Krebs *et al.* concluded that Notch4 and Notch1 genes have partially overlapping roles during embryogenesis (Krebs et al., 2000). Mutants mice with constitutive overexpression of Notch4 developed brain arteriovenous malformations, suggesting Notch pathway to be an inhibitor of vessel sprouting (Murphy et al., 2008).

3.9.2 Dominant inheritance Analysis

Considering possibility of dominant disease in pedigrees with protein sensitive HH, filters were applied to exome sequencing data of trios (proband and both parents) to identify de novo heterozygous deleterious variants. The results of filtering for dominant variants are shown in the figures 3.6, 3.7, 3.8 and 3.9. The novel *de novo* exonic variants in probands B, C, G and H are shown in table 3.12.

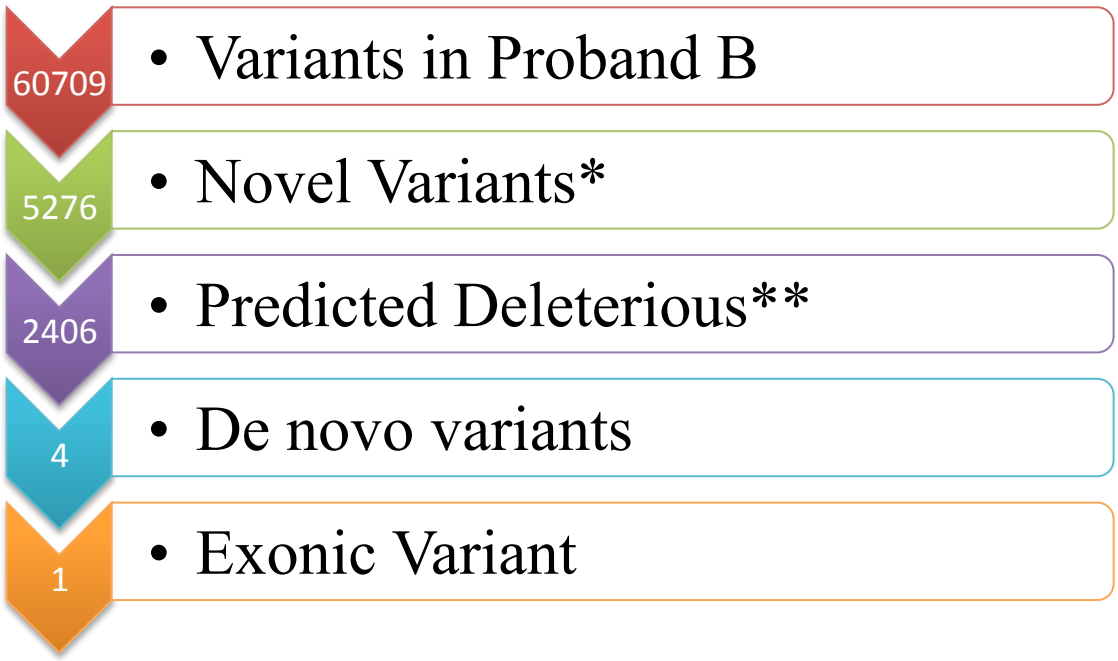

Figure 3.6: *De Novo* Variant Analysis Of Proband B (* Novel variants include variants present in at least 3% minor allele frequency in 1000 Genomes Project, Complete Genomics genomes and NHLBI ESP exomes excluded; ** Predicted deleterious variants included non-synonymous coding, splice site, frameshift, stop gain variants)

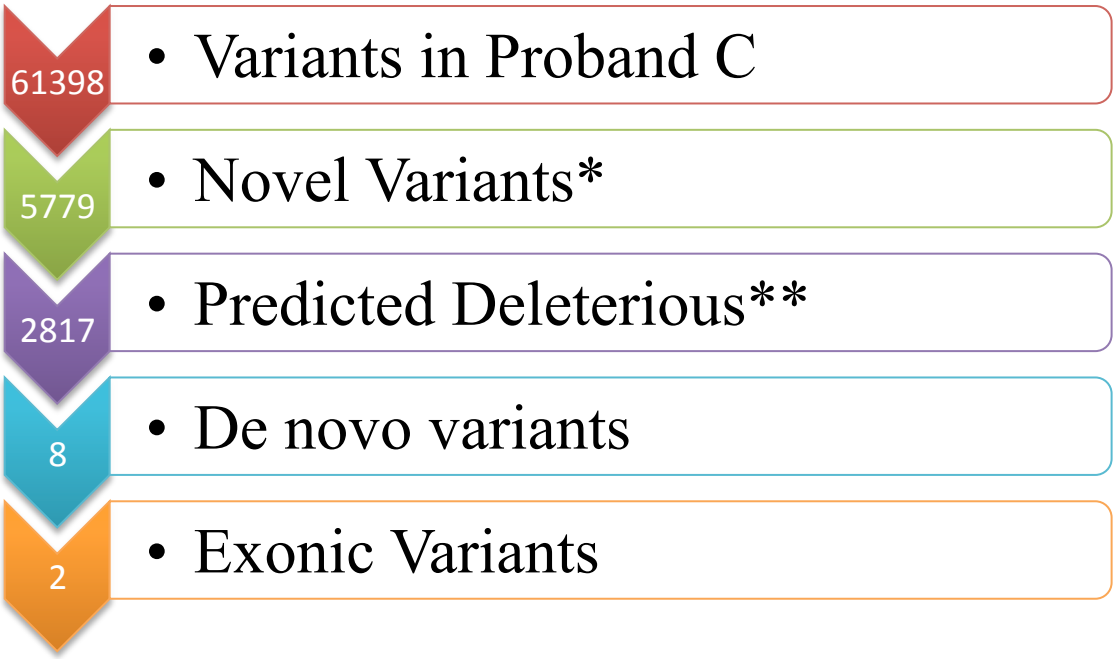

Figure 3.7: *De Novo* Variant Analysis Of Proband C (* Novel variants include variants present in at least 3% minor allele frequency in 1000 Genomes Project, Complete Genomics genomes and NHLBI ESP exomes excluded; ** Predicted deleterious variants included non-synonymous coding, splice site, frameshift, stop gain variants)

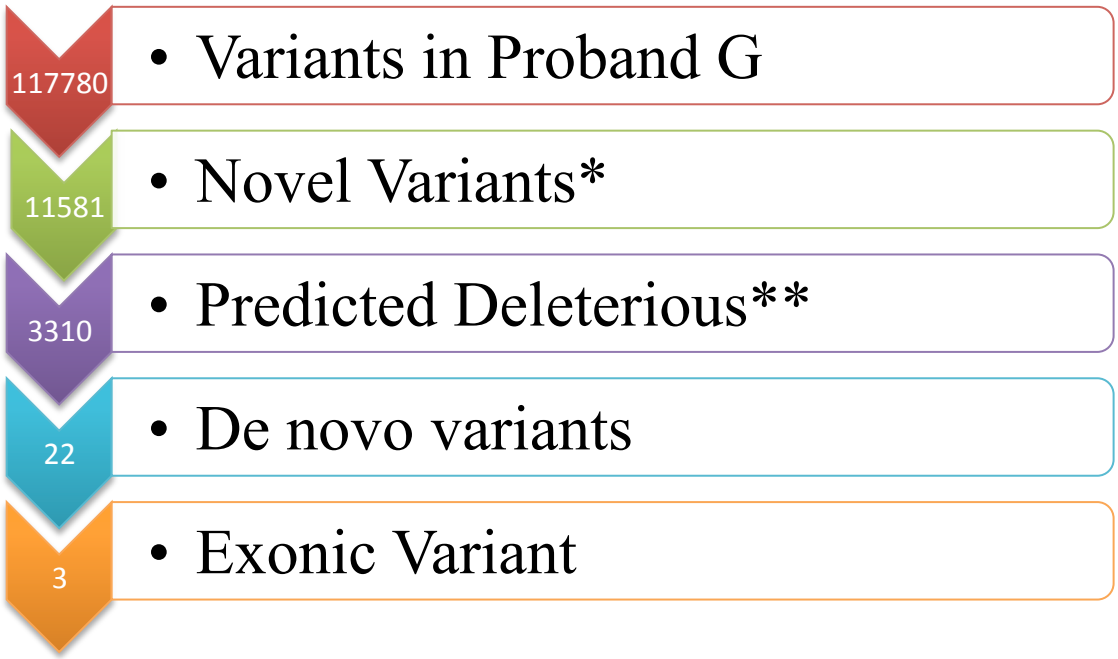

Figure 3.8: *De Novo* Variant Analysis Of Proband G (* Novel variants include variants present in at least 3% minor allele frequency in 1000 Genomes Project, Complete Genomics genomes and NHLBI ESP exomes excluded; ** Predicted deleterious variants included non-synonymous coding, splice site, frameshift, stop gain variants)

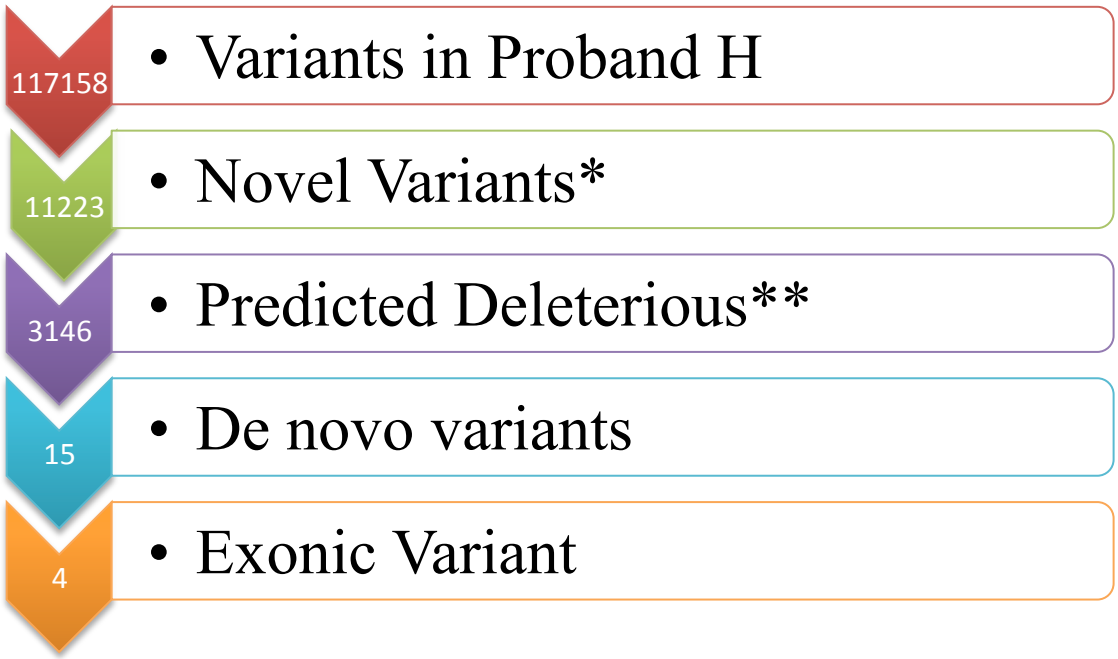

Figure 3.9: *De Novo* Variant Analysis Of Proband H (* Novel variants include variants present in at least 3% minor allele frequency in 1000 Genomes Project, Complete Genomics genomes and NHLBI ESP exomes excluded; ** Predicted deleterious variants included non-synonymous coding, splice site, frameshift, stop gain variants)

Table 3.12: List Of Novel Predicted Deleterious *De Novo* Variants In Probands With Protein Sensitive HH

Gene	Gene Region	Chromosome	Variant Position	Protein
Proband B				
TNFSF12	Exonic	17	7463171	p.S116P
Proband C				
AIM1L	Exonic	1	26671690	p.S487P
CAMKK2	Exonic	12	121678327	p.G539fs*4
Proband G				
PRIM2	Exonic	6	57398226	p.G310V
RCOR1	Exonic	14	103059287	p.A22_A28del
SNRPB	Exonic	20	2443385	p.P193_G194del
Proband H				
LGALS8	Splice site	1	236714292	p.??
HLA-DRB5	Exonic	6	32489766	p.F96L
TMEM67	Exonic	8	94793924	p.I258M,p.I339M

Out of these variants identified by the recessive and dominant inheritance filtering strategy in four probands with protein sensitive HH, no variant could explain the phenotype of protein sensitive HH based on the biological information known about these genes. A brief description of the genes in which predicted deleterious variants were found is shown below.

***TNFSF12* (Tumor Necrosis Factor [Ligand] Superfamily, Member 12)**

This gene codes for a cytokine that belongs to the tumor necrosis factor (TNF) ligand family. The encoded protein has a role in apoptosis, angiogenesis and induction of other inflammatory cytokines (Chicheportiche et al., 1997).

***AIM1L* (Absent In Melanoma 1-Like)**

AIM1L codes for Absent In Melanoma 1-Like protein. *AIM1* expression was reported to be associated with the experimental reversal of tumorigenicity of human malignant melanoma (Ray et al., 1997). Not much knowledge is available about this gene.

***CAMKK2* (Calcium/Calmodulin-Dependent Protein Kinase Kinase 2, Beta)**

Using RT-PCR, Nagase *et al.* detected high expression of *CAMKK2* in lung and ovaries (Nagase et al., 1998). A very low expression was detected in pancreas. Human CAMKK2 was found to phosphorylate CAMK1 and activate its kinase activity in the presence of Ca^{2+}/calmodulin (Hsu et al., 1998). Calmodulin-dependent kinases (CAMK) are a family of serine/threonine kinases that are responsible for many of the second messenger effects of Ca^{2+} (Anderson et al., 1998). Most CAMKs are expressed ubiquitously.

***PRIM2* (Primase, DNA, Polypeptide 2 [58kDa])**

This gene encodes a subunit of enzyme, DNA primase. DNA primase plays an important role in DNA replication by synthesizing small RNA primers for the Okazaki fragments (Shiratori et al., 1995).

***RCOR1* (REST Corepressor 1)**

The RCOR1 gene encodes a functional corepressor required for regulation of neural-specific gene expression. By association with REST (RE1-Silencing Transcription Factor), RCOR1 recruits molecular machinery for silencing neuronal-specific genes (Lunyak et al., 2002).

***SNRPB* (Small Nuclear Ribonucleoprotein Polypeptides B and B1)**

The SNRPB protein is one of the several nuclear proteins found in small ribonucleoprotein particles (snRNPs) (van Dam et al., 1989). These snRNPs are involved in pre-mRNA splicing.

***LGALS8* (Lectin, Galactoside-Binding, Soluble, 8)**

This gene encodes an animal lectin (carbohydrate-binding protein) that binds with beta-galactoside. They have conserved carbohydrate recognition domains. These lectins have a role in cell-cell adhesion, cell signaling and cell migration. *LGALS8* is expressed in the intestinal tract where the protein recognizes and kills E.coli expressing blood group antigen (Stowell et al., 2010).

***HLA-DRB5* (Major Histocompatibility Complex, Class II, DR Beta 5)**

HLA-DRB5 belongs to the HLA class II beta chain paralogues. The class II molecules are expressed in antigen presenting cells and present peptides on the cell surface for recognition by the CD4 T-cells. The class II molecule is a heterodimer of an alpha (DRA) and a beta (DRB) chain (Tieber et al., 1986). The polymorphisms within the beta chain determine the peptide binding specificities.

***TMEM67* (Transmembrane Protein 67)**

This gene has been linked to the phenotypes of Meckel syndrome 3, Joubert syndrome 6 and modifier of Bardet-Biedl syndrome 14 (Baala et al., 2007, Leitch et al., 2008, Smith et al., 2006). The highest expression of *TMEM67* was detected in spinal cord and moderate levels in adrenal tissue, brain and kidney by real-time quantitative PCR analysis of human embryonic tissues (Smith et al., 2006).

FAMILY D

3.10 CLINICAL INFORMATION (FAMILY D)

This consanguineous family had two siblings (probands D1 and D2) with congenital HH. The pedigree of the family D is shown in figure 3.10. The elder sibling (proband D1), aged 8 years, presented at 4 months of age with hypoglycaemic seizures. She was born at term gestation weighing 2450 grams. Investigations confirmed HH (table 3.13) with elevated serum ammonia. She showed good response to diazoxide treatment.

Table 3.13: Controlled Diagnostic Fast (Family D)

Investigations	Proband D1	Proband D2
Blood glucose (mmol/L)	1.7	2.1
Serum Insulin (mU/L)	5.6	2.9
Acetoacetate (mmol/L)	<0.05	<0.05
Beta-hydroxyl butyrate (mmol/L)	<0.05	<0.05
Lactate (mmol/L)	2.94	1.3
Serum Ammonia (µmol/L)	140; 169	163; 159
Plasma amino acids	Increased concentrations of tyrosine, methionine and proline	Increased concentrations of Arginine, reduced concentration of valine
Urine aminoacids	Generalized aminoaciduria	Dibasic aminoaciduria
Carnitine (Free and Total)	Normal	Normal
Acyl carnitines	Normal	Normal

Further investigations showed normal glutamate dehydrogenase (GDH) activity and normal inhibition by GTP. Molecular genetic analysis was negative for *ABCC8, KCNJ11, HADH* and *GLUD1*.

The younger sibling (proband D2), currently aged 3 ½ years, was born at 37 weeks gestation weighing 2660 grams. She was given frequent feeds in view of the history of hypoglycaemia in the elder sister. At 5 months of age, she presented with lethargy and floppiness in the postprandial period. Investigations confirmed HH (table) with elevated serum ammonia. She showed good response to management with uncooked cornstarch and diazoxide. The younger sibling also had primary hypothyroidism and required thyroxine replacement.

Figure 3.10: The pedigree chart of Family D:

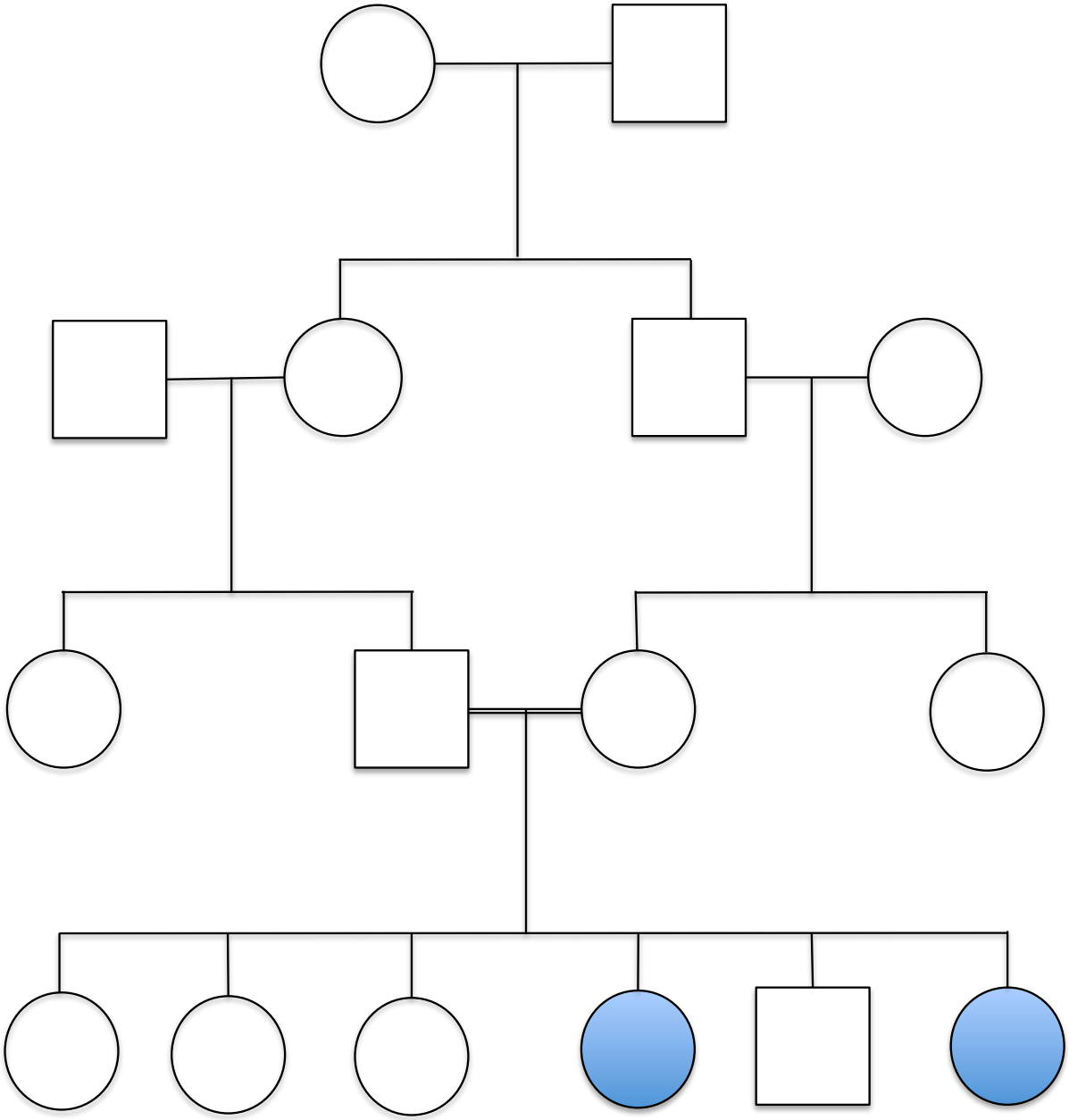

3.11 HOMOZYGOSITY MAPPING RESULTS (FAMILY D)

As this is a consanguineous pedigree, homozygosity mapping was done to locate the shared homozygous regions between two affected siblings, which were not shared with the unaffected sibling (Table 3.14). The two largest homozygous shared regions (14.5Mb and 4.73Mb) were on chromosome 3 and chromosome 19 respectively (Figure 3.11).

Table 3.14: Shared Homozygous Region Between Affected Siblings, Which Is Not Shared With Unaffected Sibling (Family D)

Chromosome	Start	End	Size (Mb)
Chr2	97358437	98637504	1.279067
Chr2	117912256	119006422	1.094166
Chr2	139489497	140900604	1.411107
Chr3	98367525	99387903	1.020378
Chr3	**126935726**	**141484860**	**14.549134**
Chr4	47682174	48931655	1.249481
Chr4	60536829	61860937	1.324108
Chr5	128747841	132181800	3.433959
Chr8	47060977	49190984	2.130007
Chr14	80441297	80468443	0.027146
Chr18	31945534	33040875	1.095341
Chr19	**35002775**	**39734923**	**4.732148**

Figure 7.8: B-allele frequency plot for chromosome 3

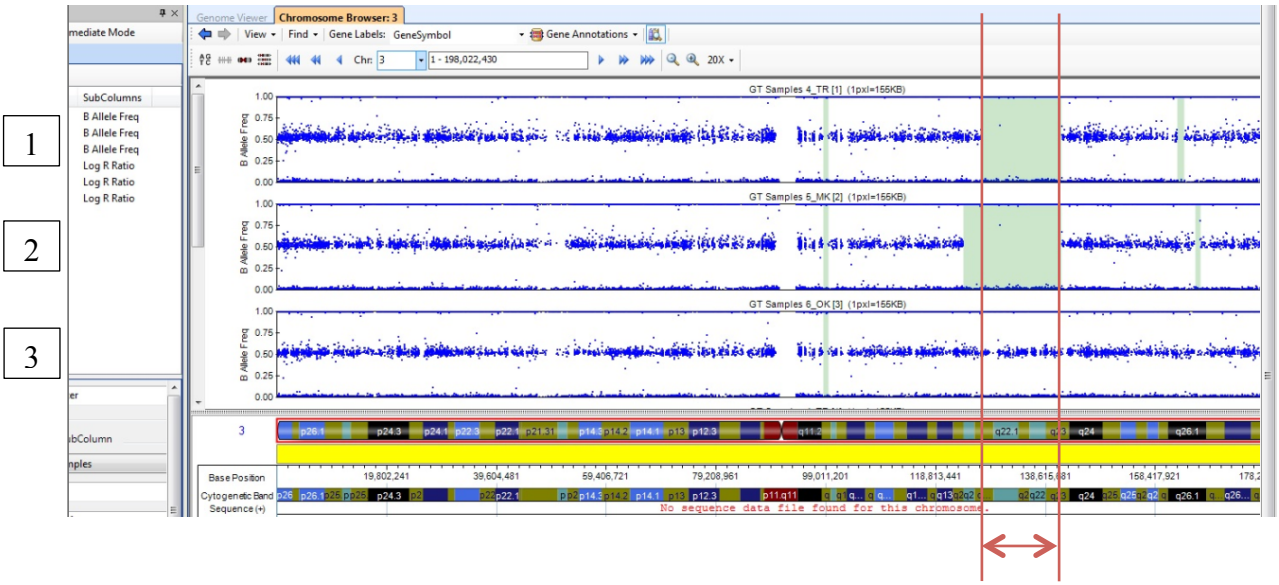

Figure 3.11: B-allele frequency plot showing the shared homozygous regions (highlighted in green) on chromosome 3. Samples 1 and 2 are the affected siblings, and sample 3 is the unaffected sibling. The shared homozygous region is between base pair position 126935726 and 141484860, and spans 14.54 Mb.

3.12 WHOLE-EXOME SEQUENCING RESULTS (FAMILY D)

In this family, four siblings (two affected and two unaffected) were studied with whole-exome sequencing. In view of consanguinity, filters were applied as outlined in figure 3.12 to the whole-exome sequencing data to determine autosomal recessive variants.

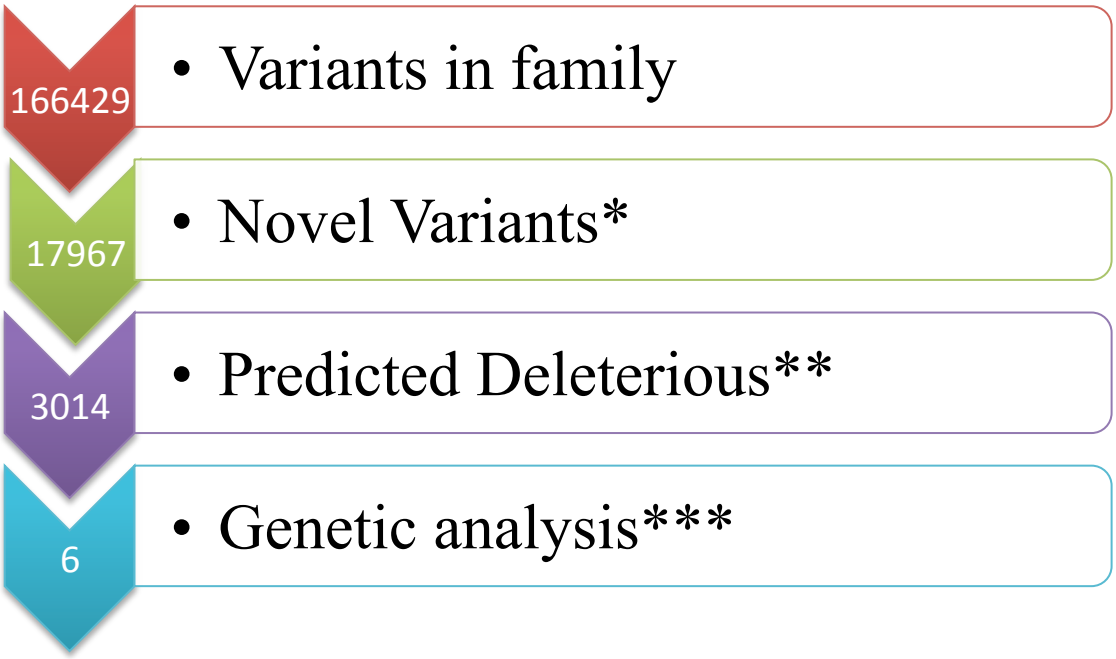

Figure 3.12: Recessive Variant Analysis Of Four Siblings (Two Affected And Two Unaffected) From Family D (* Novel variants include variants present in at less than 3% minor allele frequency in 1000 Genomes Project, Complete Genomics genomes and NHLBI ESP exomes excluded; ** Predicted deleterious variants included non-synonymous coding, splice site, frameshift, stop gain variants; *** Variants present in homozygous state in the affected siblings and not in the unaffected siblings)

The novel, predicted deleterious, autosomal recessive variants in family D are shown in table 3.15. With the available biological information about these genes, the phenotype of HH with these variants could not be explained. A very brief description about these genes is presented next.

Table 3.15: List Of Novel, Predicted Deleterious, Autosomal Recessive Variants In Family D

Gene	Chromosome	Position	Variant	Phenotype
SLCO2A1	3	133666113	p.V428F	√
AMOTL2	3	134090292	p.C53Y	
FAM187B	19	35719234	p.H117R	
ZNF793	19	38027957	p.I133V	
GGN	19	38876725	p.P393S	
PAPL	19	39591453	p.L256S	

***AMOTL2* (Angiomotin-like 2)**

Knockdown experiments in zebrafish and in cultured human umbilical vein endothelial cells indicated role of Amotl2 in polarity, migration and proliferation of angiogenic endothelial cells (Wang et al., 2011). Motin family members (*AMOT*, *AMOTL1* and *AMOTL2*) were shown to be involved in regulation of Wnt/β-catenin signaling (Li et al., 2012).

***FAM187B* (Family with Sequence Similarity 187, Member B)**

This encodes a predicted single-pass transmembrane protein. No information is available in the literature regarding the function of the gene.

***ZNF793* (Zinc finger protein 793)**

ZNF793 belongs to the Krueppel C2H2-type zinc-finger protein family. It contains 6 C2H2 zinc-finger domains one Krueppel associated box domain (Ota et al., 2004). Based on the protein sequence, this is likely to be involved in transcriptional regulation.

***GGN* (Gametogenetin, Mouse, Homolog of)**

A similar mouse gene was expressed only in testis and ovary. By yeast 2-hybrid analysis, it was shown that proteins encoded by mouse GGN gene, GGN1 and GGN3, interacted with Pog (Proliferation of germ cells) protein (Lu and Bishop, 2003).

***PAPL* (Purple Acid Phosphatase, Long form)**

PAPL is a member of a family of binuclear metallohydrolases, Purple Acid Phosphatases (PAP). A member with similar genomic sequence, *ACP5* (Phosphatase, Acid, Type 5, Tartrate-Resistant) is associated with a phenotype of spondyloenchondrodysplasia with immune dysregulation (Briggs et al., 2011).

FAMILY J

3.13 CLINICAL INFORMATION (FAMILY J)

Proband J was born at 36 weeks to non-consanguineous Caucasian parents weighing 2750g after induction of labour. She presented with history of palpitations from early childhood. Investigations revealed multiple types of tachyarrhythmia (sinus tachycardia, Supraventricular tachycardia, atrial flutter). She underwent catheter ablation for supraventricular tachycardia. She continued to have episodes of ventricular tachyarrhythmia and required implantation of defibrillator.

Along with cardiac arrhythmias, she also presented history of symptoms of hypoglycaemia within few hours of meals. Her glucose tolerance test revealed very high serum insulin measurements within 30 minutes of glucose load.

There was history of similar symptoms in her mother. Her younger sister displayed similar symptoms but unfortunately died due to unrelated cause.

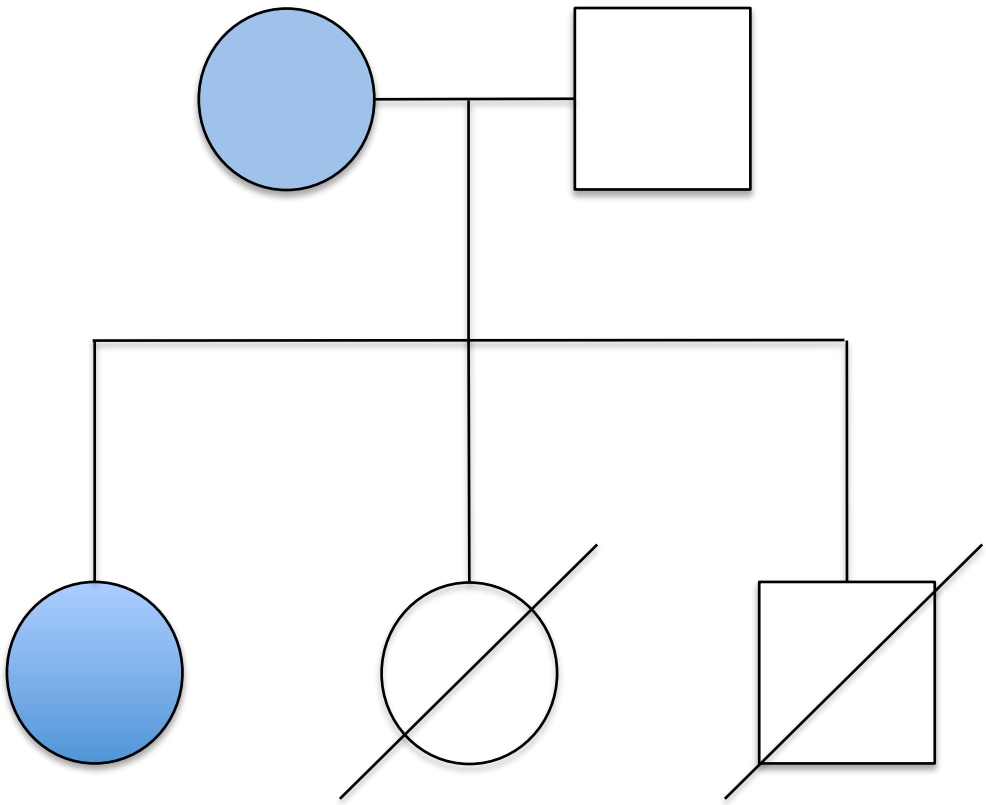

Figure 3.13: The pedigree chart of Family J

3.14 WHOLE-EXOME SEQUENCING RESULTS (FAMILY J)

In this family, the proband and her mother were studied with whole-exome sequencing. This family has a unique phenotype of HH and cardiac arrhythmias. A number of other family members had similar clinical phenotype. Assuming a dominant inheritance, filtering strategy applied to the whole-exome sequencing data of this family is shown in figure 3.14.

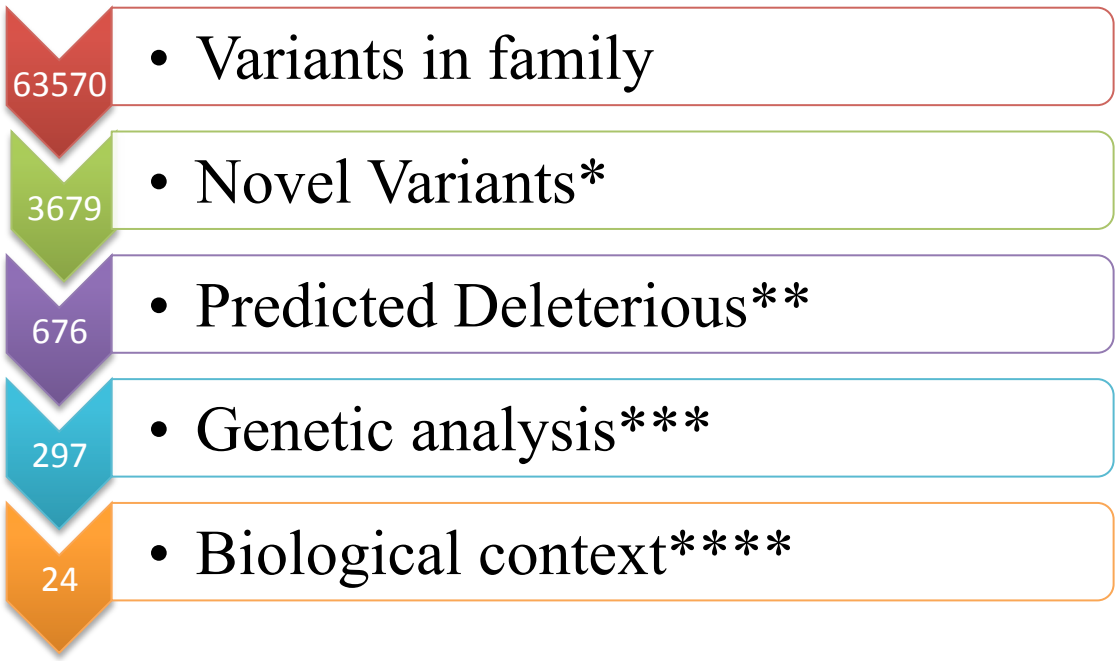

Figure 3.14: Filtering Strategy For Whole-Exome Sequencing Data Of Family J (* Novel variants include variants present in at least 3% minor allele frequency in 1000 Genomes Project, Complete Genomics genomes and NHLBI ESP exomes excluded; ** Predicted deleterious variants included non-synonymous coding, splice site, frameshift, stop gain variants; *** Variants present in heterozygous state in the proband and her mother; **** Variants with biological role related to the clinical phenotype of hyperinsulinaemic hypoglycaemia and cardiac arrhythmias)

The potential candidate genes and their locations are shown in table 3.16. A brief description about these genes is presented next.

Table 3.16: List Of Novel Predicted Deleterious Heterozygous Variants In Family J

Gene	Chromosome	Position	Variant	Phenotype
NBPF10	1	144871755	p.V1736E	
TTN	2	179596554	p.Y4439C	√
FN1	2	216251538	p.R1405W	√
MST1	3	49721812	p.R651*	
HAVCR1	5	156479569	p.T155_T159del	
HLA-C	6	31238886	p.Y195H	
HLA-B	6	31324100	p.R155S	
KCNK17	6	39278695	p.F108del	
PRSS1	7	142460335	p.K170E	√
KMT2C	7	151945007; 151945071	p.G838S; p.Y816*	
TET1	10	70404588	p.S701N	
CACNA2D4	12	1940199	p.G56S	√
POLG	15	89876827	p.Q55dup	√
ABCC1	16	16208631	p.V1030M	
IRX6	16	55363223	p.A445T	
KCNJ12	17	21318867; 21319208	p.M71I; p.A185V	
KCNG2	18	77659680	p.A422V	
COL5A3	19	10084460	p.V1195A	
LILRA6	19	54746051; 54746081	p.W69L; p.Q59R	

***NBPF10* (Neuroblastoma Breakpoint Family, Member 10)**

NBPF10 is a member of NBPF family, which has 22 genes and pseudogenes. The name NBPF was given to this family as one member of this family was disrupted by a chromosomal translocation in a neuroblastoma patient. The encoded proteins contain a highly conserved domain of unknown function (Vandepoele et al., 2005). Members of this family were found to be abundantly expressed in breast, liver, lung and kidney (Vandepoele et al., 2005). The exact function of the NBPF10 is unknown.

***MST1* (Macrophage stimulating 1)**

In view of the identical domain structure of the protein to that of hepatic growth factor (HGF), the protein's alternative name is HGF-like (HGFL) (Han et al., 1991). Hgfl-/- mice did not show obvious phenotypical abnormalities (Bezerra et al., 1998).

***HAVCR1* (Hepatitis A virus Cellular Receptor 1)**

This gene encodes for the cellular receptor of Hepatitis A virus and is expressed ubiquitously with highest expression in kidney and testis.

***KMT2C* (Lysine-specific methyltransferase 2C)**

This gene is a member of myeloid/lymphoid or mixed-lineage leukemia 3 (MLL3) family. The protein methylates 'Lys-4' of histone H3. H3'Lys-4' methylation is a specific event for epigenetic transcriptional activation (Daniel et al., 2010).

***TET1* (Tet Oncogene family, member 1)**

TET1 is a member of a family of methylcytosine dioxygenases that is required for cytosine demethylation and gene activation (Ito et al., 2011).

***ABCC1* (ATP Binding Cassette, Subfamily C, Member 1)**

This encodes a transporter protein (multidrug resistance protein; MRP) and was found to be overexpressed in a multidrug-resistant variant of small cell lung cancer cell line (Cole et al., 1992). The gene expression analysis detected increased expression in lung, testis and peripheral mononuclear cells. $MRP^{-/-}$ mice exhibited reduced dendritic cell migration from skin to lymph nodes and reduced mortality from Streptococcus pneumoniae as compared to wildtype mice (Robbiani et al., 2000, Schultz et al., 2001).

***IRX6* (Iroquois Homeobox Protein 6)**

Members of this gene family are involved during pattern formation in vertebrate embryos (Bosse et al., 1997).

***KCNJ12* (Potassium channel, Inward rectifying, Subfamily J, Member 12)**

This gene was cloned from human atrial RNA using primers based on the conserved regions of inward rectifying K^+ channel (Wible et al., 1995). On expression in Xenopus oocytes, the encoded protein was shown to be inward rectifying (Wible et al., 1995).

***LILRA6* (Leukocyte Immunoglobulin-Like Receptor, Subfamily A, Member 6)**

Based on the similarity of the protein sequence with LILRB4, this is predicted to function as a receptor for class 1 MHC (Major Histocompatibility Complex) antigens (Borges et al., 1997).

***COL5A3* (Collagen, Type 5, Alpha-3)**

COL5A3 encodes alpha-3 chain of type 5 collagen, which is a heterotrimer of COL5A1, COL5A2 and COL5A3 chains.

***KCNK17 (*Potassium channel, Subfamily K, Member 17)**

KCNK17 is a member of the 2-pore domain superfamily of K^+ channels and contribute to the resting membrane potential of the cell. *KCNK17* is widely expressed with high expression in the pancreas and heart (Decher et al., 2001). This gene is discussed in more detail in chapter 5.

***KCNG2* (Potassium channel, voltage-gated, subfamily G, Member 2)**

This gene is highly expressed in the heart and may contribute towards cardiac action potential repolarization (Zhu et al., 1999). This gene is also discussed in more detail in chapter 6.

FAMILY F

3.15 CLINICAL INFORMATION (FAMILY F)

Proband F was born at 39^{+4} weeks of gestation weighing 4600 grams to non-consanguineous Caucasian parents. She had transient hypoglycaemia in the neonatal period. Three episodes of generalized tonic-clonic seizures associated with low bedside blood glucose level of 1.7mmol/L resulted in referral to Congenital Hyperinsulinism team at Great Ormond Street Hospital. All these episodes happened in the morning before breakfast within a 1week period. Her growth was along the 98^{th} centile for weight and height. The pedigree of the family is shown in figure 3.15. The results of the controlled diagnostic fast are shown in table 3.17.

Figure 3.15: The pedigree chart of Family F

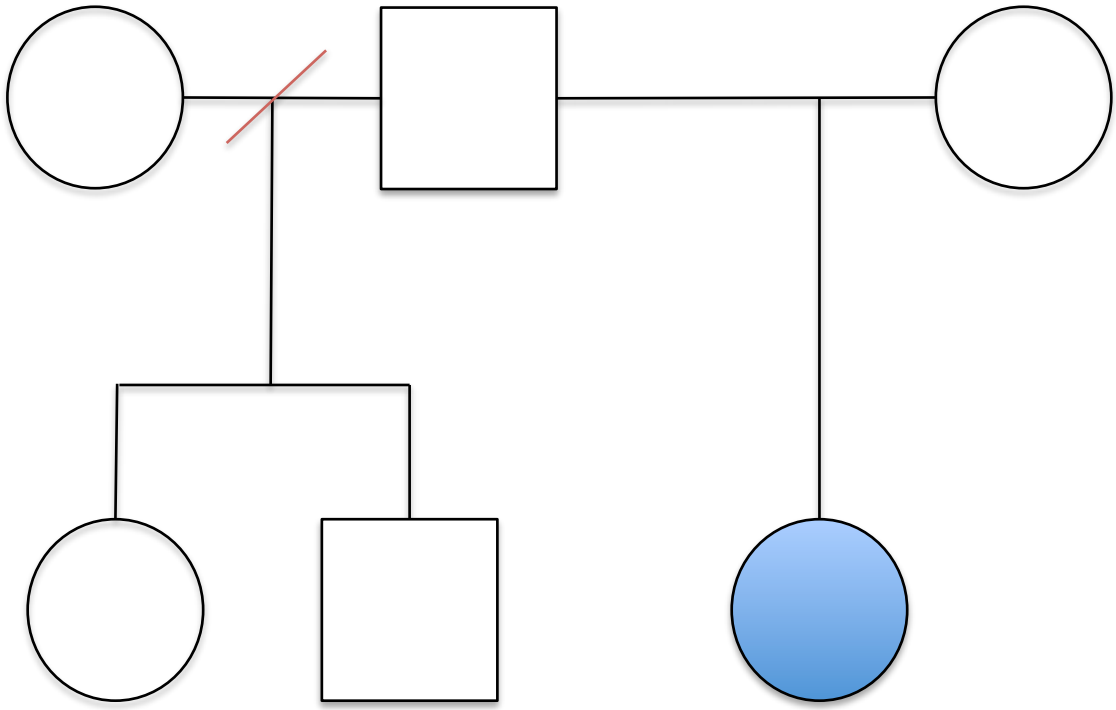

She required 10 mg/kg/min of glucose infusion to maintain blood glucose ≥ 3.5mmol/L. No response to medical management with diazoxide was seen. Molecular genetic testing performed at University Exeter School, Exeter identified a heterozygous non-stop mutation in *KCNJ11* (c.1171T>C), inherited from the father.

In view of the paternally inherited heterozygous *KCNJ11* mutation, an ^{18}F DOPA-PET CT scan was performed which identified a focal lesion in the tail of the pancreas. The lesion was laparoscopically resected and histological analysis confirmed the focal lesion in the tail. Microsatellite analysis of the chromosome 11p15 region of the resected pancreatic tissue showed maternal loss of heterozygosity.

Post-resection of the focal lesion, however, the proband continued to have hypoglycaemic episodes and could not be weaned off intravenous dextrose fluids. A second ^{18}F DOPA-PET CT scan did not identify focal uptake in the pancreas. A second pancreatectomy was done in which further pancreatic tissue around the tail (the site of focal lesion) was resected. Histological analysis of the pancreatic tissue identified well-demarcated margins of the focal lesion. However the pancreatic tissue around the focal lesion did not have normal histological appearance. Microsatellite analysis of the chromosome 11p15 region of the pancreatic tissue resected in the second pancreatectomy did not show maternal loss of heterozygosity.

The proband continued to have inappropriate fasting tolerance even after the second pancreatectomy. She was recommenced on diazoxide, which was gradually increased to the maximum dose of 15mg/kg/day. She showed some improvement in her fasting tolerance with diazoxide. A repeat ^{18}F DOPA-PET CT scan revealed diffuse uptake throughout pancreas.

Table 3.17: Controlled Diagnostic Fast (Proband F)

Investigations	**At local hospital**	**At GOSH**	**After 1st surgery**	**After 2nd surgery**
Blood glucose (mmol/L)	2.5	2.2	2.7	2.5
Serum Insulin (mU/L)	53	7	12.1	6.8
C-peptide (pmol/L)	459			
Serum Cortisol (nmol/L)	628		458	604
Non-esterified fatty acids (mmol/L)	0.4	<0.05	1	1.60
β-hydroxybutyrate (mmol/L)	<0.1	<0.05	1.41	1.43
Serum ammonia (µmol/L)	37	22		26
Serum Lactate (mmol/L)	1.5	1		1.6
Plasma Acylcarnitine profile	Normal			
Plasma Amino acids	Normal			

FAMILY I

3.16 CLINICAL INFORMATION (FAMILY I)

The proband I1 was born at term gestation by normal vaginal delivery to Caucasian non-consanguineous parents weighing 5370g. Her mother's antenatal period was uneventful. She required resuscitation after birth and was ventilated. In the neonatal period, she required high glucose infusion to maintain blood glucose above 3.5mmol/L. Her controlled diagnostic fast was suggestive of HH (table 3.18).

Table 3.18: Controlled Diagnostic Fast (Proband I)

Investigation	I1	I2
Blood Glucose (mmol/L)	2.7	0.1
Serum Insulin (mU/L)	<2.0	25.7
C-peptide (pmol/L)	159	
Serum Cortisol (nmol/L)	433	
Serum Growth hormone (ng/mL)	7.4	
Non-esterified fatty acids (mmol/L)	0.31	<0.05
Beta-hydroxybutyrate (mmol/L)	<0.05	<0.05
Serum Ammonia (mmol/L)	29	25
Serum Lactate (mmol/L)	1.2	1.6
Plasma Amino acids	Normal	Normal
Urine Organic acids	Normal	Normal
Serum Carnitine profile	Normal	Normal

She responded well to 3 mg/kg/day of diazoxide. Her HH was transient and she was successfully weaned off the medications by 3 months of age.

The proband's maternal cousin (proband I2; see figure 3.16 for pedigree) also had transient HH. He was born at 31 weeks gestation with a birth weight of 1815g. In view of requirement of high glucose infusion rate, a controlled diagnostic fast was done which confirmed HH (table 3.18). He was successfully managed with 5mg/kg/day of diazoxide, which could be weaned by 8 weeks of age.

Molecular genetic analysis identified a maternally inherited heterozygous *ABCC8* mutation (c.4547C > T; p.Thr1516Met) in both probands.

Figure 3.16: The pedigree chart of Family I

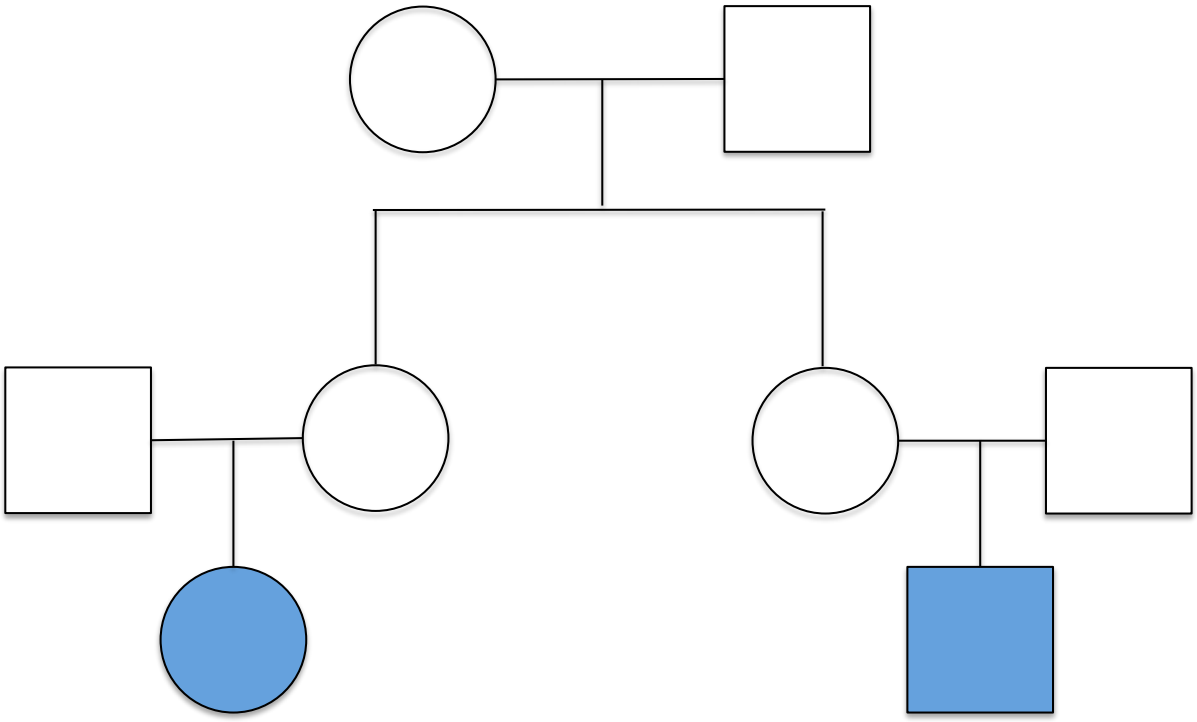

CHAPTER 4

BASIC PRINCIPLES OF PATCH-CLAMP ELECTROPHYSIOLOGY

4.1 SUMMARY OF CHAPTER 4

The patch clamp technique is the 'gold standard' for studying ion channel function. This chapter provides a brief introduction to electrophysiology, followed by a protocol of how the experiments were conducted and analyzed.

These electrophysiological experiments were performed at the William Harvey Heart Institute, Queen Mary University in Professor Andrew Tinker's laboratory. Dr Qadeer Aziz Hussain, a post-doc in Professor Tinker's laboratory, supervised these experiments.

4.2 MEMBRANE BIOLOGY

All living cells are enveloped by a plasma membrane, which is mainly constituted of phospholipid bilayer. Phospholipids have lipophilic residue (tail) at one end and hydrophilic (head) at the other end. In a phospholipid bilayer, these phospholipid molecules arrange themselves so that lipophilic residues face each other. This bilayer acts as a barrier between the cytoplasm and the extracellular space. Within this bilayer are embedded other membrane constituents (ion channel proteins), which allow communication between the cytoplasm and the extracellular space.

As shown in table 4.1, there are striking differences in the concentrations of inorganic ions in the extracellular and intracellular medium. These concentration differences induce the movement of ions along their concentration gradient through the ion channels and generate an electrical potential across the plasma membrane.

Table 4.1: Intracellular and extracellular distribution of the main ions

Ion	Intracellular range (mM)	Extracellular range (mM)
Na^+	5-20	130-160
K^+	130-160	4-8
Ca^{2+}	50-1000 nM	1.2-4
Mg^{2+}	10-20	1-5
Cl^-	1-60	100-140
HCO_3^-	1-3	20-30

4.2.1 Nernst equation

As mentioned in the previous section, the concentration gradients of various ions induce the movement from higher to lower concentrations. However as these ions are charged molecules, this movement generates an electrical force, opposing this diffusion. When the two opposing forces are in equilibrium, there is no net movement of ions. The relation describing this equilibrium is described by the following equation:

$$-RT\ In\frac{[ion]o}{[ion]i} = -EzF$$

This relation can be rearranged to provide the electrical potential at which a certain ion gradient is in equilibrium and there is no net movement.

$$E\ = \frac{RT}{zF}In\frac{[ion]o}{[ion]i}$$

- E is the equilibrium potential for the ion under consideration
- R is the universal gas constant (8.31 Joules mol^{-1} $Kelvin^{-1}$)
- T is the temperature in Kelvin
- Z is the oxidation state of the ion under consideration
- F is the Faraday constant (9.65×10^4 Coulombs mol^{-1})
- [ion]*o* and [ion]*i* are the extracellular and intracellular concentrations of the ion

4.2.2 Membrane Potential

At rest, the inside of all cells is more negatively charged than the outside (resting membrane potential). This imbalance is due to differences in the distribution of various ions on either side of the membrane and the relative permeability of the plasma membrane to each of the ions. The Goldman Hodgkin-Katz (GHK) equation, which takes into account the ion concentrations on either side of the membrane as well as the membrane permeability, can be used to determine the resting membrane potential.

$$E_m = \frac{RT}{F}\ In\ [\frac{P_K[K^+]out + P_{Na}[Na^+]out + P_{Cl}[Cl^-]in}{P_K[K^+]in + P_{Na}[Na^+]in + P_{Cl}[Cl^-]out}]$$

If the plasma membrane was to be permeable only to K+ ions, the resting membrane potential of the cell will be equal to the equilibrium potential for potassium ions (E_K). This can be calculated by the Nernst equation described in the previous section, which is between -80 to -90 mV. However, plasma membrane is permeable to other ions as well and their equilibrium potentials are more positive than E_K. Hence the membrane potential is slightly more positive than E_K and is typically -50 to -80mV.

4.3 ELECTRICAL PROPERTIES OF THE CELL MEMBRANE

4.3.1 Membrane Resistance

At resting membrane potential, the membrane potential is equivalent to the diffusing force and there is no net movement of ions across the cell membrane. As the membrane potential moves away from the resting membrane potential, the two forces (diffusing force and membrane potential) are not equal and the ions will flow across the membrane. The further

the membrane potential is from the resting membrane potential, the greater will be the flow of ions. The movement of charge is expressed in current;

$$I = \frac{dQ}{dt}$$

where I is current in amperes (A) and dQ/dt is the change in charge in coulomb over time. The size of current is determined by

1. Driving force – difference between the membrane potential and equilibrium potential
2. Resistance of the membrane

The relation between current, resistance and driving force is described by the following equation;

$$I = \frac{E_m - E_{rm}}{R_m}$$

Where $E_m - E_{rm}$ is the driving force and R_m is the membrane resistance.

4.3.2 Membrane Capacitance

In view of the unequal distribution of charge on the two sides of the membrane, the plasma membrane attracts charged particles on either side of the membrane. This storage of charge is dependent on the potential difference across the membrane and the physical dimensions of the membrane. Consequently, the higher the potential difference across the membrane and the larger the size of the cell, the more charge a membrane can store. The ability of the membrane to store charge at a given potential is described as capacitance of the cell membrane. Measurement of capacitance provides a good estimation of the membrane surface area.

The membrane capacitance plays an important role in electrophysiological experiments such as voltage clamp. Due to membrane capacitance, the voltage clamp will change the membrane potential with some delay. Hence it is very important to compensate for the capacitance in electrophysiological experiments to accurately measure the current.

4.4 ELECTROPHYSIOLOGY

Electrophysiological techniques are employed to record ion fluxes across a membrane. There are two types of electrophysiological techniques: indirect and direct. Indirect techniques include electrograms, encephalograms etc. where the electrodes to measure ion fluxes are positioned extracellularly. Direct techniques such as patch clamping require the microelectrodes to make contact with the cell of interest.

4.3.1 Voltage Clamp

As mentioned before, the movement of ions (through the ion channels across the cell membrane) generate a membrane potential. The activity of ion channels can be studied by measurement of the changes in membrane potential as a result of ion fluxes. However detailed study of the ion channel behavior is difficult by this method as the change in membrane potential can itself affect the ion channel activity e.g. many ion channels have gating mechanisms which respond to membrane potential changes. It is therefore desirable to use a technique called voltage clamp. In voltage clamp, the membrane potential is controlled by the experimenter and the current is recorded directly in response to set membrane potential.

In voltage clamp, the experimenter sets a series of different voltages (step protocol or complicated waveforms) across the membrane. As the set membrane potential is different from the actual membrane potential, this results in generation of a driving force for the ions across the membrane. The movement of ions (current) is measured and a compensatory current equal in size but opposite in direction is instantly injected to keep the membrane potential at the potential set by the experimenter. By recording the current required to be

injected to keep the membrane potential at the holding potential, the activity of the ion channels can be measured.

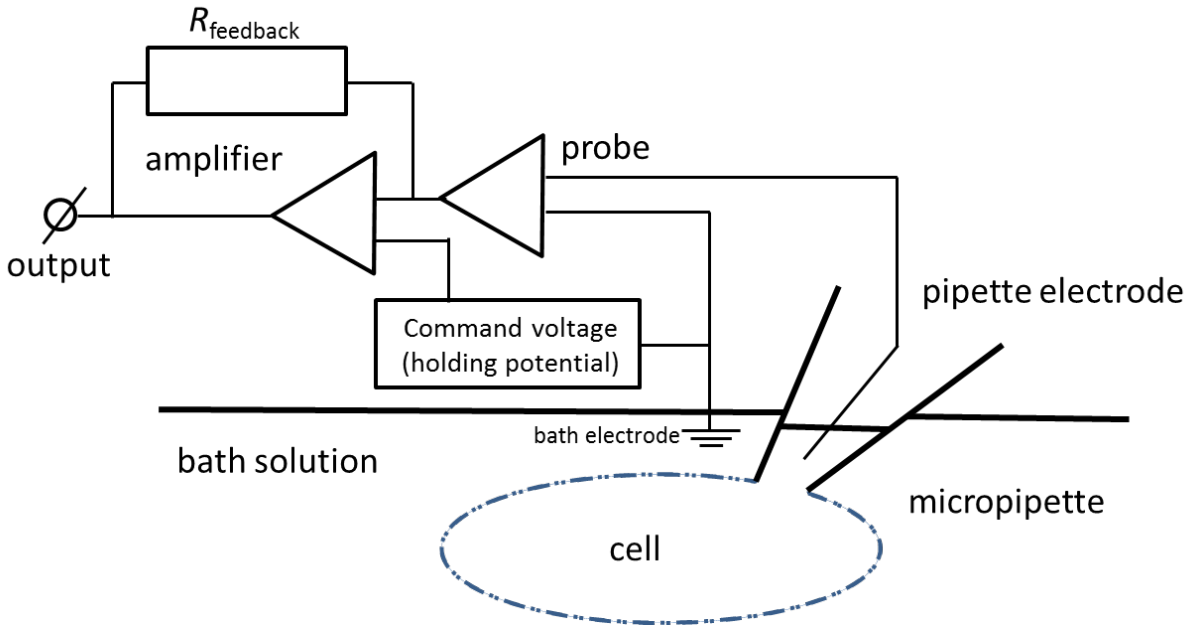

Figure 4.1: The voltage clamp principle in the whole-cell configuration. The holding potential and the measured potential between the pipette and bath electrode are continuously compared. The difference in the two potentials is instantly corrected by current injection using amplifier circuitry.

4.5 PATCH-CLAMP CONFIGURATIONS

Patch clamp technique can be used in various configurations depending upon whether individual channels or whole cell need to be studied. Different configurations also allow manipulations of the fluids on the extracellular side or the intracellular side of the membrane according to the requirements. The various patch-clamp configurations are

4.5.1 Cell attached patch mode

This is the simplest mode of patch-clamp. In this mode, the patch pipette has a very high resistance seal (GΩ) with the cell membrane (R_{patch}). This configuration is a single channel configuration and is used to study the activity of the ion channels in the tiny patch of membrane surrounded by the tip of the pipette. Although this configuration is physiological as the cell is intact, manipulation of the intracellular media is not possible and extracellular media is difficult. During voltage clamp, the membrane potential over the patch cannot be measured directly as well.

4.5.2 Whole-cell patch mode

In whole-cell mode, the patch of the membrane under the tip of the micropipette is ruptured and hence the pipette solution and the cytoplasm are in continuity. The rupture results in disruption of the membrane potential and dramatic reduction of R_{patch}, which in this configuration is named as the access resistance R_{access}. The series circuit in this configuration consists of the pipette resistance $R_{pipette}$, the access resistance R_{access} and the membrane resistance R_m. As R_m is much larger than $R_{pipette}$ and R_{access}, this configuration allows the measurement of currents through all activated single channels of the cell. The R_{access} and $R_{pipette}$ are also in series with the membrane capacitance (C_m) and form a significant RC

circuit. An RC circuit is a circuit where a resistor and a capacitor are present in series. The sum of R_{access} and $R_{pipette}$ is referred to as series resistance.

In an RC circuit, the speed of charging and discharging a capacitor upon a change in potential, such as seen during voltage clamp, is dependent on the resistor(s) in series with it. This series resistance cause delay in voltage changes and need to be compensated. In voltage clamp, the problem is reduced by over-injecting current in order to speed up the response.

Electrically, the two electrodes are on either side of the cell membrane: patch electrode on the intracellular side and ground electrode on the extracellular side. Hence the membrane potential can be directly measured. As there is mixing of the cytoplasm and the pipette solution, and the pipette solution volume is much larger than the cell volume, the composition of the intracellular fluid can be considered equal to that of the pipette solution.

4.5.3 Outside-out and Inside-out patch-modes

These are single channel configurations that require excising a patch of the membrane from the cell. The outside-out patch configuration is obtained by pulling away the patch pipette from the whole cell configuration, whereas the inside-out patch is obtained by pulling away the pipette from the cell-attached patch configuration. The patch and its ion channels can be manipulated both electrically and chemically.

4.6 PROTOCOL

4.6.1 The Patch-clamp set up (Figure 4.2)

The patch-clamp rig, where the electrophysiological experiments were performed, included the following elements:

- A stable platform with vibration dampening properties
- A microscope (Olympus 1X71) for visualizing the cells
- Micromanipulators to position the micropipette tip on the cell membrane
- Superfusion systems – a set of containers containing solutions to bath the cell preparation

The above equipment was all inside a Faraday cage to shield the experiment from surroundings.

The remaining equipment such as fluorescent lamp (for identifying the transfected cells), lamp source for visualizing cells under the microscope (Olympus TH-200), AXON CNS Digidata 1440A (Molecular Devices; low noise data acquisition system) and AXON CNS Multiclamp 700B (Molecular Devices; patch-clamp amplifier which contains the measuring and clamping circuitry and controls) were located next to the rig.

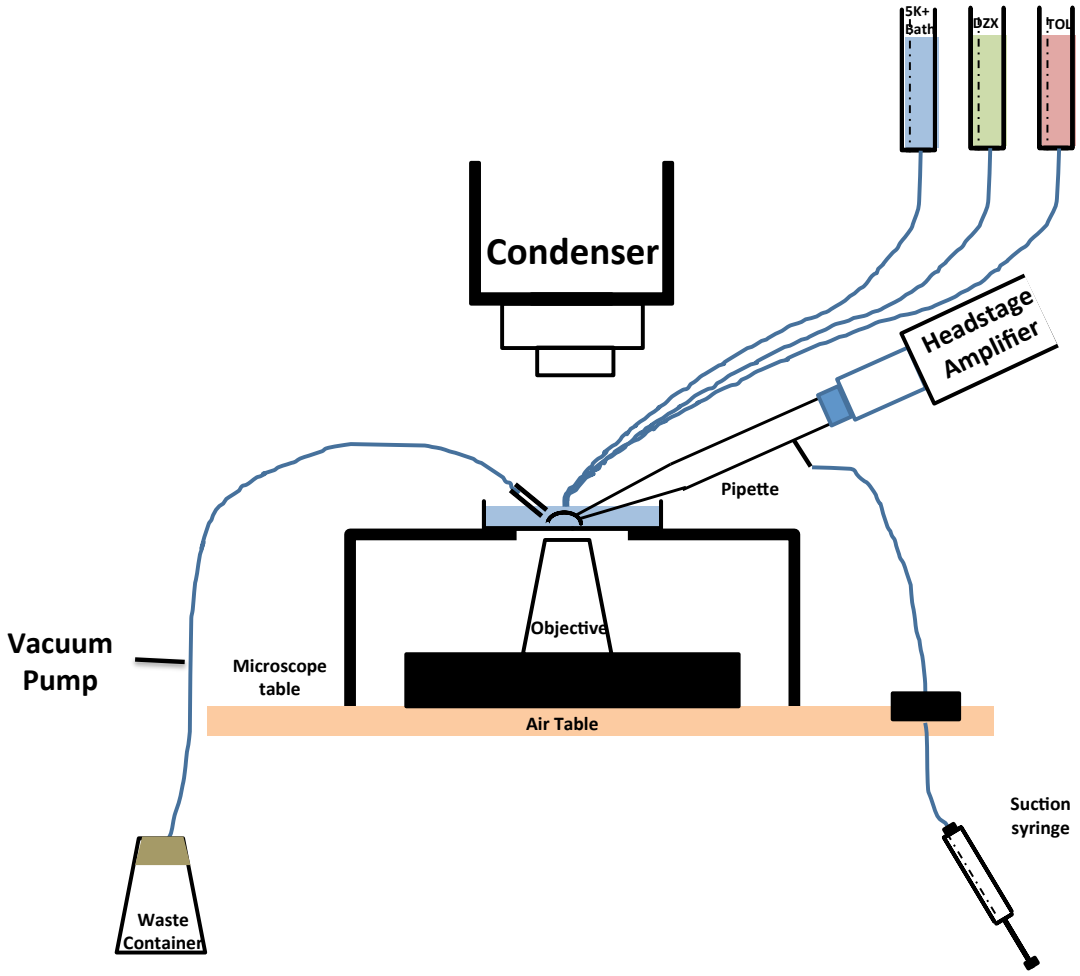

Figure 4.2: The patch-clamp set up used to make whole-cell recordings for K_{ATP} currents. The headstage amplifier was placed very close to the pipette holder. The pipette approached the cells in the chamber above the objective at an acute angle. The inverted microscope was mounted on the air table within the Faraday cage. A tube was attached to the side-port of the pipette holder to provide appropriate suction. The recording chamber was constantly superfused by solutions by a gravity driven system. A vacuum pump removed the solutions from the recording chamber to maintain a constant level.

4.6.2 Cell Culture

HEK293 cells were splitted on to the 10 mm coverslips in the 6 well plates 72 hours before the planned experiments in an appropriate dilution depending on the confluency of the cells in the T75 flask. After 24 hours, the cells were transfected with the appropriate plasmid construct along with eGFP (100ng) using FuGENE HD transfection reagent. The plasmid constructs and their amounts used in different experiments performed in this thesis are detailed in tables 4.2 and 4.3.

Table 4.2: Transfection Mixtures For Different K_{ATP} Channel Experiments

Experiments on K_{ATP} channels		
Wild type	Wild type SUR1 Construct Wild type Kir6.2 Construct	2 μg 500 ng
Mutant SUR1 T1516M	Mutant T1516M SUR1 Construct Wild type Kir6.2 Construct	2 μg 500 ng
Heterozygous SUR1 T1516M Mutant	Wild type SUR1 Construct Mutant T1516M SUR1 Construct Wild type Kir6.2 Construct	1 μg 1 μg 500 ng
Mutant Kir6.2*391Rext*94	Wild type SUR1 Construct Mutant Kir6.2*391Rext*94 Construct	2 μg 500 ng
Heterozygous Kir6.2*391Rext*94 Mutant	Wild type SUR1 Construct Wild type Kir6.2 Construct Mutant Kir6.2*391Rext*94 Construct	2 μg 250 ng 250 ng

Table 4.3: Transfection Mixtures For Different $K_{2P}17$ And K_v Channel Experiments

Experiments on $K_{2P}17$ channels		
Wild type	Wild type $K_{2P}17$ construct	2 μg
Mutant $K_{2P}17$ F108del	Mutant $K_{2P}17$ construct	2 μg
Heterozygous $K_{2P}17$ F108del	Wild type $K_{2P}17$ construct Mutant $K_{2P}17$ construct	1 μg 1 μg
Experiments on Kv Channels		
Wild type $K_v2.1$	Wild type $K_v2.1$ construct	2 μg
Wild type $K_v6.2$	Wild type $K_v6.2$ construct	2 μg
Mutant $K_v6.2$ p.A422V	Mutant $K_v6.2$ construct	2 μg
Wild type $K_v2.1$ + Wild type $K_v6.2$	Wild type $K_v2.1$ construct Wild type $K_v6.2$ construct	1 μg 1 μg
Wild type $K_v2.1$ + Mutant $K_v6.2$ p.A422V	Wild type $K_v2.1$ construct Mutant $K_v6.2$ construct	1 μg 1 μg
Wild type $K_v2.1$ + Wild type $K_v6.2$ + Mutant $K_v6.2$ p.A422V	Wild type $K_v2.1$ construct Wild type $K_v6.2$ construct Mutant $K_v6.2$ construct	1 μg 500 ng 500 ng

4.6.3 Intracellular (ICS) and Extracellular (ECS) solutions

The composition of the solutions used for whole-cell patch clamping is shown in table 4.4. The ICS for patch-clamping experiments on K_{ATP} channels was immediately stored in ~1 ml aliquots after preparing. This was then thawed on the day of the experiment and kept on ice throughout to prevent degradation of nucleotides. The ICS for patch-clamping experiments on $K_{2P}17$ and K_v channels was stored at +4°C. The ECS for all patch-clamping experiments was stored at +4°C.

Table 4.4: Composition of intracellular (ICS) and extracellular (ECS) solutions for K_{ATP}, $K_{2P}17$ and K_v Channel patch-clamping experiments.

	K_{ATP} Channels		**$K_{2P}17$ Channels**		**Kv Channels**	
	ICS (mM)	ECS (mM)	ICS (mM)	ECS (mM)	ICS (mM)	ECS (mM)
KCl	107	5	140	5	140	5
NaCl	-	140	-	140	-	140
$MgCl_2$	1.2	1	3	1.2	3	1.2
$CaCl_2$	1	1.8	-	2.6	-	2.6
EGTA	10	-	10	-	10	-
HEPES	5	10	10	10	10	10
MgATP	3	-	-	-	-	-
NaADP	1	-	-	-	-	-
Glucose	-	-	-	-	-	10
pH	7.2 (KOH)	7.4 (NaOH)	7.2 (KOH)	7.4 (NaOH)	7.2 (KOH)	7.4 (NaOH)

4.6.4 Patch Pipettes

The thin walled borosilicate glass capillaries were used to make the patch pipettes. The ends of the capillaries were fire polished using a bunsen burner. A two-stage pipette puller (Model PP-830, Narishige, Japan) was then used to heat and pull the glass into two fine pipettes. In the first pull, the capillaries were heated to 62°C. After letting it cool down for few seconds, the second pull was applied by heating to 48.8°C. These fine pipettes were filled with ICS for whole-cell recordings.

4.6.5 Obtaining the GΩ Seal

A suitably transfected cell, not touching any neighboring cells, was chosen for whole-cell recording. The cell was positioned in the centre of the field of view under the microscope. The micropipette, filled with ICS, was loaded on the pipette holder making sure that the tip of electrode filament was immersed in the ICS. The micropipette was lowered into the bath solution using the coarse manipulator. A small positive pressure was applied with the help of 1 mL syringe at this stage. Once the micropipette was in the bath solution, the pipette resistance could be measured based on the amplitude of the current in response to the test pulse. The pipettes with a resistance of ~2-4 MΩ were generally used. The pipette was gradually lowered towards the chosen cell. With the help of manipulators, the position of the pipette was adjusted in the horizontal plane so that it touches the centre of the cell on lowering.

The current was offset to zero immediately before the pipette made contact with the cell. When the pipette was very near to the cell, fine manipulators were used to control the movement of the pipette. The pipette was gently touched to the cell membrane so that its resistance has increased by ~1 MΩ. Suction was applied to the pipette through the tubing

attached to the side-port of the pipette holder, which increased the seal resistance. Once a seal resistance of >1 GΩ was achieved, the cell was in the cell-attached configuration.

4.6.6 Whole-cell Patch-Clamp Recordings

After establishing the GΩ seal, the capacitance transients were electronically compensated by using amplifier circuitry (MultiClamp 700B). Gentle mouth suction was applied to rupture the patch of membrane beneath the micropipette tip. The appearance of large capacitance spikes denoted the successful rupture of the membrane and attainment of whole-cell configuration. These transients are formed by the cell capacitance in series with the $R_{pipette}$ and R_{access} (collectively referred to as the series resistance). These transients caused by RC circuits can cause large artifacts during voltage clamp.

The capacitance spikes were cancelled and series resistance was compensated electronically by using amplifier circuitry (Multiclamp 700B). The series resistance was compensated at ~70%. The values of the membrane capacitance (C_m), membrane resistance (R_m) and access resistance (R_a) were recorded.

The cells were subsequently subjected to voltage-clamp protocol. Different protocols were used for K_{ATP}, $K_{2P}17$ and K_v channels whole-cell recordings.

For $K_{2P}17$ current recordings, the voltage protocol consisted of a holding potential of -80mV, followed by 200 milliseconds pulses at 20 mV increments from -100mV to +60mV with inter-pulse interval of 2 seconds. The recordings were performed with different pH extracellular solutions after achieving whole-cell configuration.

For K_v current recordings, the voltage protocol consisted of a holding potential of -80mV, followed by 200 milliseconds pulses at 20 mV increments from -100mV to +80mV with inter-pulse interval of 2 seconds. The recordings were performed immediately, 2 and 5 minutes after attaining whole-cell configuration.

For K_{ATP} channel current recordings, the voltage ramp protocol was used. From a holding potential of -80mV, cells were ramped from -150mV to +50mVover 1s (200mV/s) and then stepped back to -80mV. The recordings were performed in $5K^+$ bath solution, in 100 μM diazoxide solution (to activate K_{ATP} currents) and in (100 μM diazoxide + 100 μM tolbutamide) solution to block K_{ATP} currents.

The data were sampled at 5kHz and filtered at 1kHz with the filter provided in the Multiclamp 700B (4 Pole Bessel). Signals were converted from analogue to digital signals by Digidata 1440A (*Molecular Devices*). Recordings were acquired and analyzed using pClamp10 and Clampfit 10 (*Axon Instruments*), respectively.

4.6.7 Data Analysis

The data for whole-cell recordings were analyzed using the Clampfit 10.4 software, Microsoft Excel and Graph Pad Prism 6. The current-voltage (I-V) relationship was plotted using the Clampfit 10.4 software. Whole-cell currents were the normalized to the size (C_m) of the cell (pA/pF). The mean, standard deviation and standard error were calculated.

Student's paired t-test was used to calculate the significance of difference between the current recordings from the same cell under different conditions. Student's unpaired t-test with

Welch's correction was used to calculate the difference between the current recordings from wild type, mutant and heterozygous mutant channels.

CHAPTER 5

TWO-PORE DOMAIN POTASSIUM CHANNELS (K_{2P}) AND ELECTROPHYSIOLOGICAL ANALYSIS OF K_{2P}17 WILD TYPE AND p.F108del MUTANT

5.1 SUMMARY OF CHAPTER 5

Chapter 5 provides an introduction to two-pore domain potassium channels (K_{2P}) family followed by method used to create $K_{2P}17$ mutant construct and results of whole-cell patch clamping. The chapter ends with the discussion of the results in context with the phenotype of the patient.

5.2 INTRODUCTION

The high resting potassium conductance of the plasma membrane has been known for a long time and was thought to be due to the presence of background K^+ current conducted through potassium selective pores in the plasma membrane (Enyedi and Czirjak, 2010, Hodgkin and Huxley, 1947). The first member of the molecular entities responsible for the background K^+ currents, two-pore domain potassium channels, were identified in 1966 long after the identification of all the other major K^+ channel families (voltage-gated, inwardly rectifying, and calcium dependent K^+ channels) (Lesage et al., 1996).

The name of the family "two-pore domain" potassium channels (K_{2P}) was given on the basis of the topology of the K^+ channel subunits. Each subunit contains two K^+ channel pore loop-forming (P) domains (Enyedi and Czirjak, 2010). However other K^+ channel families contain one P domain per one subunit. Two K_{2P} subunits dimerize to constitute the functional K^+ selectivity filter containing four pore loop domains (Enyedi and Czirjak, 2010).

Each K_{2P} channel subunit has four transmembrane (TM) segments and thus has a characteristic 4TM/2P topology (figure 5.1) (Enyedi and Czirjak, 2010). The probability of opening (Po) of these channels is the same at all membrane potentials; K^+ current through these channels is not voltage dependent. These channels are also time independent; the amplitude of the current instantaneously follows the changes of the membrane potential (Lesage et al., 1996). In view of these characteristics of K_{2P} channels, a voltage step in a voltage-clamp experiment induces a square wave-like K^+ current.

The background current through these K_{2P} channels is not rectifying; equal but opposite voltage steps induce opposite currents of equal amplitude. The apparent rectification seen in

physiological solutions is caused by the unequal K^+ concentrations in the intracellular and extracellular compartment (Enyedi and Czirjak, 2010).

Many members of K_{2P} channel family encoded by different genes have been found. These members have been subdivided into six subfamilies bases on sequence similarity and functional resemblance (Enyedi and Czirjak, 2010).

1. TWIK (Tandem of Pore Domains in a Weak Inward Rectifying K^+ Channel)
2. TREK (TWIK-Related K^+ channel)
3. TASK (TWIK-Related Acid-Sensitive K^+ Channel)
4. TALK (TWIK-Related Alkaline pH-Activated K^+ Channel)
5. THIK (Tandem Pore Domain Halothane-Inhibited K^+ Channel)
6. TRESK (TWIK-Related Spinal Cord K^+ Channel)

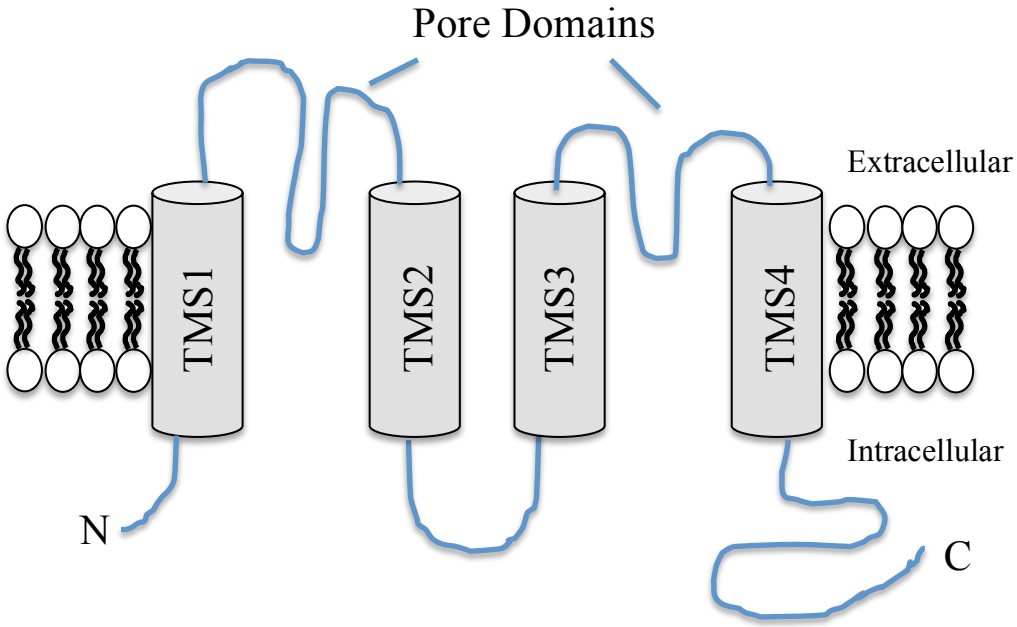

Figure 5.1: Schematic transmembrane topology of human two-pore domain potassium (K_{2P}) channels. Transmembrane segments are indicated by TMS1-4. One subunit of the functional dimer is depicted.

5.2.1 TALK subfamily

Based on the alkaline range of pH sensitivity, this subfamily has three members: TASK-2 ($K_{2P}5$), TALK-1 ($K_{2P}16$) and TALK-2 ($K_{2P}17$) (Girard et al., 2001, Decher et al., 2001). The first member of this subfamily identified was TASK-2 (Reyes et al., 1998). TALK-1 and TALK-2 are more closely related to each other than to TASK-2.

5.2.2 $K_{2P}17$ (TALK-2 or TASK-4)

Decher *et al.* cloned full-length cDNA of TASK-4 (TALK-2) channel from adrenal cDNA library (Decher et al., 2001). They named it TASK-4 but later on it was reassigned to the TALK subfamily. The full length TASK-4 cDNA encoded a protein of 343 amino acids with a predicted molecular mass of ≈ 38 kDa. TASK-4 has an extended extracellular M1P1 interdomain, which is a characteristic of this channel family (Enyedi and Czirjak, 2010). The human TASK-4 protein sequence has two consensus sites for N-glycosylation at residues 65 and 94 within this M1P1 interdomain. The cysteine at residue 68, which is conserved in members of K_{2P} channel family, is involved in homodimer formation. TASK-4 does not possess a histidine immediately downstream of the "GYG" pore motif. This histidine residue mediates proton block in TASK-3.

In addition to cloning TASK-4, Decher *et al.* also studied the expression of TASK-4 in human tissues by RT-PCR. Strongest TASK-4 signals were observed in liver, lung, placenta, pancreas, small intestine and aorta. TASK-4 was also detected in human heart where it is preferentially expressed in the atrial regions. Expression by insitu hybridization suggested

that TALK-2 transcripts are present in acinar cells and not in islets of Langerhans (Decher et al., 2001).

Experiments in Xenopus oocytes after injection of TASK-4 cRNA show quasi-instantaneous and non-inactivating currents on exposure to alkaline pH (Decher et al., 2001). The current-voltage (I-V) relationships show outwardly rectifying currents and almost no inward currents were recorded with 2mM K^+ in the extracellular fluid. Like other members of the TASK family, TASK-4 is open at all membrane potentials once extracellular fluid pH is increased. At pH 8.5, the classical K^+ channel blockers tetraethylammonium (TEA, 3mM), 4-aminopyridine (4-AP, 2mM) and Cs^+ (2mM) are inactive on the recorded currents (Decher et al., 2001). Although TASK-4 has potential phosphorylation sites for protein kinase A and protein kinase C, it does not appear TASK-4 is regulated by them.

A basic amino acid is conserved at position 242 in TALK-2 (K242). By modeling the structure of TALK-2 pore using Kv1.2 as a template, K242 was identified to occupy a position at the outermost portion of helix TM4 and close to the pore region. By mutating this lysine residue at position 242 to alanine (K242A), it was shown that sizeable currents are present at neutral pH. This suggests that lysine at position 242 acts as the pH sensor in TALK-2 channels (Niemeyer et al., 2007).

Based on the pH sensitivity, it was postulated that TASK-4 might be of great relevance in tissues such as pancreas where physiological pH can range from 7.5 to 8.5. In addition, pathophysiological situations can also cause pH shifts. It is also possible that native TASK-4 channels display a different pH dependency to that observed in heterologous expression system.

Friedrich *et al.* reported a heterozygous (c.262G>A; pGly88Arg) mutation in a TASK-4 channel in a patient with severe cardiac conduction disorder (Friedrich et al., 2014). With quantitative PCR experiments, strongest expression of TASK-4 was found in Purkinje fibers and the AV-node, followed by expression in the atrial and sinoatrial (SA)-node. By heterologously expressing the G88R mutant TASK-4 channels in Xenopus laevis oocytes and recording current voltage relationships of wild-type and mutant TASK-4 channels, threefold more outward currents were generated by mutant TASK-4 channels compared to wild-type channels. Similar cell surface expression of mutant and wild-type TASK-4 channels was shown with a chemiluminometric assay. Further experiments with G88K (p.Gly88Lys), G88E (p.Gly88Glu) and G88A (p.Gly88Ala) mutants indicated that a small residue (glycine or alanine) at position 88 is essential for normal TASK-4 channel gating.

By transfecting HL-1 cells with wild type or G88R mutants, it was shown that while wild-type TASK-4 also slowed the action potential frequency as expected from overexpression of a tandem K+ channel in cells with less hyperpolarized membrane potential, mutant G88R TASK-4 transfection caused a significantly more pronounced slowing of the spontaneous beating frequency (Friedrich et al., 2014). Patch clamp experiments of wild type and G88R mutant transfected HL-1 cells showed shortening of the action potential duration and more pronounced after hyperpolarization following the action potential.

Based on the available biological information about K_{2P} channel family (role in maintaining cellular resting membrane potential, strong expression in pancreas and heart, heterozygous $K_{2P}17$ mutation resulting in cardiac arrhythmias, the p.F108del $K_{2P}17$ mutation, identified in whole-exome sequencing of family J with cardiac and hypoglycaemia phenotype, was studied in HEK293 cell line by patch-clamping.

5.3 METHODS

5.3.1 Site-Directed Mutagenesis

The construct containing cDNA for human *KCNK17* ($K_{2P}17$) was purchased from Thermofisher Scientific Biosciences (pCMV-SPORT6). Mutation (p.F108del) was created by site-directed mutagenesis as explained in the methodology chapter. The sequences of the mutagenic primers used to create the mutation are shown in table 5.1. The $K_{2P}17$ cDNA in the construct was then sequenced to confirm the creation of the mutation using the primers shown in table 5.1.

Table 5.1: Sequences of the mutagenic and sequencing primers for *KCNK17* construct

Mutagenic Primers	**Primer Sequence**
*KCNK17*_Primer 1	GCTCGTGGGCTCCTTCTTTTCTGTGTCCACCATCAC
*KCNK17*_Primer 2	GTGATGGTGGACACAGAAAAGAAGGAGCCCACGAGC
Sequencing Primers	
*KCNK17*_attB1	ACAAGTTTGTACAAAAAAGCAGG
*KCNK17*_T7 Promoter	AATACGACTCACTATAGGG
*KCNK17*_1F	CTTCCAGCGCGACAAGTG
*KCNK17*_1R	AAAGAAGAAGGAGCCCACGA
*KCNK17*_2F	CCGCCTCTTCTGCATCTTCT
*KCNK17*_2R	CTGGGAGGGGTTCATTCCAA

5.3.2 Whole-Cell Patch Clamping

Pulse protocol was used for measuring currents through two-pore domain potassium channels subtype 17 ($K_{2P}17$) transiently expressed in HEK293 cells. After achieving the whole-cell configuration and compensating for capacitance transients and series resistance, currents were evoked by stepwise changes in the holding potential. The voltage protocol consisted of a holding potential of -80mV, followed by 200 milliseconds pulses at 20 mV increments from -100mV to +60mV with inter-pulse interval of 2 seconds. The recordings were performed with different pH extracellular solutions after achieving whole-cell configuration.

The patch-clamp amplifier software recorded the whole-cell current (pA) at different voltages during the voltage-clamp recordings. The whole-cell current (pA) was normalized for the size of the cell (whole-cell capacitance; pF) to calculate the current density (pA/pF) at different voltages.

HEK293 cells were transfected with cDNA of wild type K2P 17 (WT $K_{2P}17$), p.F108del $K_{2P}17$ mutant, and 1:1 mixture of wild type $K_{2P}17$ and p.F108del $K_{2P}17$ mutant (heterozygous p.108del $K_{2P}17$ mutant) to measure currents with different pH extracellular solutions.

5.4 RESULTS

The current-voltage relationship, mean current density (pA/pF) at +60 mV and representative traces, of wild type $K_{2P}17$ channels, p.F108del $K_{2P}17$ mutant channels and heterozygous p.F108del $K_{2P}17$ mutant channels after attaining whole-cell configurations with different pH extracellular solutions (pH 7.4, 8.5 and 10.0) are shown in figures 5.2, 5.3 and 5.4 respectively. There was significantly reduced current density (pA/pF) at +60mV with extracellular solution pH 10.0 with p.F108del $K_{2P}17$ mutant and heterozygous p.F108del $K_{2P}17$ mutant channels as compared to wild type $K_{2P}17$ channels (figure 5.5).

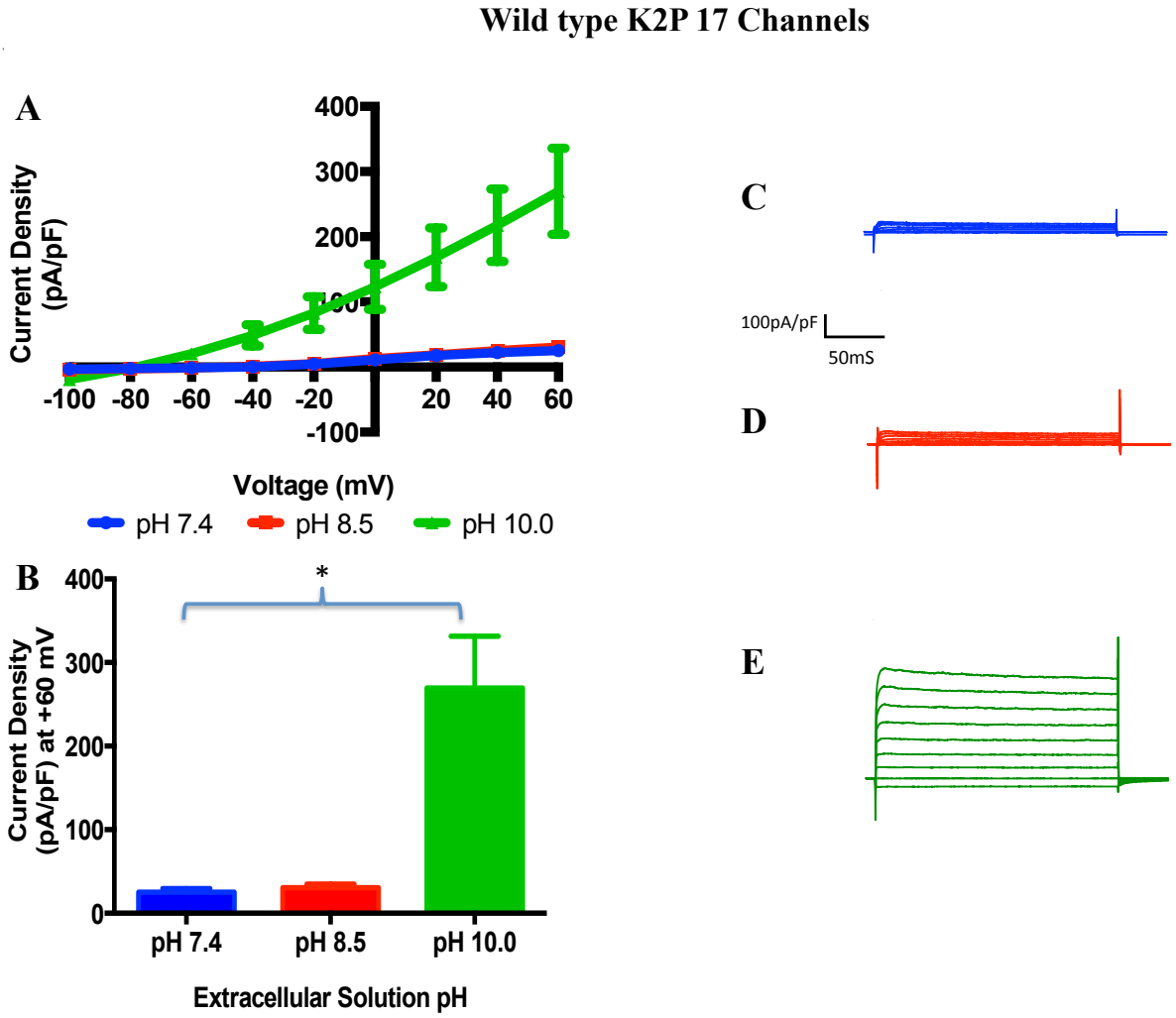

Figure 5.2. A: Current – Voltage relationships of wild type two-pore domain potassium channel subtype 17 ($K_{2P}17$) with different pH extracellular solution (pH 7.4, 8.5 and 10.0). The voltage protocol consisted of a holding potential of -80mV, followed by 200 milliseconds length pulses at 20mV increments from -100mV to +60mV with inter-pulse interval of 2 seconds. **B**: Graph showing mean current density (pA/pF) at +60mV. Data was analyzed using paired t test. *$p = 0.006$, $n = 8$. **C, D and E:** Representative traces for whole-cell recordings from HEK293 cells transfected with wild type $K_{2P}17$ with extracellular solution pH 7.4 (**C**), 8.5 (**D**) and 10.0 (**E**).

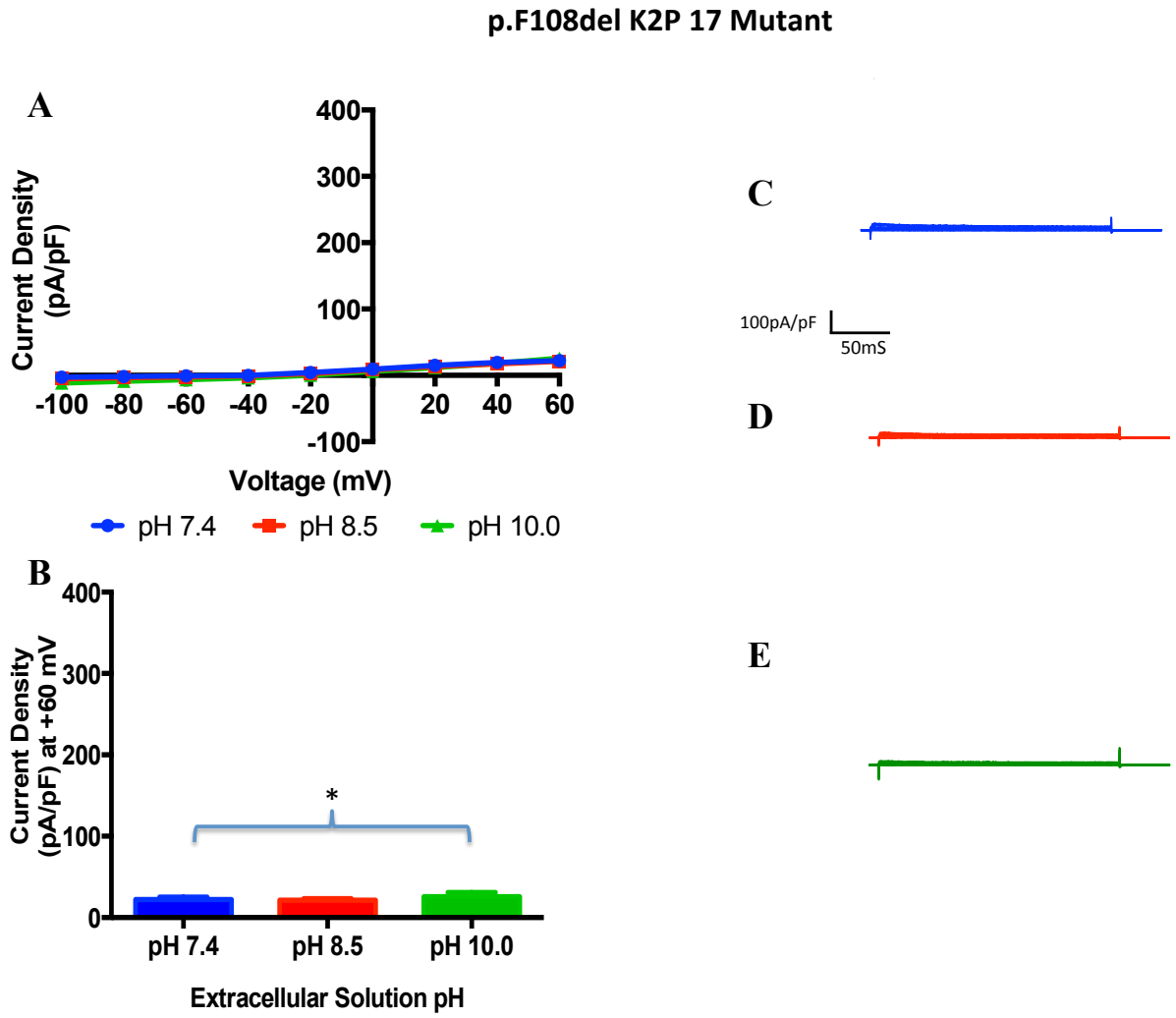

Figure 5.3. A: Current – Voltage relationships of p.F108del mutant two-pore domain potassium channel subtype 17 (p.F108del $K_{2P}17$) with different pH extracellular solution (pH 7.4, 8.5 and 10.0). The voltage protocol consisted of a holding potential of -80mV, followed by 200 milliseconds length pulses at 20mV increments from -100mV to +60mV with inter-pulse interval of 2 seconds. **B**: Graph showing mean current density (pA/pF) at +60mV. Data was analyzed using paired t test. *$p = 0.27$, $n = 7$. **C, D and E:** Representative traces for whole-cell recordings from HEK293 cells transfected with p.F108del $K_{2P}17$ mutant with extracellular solution pH 7.4 (**C**), 8.5 (**D**) and 10.0 (**E**).

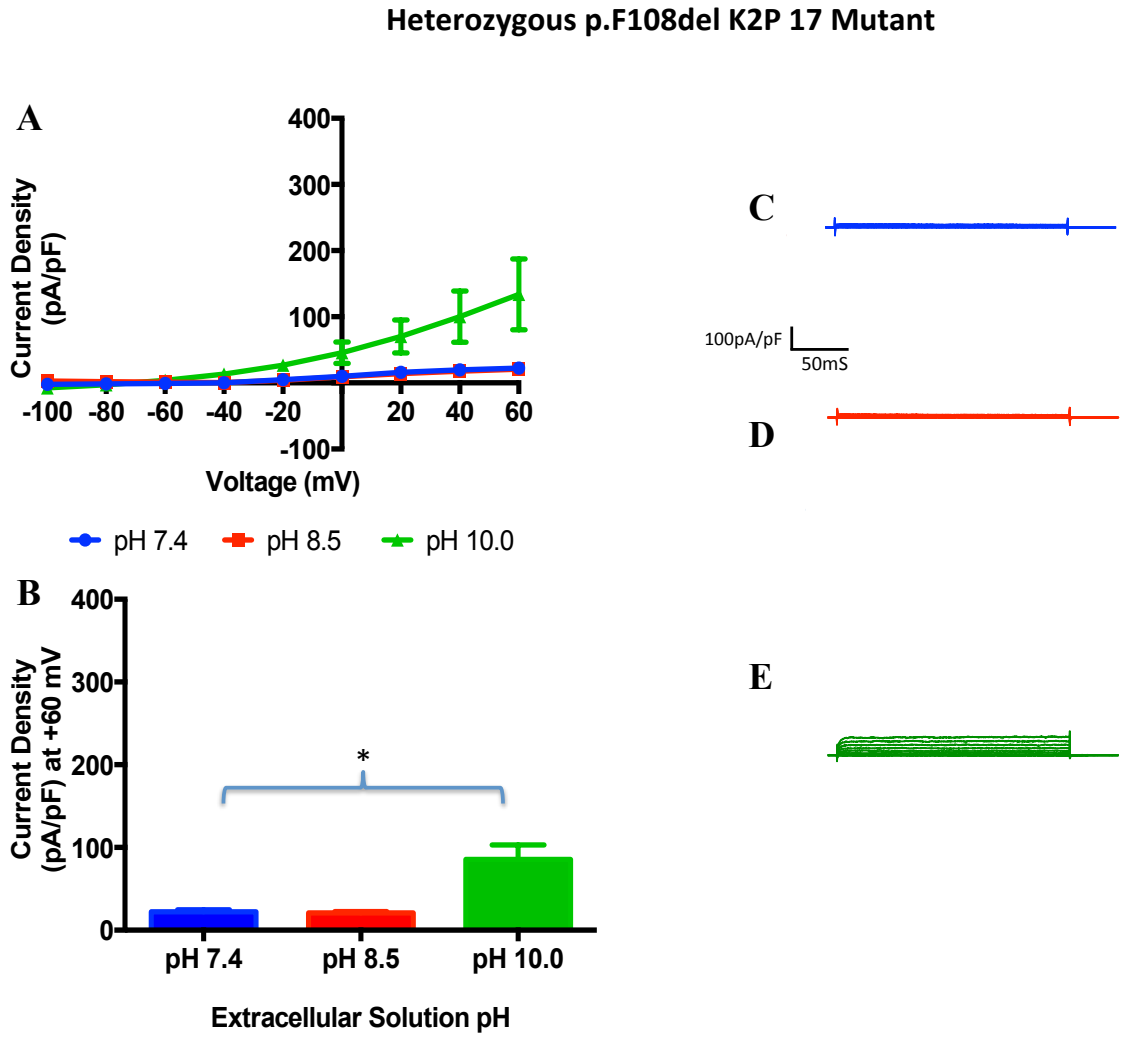

Figure 5.4. A: Current – Voltage relationships of heterozygous p.F108del mutant two-pore domain potassium channel subtype 17 (heterozygous p.F108del $K_{2P}17$) with different pH extracellular solution (pH 7.4, 8.5 and 10.0). The voltage protocol consisted of a holding potential of -80mV, followed by 200 milliseconds length pulses at 20mV increments from -100mV to +60mV with inter-pulse interval of 2 seconds. **B**: Graph showing mean current density (pA/pF) at +60mV. Data was analyzed using paired t test. *$p = 0.005$, $n = 10$. **C, D and E:** Representative traces for whole-cell recordings from HEK293 cells transfected with heterozygous p.F108del mutant $K_{2P}17$ with extracellular solution pH 7.4 (**C**), 8.5 (**D**) and 10.0 (**E**).

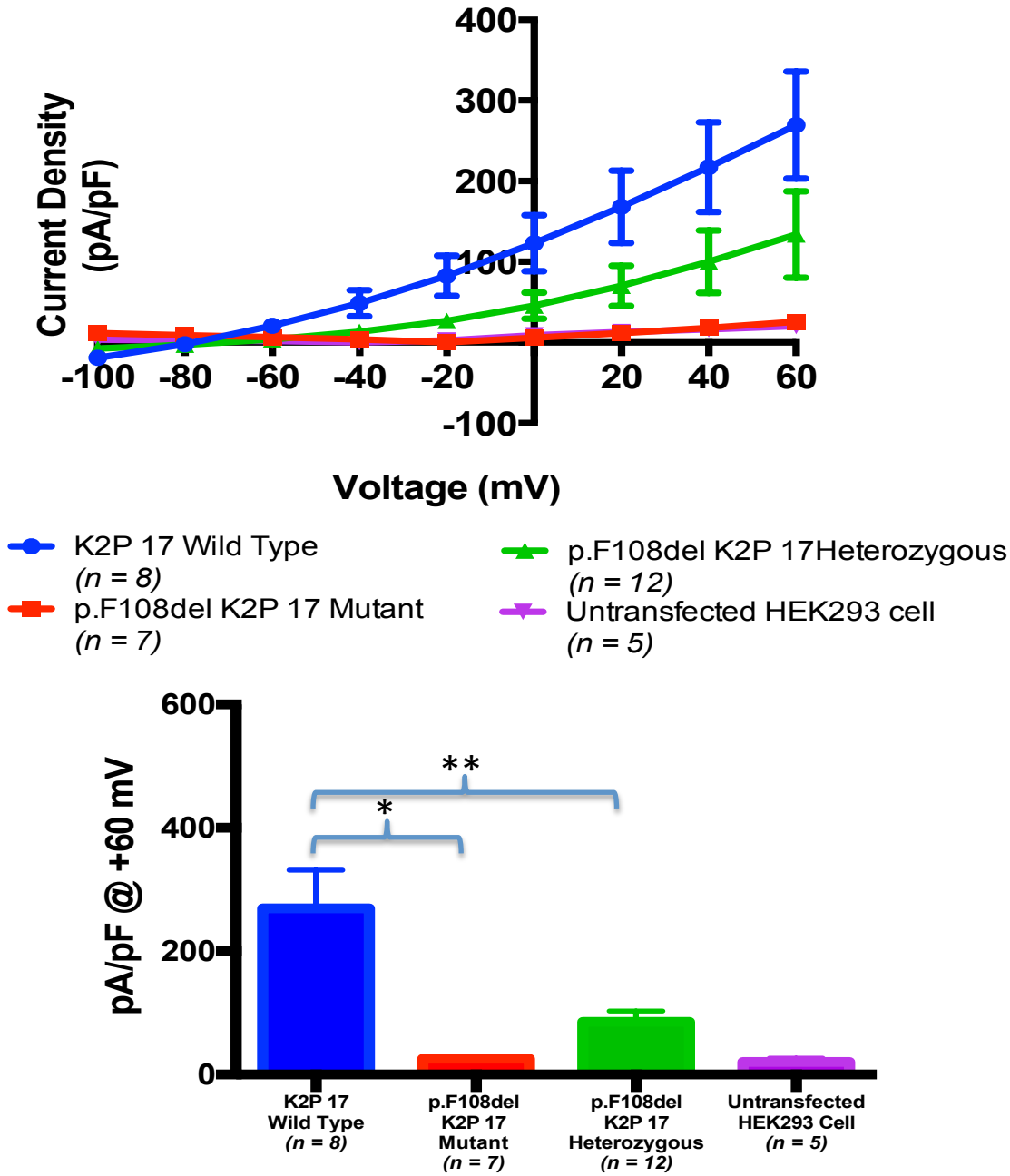

Figure 5.5. A: Current – Voltage relationships of wild type $K_{2P}17$ channels, p.F108del $K_{2P}17$ Mutant channels, heterozygous p.F108del $K_{2P}17$ mutant channels and untransfected HEK293 cells with pH 10.0 extracellular solution. **B:** Graph showing mean current density (pA/pF) at +60mV with pH 10.0 extracellular solution. Data was analyzed using unpaired t test with Welch's correction, * p = 0.006, ** p = 0.02.

5.5 DISCUSSION

The two-pore domain potassium channel subtype 17 ($K_{2P}17$) belongs to the K_{2P} family. These channels are composed of two K_{2P} subunits, each of which contains two pore-forming domains. K_{2P} channels family are responsible for the high resting potassium conductance of the plasma membrane and contribute to the cellular resting membrane potential (Enyedi and Czirjak, 2010). $K_{2P}17$ is sensitive to alkaline pH and is grouped under TALK (TWIK-Related Alkaline pH-Activated K^+ Channel) subfamily (Enyedi and Czirjak, 2010). Strong expression in human heart and pancreas has been demonstrated with RT-PCR and Northern blot analysis (Girard et al., 2001, Decher et al., 2001).

Oocytes expressing TALK-2 ($K_{2P}17$) displayed almost instantaneous (<10ms) and non-inactivating currents, which were not present in non-injected oocytes. The current-voltage (I-V) curves were outwardly rectifying in physiological K^+ solution and became linear in symmetrical K^+ solution (Girard et al., 2001). When expressed in COS cells, the current-voltage curves were similar to those recorded in oocytes (Girard et al., 2001). The reversal potentials measured in physiological K^+ (-78 ± 2 mV, n = 16) were strongly shifted towards positive values in symmetrical K^+ solution (6 ± 1 mV, n = 9) as expected for highly selective K^+ channels. The recorded currents at +50 mV in physiological K^+ solution (216 ± 42 pA, n = 16) were significantly larger than the small endogenous currents recorded in mock transfected cells (101 ± 10 pA, n = 16). Alkalization of the external solution increased TALK-2 ($K_{2P}17$) currents without altering the current kinetics or the voltage dependency (Girard et al., 2001).

In this study, HEK293 cells transfected with wild-type $K_{2P}17$ channels displayed equivalent current to the endogenous HEK293 cell current at +60 mV in physiological K^+ solution at pH 7.4 (25.28 ± 4.45 pA/pF [n = 8] *vs.* 24.53 ± 6.03 pA/pF [n = 5]; p = 0.11). Alkalinizing the

pH of the external solution from 7.4 to 8.5 did not significantly increase the $K_{2P}17$ current at +60 mV in physiological K^+ solution (25.28 ± 4.45 pA/pF, n = 8 vs. 30.47 ± 4.54 pA/pF, n = 8; p = 0.41). However increasing the pH of the external solution further to 10.0 significantly increased the $K_{2P}17$ current at +60 mV in comparison to pH 7.4 external solution (269.6 ± 61.98 pA/pF, n = 8 *vs.* 25.28 ± 4.45 pA/pF, n = 8; p = 0.006).

For p.F108del $K_{2P}17$ mutant channels, increasing the pH of the external solution from 7.4 to 10.0 did not significantly increase the current density (17.96 ± 1.95 pA/pF, n = 5 vs. 25.78 ± 4.99 pA/pF, n = 5; p = 0.27).

Although for heterozygous p.F108del $K_{2P}17$ mutant channels, increasing the pH of the external solution from 7.4 to 10.0 increased the current density significantly (22.57 ± 2.89 pA/pF vs. 85.40 ± 17.61 pA/pF, n = 10; p = 0.005), the current density was significantly less than that for wild-type $K_{2P}17$ channels (85.40 ± 17.61 pA/pF, n = 10 vs. 269.6 ± 61.98 pA/pF, n = 8; p = 0.02).

These results clearly indicate that p.F108del mutation affects the function of the $K_{2P}17$ channel and the mutant $K_{2P}17$ subunit has a dominant negative effect on the wild type $K_{2P}17$ subunit. As $K_{2P}17$ channels are responsible for the cellular resting membrane potential and have a significant expression in the pancreas and heart, it is plausible that the p.F108del $K_{2P}17$ mutation results in unstable resting membrane potential in the pancreatic β-cells and conducting system of the heart. Unstable resting membrane potential is possibly predisposing these cells to persistent depolarization and action potential.

There is very little known about the function of the $K_{2P}17$ channel in humans, as mice do not functionally express $K_{2P}17$ channels. A heterozygous mutation (p.G88R) in the $K_{2P}17$ channel was recently identified in a patient with progressive and severe cardiac conduction disorder combined with idiopathic ventricular fibrillation (Friedrich et al., 2014). As opposed to p.F108del mutant studied in this thesis, p.G88R $K_{2P}17$ mutation was a gain-of-function mutation and generated threefold increased currents. When p.G88R mutation was expressed in spontaneously beating HL-1 cell line, the action potential frequency was reduced and there was more pronounced after hyperpolarization following the action potential. Extrapolating these observations to a loss-of-function mutation like p.F108del studied in this thesis, predisposition to enhanced depolarization would be expected with pF108del mutation. This enhanced depolarization can explain the phenotype of cardiac tachyarrhythmia and enhanced glucose-induced insulin release from pancreatic β-cells based on the expression pattern of $K_{2P}17$ channels.

Expressing the p.F108del $K_{2P}17$ mutation in an insulin producing cell line and measuring the glucose-stimulated insulin-release in response would help in confirming the role of $K_{2P}17$ channels in insulin secretion from pancreatic β-cells. Sequencing *KCNK17* in genetically yet undiagnosed cases of HH can be another strategy to establish its function.

CHAPTER 6

VOLTAGE GATED POTASSIUM (K_V) CHANNELS AND ELECTROPHYSIOLOGICAL ANALYSIS OF p.A422V K_V6.2 MUTANT

6.1 SUMMARY OF CHAPTER 6

Chapter 6 provides an introduction to voltage-gated potassium channels (K_v) family, their role in insulin secretion followed by method used to create K_v6.2 mutant construct and results of whole-cell patch clamping in HEK293 cell line. The chapter ends with the discussion of the results in context with the phenotype of the patient.

6.2 INTRODUCTION

Voltage-gated potassium channels (K_v) are transmembrane channels specific for potassium and are sensitive to voltage changes in the plasma membrane potential. Typically, K_v channels are tetramers of four identical subunits (alpha subunits) arranged as a ring around a pore (Gutman et al., 2005). Each subunit has six membrane spanning hydrophobic α-helical sequences (Gutman et al., 2005). These alpha units can be subdivided into 12 classes ($K_v\alpha$1-12) on the basis of sequence homology of the hydrophobic transmembrane region. Based on the function, the alpha subunits can be grouped into 6 groups.

1. Delayed rectifier
2. A-type potassium channel
3. Outward-rectifying
4. Inward-rectifying
5. Slowly activating
6. Modifier/silencer

The delayed rectifier group can be further sub grouped into 5 subgroups based on K_v sequence homology.

1. $K_v\alpha$1.x – Shaker-related
2. $K_v\alpha$2.x – Shab-related
3. $K_v\alpha$3.x – Shaw-related
4. $K_v\alpha$7.x
5. $K_v\alpha$10.x

Based on K_v sequence homology, the modifier/silencer group can be sub grouped into 4 subgroups.

1. $K_v\alpha5.x$
2. $K_v\alpha6.x$
3. $K_v\alpha8.x$
4. $K_v\alpha9.x$

The members of the modifier/silence group are unable to form functional channels as homotetramers like other groups such as delayed rectifier K_v channels, A-type potassium channel etc. Instead the members of this group heterotetramerize with $K_v\alpha2$ family members to form conductive channels (Gutman et al., 2005).

K_v channels have a K^+ selectivity filter at the narrowest part of the transmembrane pore. The amino acid sequence (Thr-Val-Gly-Phe-Gly) or (Thr-Val-Gly-Phe-Gly) is typical to the selectivity filter of K_v channels. K^+ ions interacts with specific atomic components of Thr-Val-Gly-Tyr/Phe-Gly sequence from the four channel subunits.

6.3 ROLE OF K_V CHANNELS IN REGULATION OF INSULIN SECRETION

Following action potential due to Ca^{2+} entry through voltage-dependent Ca^{2+} channels, action potential repolarization results from activation of a delayed outward potassium current, with some contribution from Ca^{2+} activated K^+ channels. Kelly *et al.* from studies on human pancreatic islets showed that the delayed outward current activated at about -20mV and increased linearly with further depolarization (Kelly et al., 1991). The reversal of current

direction at -70mV suggested that this current is carried primarily by potassium ions. By replacing internal K^+ with impermeant cation N-methyl-D-glucamine (NMG), the authors noticed this outward current could be abolished which provide further support to the idea that this current is a potassium current (Kelly et al., 1991).

Similar delayed outward K^+ current have been described in mouse and rat β-cells and in the insulin-secreting cell lines RINm5F and HIT T15. This delayed rectifier current is sensitive to tetraethylammonium (TEA), quinine and forskolin, but not to sulfonylureas.

In a study by Henquin JC, low concentrations of TEA, which inhibits voltage sensitive K^+ channels, produced increase in glucose-induced electrical activity in mouse pancreatic β-cells. Insulin release was also slightly increased with TEA (Henquin, 1990). He concluded that voltage sensitive K^+ channels play a role in the repolarization of the spikes of β-cells (seen at high concentration of glucose) but not that of the slow waves (Henquin, 1990).

6.4 MOLECULAR ENTITIES RESPONSIBLE FOR DELAYED RECTIFIER K^+ CURRENT

Of the more than 40 known human voltage-gated potassium channel related genes that have been reported, only a subset encodes membrane proteins that produce delayed rectifier voltage-sensitive outward K^+ currents similar to those found in the β-cells. They have been named according to the single Drosophila gene locus they are most similar to: Shaker ($K_v1.x$), Shab ($K_v2.x$), and Shaw ($K_v3.x$).

Using RT-PCR, Roe *et al.* found the expression of the K^+ channel gene $K_v2.1$ in βTC3-neo (transgenically derived insulinoma) cells and β-cells purified from rodent pancreatic islets of

Langerhans (Roe et al., 1996). This was confirmed by immunoblotting of the membrane proteins in the insulinoma cells with anti-$K_v2.1$ antibody. With whole-cell patch clamping, they demonstrated the presence of delayed rectifier K^+ currents inhibited by TEA and 4-aminopyridine, with similar K_d values to that of $K_v2.1$, correlating delayed rectifier gene expression with the K^+ currents. They also showed that TEA activated large amplitude intracellular Ca^{2+} concentration oscillations and potentiated insulin secretion in the presence of glucose in the insulinoma cells (Roe et al., 1996).

In another study, high level protein expression and mRNA transcripts of $K_v1.4$, $K_v1.6$ and $K_v2.1$ were detected in rat islets and insulinoma cells (MacDonald et al., 2001). With TEA, delayed rectifier current (I_{DR}) decreased by approximately 85% and glucose-stimulated insulin secretion increased 2- to 4-fold. With the use of adenovirus-mediated expression of C-terminal truncated $K_v2.1$ subunit and $K_v1.4$ subunit, the authors established that K_v2 and K_v1 channel homologs mediate the majority of repolarizing delayed rectifier current in HIT-T15 cells and rat islet cells (MacDonald et al., 2001).

Philipson *et al.* studied the overexpression of delayed rectifier K^+ current in transgenic islets and βTC3 insulinoma cells (Philipson et al., 1994). They constructed transgenic mice and overexpressed delayed rectifier K^+ channel gene, $hK_v1.5$. The $hK_v1.5$ had previously been shown to produce TEA-resistant K^+ currents (Philipson et al., 1991). With whole-cell patch experiments, the authors confirmed the appearance of TEA-resistant K^+ currents in transgenic islet cells, the expression of which correlated with hyperglycaemia and hypoinsulinaemia (Philipson et al., 1994). Stable overexpression of $K_v1.5$ channel in insulinoma cells attenuated glucose-activated increases in intracellular Ca^{2+} concentration and also prevented the induction of TEA-dependent Ca^{2+} concentration oscillations (Philipson et al., 1994).

Zhu et al. cloned rat and human $K_v6.2$, and noticed the expression of human $K_v6.2$ mRNA in heart, liver, skeletal muscle, kidney and pancreas (Zhu et al., 1999). When expressed alone in *Xenopus* oocytes or Chinese Hamster Ovary (CHO) or HEK 293 cells, no functional $K_v6.2$ channels were noticed. However coexpression with $K_v2.1$ subunits yielded K_v channel currents distinct from those of homomultimeric $K_v2.1$ channels (Zhu et al., 1999).

Yan *et al.* investigated the expression of 26 subtypes of voltage gated potassium channels in human and rhesus pancreatic islets by RT-PCR (Yan et al., 2004). PCR fragments for 17 channel subtypes ($K_v1.3$, 1.6, 1.7, 2.1, 2.2, 3.1, 3.2, 3.3, 4.1, 4.4, 6.1, 6.2, 9.1, 9.2, 9.3, 10.1, and 11.1) were present in the pancreatic islet preparation. With insitu hybridization and immunohistochemistry, the authors showed that $K_v2.1$ mRNA-positive cells exclusively co-localized with the insulin-containing cells and confirmed the presence of $K_v2.1$ in β-cells (Yan et al., 2004). On probing the human pancreatic sections with labeled antisense oligonucleotides for $K_v6.1$ and $K_v6.2$ channels and will cell marker-specific antibodies, the authors demonstrated that $K_v6.1$ colocalized with glucagon and $K_v6.2$ with insulin containing cells (Yan et al., 2004). They hypothesized that as seen in heterologous expression systems, silent subunits ($K_v6.2$ and $K_v9.3$) coassemble with subunits from either K_v2 or K_v3 families in the human β-cells and modify their function (Yan et al., 2004).

Jacobson *et al.* investigated the role of $K_v2.1$ in β-cells from a $K_v2.1^{-/-}$ mouse model (Jacobson et al., 2007). They demonstrated that $K_v2.1$ null mice have reduced fasting blood glucose levels and elevated serum insulin as compared to control animals. In isolated islets from $K_v2.1$ null mice, they demonstrated that β-cells have reduced K_v currents (83% less at +50 mV) as compared with control cells.

Another line of evidence of involvement of K_v channels in insulin regulation comes from studies on ghrelin. Ghrelin and its receptor (Growth hormone secretagogue-receptor; GHS-R) have been shown to be located in pancreatic islets (Dezaki et al., 2004, Gnanapavan et al., 2002). It has also been shown that ghrelin inhibits insulin release in mice, rats and humans (Broglio et al., 2001, Dezaki et al., 2004). Dezaki *et al.* showed that ghrelin-induced attenuation of glucose-induced insulin release was linked to enhanced K_v channel conductance in rat islet β-cells (Dezaki et al., 2007).

Glucagon-like peptide-1 (GLP-1) that potentiates glucose-stimulated insulin secretion (GSIS) from pancreatic β-cells is hypothesized to mediate its effects through several mechanisms, including antagonism of ATP-sensitive K^+ channels, potentiation of voltage-dependent Ca^{2+} channels, release of intracellular Ca^{2+} stores etc. MacDonald *et al.* reported that GLP-1 signaling also regulates the activity of β-cell K_v channels (MacDonald et al., 2002). GLP-1 receptor activation in rat β-cells antagonized K_v currents by 43%. They implicated cAMP signaling in GLP-1 receptor modulation of β-cell K_v currents.

Based on the biological information about K_v channels, p.A422V mutation in K_v6.2 modifier subunit identified on whole-exome sequencing in family J, may reduce the delayed outward potassium current, which repolarize the cell membrane. Impaired repolarization of the pancreatic β-cells and heart as a result may result in the combined phenotype of cardiac arrhythmia and HH. The p.A422V K_v6.2 mutation was studied by patch clamping. As K_v6.2 subunits do not form homotetrameric channels, HEK293 cell line was co-transfected with K_v2.1 and K_v6.2 subunits to study the impact of p.A422V K_v6.2 mutation on the delayed outward potassium current.

6.5 METHODS

6.5.1 Site-Directed Mutagenesis

The construct containing cDNA for human *KCNG2* (K_v6.2) was purchased from Origene (pCMV-XL4). Mutation (p.A422V) was created by site-directed mutagenesis as explained in the methodology chapter. The sequences of the mutagenic primers used to create the mutation are shown in table 6.1. The K_v6.2 cDNA in the construct was then sequenced to confirm the successful creation of the mutation using the primers shown in table 6.1. The construct containing cDNA for rat *KCNB1* (K_v2.1) was kindly provided by Professor Michael Tamkun from Colorado State University, USA.

Table 6.1: Sequences Of The Mutagenic And Sequencing Primers For *KCNG2* Construct

Mutagenic Primers	**Primer Sequence**
*KCNG2*_Primer 1	CAAGGAGCAGCAGCAGCGCGTGGCCAGCCCCGAGCCGGC
*KCNG2*_Primer 2	GCCGGCTCGGGGCTGGCCACGCGCTGCTGCTGCTCCTTG
Sequencing Primers	**Primer Sequence**
*KCNG2*_VP1.5	GGACTTTCCAAAATGTCG
*KCNG2*_XL39	ATTAGGACAAGGCTGGTGGG
*KCNG2*_1F	GAGTTCTTCTTCGACCGCAG
*KCNG2*_1R	GGTCTCCAGCACGAACAGG
*KCNG2*_2F	CGTGTCCGTGTCCTTCGT
*KCNG2*_2R	AGGTGTGGAAGATGGAGGTG
*KCNG2*_Reverse	TCAGCGCCCTGCCCGCACCC

6.5.2 Whole-Cell Patch Clamping

Pulse protocol was used for measuring currents through voltage-gated potassium channels. After achieving the whole-cell configuration and compensating for capacitance transients and series resistance, voltage-activated currents were evoked by stepwise changes in the holding potential. The voltage protocol consisted of a holding potential of -80mV, followed by 200 milliseconds pulses at 20 mV increments from -100mV to +80mV with inter-pulse interval of 2 seconds.

The patch-clamp amplifier software recorded the whole-cell current (pA) at different voltages during the voltage-clamp recordings. The recordings were performed immediately, 2 and 5 minutes after achieving whole-cell configuration. The whole-cell current (pA) was normalized for the size of the cell (whole-cell capacitance; pF) to calculate the current density (pA/pF) at different voltages.

HEK293 cells were transfected with following different cDNA combinations of Voltage-gated potassium channel (Kv) subunits to measure voltage-activated currents.

1. Kv2.1 subunit only (2µg)
2. Kv6.2 wild-type subunit only (2µg)
3. Kv6.2 mutant subunit only (2µg)
4. Kv2.1 subunit (1µg) *plus* Kv6.2 wild-type subunit (1µg)
5. Kv2.1 subunit (1µg) *plus* Kv6.2 mutant subunit (1µg)
6. Kv2.1 subunit (1µg) *plus* Kv6.2 wild-type subunit (500 ng) *plus* Kv6.2 mutant subunit (500 ng)
7. No transfection (Control)

6.6 RESULTS

The current-voltage relationship and mean current density (pA/pF) at +40 mV, of voltage gated potassium channels formed of different combinations of Kv2.1, Kv6.2 WT and Kv6.2 mutant subunits in HEK293 cells, immediately, 2 and 5 minutes after attaining whole-cell configurations are shown in figures 6.1, 6.2 and 6.3 respectively. There was significantly reduced voltage-activated currents seen with voltage-gated potassium channels formed of Kv6.2 mutant subunits, as compared to voltage-gated potassium channels formed of Kv6.2 wild-type subunits *($p < 0.05$)*.

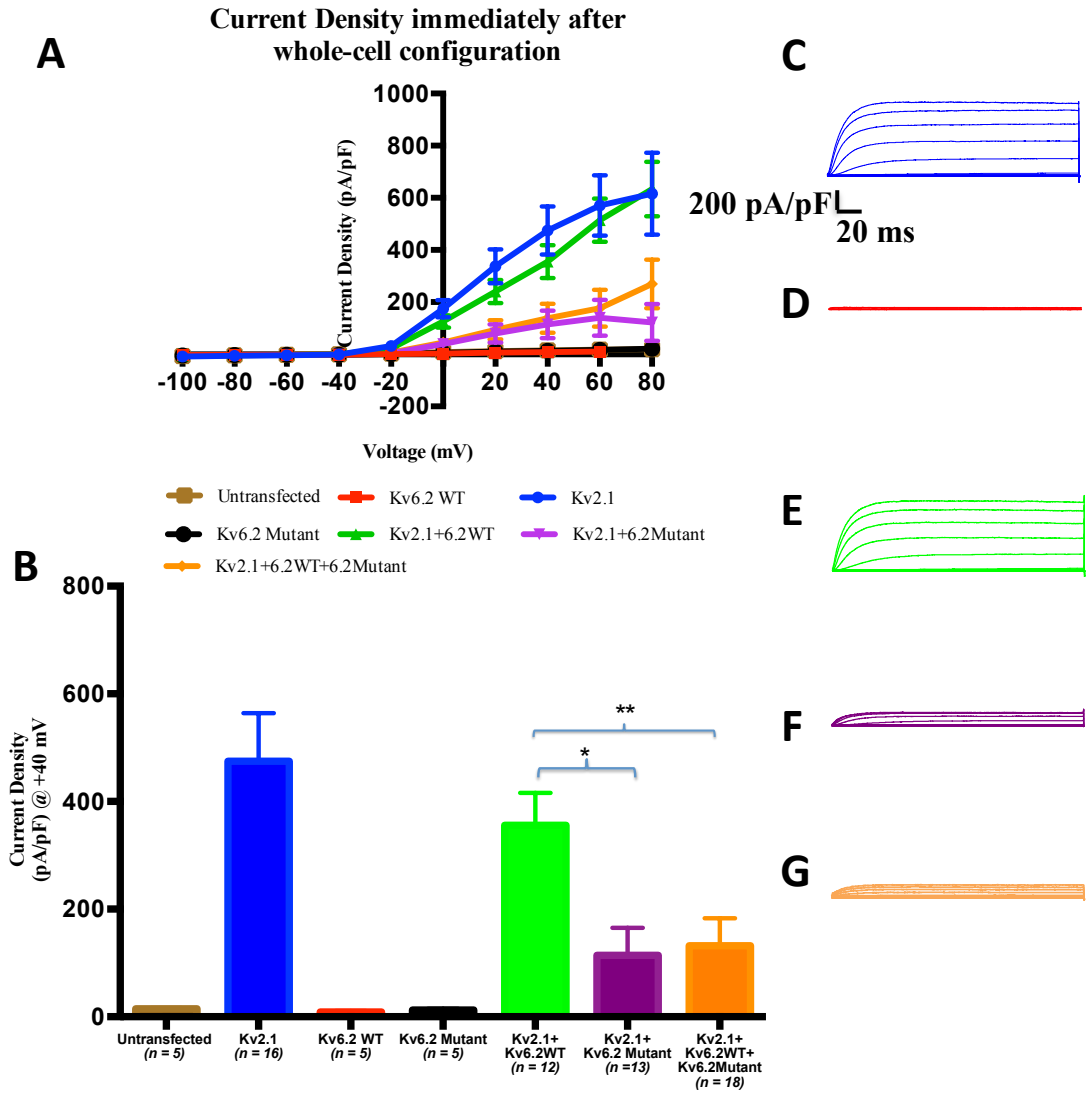

Figure 6.1. A: Current-Voltage relationships of Voltage-gated Potassium Channels (Kv Channels), formed of different combination of subunits (Kv2.1, Kv6.2WT and Kv6.2 Mutant), expressed in HEK293 cells. The recording was performed immediately after attaining whole-cell configuration. The voltage protocol consisted of a holding potential of -80mV, followed by 200 milliseconds length pulses at 20 mV increments from -100mV to +80mV with inter-pulse interval of 2 seconds. **B:** Graph showing mean current density (pA/pF) at +40 mV. The number of recordings *(n)* performed for each transfection is shown in the brackets along the x-axis. Data was analyzed using unpaired t test with Welch's correction. * $p = 0.006$ ** $p = 0.009$. **C D E F and G:** Representative traces from whole-cell patch-clamp recordings for voltage-gated potassium channels formed of Kv2.1 subunit only **(C)**, Kv6.2 wild type subunit only **(D)**, 1:1 ratio of Kv2.1 and Kv6.2 wild type subunits **(E)**, 1:1 ratio of Kv2.1 and Kv6.2 mutant subunits **(F)** and 2:1:1 ratio of Kv2.1, Kv6.2 wild-type and Kv6.2 mutant subunits **(G).** Representative traces for untransfected HEK293 cells and

cells transfected with Kv6.2 mutant were similar to the representative trace for cells transfected with Kv6.2 wild-type subunit.

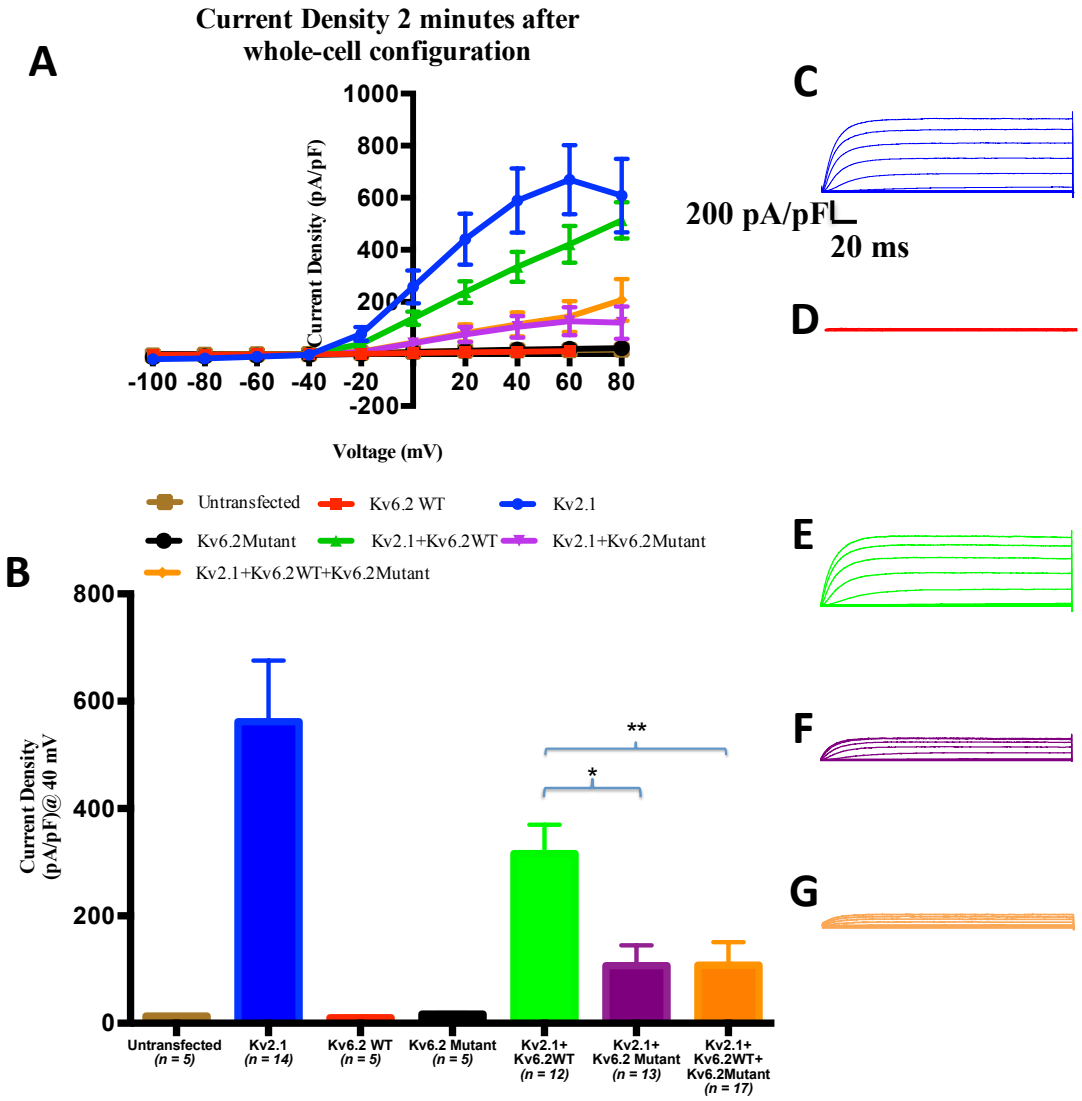

Figure 6.2. A: Current-Voltage relationships of Voltage-gated Potassium Channels (Kv Channels), formed of different combination of subunits (Kv2.1, Kv6.2WT and Kv6.2 Mutant), expressed in HEK293 cells. The recording was performed 2 minutes after attaining whole-cell configuration. The voltage protocol consisted of a holding potential of -80mV, followed by 200 milliseconds length pulses at 20 mV increments from -100mV to +80mV with inter-pulse interval of 2 seconds. **B:** Graph showing mean current density (pA/pF) at +40 mV. The number of recordings *(n)* performed for each transfection is shown in the brackets along the x-axis. Data was analyzed using unpaired t test with Welch's correction. * $p = 0.004$ ** $p = 0.006$. **C D E F and G:** Representative traces from whole-cell patch-clamp recordings for voltage-gated potassium channels formed of Kv2.1 subunit only **(C)**, Kv6.2 wild type subunit only **(D)**, 1:1 ratio of Kv2.1 and Kv6.2 wild type subunits **(E)**, 1:1 ratio of Kv2.1 and Kv6.2 mutant subunits **(F)** and 2:1:1 ratio of Kv2.1, Kv6.2 wild-type and Kv6.2 mutant subunits **(G).** Representative traces for untransfected HEK293 cells and cells

transfected with Kv6.2 mutant were similar to the representative trace for cells transfected with Kv6.2 wild-type subunit.

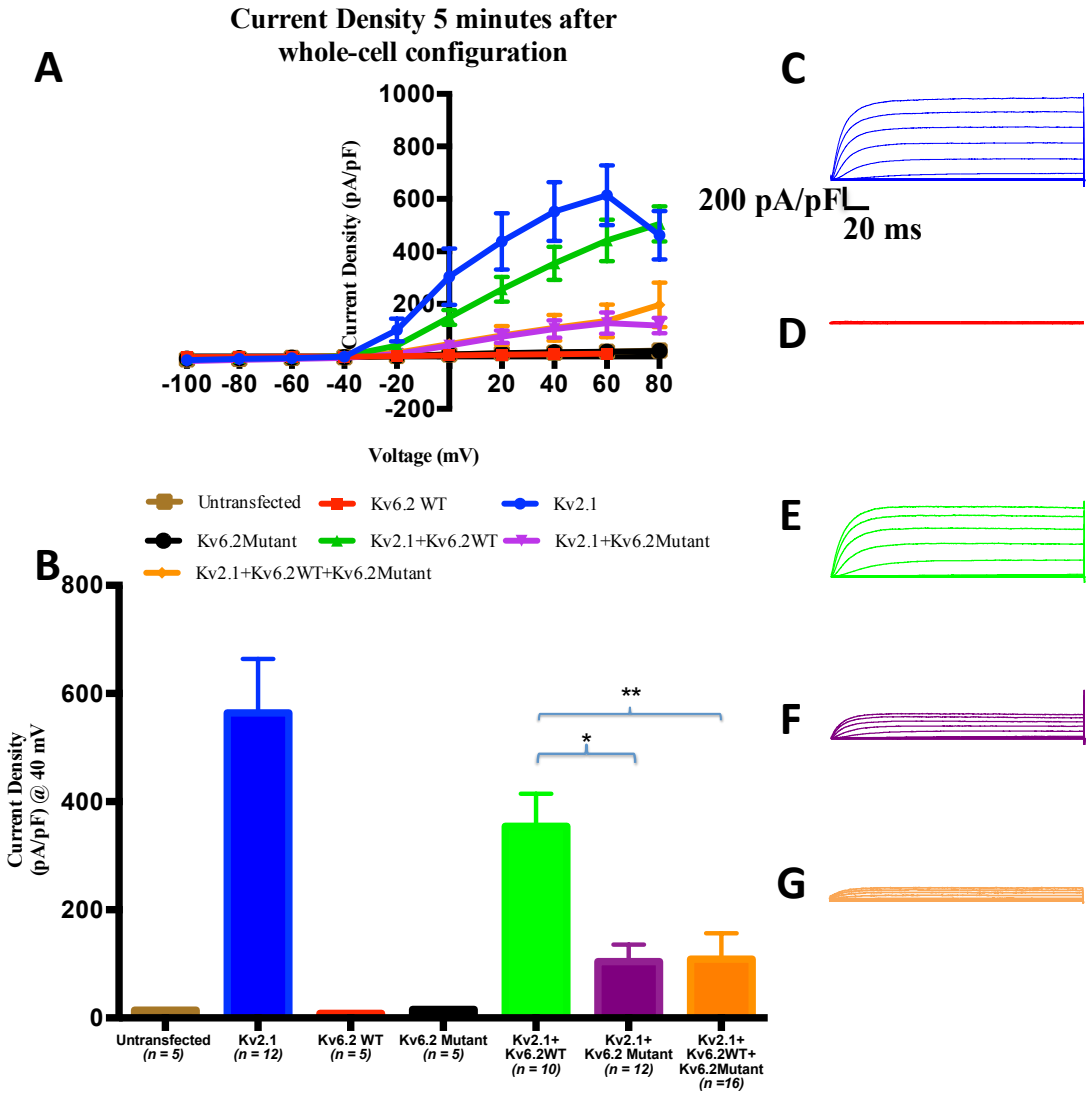

Figure 6.3. A: Current-Voltage relationships of Voltage-gated Potassium Channels (Kv Channels), formed of different combination of subunits (Kv2.1, Kv6.2WT and Kv6.2 Mutant), expressed in HEK293 cells. The recording was performed 5 minutes after attaining whole-cell configuration. The voltage protocol consisted of a holding potential of -80mV, followed by 200 milliseconds length pulses at 20 mV increments from -100mV to +80mV with inter-pulse interval of 2 seconds. **B:** Graph showing mean current density (pA/pF) at +40 mV. The number of recordings *(n)* performed for each transfection is shown in the brackets along the x-axis. Data was analyzed using unpaired t test with Welch's correction. * $p = 0.003$ ** $p = 0.005$. **C D E F and G:** Representative traces from whole-cell patch-clamp recordings for voltage-gated potassium channels formed of Kv2.1 subunit only **(C)**, Kv6.2 wild type subunit only **(D)**, 1:1 ratio of Kv2.1 and Kv6.2 wild type subunits **(E)**, 1:1 ratio of Kv2.1 and Kv6.2 mutant subunits **(F)** and 2:1:1 ratio of Kv2.1, Kv6.2 wild-type and Kv6.2 mutant subunits **(G).** Representative traces for untransfected HEK293 cells and cells

transfected with Kv6.2 mutant were similar to the representative trace for cells transfected with Kv6.2 wild-type subunit.

6.7 DISCUSSION

Voltage activated delayed outward potassium currents are responsible for repolarization after action potential (Kelly et al., 1991). Inhibition of this voltage-activated outward potassium currents by tetraethylammonium (TEA) resulted in increased glucose-induced electrical activity in mouse pancreatic β-cells as well as increased insulin secretion.

Expression studies in βTC3-neo (transgenically derived insulinoma) cells and β-cells purified from rodent pancreatic islets of Langerhans, and whole-cell patch clamping experiments suggested $K_v2.1$ channels to be responsible for these delayed outwards potassium currents (Roe et al., 1996). Other groups also reported the expression of $K_v2.1$ in human, rhesus and rat pancreatic islets as well as insulinoma cells (Yan et al., 2004, MacDonald et al., 2001).

Zhu *et al.* cloned and functionally characterized $K_v6.2$ subunit of voltage-gated potassium channels (Zhu et al., 1999). The authors demonstrated that when $K_v6.2$ was coexpressed with $K_v2.1$ subunits, heteromultimeric K_v channels were formed mediating voltage-activated delayed-rectifier type outward currents. The kinetics and conductance-voltage relationship were different than homomultimeric $K_v2.1$ channels. Preferential expression of $K_v6.2$ mRNA was seen in rat and human myocardium. Yan *et al.* reported the expression of $K_v6.2$ subunits in human pancreatic sections and also demonstrated the colocalisation of $K_v6.2$ with insulin containing cells (Yan et al., 2004).

Based on the information from the literature, it is plausible that $K_v2.1$ and $K_v6.2$ subunits coassemble to form heteromultimeric K_v channels in the pancreatic β-cells and heart, which contribute to the repolarization of the action potential. Reduced outward delayed-rectifier

potassium current due to loss-of-function mutation in $K_v2.1$ or $K_v6.2$ subunits could result in prolonged depolarization of the pancreatic β-cells and excessive insulin secretion.

In this study, the K_v channels formed of $K_v2.1$ wild type and $K_v6.2$ mutant subunits expressed significantly reduced outward potassium current as compared to K_v channels formed of $K_v2.1$ wild type and $K_v6.2$ wild type subunits.

As the K_v channels are formed of four subunits, even the heterozygous mutation is likely to result in reduced delayed rectifying outward potassium current as the mutant subunits coassemble with the wild type subunits (dominant-negative effect). In this study as well, coexpression of the mutation with wild type allele resulted in significantly reduced delayed-rectifier outward potassium current.

Reduced fasting blood glucose and elevated serum insulin were noticed in $K_v2.1^{-/-}$ mice. The β-cells from islets isolated from $K_v2.1$ null mice had reduced K_v currents as compared to control β-cells (Jacobson et al., 2007). Overexpression of delayed-rectifier potassium current in transgenic islets and βTC3 insulinoma cells resulted in the opposite phenotype of hyperglycaemia and hypoinsulinaemia (Philipson et al., 1994).

Mouse and rat β-cells as well as insulin secreting cell lines RINm5F and HIT T15 show similar delayed outward potassium current.

It is quite clear from the results that heterozygous Kv6.2 mutation resulted in reduced current through voltage-activated potassium channels.

Chapter 7

EXPRESSION OF KIR6.2 MUTANT TRANSCRIPT IN THE PANCREATIC TISSUE AND ELECTROPHYSIOLOGICAL ANALYSIS OF K_{ATP} CHANNEL MUTATIONS IN HEK293 CELLS

7.1 SUMMARY OF THE CHAPTER

The results of whole-cell patch-clamping electrophysiology experiments of two K_{ATP} channel mutants (p.T1516M SUR1 mutant and p.*391Rext*94 Kir6.2 mutant) are discussed in the current chapter. The p.*391Rext*94 Kir6.2 mutation replaces the termination codon with the amino acid arginine at codon 391 and results in addition of an extra 94 amino acids to the carboxyl terminus of Kir6.2 protein. Although it can be assumed that the normal open reading frame will simply be extended until the next in-frame stop codon is encountered, only a few human nonstop mutations have so far been characterized at either the mRNA or the protein level. In view of this, cDNA synthesized from the pancreatic tissue of the patient was sequenced as well as Western blot on the pancreatic tissue sample was performed before studying the p.*391Rext*94 Kir6.2 mutation electrophysiologically.

7.2 COMPLEMENTARY DNA (cDNA) SEQUENCING

The RNA sample was extracted from the pancreatic tissue of the patient according to the method described in the methodology chapter. The RNA was reverse-transcribed into cDNA using random hexamers as described under cDNA synthesis in Section 3.4 using SuperScript® III First-Strand Synthesis System (Invitrogen). The cDNA was amplified by PCR reaction and sequenced. Pancreatic tissue sample from another patient without *KCNJ11* mutation was used as control. The chromatogram from sequencing is shown in figure 7.1.

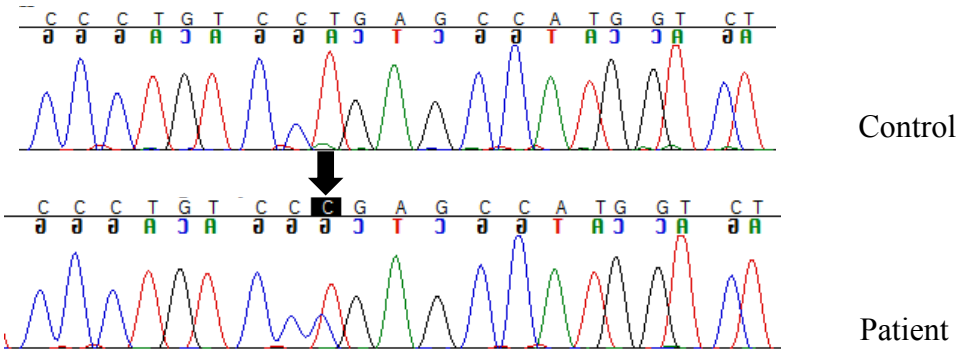

Figure 7.1: Chromatogram showing heterozygous T > C change at the termination codon (TGA) in the cDNA synthesized from the RNA extracted from the pancreatic sample of the patient. Presence of the transcript with nucleotide C at the marker position (arrow) implies the incomplete (or no) degradation of the mutant transcript by non-stop decay phenomenon.

7.3 WESTERN BLOTTING

Along with RNA, protein was also extracted from the pancreatic tissue sample of the patient with heterozygous non-stop *KCNJ11* mutation according to the method described in the methodology chapter. The protein was quantified and 20 µg sample was separated by SDS-PAGE (8%), transferred to nitrocellulose, probed with primary Kir6.2 antibody (raised in goat) followed by horseradish peroxidase (HRP)-conjugated anti-goat secondary antibody, and visualized by enhanced chemiluminescence. Protein extracted from control pancreatic tissue was run in an adjacent well as a control along with molecular weight markers. The molecular weight of Kir6.2 protein is 42kDa and the molecular weight of protein translated from *KCNJ11* transcript carrying non-stop mutation is predicted to be 52.1kDa. The western blot analysis is shown in figure 7.2

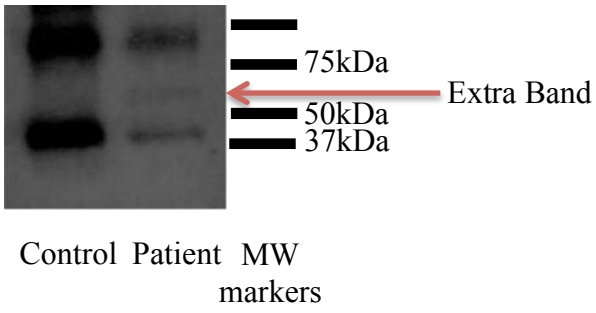

Figure 7.2: Western blot analysis of Kir6.2 proteins extracted from the pancreatic tissue of the patient and control with molecular weight markers. An extra faint band corresponding to the molecular weight of Kir6.2 protein with 94 additional amino acids was visualized in the patient, which was absent in the control pancreatic tissue. The normal sized Kir6.2 protein band was fainter as well in the patient due to translation from only one transcript.

7.4 WHOLE-CELL PATCH CLAMPING

The patch-clamp amplifier software recorded the whole-cell current (pA) at different voltages during the voltage-clamp recordings. The whole-cell current (pA) was normalized for the size of the cell (whole-cell capacitance; pF) to calculate the current density (pA/pF) at different voltages.

The recordings were performed under three different settings:

1. Immediately after attaining whole-cell configuration,
2. In the presence of diazoxide only (100 μM). This measured K_{ATP} current and endogenous HEK293 current, and
3. In the presence of diazoxide (100 μM) and tolbutamide (100 μM). This measured endogenous HEK293 current as the K_{ATP} current is inhibited by tolbutamide.

By subtracting current recorded during recording (3) from recording (2), the tolbutamide sensitive current was calculated, which is an indicator of K_{ATP} current.

For steps (2) and (3) recordings, sufficient time was given for the current to reach plateau phase. An average of four recording sweeps was used to calculate current density (pA/pF) for statistical analysis.

7.5 EXPRESSION OF WT AND MUTANT K_{ATP} CHANNELS IN HEK293 CELLS

WT SUR1/Kir6.2 Channels Expression

The whole-cell patch clamp data of HEK293 cells transfected with cDNA of hamster wild type SUR1 and mouse Kir6.2 are shown in figure 7.3. The WT K_{ATP} channels were activated with 100 μM DZX and inhibited by 100 μM TOL, as is evident from figure 7.3B. The

reversal potential for the K_{ATP} current was approximately -80 mV, which is the reversal potential for K^+.

T1516M SUR1 Mutant/WT Kir6.2 Channels Expression

The HEK293 cells transfected with cDNA for hamster T1516M SUR1 mutant and mouse WT Kir6.2 showed negligible K_{ATP} current (Figure 7.4). There was no significant change in current on exposure to diazoxide suggesting absence of K_{ATP} current. The T1516M mutation is located in the nucleotide-binding domain 2 (NBD2) region of SUR1 protein.

To simulate the heterozygous expression conditions (as seen in the proband), whole-cell patch clamp recordings were done on HEK293 cells transfected with cDNA of WT SUR1 and T1516M SUR1 mutant in 1:1 ratio along with Kir6.2 (Figure 7.5). The data suggested presence of K_{ATP} current equivalent to that seen in WT K_{ATP} channels ($p = 0.28$; Figure 7.6).

WT SUR1/p.*391REXT*94 Kir6.2 MUTANT CHANNELS EXPRESSION

Similar to p.T1516 SUR1 mutant, HEK293 cells transfected with cDNA for hamster WT SUR1 and human p.*391Rext*94 Kir6.2 mutant did not show any significant K_{ATP} current (Figure 7.7). The *391Rext*94 Kir6.2 mutant is the result of a non-stop mutation which results in addition of an extra 94 amino acids to the carboxy terminus of Kir6.2 protein.

To simulate the heterozygous expression conditions (as seen in the proband), whole-cell patch clamp recordings were done on HEK293 cells transfected with cDNA of WT Kir6.2 and p.*391Rext94* Kir6.2 mutant in 1:1 ratio along with SUR1 (Figure 7.8). The data suggested dominant negative effect of p.*391Rext94* Kir6.2 Mutant on the WT Kir6.2

protein, as evidenced by significantly reduced K_{ATP} current in the heterozygous conditions as compared to that seen in WT K_{ATP} channels ($p = 0.03$; Figure 7.9).

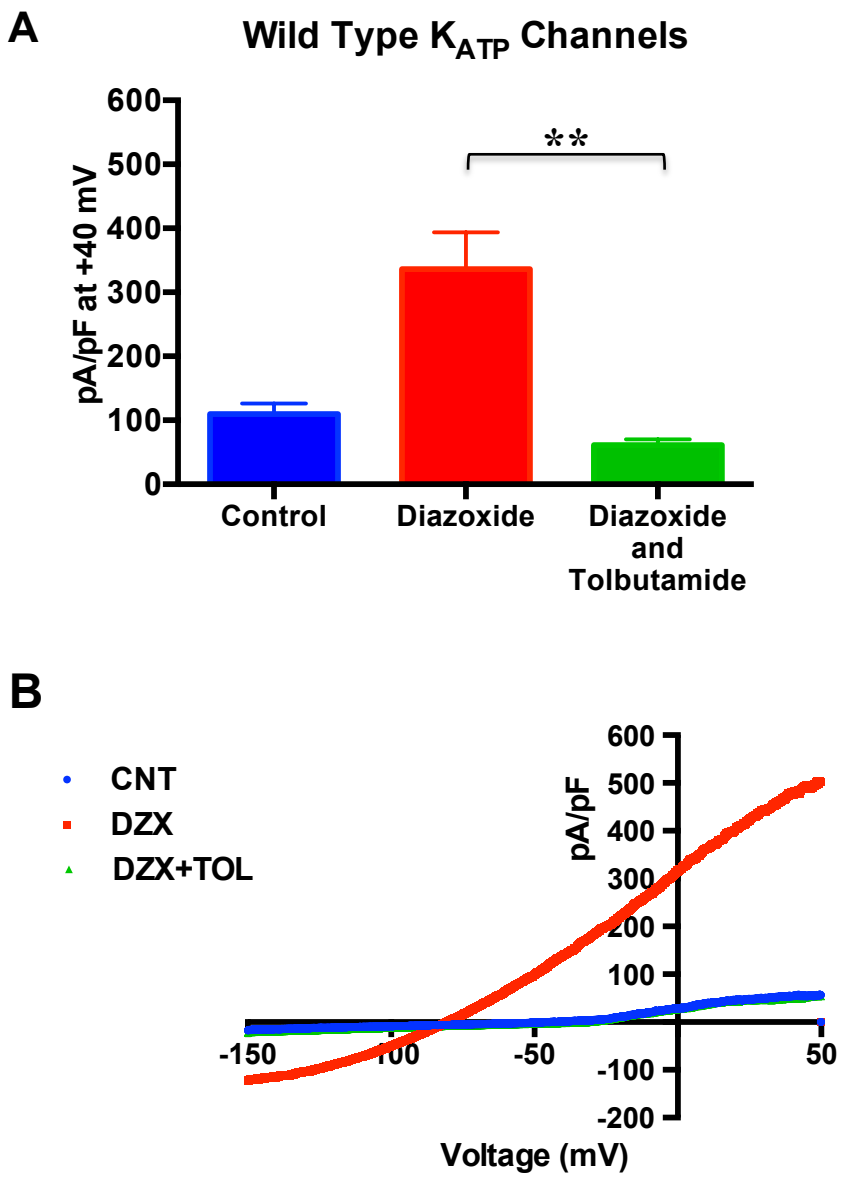

Figure 7.3: The effect of diazoxide (DZX) and tolbutamide (TOL) on the activity of wild type K_{ATP} channels (SUR1/Kir6.2) transiently expressed in HEK293 cells. After attaining whole-cell configuration, cells were voltage-clamped. The voltage-clamp protocol consisted of a holding potential of -80 mV, after which the cells were ramped from -150 mV to 50 mV over 1 second (200mV/s) and then stepped back to -80 mV. Cells were superfused with 5 K^+ bath solution (CNT), followed by 100 µM DZX to activate K_{ATP} currents, and 100 µM DZX and 100 µM Tolbutamide (DZX+TOL) to inhibit K_{ATP} currents. **A:** Graph showing mean pA/pF at +40 mV. Data was analyzed using Wilcoxon matched-pairs signed rank test, WT n = 12, **p = 0.0005. **B:** Representative trace from whole-cell patch-clamp recordings for WT cells.

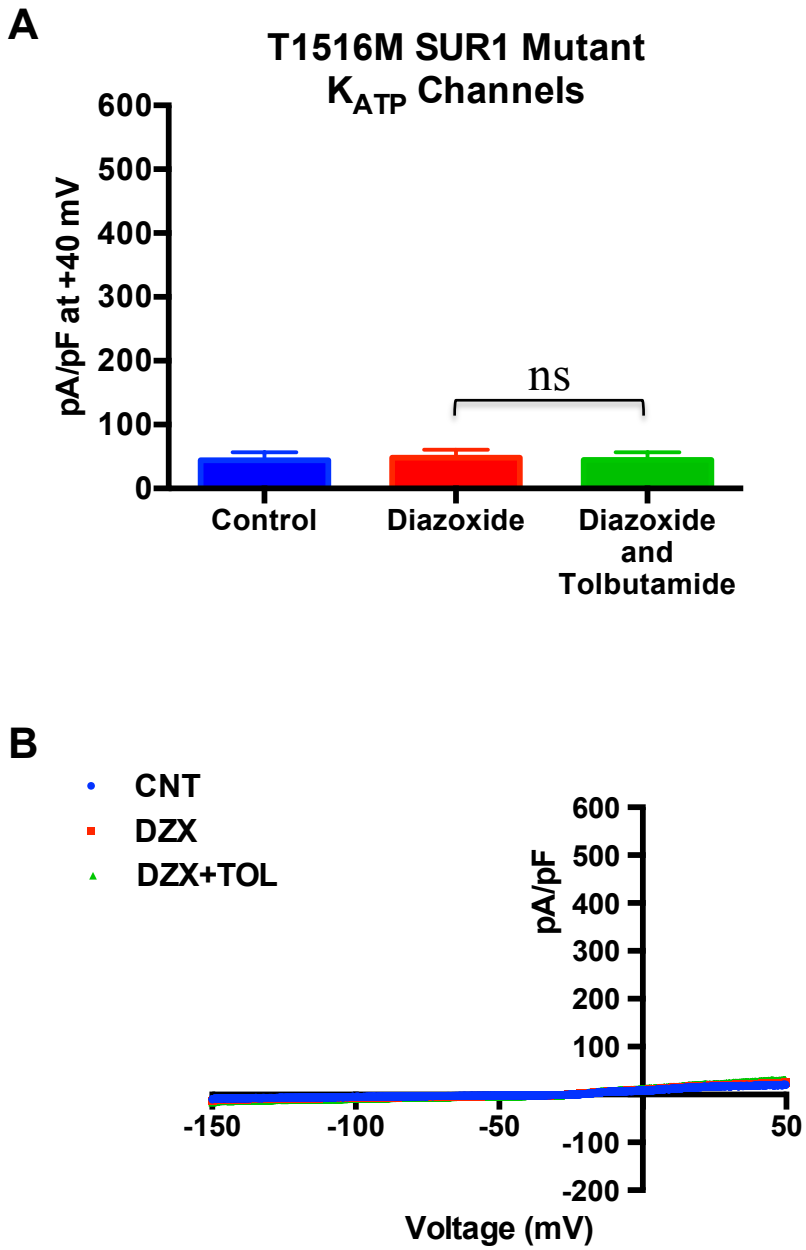

Figure 7.4: The effect of diazoxide (DZX) and tolbutamide (TOL) on the activity of mutant K_{ATP} channels (T1516M SUR1 Mutant/Kir6.2) transiently expressed in HEK293 cells. After attaining whole-cell configuration, cells were voltage-clamped. The voltage-clamp protocol consisted of a holding potential of -80 mV, after which the cells were ramped from -150 mV to 50 mV over 1 second (200mV/s) and then stepped back to -80 mV. Cells were superfused with 5 K^+ bath solution (CNT), followed by 100 µM DZX to activate K_{ATP} currents, and 100 µM DZX and 100 µM Tolbutamide (DZX+TOL) to inhibit K_{ATP} currents. **A:** Graph showing mean pA/pF at +40 mV. Data was analyzed using Wilcoxon matched-pairs signed rank test, WT n = 7, p = 0.58 (not significant [ns]). **B:** Representative trace from whole-cell patch-clamp recordings for T1516M SUR1mutant.

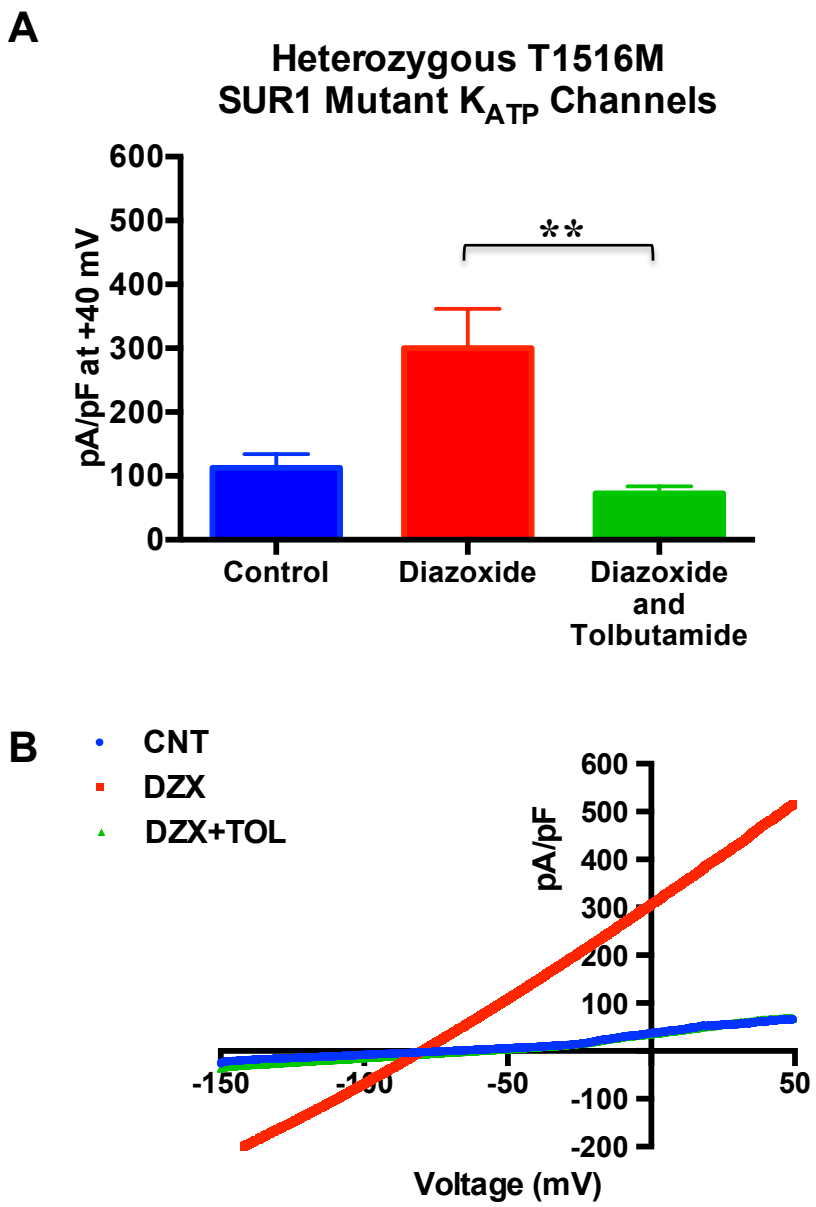

Figure 7.5: The effect of diazoxide (DZX) and tolbutamide (TOL) on the activity of heterozygous mutant K_{ATP} channels (Heterozygous T1516M SUR1 Mutant/Kir6.2) transiently expressed in HEK293 cells. After attaining whole-cell configuration, cells were voltage-clamped. The voltage-clamp protocol consisted of a holding potential of -80 mV, after which the cells were ramped from -150 mV to 50 mV over 1 second (200mV/s) and then stepped back to -80 mV. Cells were superfused with 5 K^+ bath solution (CNT), followed by 100 µM DZX to activate K_{ATP} currents, and 100 µM DZX and 100 µM Tolbutamide (DZX+TOL) to inhibit K_{ATP} currents. **A:** Graph showing mean pA/pF at +40 mV. Data was analyzed using Wilcoxon matched-pairs signed rank test, WT n = 12, **p = 0.001. **B:** Representative trace from whole-cell patch-clamp recordings for heterozygous T1516M SUR1mutant.

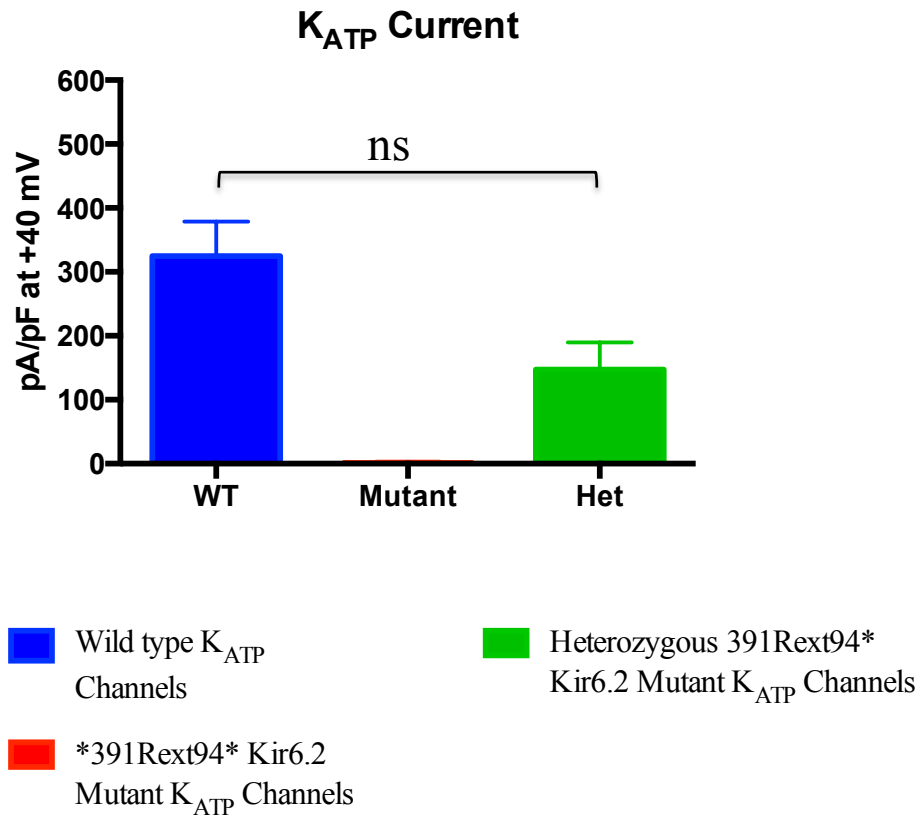

Figure: 7.6: Graph showing K_{ATP} current at +40 mV from HEK293 cells transfected with cDNA of mouse Kir6.2 along with cDNA of WT SUR1, T1516M SUR1 Mutant and 1:1 ratio of WT and T1516M SUR1 Mutant. This data was derived by subtracting the current that remained after superfusion of cells with (100 μM DZX + 100 μM TOL) from the current seen after the superfusion with 100 μM DZX only during whole-cell recordings. Data is presented as Mean ± SEM, and was analyzed using Mann-Whitney test, p = 0.28 (not significant [ns]), n = 7-12 cells.

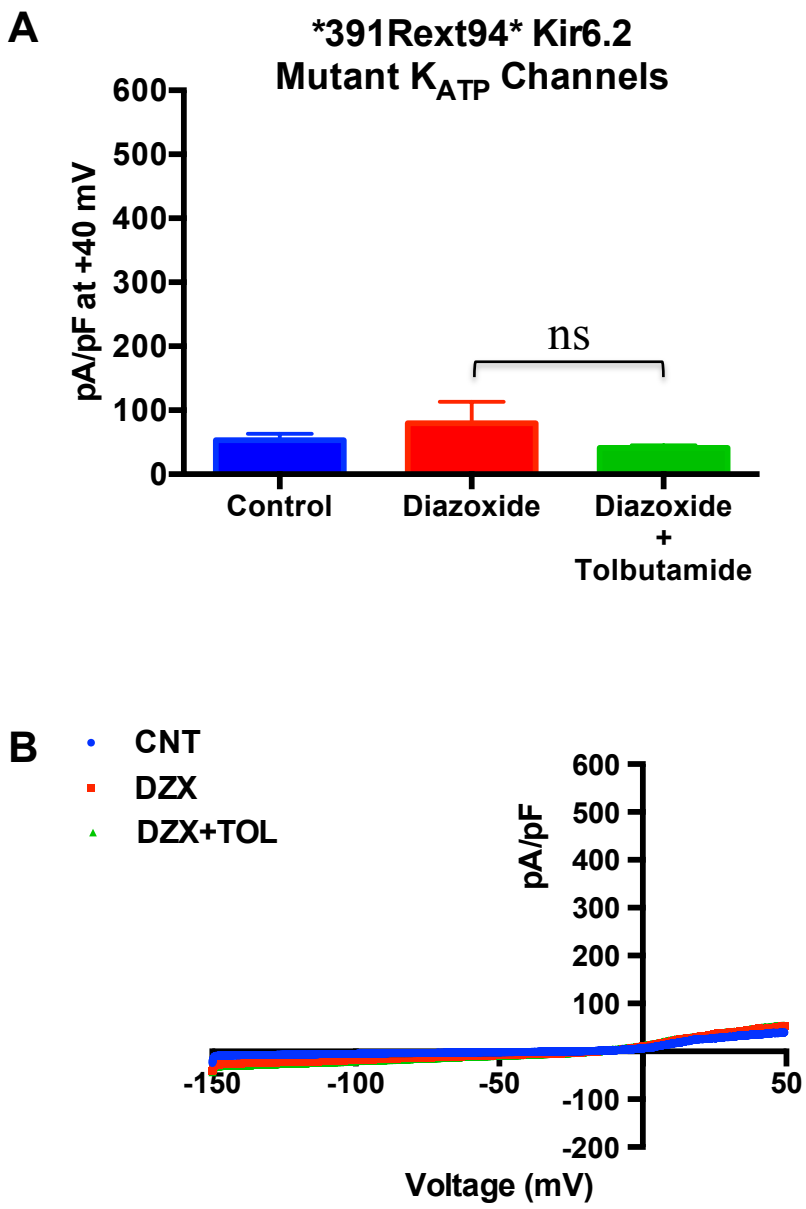

Figure 7.7: The effect of diazoxide (DZX) and tolbutamide (TOL) on the activity of mutant K_{ATP} channels (WT SUR1/*391Rext94* Kir6.2 Mutant) transiently expressed in HEK293 cells. After attaining whole-cell configuration, cells were voltage-clamped. The voltage-clamp protocol consisted of a holding potential of -80 mV, after which the cells were ramped from -150 mV to 50 mV over 1 second (200mV/s) and then stepped back to -80 mV. Cells were superfused with 5 K^+ bath solution (CNT), followed by 100 µM DZX to activate K_{ATP} currents, and 100 µM DZX and 100 µM Tolbutamide (DZX+TOL) to inhibit K_{ATP} currents. **A:** Graph showing mean pA/pF at +40 mV. Data was analyzed using Wilcoxon matched-pairs signed rank test, n = 6, p = 0.22 (not significant [ns]). **B:** Representative trace from whole-cell patch-clamp recordings for *391Rext94* Kir6.2 Mutant.

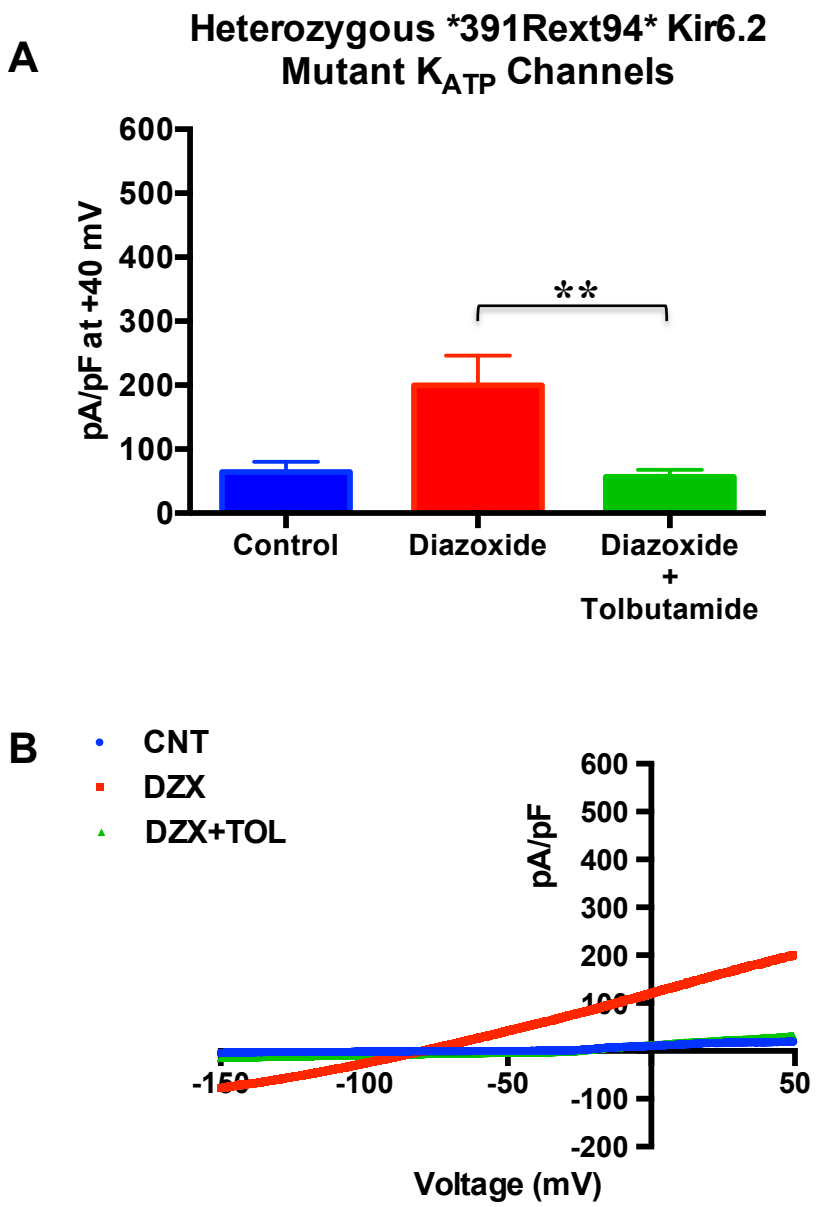

Figure 7.8: The effect of diazoxide (DZX) and tolbutamide (TOL) on the activity of heterozygous mutant K_{ATP} channels (Heterozygous WT SUR1/*391Rext94* Kir6.2 Mutant) transiently expressed in HEK293 cells. After attaining whole-cell configuration, cells were voltage-clamped. The voltage-clamp protocol consisted of a holding potential of -80 mV, after which the cells were ramped from -150 mV to 50 mV over 1 second (200mV/s) and then stepped back to -80 mV. Cells were superfused with 5 K^+ bath solution (CNT), followed by 100 µM DZX to activate K_{ATP} currents, and 100 µM DZX and 100 µM Tolbutamide (DZX+TOL) to inhibit K_{ATP} currents. **A:** Graph showing mean pA/pF at +40 mV. Data was analyzed using Wilcoxon matched-pairs signed rank test, WT n = 12, **p = 0.002. **B:** Representative trace from whole-cell patch-clamp recordings for heterozygous *391Rext94* Kir6.2 mutant.

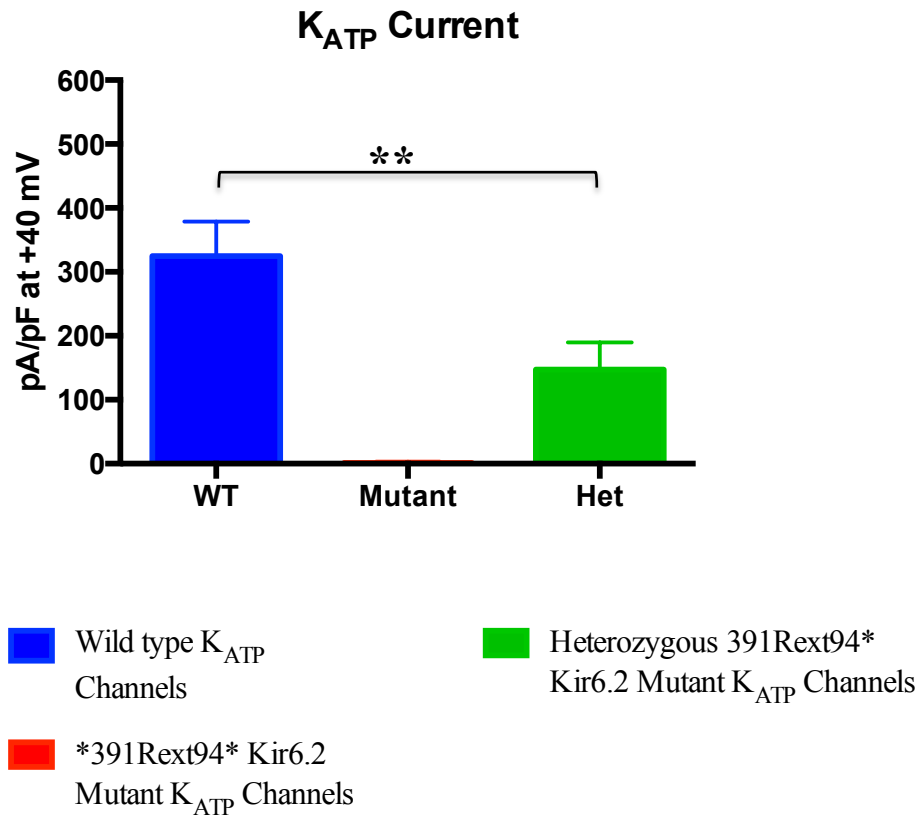

Figure: 7.9: Graph showing K_{ATP} current at +40 mV from HEK293 cells transfected with cDNA of hamster SUR1 along with human cDNA of WT Kir6.2, *391Rext94* Kir6.2 Mutant and 1:1 ratio of WT and *391Rext94* Kir6.2Mutant. This data was derived by subtracting the current that remained after superfusion of cells with (100 μM DZX + 100 μM TOL) from the current seen after the superfusion with 100 μM DZX only during whole-cell recordings. Data is presented as Mean ± SEM, and was analyzed using Mann-Whitney test, **p = 0.03, n = 6-10 cells.

7.6 DISCUSSION

The p.T1516M SUR1 and p.*391Rext*94 Kir6.2 mutants under homozygous expression conditions did not show any response to diazoxide or tolbutamide. However under heterozygous expression, the HEK293 cells transfected with p.T1516M SUR1 mutant displayed equivalent K_{ATP} current as that seen with the wild type K_{ATP} channels. In comparison, HEK293 cells transfected with p.*391Rext*94 Kir6.2 mutant under heterozygous expression conditions displayed significantly reduced K_{ATP} current as compared to the WT K_{ATP} channels. These results correlate well with the clinical phenotype observed in the patients carrying these two K_{ATP} channel mutations. In the family with p.T1516M SUR1 mutation, HH resolved in both the patients (recruited in this thesis) within the first few weeks of life, which suggests that the wild type SUR1 subunits was able to rescue the function of p.T1516M SUR1 mutant subunits. The other explanation could be that the K_{ATP} channels under heterozygous conditions were formed by only wild type SUR1 subunits, and the mutant p.T1516M SUR1 subunits were retained in the endoplasmic reticulum and not trafficked to the plasma membrane.

With regard to the Kir6.2 mutant (p.*391Rext*94 mutation), the WT Kir6.2 subunits were able to rescue the function of mutant subunits but not completely as the K_{ATP} current under simulated heterozygous conditions was significantly reduced as compared to WT K_{ATP} channels. To exclude the possibility of complete degradation of the mutated transcript by nonstop mRNA decay and no translation from the mutated transcript, RNA and protein was extracted from the pancreatic tissue of the patient with heterozygous nonstop Kir6.2 mutation.

Non-stop mRNA decay is a cellular mechanism of mRNA surveillance to detect mRNA molecules lacking a stop codon and prevent these mRNAs from translation (Frischmeyer et al., 2002). In yeast, nonstop mRNAs are recognized by the protein Ski7 on ribosomes that have become stalled at the 3´ ends of the mRNAs (van Hoof et al., 2002). These RNAs are then targeted by exosome-mediated degradation (van Hoof et al., 2002). Precisely how effective nonstop mRNA decay is in humans is unclear. Evidence points towards this to be a gene- and mutation-dependent process (Danckwardt et al., 2008).

With the techniques of cDNA synthesis and sequencing, and Western blotting, the presence of mutated transcript and protein in the pancreatic tissue was established before conducting electrophysiological experiments in the HEK293 cells transfected with the Kir6.2 mutants.

The significantly reduced K_{ATP} current under the heterozygous expression conditions of p.*391Rext*94 Kir6.2 mutant as compared to wild type K_{ATP} channels suggest dominant negative effect of the mutant. However the reduced K_{ATP} current under the heterozygous expression conditions could be due to haploinsufficiency.

Dominantly inherited K_{ATP} mutant subunits usually traffic normally to the plasma membrane. Pinney *et al* studied the surface expression and functional properties of 14 K_{ATP} channel mutants (*ABCC8* – 11; *KCNJ11* – 3) in COSm6 cells using immunofluorescence staining and quantitative chemiluminescence assay (Pinney et al., 2008). The authors observed that the surface expression of the various K_{ATP} channel mutants varied between 64.7 ± 12.9 % to 126.7 ± 7.5% relative to the WT K_{ATP} channel expression. A number of mutants studied by the authors (E1507K, I1512T, and R1539E) were located very near to the location of T1516M mutant studied in this thesis, suggesting that the trafficking of T1516M mutant to

the plasma membrane surface would be unaffected. However the surface expression of T1516M mutant was not studied in this thesis.

Huopio *et al* described the first dominantly inherited SUR1 mutation, E1506K, which caused CHI (Huopio et al., 2000). However, the authors used a different numbering system and according to the 1582 amino acid transcript (NM_000352.3), this mutation actually is E1507K. To avoid confusion, the E1506K mutation will be referred as E1507K from here onwards. The authors studied the function of the mutant by two-electrode voltage-clamp studies in the oocytes of Xenopus laevis. They noticed that although metabolic poisoning induced little effect on the currents recorded from oocytes injected with Kir6.2/SUR1-E1507K, subsequent addition of diazoxide activated currents that were blocked by tolbutamide. These results indicated that SUR1-E1507K subunits were capable of forming functional K_{ATP} channels with Kir6.2. The authors also observed that the failure of Kir6.2/SUR1-E1507K channels to respond to metabolic inhibition was not a consequence of an altered ATP sensitivity, but possibly due to lack of MgADP activation.

When Huopio *et al* coexpressed Kir6.2 with a 1:1 mixture of wild type and mutant SUR1 subunits, they observed that the amplitude of K_{ATP} currents activated by metabolic inhibition in oocytes expressing Kir6.2 and a 1:1 mixture of wild type and mutant SUR1 was approximately half that found for oocytes expressing wild type Kir6.2/SUR1 channels (Huopio et al., 2000). The authors did not perform statistical analysis to look whether the difference in the K_{ATP} current between wild type Kir6.2/SUR1 channels and those channels with Kir6.2 and 1:1 mixture of wild type and mutant SUR1 subunits was statistically significant. They concluded that E1507K mutation does not have a dominant negative effect.

Thornton *et al* functionally characterized a trinucleotide deletion in SUR1 exon 34 (delSer1387) (Thornton et al., 2003). The authors reconstituted mutant SUR1 subunits with wild type Kir6.2 to form mutant KATP channels in COSm6 cells. By photolabeling the cells with a high affinity sulfonylurea ligand [^{125}I]azido-glibenclamide and surface immunofluorescence studies, the authors demonstrated that delSer1387 SUR1 mutant K_{ATP} channels trafficked normally to the plasma membrane, similar to wild-type. On glibenclamide-inhibitable [$^{86}Rb^{+}$] efflux studies, no rubidium efflux was noticed in response to metabolic inhibition and in the presence of diazoxide, indicating that the mutant K_{ATP} channels were non-functional.

However expression studies with equimolar mixtures of wild type and delSer1387 SUR1 resulted in rubidium efflux similar to control. The authors commented that the mechanism of hyperinsulinism associated with heterozygosity for the delSer1387 mutation remains speculative. It might be due to reduction in the number of active K_{ATP} channels to a point that the plasma membrane is partly, but not completely depolarized. Patients with heterozygous SUR1 mutants that traffic normally to the plasma membrane would be predicted to have only 1/16 the normal number of channels, as compared to ½ expected with mutations that result in defective trafficking to the plasma membrane surface. Significantly less number of normal K_{ATP} channels in dominantly acting mutations could result in partial depolarization of the β-cell plasma membrane. However what is puzzling is that when the heterozygous conditions are simulated in vitro by using equimolar mixture of wild type and mutant subunits, the K_{ATP} current observed is equivalent to wild type K_{ATP} channels.

Recently, the same group from Philadelphia reported 13 different dominant SUR1 mutations causing diazoxide-unresponsive CHI in 15 families (Macmullen et al., 2011). Twelve of the 13 mutations were novel. Expression of mutations in COSm6 cells revealed normal

trafficking of channels but severely impaired responses to diazoxide or MgADP. Of these 13 mutations studied, they reported results under simulated heterozygous conditions for only S1387Y mutant. The MgADP response and diazoxide response (calculated as the current in K-INT solution plus 0.1mmol/L ATP, 0.5mmol/L ADP or 0.2mmol/L diazoxide, and 1 mmol/L free Mg^{2+} relative to that in plain K-INT solution) was approximately 10 and 25% respectively. The difference between homozygous and heterozygous expression was not as pronounced as one would expect from only $1/16^{th}$ normal number of channels in dominant acting SUR1 mutations. The authors mentioned that their previous speculation of "spare normal channels" is not sufficient in light of their data. Other non-genetic factors such as chance exposure to fasting stress or protein meals, or possibly epigenetic modifiers might play a role.

7.7 CONCLUSIONS

Under homozygous expression, both the K_{ATP} mutants (p.T1516M SUR1 and p.*391Rext*94 Kir6.2) studied in this thesis were disease causing mutants. Under heterozygous expression conditions, wild type SUR1 subunits were able to rescue the function of p.T1516M SUR1 subunits, and generate K_{ATP} current equivalent to wild type K_{ATP} channels. These results are partly consistent with the clinical phenotype of transient HH with heterozygous p.T1516M SUR1 mutation. However, it is unclear how in the first few weeks, heterozygous p.T1516M mutation resulted in reduced K_{ATP} current in the pancreatic β-cell to cause HH. There is likely to be involvement of other genetic (epigenetic modifiers) or non-genetic factors.

The p.*391Rext*94 Kir 6.2 mutant, under heterozygous expression, displayed significantly reduced K_{ATP} current as compared to wild-type K_{ATP} channels. These results are in keeping with the phenotype of diazoxide-responsive HH in the patient. However, this patient earlier was diazoxide-unresponsive and had a focal HH on ^{18}F DOPA PET scan, which was removed surgically and confirmed histologically and by microsatellite markers analysis. The focal lesion would have the p.*391Rext*94 Kir6.2 mutation in a homozygous state due to loss of the normal maternal allele. The K_{ATP} currents measured under homozygous p.*391Rext*94 Kir6.2 mutant expression is indicative of the state of the pancreatic β-cells in the focal lesion. As no K_{ATP} currents were present under homozygous p.*391Rext*94 Kir6.2 mutant expression, not surprisingly the patient was diazoxide-unresponsive before the focal lesion was removed. To summarize, the clinical phenotype and whole-cell patch clamping data suggest p.*391Rext*94 Kir6.2 mutation to be both recessive and dominant acting K_{ATP} channel mutation.

CHAPTER 8

GENERAL DISCUSSION

8.1 GENERAL DISCUSSION

Hyperinsulinaemic hypoglycaemia (HH) is the most common cause of persistent and severe hypoglycaemia in neonates, infants and children (Aynsley-Green et al., 2000). Mutations in nine different key genes involved in insulin secretion have been found as a cause of HH (Arya et al., 2014). Mutations in *ABCC8* and *KCNJ11* account for the majority of the cases in which genetic aetiology is identified (Kapoor et al., 2013, Snider et al., 2013). *ABCC8* and *KCNJ11* encode SUR1 and Kir6.2 subunits of ATP-sensitive potassium channel (K_{ATP} channel) respectively, which are present on the surface of pancreatic β-cells. K_{ATP} channels play an important role in regulating insulin secretion from pancreatic β-cells.

Diazoxide, a K_{ATP} channel agonist, is the first line of treatment for HH (Aynsley-Green et al., 2000). Based on responsiveness to diazoxide, HH can be classified into two broad groups – diazoxide-responsive HH and diazoxide-unresponsive HH. Mutations in K_{ATP} channel genes (*ABCC8* and *KCNJ11*) are identified in >90% of diazoxide-unresponsive HH (Kapoor et al., 2013, Snider et al., 2013). However, the underlying genetic aetiology is not identified in the majority of diazoxide-responsive HH (Kapoor et al., 2013, Snider et al., 2013). Both recessive and dominant acting K_{ATP} channel mutations have been described.

Histologically, there are two types of HH – diffuse and focal. In diffuse HH, the islets throughout the pancreas are enlarged and contain distinctly hypertrophied insulin producing β-cells. In focal HH, there is focal nodular hyperplasia of islet-like cell clusters, including ductuloinsular complexes and giant β-cell nuclei surrounded by a histologically and functionally normal pancreatic tissue. These two types have different underlying genetic mechanisms (Kapoor et al., 2009c).

Mutations in *GLUD1* and *HADH* are characterized by a unique clinical phenotype of protein sensitive HH (Kapoor et al., 2009b, Palladino and Stanley, 2010). Serum ammonia is mildly elevated in *GLUD1* mutations, whereas *HADH* mutations are characterized by abnormal plasma acylcarnitine profile and urine amino acid analysis (Clayton et al., 2001).

In a cohort of more than 300 congenital HH patients enrolled under Professor Khalid Hussain at Great Ormond Street Hospital, genetic aetiology was identified in only 47.6% of the patients (Kapoor et al., 2013). This cohort included patients with complex phenotypes such as protein sensitive HH with normal serum ammonia, HH with cardiac arrhythmias, and siblings from consanguineous and non-consanguineous families with unidentified genetic aetiology. A selection of these patients was studied by whole-exome sequencing.

Whole-exome sequencing is a new and powerful technique to identify genetic basis of a disease (Bamshad et al., 2011). It involves sequencing of the protein coding regions of the genome. Whole-exome sequencing has successfully identified the causal alleles for several Mendelian disorders (Bilguvar et al., 2010, Johnson et al., 2010, Walsh et al., 2010).

Whole-exome sequencing identified two potential disease-causing variants in a family with HH and cardiac arrhythmias. Whole-exome sequencing was performed on two affected members of this family (proband and her mother). Filtering whole-exome sequence data for novelty against polymorphisms available in public databases (dbSNP, 1000 Genome Project, and Exome Variant Server) identified 19 heterozygous potential disease-causing variants. Based on the biological information available about these genes in the literature, two variants (p.F108del $K_{2P}17$ and p.A422V $K_V6.2$) were strong candidates for the disease phenotype.

Whole-exome sequencing in the other families (protein sensitive HH with normal serum ammonia and families with two affected siblings) did not identify any variants in the genes after filtering, which could be considered strong candidates based on the biological information about them in the literature. This could either be due to a number of reasons. Firstly, the capture method used in the project could only capture approximately 80% of the target region and it is possible that the disease-causing variant was hence not sequenced. Secondly, may be the disease-causing variant was eliminated due to the contamination of pathogenic alleles in the public SNP databases (Bamshad et al., 2011). Last but not the least, clinical and locus heterogeneity may have accounted for the absence of potential disease-causing variants in the other families (Kapoor et al., 2012).

The $K_{2P}17$ (two-pore potassium channel subtype 17) is a K_{2P} family member and dimerize to form $K_{2P}17$ channels (Enyedi and Czirjak, 2010). These channels are responsible for the cellular resting membrane potential and are sensitive to alkaline pH (Enyedi and Czirjak, 2010, Girard et al., 2001, Decher et al., 2001). Previous studies have established strong expression of $K_{2P}17$ in human heart and pancreas (Decher et al., 2001, Girard et al., 2001). In heterologous system, p.F108del $K_{2P}17$ mutant channels (in homozygous as well as heterozygous expression) generated significantly less current as compared to wild type $K_{2P}17$ channels. Hence heterozygous p.F108del $K_{2P}17$ mutant channels could result in unstable resting membrane potential in the pancreatic β-cells and heart, and contribute/account for the clinical phenotype of HH and cardiac arrhythmias.

$K_v6.2$ subunit belongs to the modifier/silencer group of the voltage-gated potassium channels, which are tetramers arranged as a ring around a pore (Gutman et al., 2005). These subunits do not form homotetramers but form heterotetramers with $K_v\alpha2$ ($K_v2.1$ or $K_v2.2$) family

members to form conductive channels (Zhu et al., 1999). The expression in heart and pancreas of human $K_v6.2$ is well established (Yan et al., 2004, Zhu et al., 1999). Yan *et al.* also demonstrated the colocalisation of $K_v6.2$ with insulin containing cells in the human pancreatic sections.

$K_v2.1$ homotetrameric channels account for the delayed rectifier potassium current seen in βTC3-neo (transgenically derived insulinoma) cells, HIT-T15 cells and β-cells purified from rodent pancreatic islets of Langerhans (Roe et al., 1996, MacDonald et al., 2001). As $K_v6.2$ subunit is expressed in the heart and pancreas and can form channels with $K_v2.1$ subunits, it is plausible that $K_v2.1/K_v6.2$ heterotetrameric channels account for the delayed rectifier potassium current as well (Zhu et al., 1999, Yan et al., 2004). Inhibition of delayed rectifier potassium current resulted in increased glucose-induced insulin secretion in the insulinoma cells (MacDonald et al., 2001, Roe et al., 1996). Overexpression of delayed rectifier potassium current in transgenic islets and βTC3 insulinoma cells correlated with hypoinsulinaemia and hyperglycaemia (Philipson et al., 1994). The β-cells isolated from $K_v2.1^{-/-}$ mice have reduced Kv currents and $K_v2.1^{-/-}$ mice show a phenotype of reduced fasting blood glucose and elevated serum insulin as compared to control animals (Jacobson et al., 2007).

In this study, $K_v2.1$/p.A422V $K_v6.2$ mutant heterotetrameric channels generated significantly reduced K_v currents as compared to $K_v2.1$/wild type $K_v6.2$ heterotetrameric channels. This reduction in K_v current due to p.A422V $K_v6.2$ mutation is expected to result in increased glucose-induced insulin secretion from pancreatic β-cells, similar to as was observed by inhibition of K_v delayed rectifier current by TEA in HIT-T15 and rat islet cells (Roe et al., 1996, MacDonald et al., 2001).

In addition to identification of novel genetic mechanisms for congenital HH by whole-exome sequencing of patients with unidentified genetic aetiology, two K_{ATP} channel mutations associated with a unique clinical phenotype were molecularly characterized. The p.T1516M SUR1 heterozygous mutation was associated with transient HH in two cousins, whereas p.*391Rext*94 Kir6.2 heterozygous mutation was associated with a combined diffuse and focal HH phenotype.

When p.T1516M SUR1 mutant was expressed in homozygous conditions with wild type Kir6.2 in HEK293 cell line, no K_{ATP} currents were recorded, indicating that the p.T1516M SUR1 mutation was a pathogenic mutation. However under heterozygous expression conditions, K_{ATP} currents equivalent to wild type K_{ATP} channels were recorded. This indicated that either the wild type SUR1 subunits were able to rescue the function of p.T1516M SUR1 mutant subunits or the K_{ATP} channels in simulated heterozygous conditions were formed only by wild type SUR1 subunits. However for K_{ATP} channels to be formed only of wild type SUR1 subunits, mutant p.T1516M subunits would need to be retained in the endoplasmic reticulum. Whereas, dominant K_{ATP} mutations studied so far have been reported to traffic to the plasma membrane normally (Pinney et al., 2008, Thornton et al., 2003, Macmullen et al., 2011). The trafficking of p.T1516M mutation was not studied in this thesis.

Under simulated heterozygous conditions for dominant acting K_{ATP} mutations previously reported, authors have found results similar to control. Expression studies with equimolar mixtures of wild type and delSer1387 SUR1 mutant resulted in rubidium efflux similar to control (Thornton et al., 2003).

Based on these results, it is difficult to explain HH with heterozygous p.T1516M SUR1 mutation in the first few weeks of life. It has been suggested that non-genetic factors such as chance exposure to fasting or possibly epigenetic modifiers play a role (Macmullen et al., 2011, Pinney et al., 2008). Possibly, high K_{ATP} currents are required in the newborn period to suppress insulin secretion from pancreatic β-cells. A small reduction in K_{ATP} current as seen in heterozygous p.T1516 SUR1 mutation might be enough to cause HH in the neonatal period.

When p.*391Rext*94 Kir6.2 mutant was expressed in homozygous conditions with wild type SUR1 in HEK293 cell line, no K_{ATP} currents were recorded, indicating that the p.*391Rext*94 Kir6.2 mutation was a pathogenic mutation. Under heterozygous expression conditions, significantly less K_{ATP} current was recorded with wild type SUR1/ p.*391Rext*94 Kir6.2 mutant channels as compared to wild type K_{ATP} channels. The reduction in K_{ATP} current is likely to be due to dominant negative effect of p.*391Rext*94 Kir6.2 mutant rather than haploinsufficiency as the Western blotting and cDNA sequencing from the pancreatic tissue of the patient with p.*391Rext*94 Kir6.2 mutation showed the presence of the protein and transcript from both alleles. These results correlate well with the patient's phenotype of combined diazoxide-unresponsive focal and diazoxide-responsive diffuse HH.

8.2 CONCLUSIONS

In this project, a novel molecular mechanism of HH and cardiac arrhythmia phenotype was identified. Whole-exome sequencing identified two strong causative variants in a family with a phenotype of HH and cardiac arrhythmia. Electrophysiological analysis of the variants (p.F108del $K_{2P}17$ and p.A422V $K_v6.2$) proved both to be pathogenic in heterozygous expression. Strong expression of both the genes has previously been shown in pancreas and heart.

$K_{2P}17$ contribute to the cellular resting membrane potential, whereas $K_v6.2$ in combination with $K_v2.1$ subunits form heterotetrameric voltage gated potassium channels responsible for delayed rectifier repolarizing potassium currents. Inactivating mutations in $K_{2P}17$ and $K_v6.2$ are likely to result in increased glucose-induced insulin secretion (HH) and cardiac arrhythmias. Screening of more patients with the described phenotype is needed.

In this project, the molecular basis of a transient type of HH and a novel combined phenotype of focal and diffuse HH was also identified. The heterozygous SUR1 (p.T1516M) mutation was associated with transient HH, whereas Kir6.2 (p.*391Rext*94) mutation was associated with combined diffuse and focal HH phenotype. The p.*391Rext*94 Kir6.2 mutation was a non-stop mutation. The transcripts containing non-stop mutations are at risk of non-stop mRNA decay. Analysis of pancreatic tissue from the patient by cDNA sequencing and Western blotting established presence of transcript and protein with non-stop mutation. Electrophysiological analysis of p.T1516M SUR1 and p.*391Rext*94 Kir6.2 mutants was indicative of pathogenic nature of the mutation.

8.3 FUTURE WORK

Based on the results from this project, Sanger sequencing *KCNG2* and *KCNK17* in more patients with similar phenotype (HH and cardiac arrhythmias) is planned to establish the causality. Expressing the WT and mutant *KCNG2* and *KCNK17* in an insulin-producing cell line and studying the resultant effect on basal as well as glucose-induced insulin release would be another strategy to clarify the potential role of *KCNG2* and *KCNK17* in insulin release.

CHAPTER 9

REFERENCES

AGUILAR-BRYAN, L., NICHOLS, C. G., WECHSLER, S. W., CLEMENT, J. P. T., BOYD, A. E., 3RD, GONZALEZ, G., HERRERA-SOSA, H., NGUY, K., BRYAN, J. & NELSON, D. A. 1995. Cloning of the beta cell high-affinity sulfonylurea receptor: a regulator of insulin secretion. *Science,* 268**,** 423-6.

AHREN, B. 2000. Autonomic regulation of islet hormone secretion--implications for health and disease. *Diabetologia,* 43**,** 393-410.

AIZAWA, T., SATO, Y., ISHIHARA, F., TAGUCHI, N., KOMATSU, M., SUZUKI, N., HASHIZUME, K. & YAMADA, T. 1994. ATP-sensitive K+ channel-independent glucose action in rat pancreatic beta-cell. *Am J Physiol,* 266**,** C622-7.

AL-OTAIBI, H., SENNIAPPAN, S., ALAM, S. & HUSSAIN, K. 2013. Biochemical studies in patients with hyperinsulinaemic hypoglycaemia. *Eur J Pediatr*.

AL-SHANAFEY, S. 2009. Laparoscopic vs open pancreatectomy for persistent hyperinsulinemic hypoglycemia of infancy. *J Pediatr Surg,* 44**,** 957-61.

ANDERSON, K. A., MEANS, R. L., HUANG, Q. H., KEMP, B. E., GOLDSTEIN, E. G., SELBERT, M. A., EDELMAN, A. M., FREMEAU, R. T. & MEANS, A. R. 1998. Components of a calmodulin-dependent protein kinase cascade. Molecular cloning, functional characterization and cellular localization of Ca2+/calmodulin-dependent protein kinase kinase beta. *J Biol Chem,* 273**,** 31880-9.

ANTONARAKIS, S. E. & BECKMANN, J. S. 2006. Mendelian disorders deserve more attention. *Nat Rev Genet,* 7**,** 277-82.

ARYA, V. B., FLANAGAN, S. E., KUMARAN, A., SHIELD, J. P., ELLARD, S., HUSSAIN, K. & KAPOOR, R. R. 2013. Clinical and molecular characterisation of hyperinsulinaemic hypoglycaemia in infants born small-for-gestational age. *Arch Dis Child Fetal Neonatal Ed,* 98**,** F356-8.

ARYA, V. B., MOHAMMED, Z., BLANKENSTEIN, O., DE LONLAY, P. & HUSSAIN, K. 2014. Hyperinsulinaemic hypoglycaemia. *Hormone and metabolic research,* 46**,** 157-70.

ASHCROFT, F. M., HARRISON, D. E. & ASHCROFT, S. J. 1984. Glucose induces closure of single potassium channels in isolated rat pancreatic beta-cells. *Nature,* 312**,** 446-8.

AYNSLEY-GREEN, A., HUSSAIN, K., HALL, J., SAUDUBRAY, J. M., NIHOUL-FEKETE, C., DE LONLAY-DEBENEY, P., BRUNELLE, F., OTONKOSKI, T., THORNTON, P. & LINDLEY, K. J. 2000. Practical management of hyperinsulinism in infancy. *Arch Dis Child Fetal Neonatal Ed,* 82**,** F98-F107.

BAALA, L., ROMANO, S., KHADDOUR, R., SAUNIER, S., SMITH, U. M., AUDOLLENT, S., OZILOU, C., FAIVRE, L., LAURENT, N., FOLIGUET, B., MUNNICH, A., LYONNET, S., SALOMON, R., ENCHA-RAZAVI, F., GUBLER, M. C., BODDAERT, N., DE LONLAY, P., JOHNSON, C. A., VEKEMANS, M., ANTIGNAC, C. & ATTIE-BITACH, T. 2007. The Meckel-Gruber syndrome gene, MKS3, is mutated in Joubert syndrome. *Am J Hum Genet,* 80**,** 186-94.

BAHI-BUISSON, N., EL SABBAGH, S., SOUFFLET, C., ESCANDE, F., BODDAERT, N., VALAYANNOPOULOS, V., BELLANE-CHANTELOT, C., LASCELLES, K., DULAC, O., PLOUIN, P. & DE LONLAY, P. 2008. Myoclonic absence epilepsy with photosensitivity and a gain of function mutation in glutamate dehydrogenase. *Seizure,* 17**,** 658-64.

BAMSHAD, M. J., NG, S. B., BIGHAM, A. W., TABOR, H. K., EMOND, M. J., NICKERSON, D. A. & SHENDURE, J. 2011. Exome sequencing as a tool for Mendelian disease gene discovery. *Nat Rev Genet,* 12**,** 745-55.

BAUKROWITZ, T., SCHULTE, U., OLIVER, D., HERLITZE, S., KRAUTER, T., TUCKER, S. J., RUPPERSBERG, J. P. & FAKLER, B. 1998. PIP2 and PIP as determinants for ATP inhibition of KATP channels. *Science,* 282**,** 1141-4.

BEALE, E., ANDREONE, T., KOCH, S., GRANNER, M. & GRANNER, D. 1984. Insulin and glucagon regulate cytosolic phosphoenolpyruvate carboxykinase (GTP) mRNA in rat liver. *Diabetes,* 33**,** 328-32.

BEZERRA, J. A., CARRICK, T. L., DEGEN, J. L., WITTE, D. & DEGEN, S. J. 1998. Biological effects of targeted inactivation of hepatocyte growth factor-like protein in mice. *J Clin Invest,* 101**,** 1175-83.

BILGUVAR, K., OZTURK, A. K., LOUVI, A., KWAN, K. Y., CHOI, M., TATLI, B., YALNIZOGLU, D., TUYSUZ, B., CAGLAYAN, A. O., GOKBEN, S., KAYMAKCALAN, H., BARAK, T., BAKIRCIOGLU, M., YASUNO, K., HO, W., SANDERS, S., ZHU, Y., YILMAZ, S., DINCER, A., JOHNSON, M. H., BRONEN, R. A., KOCER, N., PER, H., MANE, S., PAMIR, M. N., YALCINKAYA, C., KUMANDAS, S., TOPCU, M., OZMEN, M., SESTAN, N., LIFTON, R. P., STATE, M. W. & GUNEL, M. 2010. Whole-exome sequencing identifies recessive WDR62 mutations in severe brain malformations. *Nature,* 467**,** 207-10.

BOND, C. T., SPRENGEL, R., BISSONNETTE, J. M., KAUFMANN, W. A., PRIBNOW, D., NEELANDS, T., STORCK, T., BAETSCHER, M., JERECIC, J., MAYLIE, J., KNAUS, H. G., SEEBURG, P. H. & ADELMAN, J. P. 2000. Respiration and parturition affected by conditional overexpression of the Ca2+-activated K+ channel subunit, SK3. *Science,* 289**,** 1942-6.

BORGES, L., HSU, M. L., FANGER, N., KUBIN, M. & COSMAN, D. 1997. A family of human lymphoid and myeloid Ig-like receptors, some of which bind to MHC class I molecules. *J Immunol,* 159**,** 5192-6.

BOSSE, A., ZULCH, A., BECKER, M. B., TORRES, M., GOMEZ-SKARMETA, J. L., MODOLELL, J. & GRUSS, P. 1997. Identification of the vertebrate Iroquois homeobox gene family with overlapping expression during early development of the nervous system. *Mech Dev,* 69**,** 169-81.

BOURCIER, M. E., SHERROD, A., DIGUARDO, M. & VINIK, A. I. 2009. Successful control of intractable hypoglycemia using rapamycin in an 86-year-old man with a pancreatic insulin-secreting islet cell tumor and metastases. *J Clin Endocrinol Metab,* 94**,** 3157-62.

BRIGGS, T. A., RICE, G. I., DALY, S., URQUHART, J., GORNALL, H., BADER-MEUNIER, B., BASKAR, K., BASKAR, S., BAUDOUIN, V., BERESFORD, M. W., BLACK, G. C., DEARMAN, R. J., DE ZEGHER, F., FOSTER, E. S., FRANCES, C., HAYMAN, A. R., HILTON, E., JOB-DESLANDRE, C., KULKARNI, M. L., LE MERRER, M., LINGLART, A., LOVELL, S. C., MAURER, K., MUSSET, L., NAVARRO, V., PICARD, C., PUEL, A., RIEUX-LAUCAT, F., ROIFMAN, C. M., SCHOLL-BURGI, S., SMITH, N., SZYNKIEWICZ, M., WIEDEMAN, A., WOUTERS, C., ZEEF, L. A., CASANOVA, J. L., ELKON, K. B., JANCKILA, A., LEBON, P. & CROW, Y. J. 2011. Tartrate-resistant acid phosphatase deficiency causes a bone dysplasia with autoimmunity and a type I interferon expression signature. *Nature genetics,* 43**,** 127-31.

BROGLIO, F., ARVAT, E., BENSO, A., GOTTERO, C., MUCCIOLI, G., PAPOTTI, M., VAN DER LELY, A. J., DEGHENGHI, R. & GHIGO, E. 2001. Ghrelin, a natural GH secretagogue produced by the stomach, induces hyperglycemia and reduces insulin secretion in humans. *J Clin Endocrinol Metab,* 86**,** 5083-6.

CALABRIA, A. C., LI, C., GALLAGHER, P. R., STANLEY, C. A. & DE LEON, D. D. 2012. GLP-1 receptor antagonist exendin-(9-39) elevates fasting blood glucose levels

in congenital hyperinsulinism owing to inactivating mutations in the ATP-sensitive K+ channel. *Diabetes,* 61**,** 2585-91.

CARTIER, E. A., CONTI, L. R., VANDENBERG, C. A. & SHYNG, S. L. 2001a. Defective trafficking and function of KATP channels caused by a sulfonylurea receptor 1 mutation associated with persistent hyperinsulinemic hypoglycemia of infancy. *Proceedings of the National Academy of Sciences of the United States of America,* 98**,** 2882-7.

CARTIER, E. A., CONTI, L. R., VANDENBERG, C. A. & SHYNG, S. L. 2001b. Defective trafficking and function of KATP channels caused by a sulfonylurea receptor 1 mutation associated with persistent hyperinsulinemic hypoglycemia of infancy. *Proc Natl Acad Sci U S A,* 98**,** 2882-7.

CASTANO, J. G., NIETO, A. & FELIU, J. E. 1979. Inactivation of phosphofructokinase by glucagon in rat hepatocytes. *J Biol Chem,* 254**,** 5576-9.

CHICHEPORTICHE, Y., BOURDON, P. R., XU, H., HSU, Y. M., SCOTT, H., HESSION, C., GARCIA, I. & BROWNING, J. L. 1997. TWEAK, a new secreted ligand in the tumor necrosis factor family that weakly induces apoptosis. *J Biol Chem,* 272**,** 32401-10.

CHOUFANI, S., SHUMAN, C. & WEKSBERG, R. 2010. Beckwith-Wiedemann syndrome. *American journal of medical genetics. Part C, Seminars in medical genetics,* 154C**,** 343-54.

CHRIST, B., NATH, A., BASTIAN, H. & JUNGERMANN, K. 1988. Regulation of the expression of the phosphoenolpyruvate carboxykinase gene in cultured rat hepatocytes by glucagon and insulin. *Eur J Biochem,* 178**,** 373-9.

CHRISTESEN, H. B., JACOBSEN, B. B., ODILI, S., BUETTGER, C., CUESTA-MUNOZ, A., HANSEN, T., BRUSGAARD, K., MASSA, O., MAGNUSON, M. A., SHIOTA,

C., MATSCHINSKY, F. M. & BARBETTI, F. 2002. The second activating glucokinase mutation (A456V): implications for glucose homeostasis and diabetes therapy. *Diabetes,* 51**,** 1240-6.

CHRISTESEN, H. B., TRIBBLE, N. D., MOLVEN, A., SIDDIQUI, J., SANDAL, T., BRUSGAARD, K., ELLARD, S., NJOLSTAD, P. R., ALM, J., BROCK JACOBSEN, B., HUSSAIN, K. & GLOYN, A. L. 2008. Activating glucokinase (GCK) mutations as a cause of medically responsive congenital hyperinsulinism: prevalence in children and characterisation of a novel GCK mutation. *Eur J Endocrinol,* 159**,** 27-34.

CIUDAD, C., CAMICI, M., AHMAD, Z., WANG, Y., DEPAOLI-ROACH, A. A. & ROACH, P. J. 1984. Control of glycogen synthase phosphorylation in isolated rat hepatocytes by epinephrine, vasopressin and glucagon. *Eur J Biochem,* 142**,** 511-20.

CLAYTON, P. T., EATON, S., AYNSLEY-GREEN, A., EDGINTON, M., HUSSAIN, K., KRYWAWYCH, S., DATTA, V., MALINGRE, H. E., BERGER, R. & VAN DEN BERG, I. E. 2001. Hyperinsulinism in short-chain L-3-hydroxyacyl-CoA dehydrogenase deficiency reveals the importance of beta-oxidation in insulin secretion. *J Clin Invest,* 108**,** 457-65.

COLE, S. P., BHARDWAJ, G., GERLACH, J. H., MACKIE, J. E., GRANT, C. E., ALMQUIST, K. C., STEWART, A. J., KURZ, E. U., DUNCAN, A. M. & DEELEY, R. G. 1992. Overexpression of a transporter gene in a multidrug-resistant human lung cancer cell line. *Science,* 258**,** 1650-4.

COMBETTES-SOUVERAIN, M. & ISSAD, T. 1998. Molecular basis of insulin action. *Diabetes Metab,* 24**,** 477-89.

CONTI, L. R., RADEKE, C. M. & VANDENBERG, C. A. 2002. Membrane targeting of ATP-sensitive potassium channel. Effects of glycosylation on surface expression. *J Biol Chem,* 277**,** 25416-22.

COOK, D. L. & HALES, C. N. 1984. Intracellular ATP directly blocks K+ channels in pancreatic B-cells. *Nature,* 311**,** 271-3.

CRANE, A. & AGUILAR-BRYAN, L. 2004. Assembly, maturation, and turnover of K(ATP) channel subunits. *J Biol Chem,* 279**,** 9080-90.

CRYER, P. E. 1993. Glucose counterregulation: prevention and correction of hypoglycemia in humans. *The American journal of physiology,* 264**,** E149-55.

CRYER, P. E., AXELROD, L., GROSSMAN, A. B., HELLER, S. R., MONTORI, V. M., SEAQUIST, E. R. & SERVICE, F. J. 2009. Evaluation and management of adult hypoglycemic disorders: an Endocrine Society Clinical Practice Guideline. *The Journal of clinical endocrinology and metabolism,* 94**,** 709-28.

CUESTA-MUNOZ, A. L., HUOPIO, H., OTONKOSKI, T., GOMEZ-ZUMAQUERO, J. M., NANTO-SALONEN, K., RAHIER, J., LOPEZ-ENRIQUEZ, S., GARCIA-GIMENO, M. A., SANZ, P., SORIGUER, F. C. & LAAKSO, M. 2004. Severe persistent hyperinsulinemic hypoglycemia due to a de novo glucokinase mutation. *Diabetes,* 53**,** 2164-8.

DANCKWARDT, S., HENTZE, M. W. & KULOZIK, A. E. 2008. 3' end mRNA processing: molecular mechanisms and implications for health and disease. *EMBO J,* 27**,** 482-98.

DANIEL, J. A., SANTOS, M. A., WANG, Z., ZANG, C., SCHWAB, K. R., JANKOVIC, M., FILSUF, D., CHEN, H. T., GAZUMYAN, A., YAMANE, A., CHO, Y. W., SUN, H. W., GE, K., PENG, W., NUSSENZWEIG, M. C., CASELLAS, R., DRESSLER, G. R., ZHAO, K. & NUSSENZWEIG, A. 2010. PTIP promotes

chromatin changes critical for immunoglobulin class switch recombination. *Science,* 329**,** 917-23.

DAVIS, E. A., CUESTA-MUNOZ, A., RAOUL, M., BUETTGER, C., SWEET, I., MOATES, M., MAGNUSON, M. A. & MATSCHINSKY, F. M. 1999. Mutants of glucokinase cause hypoglycaemia- and hyperglycaemia syndromes and their analysis illuminates fundamental quantitative concepts of glucose homeostasis. *Diabetologia,* 42**,** 1175-86.

DE LEON, D. D., LI, C., DELSON, M. I., MATSCHINSKY, F. M., STANLEY, C. A. & STOFFERS, D. A. 2008. Exendin-(9-39) corrects fasting hypoglycemia in SUR-1-/- mice by lowering cAMP in pancreatic beta-cells and inhibiting insulin secretion. *The Journal of biological chemistry,* 283**,** 25786-93.

DE LEON, D. D. & STANLEY, C. A. 2007. Mechanisms of Disease: advances in diagnosis and treatment of hyperinsulinism in neonates. *Nature clinical practice. Endocrinology & metabolism,* 3**,** 57-68.

DE LONLAY-DEBENEY, P., POGGI-TRAVERT, F., FOURNET, J. C., SEMPOUX, C., VICI, C. D., BRUNELLE, F., TOUATI, G., RAHIER, J., JUNIEN, C., NIHOUL-FEKETE, C., ROBERT, J. J. & SAUDUBRAY, J. M. 1999. Clinical features of 52 neonates with hyperinsulinism. *The New England journal of medicine,* 340**,** 1169-75.

DEAN, P. M., MATTHEWS, E. K. & SAKAMOTO, Y. 1975. Pancreatic islet cells: effects of monosaccharides, glycolytic intermediates and metabolic inhibitors on membrane potential and electrical activity. *J Physiol,* 246**,** 459-78.

DECHER, N., MAIER, M., DITTRICH, W., GASSENHUBER, J., BRUGGEMANN, A., BUSCH, A. E. & STEINMEYER, K. 2001. Characterization of TASK-4, a novel member of the pH-sensitive, two-pore domain potassium channel family. *FEBS Lett,* 492**,** 84-9.

DEKEL, B., LUBIN, D., MODAN-MOSES, D., QUINT, J., GLASER, B. & MEYEROVITCH, J. 2002. Compound heterozygosity for the common sulfonylurea receptor mutations can cause mild diazoxide-sensitive hyperinsulinism. *Clin Pediatr (Phila),* 41**,** 183-6.

DEZAKI, K., HOSODA, H., KAKEI, M., HASHIGUCHI, S., WATANABE, M., KANGAWA, K. & YADA, T. 2004. Endogenous ghrelin in pancreatic islets restricts insulin release by attenuating Ca2+ signaling in beta-cells: implication in the glycemic control in rodents. *Diabetes,* 53**,** 3142-51.

DEZAKI, K., KAKEI, M. & YADA, T. 2007. Ghrelin uses Galphai2 and activates voltage-dependent K+ channels to attenuate glucose-induced Ca2+ signaling and insulin release in islet beta-cells: novel signal transduction of ghrelin. *Diabetes,* 56**,** 2319-27.

DOUGLAS, J., CILLIERS, D., COLEMAN, K., TATTON-BROWN, K., BARKER, K., BERNHARD, B., BURN, J., HUSON, S., JOSIFOVA, D., LACOMBE, D., MALIK, M., MANSOUR, S., REID, E., CORMIER-DAIRE, V., COLE, T. & RAHMAN, N. 2007. Mutations in RNF135, a gene within the NF1 microdeletion region, cause phenotypic abnormalities including overgrowth. *Nature genetics,* 39**,** 963-5.

DULLAART, R. P., HOOGENBERG, K., ROUWE, C. W. & STULP, B. K. 2004. Family with autosomal dominant hyperinsulinism associated with A456V mutation in the glucokinase gene. *J Intern Med,* 255**,** 143-5.

DUNNE, M. J., COSGROVE, K. E., SHEPHERD, R. M., AYNSLEY-GREEN, A. & LINDLEY, K. J. 2004. Hyperinsulinism in infancy: from basic science to clinical disease. *Physiological reviews,* 84**,** 239-75.

DUNNE, M. J., KANE, C., SHEPHERD, R. M., SANCHEZ, J. A., JAMES, R. F., JOHNSON, P. R., AYNSLEY-GREEN, A., LU, S., CLEMENT, J. P. T., LINDLEY, K. J., SEINO, S. & AGUILAR-BRYAN, L. 1997. Familial persistent

hyperinsulinemic hypoglycemia of infancy and mutations in the sulfonylurea receptor. *N Engl J Med,* 336**,** 703-6.

DUNNE, M. J. & PETERSEN, O. H. 1986. Intracellular ADP activates K+ channels that are inhibited by ATP in an insulin-secreting cell line. *FEBS Lett,* 208**,** 59-62.

DUNNE, M. J. & PETERSEN, O. H. 1991. Potassium selective ion channels in insulin-secreting cells: physiology, pharmacology and their role in stimulus-secretion coupling. *Biochim Biophys Acta,* 1071**,** 67-82.

ENYEDI, P. & CZIRJAK, G. 2010. Molecular background of leak K+ currents: two-pore domain potassium channels. *Physiol Rev,* 90**,** 559-605.

FAFOULA, O., ALKHAYYAT, H. & HUSSAIN, K. 2006. Prolonged hyperinsulinaemic hypoglycaemia in newborns with intrauterine growth retardation. *Arch Dis Child Fetal Neonatal Ed,* 91**,** F467.

FAHIEN, L. A., MACDONALD, M. J., KMIOTEK, E. H., MERTZ, R. J. & FAHIEN, C. M. 1988. Regulation of insulin release by factors that also modify glutamate dehydrogenase. *J Biol Chem,* 263**,** 13610-4.

FAN, Z. & MAKIELSKI, J. C. 1997. Anionic phospholipids activate ATP-sensitive potassium channels. *J Biol Chem,* 272**,** 5388-95.

FINCH, A. J., HILCENKO, C., BASSE, N., DRYNAN, L. F., GOYENECHEA, B., MENNE, T. F., GONZALEZ FERNANDEZ, A., SIMPSON, P., D'SANTOS, C. S., ARENDS, M. J., DONADIEU, J., BELLANNE-CHANTELOT, C., COSTANZO, M., BOONE, C., MCKENZIE, A. N., FREUND, S. M. & WARREN, A. J. 2011. Uncoupling of GTP hydrolysis from eIF6 release on the ribosome causes Shwachman-Diamond syndrome. *Genes & development,* 25**,** 917-29.

FINEGOLD, D. N., STANLEY, C. A. & BAKER, L. 1980. Glycemic response to glucagon during fasting hypoglycemia: an aid in the diagnosis of hyperinsulinism. *The Journal of pediatrics,* 96**,** 257-9.

FLANAGAN, S. E., KAPOOR, R. R., BANERJEE, I., HALL, C., SMITH, V. V., HUSSAIN, K. & ELLARD, S. 2011a. Dominantly acting ABCC8 mutations in patients with medically unresponsive hyperinsulinaemic hypoglycaemia. *Clin Genet,* 79**,** 582-7.

FLANAGAN, S. E., PATCH, A. M., LOCKE, J. M., AKCAY, T., SIMSEK, E., ALAEI, M., YEKTA, Z., DESAI, M., KAPOOR, R. R., HUSSAIN, K. & ELLARD, S. 2011b. Genome-wide homozygosity analysis reveals HADH mutations as a common cause of diazoxide-responsive hyperinsulinemic-hypoglycemia in consanguineous pedigrees. *The Journal of clinical endocrinology and metabolism,* 96**,** E498-502.

FOURNET, J. C., MAYAUD, C., DE LONLAY, P., GROSS-MORAND, M. S., VERKARRE, V., CASTANET, M., DEVILLERS, M., RAHIER, J., BRUNELLE, F., ROBERT, J. J., NIHOUL-FEKETE, C., SAUDUBRAY, J. M. & JUNIEN, C. 2001. Unbalanced expression of 11p15 imprinted genes in focal forms of congenital hyperinsulinism: association with a reduction to homozygosity of a mutation in ABCC8 or KCNJ11. *Am J Pathol,* 158**,** 2177-84.

FRIEDRICH, C., RINNE, S., ZUMHAGEN, S., KIPER, A. K., SILBERNAGEL, N., NETTER, M. F., STALLMEYER, B., SCHULZE-BAHR, E. & DECHER, N. 2014. Gain-of-function mutation in TASK-4 channels and severe cardiac conduction disorder. *EMBO Mol Med,* 6**,** 937-51.

FRISCHMEYER, P. A., VAN HOOF, A., O'DONNELL, K., GUERRERIO, A. L., PARKER, R. & DIETZ, H. C. 2002. An mRNA surveillance mechanism that eliminates transcripts lacking termination codons. *Science,* 295**,** 2258-61.

GAL, A., RAU, I., EL MATRI, L., KREIENKAMP, H. J., FEHR, S., BAKLOUTI, K., CHOUCHANE, I., LI, Y., REHBEIN, M., FUCHS, J., FLEDELIUS, H. C., VILHELMSEN, K., SCHORDERET, D. F., MUNIER, F. L., OSTERGAARD, E., THOMPSON, D. A. & ROSENBERG, T. 2011. Autosomal-recessive posterior microphthalmos is caused by mutations in PRSS56, a gene encoding a trypsin-like serine protease. *Am J Hum Genet,* 88**,** 382-90.

GEMBAL, M., DETIMARY, P., GILON, P., GAO, Z. Y. & HENQUIN, J. C. 1993. Mechanisms by which glucose can control insulin release independently from its action on adenosine triphosphate-sensitive K+ channels in mouse B cells. *J Clin Invest,* 91**,** 871-80.

GILISSEN, C., ARTS, H. H., HOISCHEN, A., SPRUIJT, L., MANS, D. A., ARTS, P., VAN LIER, B., STEEHOUWER, M., VAN REEUWIJK, J., KANT, S. G., ROEPMAN, R., KNOERS, N. V., VELTMAN, J. A. & BRUNNER, H. G. 2010. Exome sequencing identifies WDR35 variants involved in Sensenbrenner syndrome. *Am J Hum Genet,* 87**,** 418-23.

GIRARD, C., DUPRAT, F., TERRENOIRE, C., TINEL, N., FOSSET, M., ROMEY, G., LAZDUNSKI, M. & LESAGE, F. 2001. Genomic and functional characteristics of novel human pancreatic 2P domain K(+) channels. *Biochemical and biophysical research communications,* 282**,** 249-56.

GLASER, B., CHIU, K. C., ANKER, R., NESTOROWICZ, A., LANDAU, H., BEN-BASSAT, H., SHLOMAI, Z., KAISER, N., THORNTON, P. S., STANLEY, C. A. & ET AL. 1994. Familial hyperinsulinism maps to chromosome 11p14-15.1, 30 cM centromeric to the insulin gene. *Nature genetics,* 7**,** 185-8.

GNANAPAVAN, S., KOLA, B., BUSTIN, S. A., MORRIS, D. G., MCGEE, P., FAIRCLOUGH, P., BHATTACHARYA, S., CARPENTER, R., GROSSMAN, A. B.

& KORBONITS, M. 2002. The tissue distribution of the mRNA of ghrelin and subtypes of its receptor, GHS-R, in humans. *J Clin Endocrinol Metab,* 87**,** 2988.

GOULD, G. W., THOMAS, H. M., JESS, T. J. & BELL, G. I. 1991. Expression of human glucose transporters in Xenopus oocytes: kinetic characterization and substrate specificities of the erythrocyte, liver, and brain isoforms. *Biochemistry,* 30**,** 5139-45.

GRAY, G. E., MANN, R. S., MITSIADIS, E., HENRIQUE, D., CARCANGIU, M. L., BANKS, A., LEIMAN, J., WARD, D., ISH-HOROWITZ, D. & ARTAVANIS-TSAKONAS, S. 1999. Human ligands of the Notch receptor. *Am J Pathol,* 154**,** 785-94.

GREMLICH, S., NOLAN, C., RODUIT, R., BURCELIN, R., PEYOT, M. L., DELGHINGARO-AUGUSTO, V., DESVERGNE, B., MICHALIK, L., PRENTKI, M. & WAHLI, W. 2005. Pancreatic islet adaptation to fasting is dependent on peroxisome proliferator-activated receptor alpha transcriptional up-regulation of fatty acid oxidation. *Endocrinology,* 146**,** 375-82.

GUPTA, R. K., VATAMANIUK, M. Z., LEE, C. S., FLASCHEN, R. C., FULMER, J. T., MATSCHINSKY, F. M., DUNCAN, S. A. & KAESTNER, K. H. 2005. The MODY1 gene HNF-4alpha regulates selected genes involved in insulin secretion. *The Journal of clinical investigation,* 115**,** 1006-15.

GUTMAN, G. A., CHANDY, K. G., GRISSMER, S., LAZDUNSKI, M., MCKINNON, D., PARDO, L. A., ROBERTSON, G. A., RUDY, B., SANGUINETTI, M. C., STUHMER, W. & WANG, X. 2005. International Union of Pharmacology. LIII. Nomenclature and molecular relationships of voltage-gated potassium channels. *Pharmacol Rev,* 57**,** 473-508.

HAN, S., STUART, L. A. & DEGEN, S. J. 1991. Characterization of the DNF15S2 locus on human chromosome 3: identification of a gene coding for four kringle domains with homology to hepatocyte growth factor. *Biochemistry,* 30**,** 9768-80.

HARDY, O. T., HERNANDEZ-PAMPALONI, M., SAFFER, J. R., SCHEUERMANN, J. S., ERNST, L. M., FREIFELDER, R., ZHUANG, H., MACMULLEN, C., BECKER, S., ADZICK, N. S., DIVGI, C., ALAVI, A. & STANLEY, C. A. 2007a. Accuracy of [18F]fluorodopa positron emission tomography for diagnosing and localizing focal congenital hyperinsulinism. *J Clin Endocrinol Metab,* 92**,** 4706-11.

HARDY, O. T., HOHMEIER, H. E., BECKER, T. C., MANDUCHI, E., DOLIBA, N. M., GUPTA, R. K., WHITE, P., STOECKERT, C. J., JR., MATSCHINSKY, F. M., NEWGARD, C. B. & KAESTNER, K. H. 2007b. Functional genomics of the beta-cell: short-chain 3-hydroxyacyl-coenzyme A dehydrogenase regulates insulin secretion independent of K+ currents. *Molecular endocrinology,* 21**,** 765-73.

HENQUIN, J. C. 1990. Role of voltage- and Ca2(+)-dependent K+ channels in the control of glucose-induced electrical activity in pancreatic B-cells. *Pflugers Arch,* 416**,** 568-72.

HENQUIN, J. C., SEMPOUX, C., MARCHANDISE, J., GODECHARLES, S., GUIOT, Y., NENQUIN, M. & RAHIER, J. 2013. Congenital Hyperinsulinism Caused by Hexokinase I Expression or Glucokinase-Activating Mutation in a Subset of beta-Cells. *Diabetes,* 62**,** 1689-96.

HESLEGRAVE, A. J., KAPOOR, R. R., EATON, S., CHADEFAUX, B., ACKAY, T., SIMSEK, E., FLANAGAN, S. E., ELLARD, S. & HUSSAIN, K. 2012. Leucine-sensitive hyperinsulinaemic hypoglycaemia in patients with loss of function mutations in 3-Hydroxyacyl-CoA Dehydrogenase. *Orphanet journal of rare diseases,* 7**,** 25.

HODGKIN, A. L. & HUXLEY, A. F. 1947. Potassium leakage from an active nerve fibre. *J Physiol,* 106**,** 341-67.

HOISCHEN, A., VAN BON, B. W., GILISSEN, C., ARTS, P., VAN LIER, B., STEEHOUWER, M., DE VRIES, P., DE REUVER, R., WIESKAMP, N., MORTIER, G., DEVRIENDT, K., AMORIM, M. Z., REVENCU, N., KIDD, A., BARBOSA, M., TURNER, A., SMITH, J., OLEY, C., HENDERSON, A., HAYES, I. M., THOMPSON, E. M., BRUNNER, H. G., DE VRIES, B. B. & VELTMAN, J. A. 2010. De novo mutations of SETBP1 cause Schinzel-Giedion syndrome. *Nat Genet,* 42**,** 483-5.

HOUSLAY, M. D. & SIDDLE, K. 1989. Molecular basis of insulin receptor function. *British medical bulletin,* 45**,** 264-84.

HSU, B. Y., KELLY, A., THORNTON, P. S., GREENBERG, C. R., DILLING, L. A. & STANLEY, C. A. 2001. Protein-sensitive and fasting hypoglycemia in children with the hyperinsulinism/hyperammonemia syndrome. *J Pediatr,* 138**,** 383-9.

HSU, L. S., TSOU, A. P., CHI, C. W., LEE, C. H. & CHEN, J. Y. 1998. Cloning, expression and chromosomal localization of human Ca2+/calmodulin-dependent protein kinase kinase. *J Biomed Sci,* 5**,** 141-9.

HUNG, L. W., WANG, I. X., NIKAIDO, K., LIU, P. Q., AMES, G. F. & KIM, S. H. 1998. Crystal structure of the ATP-binding subunit of an ABC transporter. *Nature,* 396**,** 703-7.

HUOPIO, H., REIMANN, F., ASHFIELD, R., KOMULAINEN, J., LENKO, H. L., RAHIER, J., VAUHKONEN, I., KERE, J., LAAKSO, M., ASHCROFT, F. & OTONKOSKI, T. 2000. Dominantly inherited hyperinsulinism caused by a mutation in the sulfonylurea receptor type 1. *J Clin Invest,* 106**,** 897-906.

HUSSAIN, K., BRYAN, J., CHRISTESEN, H. T., BRUSGAARD, K. & AGUILAR-BRYAN, L. 2005a. Serum glucagon counterregulatory hormonal response to hypoglycemia is blunted in congenital hyperinsulinism. *Diabetes,* 54**,** 2946-51.

HUSSAIN, K., CLAYTON, P. T., KRYWAWYCH, S., CHATZIANDREOU, I., MILLS, P., GINBEY, D. W., GEBOERS, A. J., BERGER, R., VAN DEN BERG, I. E. & EATON, S. 2005b. Hyperinsulinism of infancy associated with a novel splice site mutation in the SCHAD gene. *J Pediatr,* 146**,** 706-8.

HUSSAIN, K., HINDMARSH, P. & AYNSLEY-GREEN, A. 2003. Neonates with symptomatic hyperinsulinemic hypoglycemia generate inappropriately low serum cortisol counterregulatory hormonal responses. *The Journal of clinical endocrinology and metabolism,* 88**,** 4342-7.

INAGAKI, N., GONOI, T., CLEMENT, J. P. T., NAMBA, N., INAZAWA, J., GONZALEZ, G., AGUILAR-BRYAN, L., SEINO, S. & BRYAN, J. 1995. Reconstitution of IKATP: an inward rectifier subunit plus the sulfonylurea receptor. *Science,* 270**,** 1166-70.

INOUE, T., HOSHINA, N., NAKAZAWA, T., KIYAMA, Y., KOBAYASHI, S., ABE, T., YAMAMOTO, T. & MANABE, T. 2014. LMTK3 deficiency causes pronounced locomotor hyperactivity and impairs endocytic trafficking. *J Neurosci,* 34**,** 5927-37.

ISHIHARA, H., WANG, H., DREWES, L. R. & WOLLHEIM, C. B. 1999. Overexpression of monocarboxylate transporter and lactate dehydrogenase alters insulin secretory responses to pyruvate and lactate in beta cells. *J Clin Invest,* 104**,** 1621-9.

ISMAIL, D., SMITH, V. V., DE LONLAY, P., RIBEIRO, M. J., RAHIER, J., BLANKENSTEIN, O., FLANAGAN, S. E., BELLANNE-CHANTELOT, C., VERKARRE, V., AIGRAIN, Y., PIERRO, A., ELLARD, S. & HUSSAIN, K. 2011. Familial focal congenital hyperinsulinism. *The Journal of clinical endocrinology and metabolism,* 96**,** 24-8.

ITO, S., SHEN, L., DAI, Q., WU, S. C., COLLINS, L. B., SWENBERG, J. A., HE, C. & ZHANG, Y. 2011. Tet proteins can convert 5-methylcytosine to 5-formylcytosine and 5-carboxylcytosine. *Science,* 333**,** 1300-3.

IYNEDJIAN, P. B., AUBERGER, P., GUIGOZ, Y. & LE CAM, A. 1985. Pretranslational regulation of tyrosine aminotransferase and phosphoenolpyruvate carboxykinase (GTP) synthesis by glucagon and dexamethasone in adult rat hepatocytes. *Biochem J,* 225**,** 77-84.

JACOBSON, D. A., KUZNETSOV, A., LOPEZ, J. P., KASH, S., AMMALA, C. E. & PHILIPSON, L. H. 2007. Kv2.1 ablation alters glucose-induced islet electrical activity, enhancing insulin secretion. *Cell Metab,* 6**,** 229-35.

JARRIAULT, S., BROU, C., LOGEAT, F., SCHROETER, E. H., KOPAN, R. & ISRAEL, A. 1995. Signalling downstream of activated mammalian Notch. *Nature,* 377**,** 355-8.

JIANG, G. & ZHANG, B. B. 2003. Glucagon and regulation of glucose metabolism. *Am J Physiol Endocrinol Metab,* 284**,** E671-8.

JOHN, S. A., WEISS, J. N., XIE, L. H. & RIBALET, B. 2003. Molecular mechanism for ATP-dependent closure of the K+ channel Kir6.2. *J Physiol,* 552**,** 23-34.

JOHNSON, J. H., NEWGARD, C. B., MILBURN, J. L., LODISH, H. F. & THORENS, B. 1990. The high Km glucose transporter of islets of Langerhans is functionally similar to the low affinity transporter of liver and has an identical primary sequence. *The Journal of biological chemistry,* 265**,** 6548-51.

JOHNSON, J. O., MANDRIOLI, J., BENATAR, M., ABRAMZON, Y., VAN DEERLIN, V. M., TROJANOWSKI, J. Q., GIBBS, J. R., BRUNETTI, M., GRONKA, S., WUU, J., DING, J., MCCLUSKEY, L., MARTINEZ-LAGE, M., FALCONE, D., HERNANDEZ, D. G., AREPALLI, S., CHONG, S., SCHYMICK, J. C., ROTHSTEIN, J., LANDI, F., WANG, Y. D., CALVO, A., MORA, G., SABATELLI,

M., MONSURRO, M. R., BATTISTINI, S., SALVI, F., SPATARO, R., SOLA, P., BORGHERO, G., GALASSI, G., SCHOLZ, S. W., TAYLOR, J. P., RESTAGNO, G., CHIO, A. & TRAYNOR, B. J. 2010. Exome sequencing reveals VCP mutations as a cause of familial ALS. *Neuron,* 68**,** 857-64.

KACZMAREK, K., NIEDZIALKOWSKA, E., STUDENCKA, M., SCHULZ, Y. & GRZMIL, P. 2009. Ccdc33, a predominantly testis-expressed gene, encodes a putative peroxisomal protein. *Cytogenet Genome Res,* 126**,** 243-52.

KAKEI, M., KELLY, R. P., ASHCROFT, S. J. & ASHCROFT, F. M. 1986. The ATP-sensitivity of K+ channels in rat pancreatic B-cells is modulated by ADP. *FEBS Lett,* 208**,** 63-6.

KAPOOR, R. R., FLANAGAN, S. E., ARYA, V. B., SHIELD, J. P., ELLARD, S. & HUSSAIN, K. 2013. Clinical and molecular characterisation of 300 patients with congenital hyperinsulinism. *European journal of endocrinology,* 168**,** 557-64.

KAPOOR, R. R., FLANAGAN, S. E., ELLARD, S. & HUSSAIN, K. 2012. Congenital hyperinsulinism: marked clinical heterogeneity in siblings with identical mutations in the ABCC8 gene. *Clinical endocrinology,* 76**,** 312-3.

KAPOOR, R. R., FLANAGAN, S. E., FULTON, P., CHAKRAPANI, A., CHADEFAUX, B., BEN-OMRAN, T., BANERJEE, I., SHIELD, J. P., ELLARD, S. & HUSSAIN, K. 2009a. Hyperinsulinism-hyperammonaemia syndrome: novel mutations in the GLUD1 gene and genotype-phenotype correlations. *European journal of endocrinology / European Federation of Endocrine Societies,* 161**,** 731-5.

KAPOOR, R. R., JAMES, C., FLANAGAN, S. E., ELLARD, S., EATON, S. & HUSSAIN, K. 2009b. 3-Hydroxyacyl-coenzyme A dehydrogenase deficiency and hyperinsulinemic hypoglycemia: characterization of a novel mutation and severe dietary protein sensitivity. *J Clin Endocrinol Metab,* 94**,** 2221-5.

KAPOOR, R. R., JAMES, C. & HUSSAIN, K. 2009c. Advances in the diagnosis and management of hyperinsulinemic hypoglycemia. *Nature clinical practice. Endocrinology & metabolism,* 5**,** 101-12.

KAPOOR, R. R., LOCKE, J., COLCLOUGH, K., WALES, J., CONN, J. J., HATTERSLEY, A. T., ELLARD, S. & HUSSAIN, K. 2008. Persistent hyperinsulinemic hypoglycemia and maturity-onset diabetes of the young due to heterozygous HNF4A mutations. *Diabetes,* 57**,** 1659-63.

KELLY, R. P., SUTTON, R. & ASHCROFT, F. M. 1991. Voltage-activated calcium and potassium currents in human pancreatic beta-cells. *J Physiol,* 443**,** 175-92.

KOHLER, M., HIRSCHBERG, B., BOND, C. T., KINZIE, J. M., MARRION, N. V., MAYLIE, J. & ADELMAN, J. P. 1996. Small-conductance, calcium-activated potassium channels from mammalian brain. *Science,* 273**,** 1709-14.

KOMATSU, M., SCHERMERHORN, T., AIZAWA, T. & SHARP, G. W. 1995. Glucose stimulation of insulin release in the absence of extracellular Ca2+ and in the absence of any increase in intracellular Ca2+ in rat pancreatic islets. *Proceedings of the National Academy of Sciences of the United States of America,* 92**,** 10728-32.

KRAFCHAK, C. M., PAWAR, H., MOROI, S. E., SUGAR, A., LICHTER, P. R., MACKEY, D. A., MIAN, S., NAIRUS, T., ELNER, V., SCHTEINGART, M. T., DOWNS, C. A., KIJEK, T. G., JOHNSON, J. M., TRAGER, E. H., ROZSA, F. W., MANDAL, M. N., EPSTEIN, M. P., VOLLRATH, D., AYYAGARI, R., BOEHNKE, M. & RICHARDS, J. E. 2005. Mutations in TCF8 cause posterior polymorphous corneal dystrophy and ectopic expression of COL4A3 by corneal endothelial cells. *Am J Hum Genet,* 77**,** 694-708.

KREBS, L. T., XUE, Y., NORTON, C. R., SHUTTER, J. R., MAGUIRE, M., SUNDBERG, J. P., GALLAHAN, D., CLOSSON, V., KITAJEWSKI, J., CALLAHAN, R.,

SMITH, G. H., STARK, K. L. & GRIDLEY, T. 2000. Notch signaling is essential for vascular morphogenesis in mice. *Genes & development,* 14**,** 1343-52.

KRYUKOV, G. V., PENNACCHIO, L. A. & SUNYAEV, S. R. 2007. Most rare missense alleles are deleterious in humans: implications for complex disease and association studies. *Am J Hum Genet,* 80**,** 727-39.

KULKE, M. H., BERGSLAND, E. K. & YAO, J. C. 2009. Glycemic control in patients with insulinoma treated with everolimus. *N Engl J Med,* 360**,** 195-7.

KURLAND, I. J. & PILKIS, S. J. 1995. Covalent control of 6-phosphofructo-2-kinase/fructose-2,6-bisphosphatase: insights into autoregulation of a bifunctional enzyme. *Protein Sci,* 4**,** 1023-37.

LAJE, P., HALABY, L., ADZICK, N. S. & STANLEY, C. A. 2010. Necrotizing enterocolitis in neonates receiving octreotide for the management of congenital hyperinsulinism. *Pediatric diabetes,* 11**,** 142-7.

LAJE, P., STATES, L. J., ZHUANG, H., BECKER, S. A., PALLADINO, A. A., STANLEY, C. A. & ADZICK, N. S. 2013. Accuracy of PET/CT Scan in the diagnosis of the focal form of congenital hyperinsulinism. *Journal of pediatric surgery,* 48**,** 388-93.

LALONDE, E., ALBRECHT, S., HA, K. C., JACOB, K., BOLDUC, N., POLYCHRONAKOS, C., DECHELOTTE, P., MAJEWSKI, J. & JABADO, N. 2010. Unexpected allelic heterogeneity and spectrum of mutations in Fowler syndrome revealed by next-generation exome sequencing. *Hum Mutat,* 31**,** 918-23.

LANDER, E. S. & BOTSTEIN, D. 1987. Homozygosity mapping: a way to map human recessive traits with the DNA of inbred children. *Science,* 236**,** 1567-70.

LE QUAN SANG, K. H., ARNOUX, J. B., MAMOUNE, A., SAINT-MARTIN, C., BELLANNE-CHANTELOT, C., VALAYANNOPOULOS, V., BRASSIER, A., KAYIRANGWA, H., BARBIER, V., BROISSAND, C., FABREGUETTES, J. R.,

CHARRON, B., THALABARD, J. C. & DE LONLAY, P. 2012. Successful treatment of congenital hyperinsulinism with long-acting release octreotide. *Eur J Endocrinol,* 166**,** 333-9.

LEITCH, C. C., ZAGHLOUL, N. A., DAVIS, E. E., STOETZEL, C., DIAZ-FONT, A., RIX, S., ALFADHEL, M., LEWIS, R. A., EYAID, W., BANIN, E., DOLLFUS, H., BEALES, P. L., BADANO, J. L. & KATSANIS, N. 2008. Hypomorphic mutations in syndromic encephalocele genes are associated with Bardet-Biedl syndrome. *Nature genetics,* 40**,** 443-8.

LESAGE, F., GUILLEMARE, E., FINK, M., DUPRAT, F., LAZDUNSKI, M., ROMEY, G. & BARHANIN, J. 1996. TWIK-1, a ubiquitous human weakly inward rectifying K+ channel with a novel structure. *Embo j,* 15**,** 1004-11.

LEVITT KATZ, L. E., SATIN-SMITH, M. S., COLLETT-SOLBERG, P., THORNTON, P. S., BAKER, L., STANLEY, C. A. & COHEN, P. 1997. Insulin-like growth factor binding protein-1 levels in the diagnosis of hypoglycemia caused by hyperinsulinism. *The Journal of pediatrics,* 131**,** 193-9.

LI, C., CHEN, P., PALLADINO, A., NARAYAN, S., RUSSELL, L. K., SAYED, S., XIONG, G., CHEN, J., STOKES, D., BUTT, Y. M., JONES, P. M., COLLINS, H. W., COHEN, N. A., COHEN, A. S., NISSIM, I., SMITH, T. J., STRAUSS, A. W., MATSCHINSKY, F. M., BENNETT, M. J. & STANLEY, C. A. 2010. Mechanism of hyperinsulinism in short-chain 3-hydroxyacyl-CoA dehydrogenase deficiency involves activation of glutamate dehydrogenase. *J Biol Chem,* 285**,** 31806-18.

LI, G., YE, L., LI, J., YANG, W. & LOU, J. 2002. [Impact of islet alpha cell loss on insulin secretion]. *Zhonghua Yi Xue Za Zhi,* 82**,** 1427-31.

LI, L., HUANG, G. M., BANTA, A. B., DENG, Y., SMITH, T., DONG, P., FRIEDMAN, C., CHEN, L., TRASK, B. J., SPIES, T., ROWEN, L. & HOOD, L. 1998. Cloning,

characterization, and the complete 56.8-kilobase DNA sequence of the human NOTCH4 gene. *Genomics,* 51**,** 45-58.

LI, Z., WANG, Y., ZHANG, M., XU, P., HUANG, H., WU, D. & MENG, A. 2012. The Amotl2 gene inhibits Wnt/beta-catenin signaling and regulates embryonic development in zebrafish. *J Biol Chem,* 287**,** 13005-15.

LINTON, M. F., FARESE, R. V., JR. & YOUNG, S. G. 1993. Familial hypobetalipoproteinemia. *J Lipid Res,* 34**,** 521-41.

LOPATIN, A. N., MAKHINA, E. N. & NICHOLS, C. G. 1994. Potassium channel block by cytoplasmic polyamines as the mechanism of intrinsic rectification. *Nature,* 372**,** 366-9.

LU, B. & BISHOP, C. E. 2003. Mouse GGN1 and GGN3, two germ cell-specific proteins from the single gene Ggn, interact with mouse POG and play a role in spermatogenesis. *J Biol Chem,* 278**,** 16289-96.

LUNYAK, V. V., BURGESS, R., PREFONTAINE, G. G., NELSON, C., SZE, S. H., CHENOWETH, J., SCHWARTZ, P., PEVZNER, P. A., GLASS, C., MANDEL, G. & ROSENFELD, M. G. 2002. Corepressor-dependent silencing of chromosomal regions encoding neuronal genes. *Science,* 298**,** 1747-52.

MACDONALD, P. E., HA, X. F., WANG, J., SMUKLER, S. R., SUN, A. M., GAISANO, H. Y., SALAPATEK, A. M., BACKX, P. H. & WHEELER, M. B. 2001. Members of the Kv1 and Kv2 voltage-dependent K(+) channel families regulate insulin secretion. *Mol Endocrinol,* 15**,** 1423-35.

MACDONALD, P. E., SALAPATEK, A. M. & WHEELER, M. B. 2002. Glucagon-like peptide-1 receptor activation antagonizes voltage-dependent repolarizing K(+) currents in beta-cells: a possible glucose-dependent insulinotropic mechanism. *Diabetes,* 51 Suppl 3**,** S443-7.

MACMULLEN, C., FANG, J., HSU, B. Y., KELLY, A., DE LONLAY-DEBENEY, P., SAUDUBRAY, J. M., GANGULY, A., SMITH, T. J. & STANLEY, C. A. 2001. Hyperinsulinism/hyperammonemia syndrome in children with regulatory mutations in the inhibitory guanosine triphosphate-binding domain of glutamate dehydrogenase. *The Journal of clinical endocrinology and metabolism,* 86**,** 1782-7.

MACMULLEN, C. M., ZHOU, Q., SNIDER, K. E., TEWSON, P. H., BECKER, S. A., AZIZ, A. R., GANGULY, A., SHYNG, S. L. & STANLEY, C. A. 2011. Diazoxide-unresponsive congenital hyperinsulinism in children with dominant mutations of the beta-cell sulfonylurea receptor SUR1. *Diabetes,* 60**,** 1797-804.

MALAISSE, W. J., SENER, A., HERCHUELZ, A. & HUTTON, J. C. 1979. Insulin release: the fuel hypothesis. *Metabolism,* 28**,** 373-86.

MARTENS, G. A., VERVOORT, A., VAN DE CASTEELE, M., STANGE, G., HELLEMANS, K., VAN THI, H. V., SCHUIT, F. & PIPELEERS, D. 2007. Specificity in beta cell expression of L-3-hydroxyacyl-CoA dehydrogenase, short chain, and potential role in down-regulating insulin release. *The Journal of biological chemistry,* 282**,** 21134-44.

MARTIN, G. M., CHEN, P. C., DEVARANENI, P. & SHYNG, S. L. 2013. Pharmacological rescue of trafficking-impaired ATP-sensitive potassium channels. *Front Physiol,* 4**,** 386.

MATSCHINSKY, F. M. 1996. Banting Lecture 1995. A lesson in metabolic regulation inspired by the glucokinase glucose sensor paradigm. *Diabetes,* 45**,** 223-41.

MATSUO, M., KIOKA, N., AMACHI, T. & UEDA, K. 1999. ATP binding properties of the nucleotide-binding folds of SUR1. *J Biol Chem,* 274**,** 37479-82.

MATSUO, M., TANABE, K., KIOKA, N., AMACHI, T. & UEDA, K. 2000a. Different binding properties and affinities for ATP and ADP among sulfonylurea receptor subtypes, SUR1, SUR2A, and SUR2B. *J Biol Chem,* 275**,** 28757-63.

MATSUO, M., TRAPP, S., TANIZAWA, Y., KIOKA, N., AMACHI, T., OKA, Y., ASHCROFT, F. M. & UEDA, K. 2000b. Functional analysis of a mutant sulfonylurea receptor, SUR1-R1420C, that is responsible for persistent hyperinsulinemic hypoglycemia of infancy. *J Biol Chem,* 275**,** 41184-91.

MEISSNER, T., FRIEDMANN, B., OKUN, J. G., SCHWAB, M. A., OTONKOSKI, T., BAUER, T., BARTSCH, P. & MAYATEPEK, E. 2005. Massive insulin secretion in response to anaerobic exercise in exercise-induced hyperinsulinism. *Horm Metab Res,* 37**,** 690-4.

MODAN-MOSES, D., KOREN, I., MAZOR-ARONOVITCH, K., PINHAS-HAMIEL, O. & LANDAU, H. 2011. Treatment of congenital hyperinsulinism with lanreotide acetate (Somatuline Autogel). *The Journal of clinical endocrinology and metabolism,* 96**,** 2312-7.

MOHNIKE, K., BLANKENSTEIN, O., PFUETZNER, A., POTZSCH, S., SCHOBER, E., STEINER, S., HARDY, O. T., GRIMBERG, A. & VAN WAARDE, W. M. 2008. Long-term non-surgical therapy of severe persistent congenital hyperinsulinism with glucagon. *Hormone research,* 70**,** 59-64.

MOLVEN, A., MATRE, G. E., DURAN, M., WANDERS, R. J., RISHAUG, U., NJOLSTAD, P. R., JELLUM, E. & SOVIK, O. 2004. Familial hyperinsulinemic hypoglycemia caused by a defect in the SCHAD enzyme of mitochondrial fatty acid oxidation. *Diabetes,* 53**,** 221-7.

MUECKLER, M. 1990. Family of glucose-transporter genes. Implications for glucose homeostasis and diabetes. *Diabetes,* 39**,** 6-11.

MURPHY, P. A., LAM, M. T., WU, X., KIM, T. N., VARTANIAN, S. M., BOLLEN, A. W., CARLSON, T. R. & WANG, R. A. 2008. Endothelial Notch4 signaling induces hallmarks of brain arteriovenous malformations in mice. *Proc Natl Acad Sci U S A,* 105**,** 10901-6.

NACHMAN, M. W. & CROWELL, S. L. 2000. Estimate of the mutation rate per nucleotide in humans. *Genetics,* 156**,** 297-304.

NAGASE, T., ISHIKAWA, K., SUYAMA, M., KIKUNO, R., MIYAJIMA, N., TANAKA, A., KOTANI, H., NOMURA, N. & OHARA, O. 1998. Prediction of the coding sequences of unidentified human genes. XI. The complete sequences of 100 new cDNA clones from brain which code for large proteins in vitro. *DNA Res,* 5**,** 277-86.

NAM, K. H., YONG, W., HARVAT, T., ADEWOLA, A., WANG, S., OBERHOLZER, J. & EDDINGTON, D. T. 2010. Size-based separation and collection of mouse pancreatic islets for functional analysis. *Biomed Microdevices,* 12**,** 865-74.

NAVIAUX, R. K. & NGUYEN, K. V. 2004. POLG mutations associated with Alpers' syndrome and mitochondrial DNA depletion. *Annals of neurology,* 55**,** 706-12.

NESTOROWICZ, A., WILSON, B. A., SCHOOR, K. P., INOUE, H., GLASER, B., LANDAU, H., STANLEY, C. A., THORNTON, P. S., CLEMENT, J. P. T., BRYAN, J., AGUILAR-BRYAN, L. & PERMUTT, M. A. 1996. Mutations in the sulonylurea receptor gene are associated with familial hyperinsulinism in Ashkenazi Jews. *Human molecular genetics,* 5**,** 1813-22.

NICHOLS, C. G. 2006. KATP channels as molecular sensors of cellular metabolism. *Nature,* 440**,** 470-6.

NIEMEYER, M. I., GONZALEZ-NILO, F. D., ZUNIGA, L., GONZALEZ, W., CID, L. P. & SEPULVEDA, F. V. 2007. Neutralization of a single arginine residue gates open a

two-pore domain, alkali-activated K+ channel. *Proc Natl Acad Sci U S A,* 104**,** 666-71.

OKAR, D. A. & LANGE, A. J. 1999. Fructose-2,6-bisphosphate and control of carbohydrate metabolism in eukaryotes. *Biofactors,* 10**,** 1-14.

ORIMO, A., INOUE, S., MINOWA, O., TOMINAGA, N., TOMIOKA, Y., SATO, M., KUNO, J., HIROI, H., SHIMIZU, Y., SUZUKI, M., NODA, T. & MURAMATSU, M. 1999. Underdeveloped uterus and reduced estrogen responsiveness in mice with disruption of the estrogen-responsive finger protein gene, which is a direct target of estrogen receptor alpha. *Proc Natl Acad Sci U S A,* 96**,** 12027-32.

OTA, T., SUZUKI, Y., NISHIKAWA, T., OTSUKI, T., SUGIYAMA, T., IRIE, R., WAKAMATSU, A., HAYASHI, K., SATO, H., NAGAI, K., KIMURA, K., MAKITA, H., SEKINE, M., OBAYASHI, M., NISHI, T., SHIBAHARA, T., TANAKA, T., ISHII, S., YAMAMOTO, J., SAITO, K., KAWAI, Y., ISONO, Y., NAKAMURA, Y., NAGAHARI, K., MURAKAMI, K., YASUDA, T., IWAYANAGI, T., WAGATSUMA, M., SHIRATORI, A., SUDO, H., HOSOIRI, T., KAKU, Y., KODAIRA, H., KONDO, H., SUGAWARA, M., TAKAHASHI, M., KANDA, K., YOKOI, T., FURUYA, T., KIKKAWA, E., OMURA, Y., ABE, K., KAMIHARA, K., KATSUTA, N., SATO, K., TANIKAWA, M., YAMAZAKI, M., NINOMIYA, K., ISHIBASHI, T., YAMASHITA, H., MURAKAWA, K., FUJIMORI, K., TANAI, H., KIMATA, M., WATANABE, M., HIRAOKA, S., CHIBA, Y., ISHIDA, S., ONO, Y., TAKIGUCHI, S., WATANABE, S., YOSIDA, M., HOTUTA, T., KUSANO, J., KANEHORI, K., TAKAHASHI-FUJII, A., HARA, H., TANASE, T. O., NOMURA, Y., TOGIYA, S., KOMAI, F., HARA, R., TAKEUCHI, K., ARITA, M., IMOSE, N., MUSASHINO, K., YUUKI, H., OSHIMA, A., SASAKI, N., AOTSUKA, S., YOSHIKAWA, Y., MATSUNAWA, H.,

ICHIHARA, T., SHIOHATA, N., SANO, S., MORIYA, S., MOMIYAMA, H., SATOH, N., TAKAMI, S., TERASHIMA, Y., SUZUKI, O., NAKAGAWA, S., SENOH, A., MIZOGUCHI, H., GOTO, Y., SHIMIZU, F., WAKEBE, H., HISHIGAKI, H., WATANABE, T., SUGIYAMA, A., et al. 2004. Complete sequencing and characterization of 21,243 full-length human cDNAs. *Nature genetics,* 36**,** 40-5.

OTONKOSKI, T., KAMINEN, N., USTINOV, J., LAPATTO, R., MEISSNER, T., MAYATEPEK, E., KERE, J. & SIPILA, I. 2003. Physical exercise-induced hyperinsulinemic hypoglycemia is an autosomal-dominant trait characterized by abnormal pyruvate-induced insulin release. *Diabetes,* 52**,** 199-204.

OTONKOSKI, T., NANTO-SALONEN, K., SEPPANEN, M., VEIJOLA, R., HUOPIO, H., HUSSAIN, K., TAPANAINEN, P., ESKOLA, O., PARKKOLA, R., EKSTROM, K., GUIOT, Y., RAHIER, J., LAAKSO, M., RINTALA, R., NUUTILA, P. & MINN, H. 2006. Noninvasive diagnosis of focal hyperinsulinism of infancy with [18F]-DOPA positron emission tomography. *Diabetes,* 55**,** 13-8.

PALLADINO, A. A. & STANLEY, C. A. 2010. The hyperinsulinism/hyperammonemia syndrome. *Reviews in endocrine & metabolic disorders,* 11**,** 171-8.

PARTRIDGE, C. J., BEECH, D. J. & SIVAPRASADARAO, A. 2001a. Identification and pharmacological correction of a membrane trafficking defect associated with a mutation in the sulfonylurea receptor causing familial hyperinsulinism. *The Journal of biological chemistry,* 276**,** 35947-52.

PARTRIDGE, C. J., BEECH, D. J. & SIVAPRASADARAO, A. 2001b. Identification and pharmacological correction of a membrane trafficking defect associated with a mutation in the sulfonylurea receptor causing familial hyperinsulinism. *J Biol Chem,* 276**,** 35947-52.

PEARSON, E. R., BOJ, S. F., STEELE, A. M., BARRETT, T., STALS, K., SHIELD, J. P., ELLARD, S., FERRER, J. & HATTERSLEY, A. T. 2007. Macrosomia and hyperinsulinaemic hypoglycaemia in patients with heterozygous mutations in the HNF4A gene. *PLoS Med,* 4**,** e118.

PERMUTT, M. A., CHIRGWIN, J., ROTWEIN, P. & GIDDINGS, S. 1984. Insulin gene structure and function: a review of studies using recombinant DNA methodology. *Diabetes Care,* 7**,** 386-94.

PHILIPSON, L. H., HICE, R. E., SCHAEFER, K., LAMENDOLA, J., BELL, G. I., NELSON, D. J. & STEINER, D. F. 1991. Sequence and functional expression in Xenopus oocytes of a human insulinoma and islet potassium channel. *Proc Natl Acad Sci U S A,* 88**,** 53-7.

PHILIPSON, L. H., ROSENBERG, M. P., KUZNETSOV, A., LANCASTER, M. E., WORLEY, J. F., 3RD, ROE, M. W. & DUKES, I. D. 1994. Delayed rectifier K+ channel overexpression in transgenic islets and beta-cells associated with impaired glucose responsiveness. *J Biol Chem,* 269**,** 27787-90.

PIERRO, A. & NAH, S. A. 2011. Surgical management of congenital hyperinsulinism of infancy. *Seminars in pediatric surgery,* 20**,** 50-3.

PINNEY, S. E., MACMULLEN, C., BECKER, S., LIN, Y. W., HANNA, C., THORNTON, P., GANGULY, A., SHYNG, S. L. & STANLEY, C. A. 2008. Clinical characteristics and biochemical mechanisms of congenital hyperinsulinism associated with dominant KATP channel mutations. *J Clin Invest,* 118**,** 2877-86.

PROKS, P., CAPENER, C. E., JONES, P. & ASHCROFT, F. M. 2001. Mutations within the P-loop of Kir6.2 modulate the intraburst kinetics of the ATP-sensitive potassium channel. *J Gen Physiol,* 118**,** 341-53.

RAHIER, J., GUIOT, Y. & SEMPOUX, C. 2000. Persistent hyperinsulinaemic hypoglycaemia of infancy: a heterogeneous syndrome unrelated to nesidioblastosis. *Arch Dis Child Fetal Neonatal Ed,* 82**,** F108-12.

RAIZEN, D. M., BROOKS-KAYAL, A., STEINKRAUSS, L., TENNEKOON, G. I., STANLEY, C. A. & KELLY, A. 2005. Central nervous system hyperexcitability associated with glutamate dehydrogenase gain of function mutations. *J Pediatr,* 146**,** 388-94.

RAMACHANDRAN, C., ANGELOS, K. L. & WALSH, D. A. 1983. Hormonal regulation of the phosphorylation of glycogen synthase in perfused rat heart. Effects of insulin, catecholamines, and glucagon. *J Biol Chem,* 258**,** 13377-83.

RAY, M. E., WISTOW, G., SU, Y. A., MELTZER, P. S. & TRENT, J. M. 1997. AIM1, a novel non-lens member of the betagamma-crystallin superfamily, is associated with the control of tumorigenicity in human malignant melanoma. *Proc Natl Acad Sci U S A,* 94**,** 3229-34.

REDMON, J. B., TOWLE, H. C. & ROBERTSON, R. P. 1994. Regulation of human insulin gene transcription by glucose, epinephrine, and somatostatin. *Diabetes,* 43**,** 546-51.

REYES, R., DUPRAT, F., LESAGE, F., FINK, M., SALINAS, M., FARMAN, N. & LAZDUNSKI, M. 1998. Cloning and expression of a novel pH-sensitive two pore domain K+ channel from human kidney. *J Biol Chem,* 273**,** 30863-9.

RHODES, C. J. & WHITE, M. F. 2002. Molecular insights into insulin action and secretion. *European journal of clinical investigation,* 32 Suppl 3**,** 3-13.

RIBEIRO, M. J., BODDAERT, N., BELLANNE-CHANTELOT, C., BOURGEOIS, S., VALAYANNOPOULOS, V., DELZESCAUX, T., JAUBERT, F., NIHOUL-FEKETE, C., BRUNELLE, F. & DE LONLAY, P. 2007. The added value of

[18F]fluoro-L-DOPA PET in the diagnosis of hyperinsulinism of infancy: a retrospective study involving 49 children. *Eur J Nucl Med Mol Imaging,* 34**,** 2120-8.

ROBBIANI, D. F., FINCH, R. A., JAGER, D., MULLER, W. A., SARTORELLI, A. C. & RANDOLPH, G. J. 2000. The leukotriene C(4) transporter MRP1 regulates CCL19 (MIP-3beta, ELC)-dependent mobilization of dendritic cells to lymph nodes. *Cell,* 103**,** 757-68.

ROE, M. W., WORLEY, J. F., 3RD, MITTAL, A. A., KUZNETSOV, A., DASGUPTA, S., MERTZ, R. J., WITHERSPOON, S. M., 3RD, BLAIR, N., LANCASTER, M. E., MCINTYRE, M. S., SHEHEE, W. R., DUKES, I. D. & PHILIPSON, L. H. 1996. Expression and function of pancreatic beta-cell delayed rectifier K+ channels. Role in stimulus-secretion coupling. *J Biol Chem,* 271**,** 32241-6.

RORSMAN, P. & TRUBE, G. 1985. Glucose dependent K+-channels in pancreatic beta-cells are regulated by intracellular ATP. *Pflugers Arch,* 405**,** 305-9.

SCHULTE, C., SYNOFZIK, M., GASSER, T. & SCHOLS, L. 2009. Ataxia with ophthalmoplegia or sensory neuropathy is frequently caused by POLG mutations. *Neurology,* 73**,** 898-900.

SCHULTZ, M. J., WIJNHOLDS, J., PEPPELENBOSCH, M. P., VERVOORDELDONK, M. J., SPEELMAN, P., VAN DEVENTER, S. J., BORST, P. & VAN DER POLL, T. 2001. Mice lacking the multidrug resistance protein 1 are resistant to Streptococcus pneumoniae-induced pneumonia. *J Immunol,* 166**,** 4059-64.

SEMPOUX, C., CAPITO, C., BELLANNE-CHANTELOT, C., VERKARRE, V., DE LONLAY, P., AIGRAIN, Y., FEKETE, C., GUIOT, Y. & RAHIER, J. 2011. Morphological mosaicism of the pancreatic islets: a novel anatomopathological form of persistent hyperinsulinemic hypoglycemia of infancy. *The Journal of clinical endocrinology and metabolism,* 96**,** 3785-93.

SENDEREK, J., BERGMANN, C., STENDEL, C., KIRFEL, J., VERPOORTEN, N., DE JONGHE, P., TIMMERMAN, V., CHRAST, R., VERHEIJEN, M. H., LEMKE, G., BATTALOGLU, E., PARMAN, Y., ERDEM, S., TAN, E., TOPALOGLU, H., HAHN, A., MULLER-FELBER, W., RIZZUTO, N., FABRIZI, G. M., STUHRMANN, M., RUDNIK-SCHONEBORN, S., ZUCHNER, S., MICHAEL SCHRODER, J., BUCHHEIM, E., STRAUB, V., KLEPPER, J., HUEHNE, K., RAUTENSTRAUSS, B., BUTTNER, R., NELIS, E. & ZERRES, K. 2003. Mutations in a gene encoding a novel SH3/TPR domain protein cause autosomal recessive Charcot-Marie-Tooth type 4C neuropathy. *Am J Hum Genet,* 73**,** 1106-19.

SENNIAPPAN, S., ALEXANDRESCU, S., TATEVIAN, N., SHAH, P., ARYA, V., FLANAGAN, S., ELLARD, S., RAMPLING, D., ASHWORTH, M., BROWN, R. E. & HUSSAIN, K. 2014. Sirolimus therapy in infants with severe hyperinsulinemic hypoglycemia. *The New England journal of medicine,* 370**,** 1131-7.

SHIRATORI, A., OKUMURA, K., NOGAMI, M., TAGUCHI, H., ONOZAKI, T., INOUE, T., ANDO, T., SHIBATA, T., IZUMI, M., MIYAZAWA, H. & ET AL. 1995. Assignment of the 49-kDa (PRIM1) and 58-kDa (PRIM2A and PRIM2B) subunit genes of the human DNA primase to chromosome bands 1q44 and 6p11.1-p12. *Genomics,* 28**,** 350-3.

SHYNG, S. L., FERRIGNI, T., SHEPARD, J. B., NESTOROWICZ, A., GLASER, B., PERMUTT, M. A. & NICHOLS, C. G. 1998. Functional analyses of novel mutations in the sulfonylurea receptor 1 associated with persistent hyperinsulinemic hypoglycemia of infancy. *Diabetes,* 47**,** 1145-51.

SHYNG, S. L. & NICHOLS, C. G. 1998. Membrane phospholipid control of nucleotide sensitivity of KATP channels. *Science,* 282**,** 1138-41.

SIMPSON, M. A., IRVING, M. D., ASILMAZ, E., GRAY, M. J., DAFOU, D., ELMSLIE, F. V., MANSOUR, S., HOLDER, S. E., BRAIN, C. E., BURTON, B. K., KIM, K. H., PAULI, R. M., AFTIMOS, S., STEWART, H., KIM, C. A., HOLDER-ESPINASSE, M., ROBERTSON, S. P., DRAKE, W. M. & TREMBATH, R. C. 2011. Mutations in NOTCH2 cause Hajdu-Cheney syndrome, a disorder of severe and progressive bone loss. *Nat Genet,* 43**,** 303-5.

SLADEK, F. M., ZHONG, W. M., LAI, E. & DARNELL, J. E., JR. 1990. Liver-enriched transcription factor HNF-4 is a novel member of the steroid hormone receptor superfamily. *Genes & development,* 4**,** 2353-65.

SMITH, U. M., CONSUGAR, M., TEE, L. J., MCKEE, B. M., MAINA, E. N., WHELAN, S., MORGAN, N. V., GORANSON, E., GISSEN, P., LILLIQUIST, S., ALIGIANIS, I. A., WARD, C. J., PASHA, S., PUNYASHTHITI, R., MALIK SHARIF, S., BATMAN, P. A., BENNETT, C. P., WOODS, C. G., MCKEOWN, C., BUCOURT, M., MILLER, C. A., COX, P., ALGAZALI, L., TREMBATH, R. C., TORRES, V. E., ATTIE-BITACH, T., KELLY, D. A., MAHER, E. R., GATTONE, V. H., 2ND, HARRIS, P. C. & JOHNSON, C. A. 2006. The transmembrane protein meckelin (MKS3) is mutated in Meckel-Gruber syndrome and the wpk rat. *Nature genetics,* 38**,** 191-6.

SNIDER, K. E., BECKER, S., BOYAJIAN, L., SHYNG, S. L., MACMULLEN, C., HUGHES, N., GANAPATHY, K., BHATTI, T., STANLEY, C. A. & GANGULY, A. 2013. Genotype and phenotype correlations in 417 children with congenital hyperinsulinism. *The Journal of clinical endocrinology and metabolism,* 98**,** E355-63.

SORIA, L. F., LUDWIG, E. H., CLARKE, H. R., VEGA, G. L., GRUNDY, S. M. & MCCARTHY, B. J. 1989. Association between a specific apolipoprotein B mutation and familial defective apolipoprotein B-100. *Proc Natl Acad Sci U S A,* 86**,** 587-91.

STANESCU, D. E., HUGHES, N., KAPLAN, B., STANLEY, C. A. & DE LEON, D. D. 2012. Novel Presentations of Congenital Hyperinsulinism due to Mutations in the MODY genes: HNF1A and HNF4A. *The Journal of clinical endocrinology and metabolism*.

STANLEY, C. A. 2004. Hyperinsulinism/hyperammonemia syndrome: insights into the regulatory role of glutamate dehydrogenase in ammonia metabolism. *Mol Genet Metab,* 81 Suppl 1**,** S45-51.

STANLEY, C. A., FANG, J., KUTYNA, K., HSU, B. Y., MING, J. E., GLASER, B. & PONCZ, M. 2000. Molecular basis and characterization of the hyperinsulinism/hyperammonemia syndrome: predominance of mutations in exons 11 and 12 of the glutamate dehydrogenase gene. HI/HA Contributing Investigators. *Diabetes,* 49**,** 667-73.

STANLEY, C. A., LIEU, Y. K., HSU, B. Y., BURLINA, A. B., GREENBERG, C. R., HOPWOOD, N. J., PERLMAN, K., RICH, B. H., ZAMMARCHI, E. & PONCZ, M. 1998a. Hyperinsulinism and hyperammonemia in infants with regulatory mutations of the glutamate dehydrogenase gene. *N Engl J Med,* 338**,** 1352-7.

STANLEY, C. A., LIEU, Y. K., HSU, B. Y., BURLINA, A. B., GREENBERG, C. R., HOPWOOD, N. J., PERLMAN, K., RICH, B. H., ZAMMARCHI, E. & PONCZ, M. 1998b. Hyperinsulinism and hyperammonemia in infants with regulatory mutations of the glutamate dehydrogenase gene. *The New England journal of medicine,* 338**,** 1352-7.

STOWELL, S. R., ARTHUR, C. M., DIAS-BARUFFI, M., RODRIGUES, L. C., GOURDINE, J. P., HEIMBURG-MOLINARO, J., JU, T., MOLINARO, R. J., RIVERA-MARRERO, C., XIA, B., SMITH, D. F. & CUMMINGS, R. D. 2010.

Innate immune lectins kill bacteria expressing blood group antigen. *Nat Med,* 16**,** 295-301.

STRAUB, S. G., COSGROVE, K. E., AMMALA, C., SHEPHERD, R. M., O'BRIEN, R. E., BARNES, P. D., KUCHINSKI, N., CHAPMAN, J. C., SCHAEPPI, M., GLASER, B., LINDLEY, K. J., SHARP, G. W., AYNSLEY-GREEN, A. & DUNNE, M. J. 2001. Hyperinsulinism of infancy: the regulated release of insulin by KATP channel-independent pathways. *Diabetes,* 50**,** 329-39.

STRIFFLER, J. S., GARFIELD, S. A., CARDELL, E. L. & CARDELL, R. R. 1984. Effects of glucagon on hepatic microsomal glucose-6-phosphatase in vivo. *Diabete Metab,* 10**,** 91-7.

TASCHENBERGER, G., MOUGEY, A., SHEN, S., LESTER, L. B., LAFRANCHI, S. & SHYNG, S. L. 2002. Identification of a familial hyperinsulinism-causing mutation in the sulfonylurea receptor 1 that prevents normal trafficking and function of KATP channels. *J Biol Chem,* 277**,** 17139-46.

THOMAS, P., YE, Y. & LIGHTNER, E. 1996. Mutation of the pancreatic islet inward rectifier Kir6.2 also leads to familial persistent hyperinsulinemic hypoglycemia of infancy. *Hum Mol Genet,* 5**,** 1809-12.

THOMAS, P. M., COTE, G. J., WOHLLK, N., HADDAD, B., MATHEW, P. M., RABL, W., AGUILAR-BRYAN, L., GAGEL, R. F. & BRYAN, J. 1995. Mutations in the sulfonylurea receptor gene in familial persistent hyperinsulinemic hypoglycemia of infancy. *Science,* 268**,** 426-9.

THORNTON, P. S., MACMULLEN, C., GANGULY, A., RUCHELLI, E., STEINKRAUSS, L., CRANE, A., AGUILAR-BRYAN, L. & STANLEY, C. A. 2003. Clinical and molecular characterization of a dominant form of congenital hyperinsulinism caused by a mutation in the high-affinity sulfonylurea receptor. *Diabetes,* 52**,** 2403-10.

THORNTON, P. S., SATIN-SMITH, M. S., HEROLD, K., GLASER, B., CHIU, K. C., NESTOROWICZ, A., PERMUTT, M. A., BAKER, L. & STANLEY, C. A. 1998. Familial hyperinsulinism with apparent autosomal dominant inheritance: clinical and genetic differences from the autosomal recessive variant. *The Journal of pediatrics,* 132**,** 9-14.

TIEBER, V. L., ABRUZZINI, L. F., DIDIER, D. K., SCHWARTZ, B. D. & ROTWEIN, P. 1986. Complete characterization and sequence of an HLA class II DR beta chain cDNA from the DR5 haplotype. *J Biol Chem,* 261**,** 2738-42.

TOMPKINS, V., HAGEN, J., ZEDIAK, V. P. & QUELLE, D. E. 2006. Identification of novel ARF binding proteins by two-hybrid screening. *Cell Cycle,* 5**,** 641-6.

TREBERG, J. R., CLOW, K. A., GREENE, K. A., BROSNAN, M. E. & BROSNAN, J. T. 2010. Systemic activation of glutamate dehydrogenase increases renal ammoniagenesis: implications for the hyperinsulinism/hyperammonemia syndrome. *Am J Physiol Endocrinol Metab,* 298**,** E1219-25.

TREGLIA, G., MIRK, P., GIORDANO, A. & RUFINI, V. 2012. Diagnostic performance of fluorine-18-dihydroxyphenylalanine positron emission tomography in diagnosing and localizing the focal form of congenital hyperinsulinism: a meta-analysis. *Pediatric radiology,* 42**,** 1372-9.

TUCKER, S. J., GRIBBLE, F. M., ZHAO, C., TRAPP, S. & ASHCROFT, F. M. 1997. Truncation of Kir6.2 produces ATP-sensitive K+ channels in the absence of the sulphonylurea receptor. *Nature,* 387**,** 179-83.

URANO, T., SAITO, T., TSUKUI, T., FUJITA, M., HOSOI, T., MURAMATSU, M., OUCHI, Y. & INOUE, S. 2002. Efp targets 14-3-3 sigma for proteolysis and promotes breast tumour growth. *Nature,* 417**,** 871-5.

UYTTENDAELE, H., MARAZZI, G., WU, G., YAN, Q., SASSOON, D. & KITAJEWSKI, J. 1996. Notch4/int-3, a mammary proto-oncogene, is an endothelial cell-specific mammalian Notch gene. *Development,* 122**,** 2251-9.

VAN DAM, A., WINKEL, I., ZIJLSTRA-BAALBERGEN, J., SMEENK, R. & CUYPERS, H. T. 1989. Cloned human snRNP proteins B and B' differ only in their carboxy-terminal part. *EMBO J,* 8**,** 3853-60.

VAN HOOF, A., FRISCHMEYER, P. A., DIETZ, H. C. & PARKER, R. 2002. Exosome-mediated recognition and degradation of mRNAs lacking a termination codon. *Science,* 295**,** 2262-4.

VANDEPOELE, K., VAN ROY, N., STAES, K., SPELEMAN, F. & VAN ROY, F. 2005. A novel gene family NBPF: intricate structure generated by gene duplications during primate evolution. *Mol Biol Evol,* 22**,** 2265-74.

VEIT, F., HEINE, R. G. & CATTO-SMITH, A. G. 1994. Dumping syndrome after Nissen fundoplication. *Journal of paediatrics and child health,* 30**,** 182-5.

VENEZIALE, C. M., DEERING, N. G. & THOMPSON, H. J. 1976. Gluconeogenesis in isolated rat hepatic parenchymal cells. IX. Differential effects of glucagon and epinephrine on phosphofructokinase and pyruvate kinase. *Mayo Clinic proceedings. Mayo Clinic,* 51**,** 624-31.

VERKARRE, V., FOURNET, J. C., DE LONLAY, P., GROSS-MORAND, M. S., DEVILLERS, M., RAHIER, J., BRUNELLE, F., ROBERT, J. J., NIHOUL-FEKETE, C., SAUDUBRAY, J. M. & JUNIEN, C. 1998. Paternal mutation of the sulfonylurea receptor (SUR1) gene and maternal loss of 11p15 imprinted genes lead to persistent hyperinsulinism in focal adenomatous hyperplasia. *J Clin Invest,* 102**,** 1286-91.

VEZZOSI, D., BENNET, A., ROCHAIX, P., COURBON, F., SELVES, J., PRADERE, B., BUSCAIL, L., SUSINI, C. & CARON, P. 2005. Octreotide in insulinoma patients:

efficacy on hypoglycemia, relationships with Octreoscan scintigraphy and immunostaining with anti-sst2A and anti-sst5 antibodies. *European journal of endocrinology / European Federation of Endocrine Societies,* 152**,** 757-67.

VISSERS, L. E., DE LIGT, J., GILISSEN, C., JANSSEN, I., STEEHOUWER, M., DE VRIES, P., VAN LIER, B., ARTS, P., WIESKAMP, N., DEL ROSARIO, M., VAN BON, B. W., HOISCHEN, A., DE VRIES, B. B., BRUNNER, H. G. & VELTMAN, J. A. 2010. A de novo paradigm for mental retardation. *Nat Genet,* 42**,** 1109-12.

WALKER, J. E., SARASTE, M., RUNSWICK, M. J. & GAY, N. J. 1982. Distantly related sequences in the alpha- and beta-subunits of ATP synthase, myosin, kinases and other ATP-requiring enzymes and a common nucleotide binding fold. *EMBO J,* 1**,** 945-51.

WALSH, T., SHAHIN, H., ELKAN-MILLER, T., LEE, M. K., THORNTON, A. M., ROEB, W., ABU RAYYAN, A., LOULUS, S., AVRAHAM, K. B., KING, M. C. & KANAAN, M. 2010. Whole exome sequencing and homozygosity mapping identify mutation in the cell polarity protein GPSM2 as the cause of nonsyndromic hearing loss DFNB82. *Am J Hum Genet,* 87**,** 90-4.

WANG, Y., LI, Z., XU, P., HUANG, L., TONG, J., HUANG, H. & MENG, A. 2011. Angiomotin-like2 gene (amotl2) is required for migration and proliferation of endothelial cells during angiogenesis. *J Biol Chem,* 286**,** 41095-104.

WEINZIMER, S. A., STANLEY, C. A., BERRY, G. T., YUDKOFF, M., TUCHMAN, M. & THORNTON, P. S. 1997. A syndrome of congenital hyperinsulinism and hyperammonemia. *J Pediatr,* 130**,** 661-4.

WIBLE, B. A., DE BIASI, M., MAJUMDER, K., TAGLIALATELA, M. & BROWN, A. M. 1995. Cloning and functional expression of an inwardly rectifying K+ channel from human atrium. *Circ Res,* 76**,** 343-50.

XANTHOPOULOS, K. G., PREZIOSO, V. R., CHEN, W. S., SLADEK, F. M., CORTESE, R. & DARNELL, J. E., JR. 1991. The different tissue transcription patterns of genes for HNF-1, C/EBP, HNF-3, and HNF-4, protein factors that govern liver-specific transcription. *Proc Natl Acad Sci U S A,* 88**,** 3807-11.

YAN, L., FIGUEROA, D. J., AUSTIN, C. P., LIU, Y., BUGIANESI, R. M., SLAUGHTER, R. S., KACZOROWSKI, G. J. & KOHLER, M. G. 2004. Expression of voltage-gated potassium channels in human and rhesus pancreatic islets. *Diabetes,* 53**,** 597-607.

YAP, F., HOGLER, W., VORA, A., HALLIDAY, R. & AMBLER, G. 2004. Severe transient hyperinsulinaemic hypoglycaemia: two neonates without predisposing factors and a review of the literature. *European journal of pediatrics,* 163**,** 38-41.

YORIFUJI, T., KAWAKITA, R., HOSOKAWA, Y., FUJIMARU, R., MATSUBARA, K., AIZU, K., SUZUKI, S., NAGASAKA, H., NISHIBORI, H. & MASUE, M. 2013. Efficacy and safety of long-term, continuous subcutaneous octreotide infusion for patients with different subtypes of KATP-channel hyperinsulinism. *Clinical endocrinology,* 78**,** 891-7.

ZAMMARCHI, E., FILIPPI, L., NOVEMBRE, E. & DONATI, M. A. 1996. Biochemical evaluation of a patient with a familial form of leucine-sensitive hypoglycemia and concomitant hyperammonemia. *Metabolism,* 45**,** 957-60.

ZERANGUE, N., SCHWAPPACH, B., JAN, Y. N. & JAN, L. Y. 1999. A new ER trafficking signal regulates the subunit stoichiometry of plasma membrane K(ATP) channels. *Neuron,* 22**,** 537-48.

ZHU, X. R., NETZER, R., BOHLKE, K., LIU, Q. & PONGS, O. 1999. Structural and functional characterization of Kv6.2 a new gamma-subunit of voltage-gated potassium channel. *Receptors Channels,* 6**,** 337-50.

ZINGMAN, L. V., ALEKSEEV, A. E., BIENENGRAEBER, M., HODGSON, D., KARGER, A. B., DZEJA, P. P. & TERZIC, A. 2001. Signaling in channel/enzyme multimers: ATPase transitions in SUR module gate ATP-sensitive K+ conductance. *Neuron,* 31**,** 233-45.

CHAPTER 10

APPENDIX

Human and Hamster *ABCC8* Alignment

```
humanAbcc8        CGGGGCCCGGGGGGCGGGGGCCTGACGGCCGGGCCGGGCGGCGGAGCTGCAAGGGACAGA 60
hamsterabcc8      ------------------------------------------------------------

humanAbcc8        GGCGCGGCAGGCGCGCGGAGCCAGCGGAGCCAGCTGAGCCCGAGCCCAGCCCGCGCCCGC 120
hamsterabcc8      ------------------------------------------------------------

humanAbcc8        GCCGCCATGCCCCTGGCCTTCTGCGGCAGCGAGAACCACTCGGCCGCCTACCGGGTGGAC 180
hamsterabcc8      ------ATGCCCTTGGCCTTCTGCGGTACCGAGAACCACTCGGCCGCCTACCGGGTGGAC 54
                        ****** ************ * ********************************

humanAbcc8        CAGGGGGTCCTCAACAACGGCTGCTTTGTGGACGCGCTCAACGTGGTGCCGCACGTCTTC 240
hamsterabcc8      CAGGGCGTCCTCAACAACGGCTGCTTCGTGGACGCGCTCAACGTGGTGCCGCACGTTTTC 114
                  ***** ******************* ***************************** ***

humanAbcc8        CTACTCTTCATCACCTTCCCCATCCTCTTCATTGGATGGGGAAGTCAGAGCTCCAAGGTG 300
hamsterabcc8      CTGCTCTTCATCACCTTCCCCATCCTCTTCATCGGATGGGGCAGCCAGAGCTCCAAGGTG 174
                  ** ***************************** ******** ** ***************

humanAbcc8        CACATCCACCACAGCACATGGCTTCATTTCCCTGGGCACAACCTGCGGTGGATCCTGACC 360
hamsterabcc8      CACATCCACCACAGCACCTGGCTGCACTTTCCAGGGCACAACCTGCGCTGGATCCTTACC 234
                  ***************** ***** ** ** ** ************** ******** ***

humanAbcc8        TTCATGCTGCTCTTCGTCCTGGTGTGTGAGATTGCAGAGGGCATCCTGTCTGATGGGGTG 420
hamsterabcc8      TTCATTTTGCTCTTCGTCCTTGTGTGTGAGATCGCTGAGGGCATCCTGTCTGATGGGGTG 294
                  *****  ************* ************ ** ************************

humanAbcc8        ACCGAATCCCACCATCTGCACCTGTACATGCCAGCCGGGATGGCGTTCATGGCTGCTGTC 480
hamsterabcc8      ACAGAATCCCGCCACCTCCACCTGTACATGCCAGCCGGGATGGCGTTCATGGCTGCCATC 354
                  ** ******* *** ** ************************************  **

humanAbcc8        ACCTCCGTGGTCTACTATCACAACATCGAGACTTCCAACTTCCCCAAGCTGCTAATTGCC 540
hamsterabcc8      ACCTCTGTAGTCTACTATCATAACATCGAGACCTCCAACTTCCCCAAGCTTTTGATCGCT 414
                  ***** ** ************ ************ *****************  * ** **

humanAbcc8        CTGCTGGTGTATTGGACCCTGGCCTTCATCACCAAGACCATCAAGTTTGTCAAGTTCTTG 600
hamsterabcc8      CTGCTCATCTATTGGACCCTGGCCTTCATCACGAAGACCATCAAGTTTGTCAAGTTCTAT 474
                  *****  * ********************** ************************

humanAbcc8        GACCACGCCATCGGCTTCTCGCAGCTACGCTTCTGCCTCACAGGGCTGCTGGTGATCCTC 660
hamsterabcc8      GACCACGCCATCGGCTTCTCCCAGCTGCGCTTCTGCCTCACGGGGCTTCTGGTGATCCTG 534
                  ******************** ***** ************** ***** ************

humanAbcc8        TATGGGATGCTGCTCCTCGTGGAGGTCAATGTCATCAGGGTGAGGAGATACATCTTCTTC 720
hamsterabcc8      TATGGGATGTTGCTGCTTGTGGAGGTCAACGTCATCAGAGTGAGGAGGTACATCTTCTTC 594
                  ********* **** ** ************ ******** ******** ************

humanAbcc8        AAGACACCGAGGGAGGTGAAGCCTCCCGAGGACCTGCAAGACCTGGGGGTACGCTTCCTG 780
hamsterabcc8      AAGACGCCACGGGAGGTGAAGCCCCCTGAGGACCTGCAGGACCTGGGTGTGCGCTTTCTG 654
                  ***** **  ************* ** ************ ******** ** ***** ***

humanAbcc8        CAGCCCTTCGTGAATCTGCTGTCCAAAGGCACCTACTGGTGGATGAACGCCTTCATCAAG 840
hamsterabcc8      CAGCCCTTCGTTAACCTGCTGTCAAAGGGGACCTATTGGTGGATGAATGCCTTCATCAAG 714
                  *********** ** ******** ** ** ***** *********** ************

humanAbcc8        ACTGCCCACAAGAAGCCCATCGACTTGCGAGCCATCGGGAAGCTGCCCATCGCCATGAGG 900
hamsterabcc8      ACGGCCCACAAGAAGCCCATCGACCTGCGGGCCATCGCGAAGCTGCCCATCGCCATGAGA 774
                  ** ******************** **** ******* ********************

humanAbcc8        GCCCTCACCAACTACCAACGGCTCTGCGAGGCCTTTGACGCCCAGGTGCGGAAGGACATT 960
hamsterabcc8      GCCCTCACCAACTATCAGCGCCTCTGCGTGGCCTTCGATGCTCAGGCGCGGAAGGACACA 834
                  ************** ** ** ******* ****** ** ** **** ***********
```

```
humanAbcc8        CAGGGCACTCAAGGTGCCCGGGCCATCTGGCAGGCACTCAGCCATGCCTTCGGGAGGCGC 1020
hamsterabcc8      CAGAGCCCACAGGGTGCCCGGGCCATCTGGAGGGCTCTATGCCATGCCTTTGGGAGACGC 894
                  *** ** * ** ******************  *** **  ********** ***** ***

humanAbcc8        CTGGTCCTCAGCAGCACTTTCCGCATCTTGGCCGACCTGCTGGGCTTCGCCGGGCCACTG 1080
hamsterabcc8      CTGATCCTCAGCAGCACATTCCGCATCCTGGCTGACCTGTTGGGCTTCGCTGGACCACTC 954
                  *** ************* ********* **** ****** ********** ** *****

humanAbcc8        TGCATCTTTGGGATCGTGGACCACCTTGGGAAGGAGAACGACGTCTTCCAGCCCAAGACA 1140
hamsterabcc8      TGCATCTTTGGGATCGTGGACCACCTGGGGAAGGAGAACCACGTCTTCCAGCCCAAGACA 1014
                  ************************** ************ ********************

humanAbcc8        CAATTTCTCGGGGTTTACTTTGTCTCATCCCAAGAGTTCCTTGCCAATGCCTACGTCTTA 1200
hamsterabcc8      CAGTTTCTCGGGGTTTACTTCGTCTCTTCTCAAGAGTTCCTTGGCAATGCCTACGTCTTG 1074
                  ** ***************** ***** ** ************* ***************

humanAbcc8        GCTGTGCTTCTGTTCCTTGCCCTCCTACTGCAAAGGACATTTCTGCAAGCATCCTACTAT 1260
hamsterabcc8      GCCGTGCTTCTGTTCCTTGCCCTGCTACTGCAAAGGACATTCCTGCAAGCCTCATACTAC 1134
                  ** ******************** ***************** ******** ** *****

humanAbcc8        GTGGCCATTGAAACTGGAATTAACTTGAGAGGAGCAATACAGACCAAGATTTACAATAAA 1320
hamsterabcc8      GTCGCCATTGAAACTGGAATTAACCTGAGAGGAGCAATCCAGACCAAGATTTACAATAAA 1194
                  ** ********************** ************* ********************

humanAbcc8        ATTATGCACCTGTCCACCTCCAACCTGTCCATGGGAGAAATGACTGCTGGACAGATCTGT 1380
hamsterabcc8      ATCATGCACATGTCCACCTCCAACCTGTCAATGGGGGAAATGACTGCTGGGCAGATCTGC 1254
                  ** ****** ******************** ***** ************** ********

humanAbcc8        AATCTGGTTGCCATCGACACCAATCAGCTCATGTGGTTTTTCTTCTTGTGCCCAAACCTC 1440
hamsterabcc8      AACCTGGTGGCCATCGACACAAACCAGCTCATGTGGTTCTTCTTTCTGTGCCCAAACCTC 1314
                  ** ***** *********** ** *************** *****  **************

humanAbcc8        TGGGCTATGCCAGTACAGATCATTGTGGGTGTGATTCTCCTCTACTACATACTCGGAGTC 1500
hamsterabcc8      TGGACGATGCCAGTACAGATCATTGTGGGCGTGATCCTTCTCTACTACATCCTTGGGGTC 1374
                  *** * ********************** ***** ** *********** ** ** ***

humanAbcc8        AGTGCCTTAATTGGAGCAGCTGTCATCATTCTACTGGCTCCTGTCCAGTACTTCGTGGCC 1560
hamsterabcc8      AGTGCCTTGATTGGAGCAGCTGTCATCATTCTGCTGGCTCCTGTACAGTACTTTGTGGCC 1434
                  ******** ********************** *********** ******** ******

humanAbcc8        ACCAAGCTGTCTCAGGCCCAGCGGAGCACACTGGAGTATTCCAATGAGCGGCTGAAGCAG 1620
hamsterabcc8      ACCAAGCTCTCCCAGGCACAGCGGACGACCTTGGAGCACTCCAACGAGAGGCTGAAGCAG 1494
                  ******** ** ***** ******* **  ***** * ***** *** ***********

humanAbcc8        ACCAACGAGATGCTCCGCGGCATCAAGCTGCTGAAGCTGTACGCCTGGGAGAACATCTTC 1680
hamsterabcc8      ACCAACGAGATGCTCCGGGGCATGAAGCTGCTCAAACTGTATGCGTGGGAGAGCATCTTC 1554
                  ***************** ***** ******** ** ***** ** ******* *******

humanAbcc8        CGCACGCGGGTGGAGACGACCCGCAGGAAGGAGATGACCAGCCTCAGGGCCTTTGCCATC 1740
hamsterabcc8      TGCTCCAGGGTGGAGGTGACTCGCAGGAAGGAGATGACCAGCCTGAGGGCGTTTGCTGTC 1614
                   ** *  ********  *** ************************ ***** *****  **

humanAbcc8        TATACCTCCATCTCCATTTTCATGAACACGGCCATCCCCATTGCAGCTGTCCTCATAACT 1800
hamsterabcc8      TACACTTCCATCTCCATCTTCATGAACACAGCCATCCCCATTGCTGCCGTCCTCATCACC 1674
                  ** ** *********** *********** ************** ** ******** **

humanAbcc8        TTCGTGGGCCACGTCAGCTTCTTCAAAGAGGCCGACTTCTCGCCCTCCGTGGCCTTTGCC 1860
hamsterabcc8      TTCGTGGGCCACGTCAGCTTCTTCAAAGAGTCGGACTTGTCACCCTCGGTGGCCTTTGCC 1734
                  ****************************** * ***** ** ***** ************

humanAbcc8        TCCCTCTCCCTCTTCCATATCTTGGTCACACCGCTGTTCCTGCTGTCCAGTGTGGTCCGA 1920
hamsterabcc8      TCCCTCTCTCTCTTCCACATCCTGGTCACTCCACTGTTCCTGCTGTCTAGCGTGGTTCGG 1794
                  ******** ******** *** ******* ** ************** ** ***** **

humanAbcc8        TCTACCGTCAAAGCTCTAGTGAGCGTGCAAAAGCTAAGCGAGTTCCTGTCCAGTGCAGAG 1980
hamsterabcc8      TCCACTGTCAAAGCCCTGGTGAGCGTGCAAAAACTGAGCGAGTTCCTGTCTAGTGCAGAG 1854
                  ** ** ******** ** ************** ** ************** *********
```

```
humanAbcc8        ATCCGTGAGGAGCAGTGTGCCCCCCATGAGCCCACACCTCAGGGCCCAGCCAGCAAGTAC 2040
hamsterabcc8      ATCCGTGAGGAGCAGTGTGCCCCCCGAGAGCCTGCACCCCAAGGCCAAGCCGGCAAGTAC 1914
                  ************************  *****  **** ** **** **** ********

humanAbcc8        CAGGCGGTGCCCCTCAGGGTTGTGAACCGCAAGCGTCCAGCCCGGGAGGATTGTCGGGGC 2100
hamsterabcc8      CAGGCAGTGCCCCTCAAGGTTGTGAACCGCAAACGCCCAGCCCGGGAAGAGGTCCGGGAC 1974
                  ***** ********** *************** ** *********** **    **** *

humanAbcc8        CTCACCGGCCCACTGCAGAGCCTGGTCCCCAGTGCAGATGGCGATGCTGACAACTGCTGT 2160
hamsterabcc8      CTCCTGGGCCCACTGCAGAGGCTGGCCCCTAGCATGGACGGGGATGCTGACAACTTCTGT 2034
                  ***   ************** **** *** **    ** ** ************* ****

humanAbcc8        GTCCAGATCATGGGAGGCTACTTCACGTGGACCCCAGATGGAATCCCCACACTGTCCAAC 2220
hamsterabcc8      GTCCAGATCATCGGAGGCTTCTTCACCTGGACCCCTGATGGAATCCCCACTCTGTCCAAC 2094
                  *********** ******* ****** ******** ************** *********

humanAbcc8        ATCACCATTCGTATCCCCCGAGGCCAGCTGACTATGATCGTGGGGCAGGTGGGCTGCGGC 2280
hamsterabcc8      ATCACCATCCGTATTCCCCGAGGTCAGCTAACCATGATTGTGGGGCAGGTGGGCTGCGGC 2154
                  ******** ***** ******** ***** ** ***** ********************

humanAbcc8        AAGTCCTCGCTCCTTCTAGCCGCACTGGGGGAGATGCAGAAGGTCTCAGGGGCTGTCTTC 2340
hamsterabcc8      AAGTCCTCGCTCCTCCTCGCCACCCTGGGGGAGATGCAGAAGGTGTCGGGGGCCGTCTTC 2214
                  ************** ** *** * ******************** ** ***** ******

humanAbcc8        TGGAGCAGC---CTTCCTGACAGCGAGATAGGAGAGGACCCCAGCCCAGAGCGGGAGACA 2397
hamsterabcc8      TGGAACAGCAACCTTCCGGACAGCGAGGGAGAGGACCCCAGCAGCCCAGAGCGGGAGACA 2274
                  **** ****   ***** *********  **  **   *  ******************

humanAbcc8        GCGACCGACTTGGATATCAGGAAGAGAGGCCCCGTGGCCTATGCTTCGCAGAAACCATGG 2457
hamsterabcc8      GCAGCTGGCTCGGATATCAGGAGCAGAGGCCCCGTGGCCTACGCATCTCAGAAACCATGG 2334
                  **  * * ** ***********  ***************** ** ** ************

humanAbcc8        CTGCTAAATGCCACTGTGGAGGAGAACATCATCTTTGAGAGTCCCTTCAACAAACAACGG 2517
hamsterabcc8      CTGCTAAACGCCACCGTGGAAGAGAACATCACCTTCGAGAGTCCCTTCAATAAGCAGCGG 2394
                  ******** ***** ***** ********** *** ************** ** ** ***

humanAbcc8        TACAAGATGGTCATTGAAGCCTGCTCTCTGCAGCCAGACATCGACATCCTGCCCCATGGA 2577
hamsterabcc8      TACAAGATGGTCATCGAAGCCTGCTCCCTGCAGCCGGACATAGACATCCTGCCCCACGGA 2454
                  ************** *********** ******** ***** ************** ***

humanAbcc8        GACCAGACCCAGATTGGGGAACGGGGCATCAACCTGTCTGGTGGTCAACGCCAGCGAATC 2637
hamsterabcc8      GACCAGACTCAGATTGGGGAACGGGGCATCAACCTGTCTGGTGGTCAGCGTCAGCGTATC 2514
                  ******** ************************************ ** ***** ***

humanAbcc8        AGTGTGGCCCGAGCCCTCTACCAGCACGCCAACGTTGTCTTCTTGGATGACCCCTTCTCA 2697
hamsterabcc8      AGTGTGGCCAGAGCCCTCTACCAGCAGACCAATGTCGTCTTCTTGGATGACCCCTTCTCA 2574
                  ********* ***************  **** ** ************************

humanAbcc8        GCTCTGGATATCCATCTGAGTGACCACTTAATGCAGGCCGGCATCCTTGAGCTGCTCCGG 2757
hamsterabcc8      GCTTTGGATGTCCATCTGAGTGACCACCTGATGCAGGCCGGCATCCTTGAGCTGCTCCGG 2634
                  *** ***** ***************** * ******************************

humanAbcc8        GACGACAAGAGGACAGTGGTCTTAGTGACCCACAAGCTACAGTACCTGCCCCATGCAGAC 2817
hamsterabcc8      GATGACAAGAGGACAGTGGTCTTGGTGACCCACAAGCTACAGTATCTGCCTCATGCAGAC 2694
                  ** ******************** ********************** ***** *********


humanAbcc8        TGGATCATTGCCATGAAGGATGGCACCATCCAGAGGGAGGGTACCCTCAAGGACTTCCAG 2877
hamsterabcc8      TGGATCATTGCCATGAAGGATGGGACCATTCAGAGGGAAGGGACGCTCAAGGACTTCCAG 2754
                  ********************** ***** ******** ** ** ***************

humanAbcc8        AGGTCTGAATGCCAGCTCTTTGAGCACTGGAAGACCCTCATGAACCGACAGGACCAAGAG 2937
hamsterabcc8      AGGTCCGAGTGCCAGCTCTTTGAGCACTGGAAGACCCTCATGAACCGGCAGGACCAAGAG 2814
                  ***** ** ************************************ ************

humanAbcc8        CTGGAGAAGGAGACTGTCACAGAGAGAAAAGCCACAGAGCCACCCCAGGGCCTATCTCGT 2997
hamsterabcc8      CTGGAGAAGGAGACAGTCATGGAGAGGAAAGCCTCAGAGCCATCTCAGGGCCTGCCCCGT 2874
                  ************** ****  ***** ****** ******** * ********  * ***
```

```
humanAbcc8        GCCATGTCCTCGAGGGATGGCCTTCTGCAGGATGAGGAAGAGGAGGAAGAGGAGGCAGCT 3057
hamsterabcc8      GCCATGTCCTCCAGAGACGGCCTTCTGCTGGATGAGGAAGAGGAGGAAGAGGAGGCAGCC 2934
                  *********** ** ** ********** ******************************

humanAbcc8        GAGAGCGAGGAGGATGACAACCTGTCGTCCATGCTGCACCAGCGTGCTGAGATCCCATGG 3117
hamsterabcc8      GAAAGCGAGGAAGATGACAACTTATCTTCAGTGCTGCATCAGCGAGCTAAGATCCCCTGG 2994
                  ** ******** ********* * ** **  ******* ***** *** ******* ***

humanAbcc8        CGAGCCTGCGCCAAGTACCTGTCCTCCGCCGGCATCCTGCTCCTGTCGTTGCTGGTCTTC 3177
hamsterabcc8      CGAGCCTGCACTAAGTATCTGTCCTCTGCTGGCATTCTGCTCCTGTCCCTGCTTGTCTTC 3054
                  ********* * ***** ******** ** ***** ***********  **** ******

humanAbcc8        TCACAGCTGCTCAAGCACATGGTCCTGGTGGCCATCGACTACTGGCTGGCCAAGTGGACC 3237
hamsterabcc8      TCCCAGCTGCTCAAGCACATGGTCTTGGTGGCCATTGATTATTGGCTGGCCAAGTGGACG 3114
                  ** ********************** ********** ** ** *****************

humanAbcc8        GACAGCGCCCTGACCCTGACCCCTGCAGCCAGGAACTGCTCCCTCAGCCAGGAGTGCACC 3297
hamsterabcc8      GACAGTGCCCTGGTCCTGAGCCCCGCTGCCAGGAACTGTTCGCTCAGCCAGGAATGTGAC 3174
                  ***** ******  ***** *** ** *********** ** *********** **   *

humanAbcc8        CTCGACCAGACTGTCTATGCCATGGTGTTCACGGTGCTCTGCAGCCTGGGCATTGTGCTG 3357
hamsterabcc8      CTGGACCAGTCTGTCTATGCCATGGTATTCACCTTGCTCTGCAGCCTGGGTATCGTGCTG 3234
                  ** ****** ***************** *****  **************** ** ******

humanAbcc8        TGCCTCGTCACGTCTGTCACTGTGGAGTGGACAGGGCTGAAGGTGGCCAAGAGACTGCAC 3417
hamsterabcc8      TGCCTGGTCACCTCTGTCACTGTGGAGTGGACGGGACTGAAGGTGGCCAAGAGGCTACAC 3294
                  ***** ***** ******************** ** ***************** ** ***

humanAbcc8        CGCAGCCTGCTAAACCGGATCATCCTAGCCCCCATGAGGTTTTTTGAGACCACGCCCCTT 3477
hamsterabcc8      CGCAGCCTGCTCAACCGCATCATCCTGGCCCCCATGAGGTTCTTTGAGACCACACCCCTC 3354
                  *********** ***** ******** ************** *********** *****

humanAbcc8        GGGAGCATCCTGAACAGATTTTCATCTGACTGTAACACCATCGACCAGCACATCCCATCC 3537
hamsterabcc8      GGGAGTATCCTGAACAGATTTTCATCCGACTGTAACACCATTGACCAGCACATCCCATCC 3414
                  ***** ******************** ************** ******************

humanAbcc8        ACGCTGGAGTGCCTGAGCCGCTCCACCCTGCTCTGTGTCTCAGCCCTGGCCGTCATCTCC 3597
hamsterabcc8      ACGCTGGAGTGTCTGAGCCGGTCCACCCTGCTGTGTGTCTCCGCCCTGACTGTCATCTCC 3474
                  *********** ******** *********** ******** ****** * *********

humanAbcc8        TATGTCACACCTGTGTTCCTCGTGGCCCTCTTGCCCCTGGCCATCGTGTGCTACTTCATC 3657
hamsterabcc8      TATGTCACACCCGTGTTCCTCGTGGCCCTCTTACCCCTAGCTGTTGTGTGCTACTTCATT 3534
                  *********** ******************** ***** **  * **************

humanAbcc8        CAGAAGTACTTCCGGGTGGCGTCCAGGGACCTGCAGCAGCTGGATGACACCACCCAGCTT 3717
hamsterabcc8      CAGAAGTACTTCCGAGTGGCATCCAGGGACCTGCAGCAGCTGGACGACACGACGCAGCTC 3594
                  ************** ***** ************************ ***** ** *****

humanAbcc8        CCACTTCTCTCACACTTTGCCGAAACCGTAGAAGGACTCACCACCATCCGGGCCTTCAGG 3777
hamsterabcc8      CCGCTCGTCTCACACTTTGCTGAAACTGTGGAGGGACTCACCACCATCCGTGCCTTCAGG 3654
                  ** **  ************* ***** ** ** ***************** *********

humanAbcc8        TATGAGGCCCGGTTCCAGCAGAAGCTTCTCGAATACACAGACTCCAACAACATTGCTTCC 3837
hamsterabcc8      TACGAGGCCCGGTTCCAGCAGAAGCTTCTAGAATATACCGACTCCAACAACATCGCCTCC 3714
                  ** ************************** ***** ** ************** ** ***

humanAbcc8        CTCTTCCTCACAGCTGCCAACAGATGGCTGGAAGTCCGAATGGAGTACATCGGTGCATGT 3897
hamsterabcc8      CTCTTCCTCACGGCAGCCAACAGATGGCTGGAAGTCTGCATGGAGTACATCGGAGCGTGC 3774
                  *********** ** ********************** * ************** ** **

humanAbcc8        GTGGTGCTCATCGCAGCGGTGACCTCCATCTCCAACTCCCTGCACAGGGAGCTCTCTGCT 3957
hamsterabcc8      GTGGTACTCATTGCGGCTGCCACCTCCATCTCCAACTCCCTGCACAGGGAACTTTCTGCT 3834
                  ***** ***** ** ** *  ****************************** ** ******

humanAbcc8        GGCCTGGTGGGCCTGGGCCTTACCTACGCCCTAATGGTCTCCAACTACCTCAACTGGATG 4017
hamsterabcc8      GGCCTGGTGGGCCTGGGCCTCACCTATGCCTTGATGGTCTCCAACTACCTCAACTGGATG 3894
                  ******************** ***** *** * ***************************
```

```
humanAbcc8        GTGAGGAACCTGGCAGACATGGAGCTCCAGCTGGGGGGCTGTGAAGCGCATCCATGGGCTC 4077
hamsterabcc8      GTGAGGAACCTGGCGGACATGGAGATCCAGCTGGGGGGCTGTGAAGAGGATCCACGCACTC 3954
                  ************** ********* ******************** * ***** *  ***

humanAbcc8        CTGAAAACCGAGGCAGAGAGCTACGAGGGGCTCCTGGCACCATCGCTGATCCCAAAGAAC 4137
hamsterabcc8      CTGAAAACCGAGGCGGAGAGCTATGAGGGGCTCCTGGCGCCGTCGTTGATCCCCAAGAAC 4014
                  ************** ******** ************** ** *** ******* ******

humanAbcc8        TGGCCAGACCAAGGGAAGATCCAGATCCAGAACCTGAGCGTGCGCTACGACAGCTCCCTG 4197
hamsterabcc8      TGGCCAGACCAAGGGAAGATCCAAATTCAGAACCTGAGCGTGCGCTATGACAGCTCCCTG 4074
                  ********************** ** ******************** ************

humanAbcc8        AAGCCGGTGCTGAAGCACGTCAATGCCCTCATCGCCCCTGGACAGAAGATCGGGATCTGC 4257
hamsterabcc8      AAGCCAGTGCTGAAGCATGTCAACACCCTCATCTCCCCGGGGCAGAAGATCGGGATCTGC 4134
                  ***** ********** *****  ******** **** ** ******************

humanAbcc8        GGCCGCACCGGCAGTGGGAAGTCCTCCTTCTCTCTTGCCTTCTTCCGCATGGTGGACACG 4317
hamsterabcc8      GGCCGCACAGGCAGCGGGAAGTCCTCCTTCTCCCTGGCCTTTTTCCGAATGGTGGACATG 4194
                  ******** ***** ***************** ** ***** ***** ********** *

humanAbcc8        TTCGAAGGGCACATCATCATTGATGGCATTGACATCGCCAAACTGCCGCTGCACACCCTG 4377
hamsterabcc8      TTTGAAGGACGCATCATCATTGATGGCATCGACATCGCCAAGCTGCCACTTCACACGCTG 4254
                  ** ***** * ****************** ********** ***** ** ***** ***

humanAbcc8        CGCTCACGCCTCTCCATCATCCTGCAGGACCCCGTCCTCTTCAGCGGCACCATCCGATTT 4437
hamsterabcc8      CGCTCACGCCTGTCCATCATCCTACAGGACCCCGTCCTCTTCAGCGGCACGATCAGATTC 4314
                  *********** ********** ************************** *** ****

humanAbcc8        AACCTGGACCCTGAGAGGAAGTGCTCAGATAGCACACTGTGGGAGGCCCTGGAAATCGCC 4497
hamsterabcc8      AACCTGGACCCCGAGAAGAAATGCTCAGACAGCACACTGTGGGAGGCCCTGGAGATCGCC 4374
                  *********** **** *** ******** ********************** ******

humanAbcc8        CAGCTGAAGCTGGTGGTGAAGGCACTGCCAGGAGGCCTCGATGCCATCATCACAGAAGGC 4557
hamsterabcc8      CAGCTGAAGCTGGTAGTGAAGGCACTGCCAGGAGGCCTAGATGCCATCATCACAGAAGGA 4434
                  ************** ********************** ********************

humanAbcc8        GGGGAGAATTTCAGCCAGGGACAGAGGCAGCTGTTCTGCCTGGCCCGGGCCTTCGTGAGG 4617
hamsterabcc8      GGGGAGAATTTTAGCCAGGGCCAGAGGCAGCTGTTCTGCCTGGCCCGGGCCTTCGTGAGG 4494
                  *********** ******** ****************************************

humanAbcc8        AAGACCAGCATCTTCATCATGGACGAGGCCACGGCTTCCATTGACATGGCCACGGAAAAC 4677
hamsterabcc8      AAGACCAGCATCTTCATCATGGATGAAGCAACCGCCTCCATCGACATGGCTACGGAGAAC 4554
                  ********************** ** ** ** ** ***** ******** ***** ***

humanAbcc8        ATCCTCCAAAAGGTGGTGATGACAGCCTTCGCAGACCGCACTGTGGTCACCATCGCGCAT 4737
hamsterabcc8      ATCCTCCAGAAGGTGGTGATGACAGCCTTCGCAGACCGCACGGTGGTCACCATCGCGCAT 4614
                  ******** ******************************** ******************

humanAbcc8        CGAGTGCACACCATCCTGAGTGCAGACCTGGTGATCGTCCTGAAGCGGGGTGCCATCCTT 4797
hamsterabcc8      CGTGTGCACACCATCCTGAGTGCAGACCTGGTGATGGTCCTCAAGAGGGGTGCTATCCTG 4674
                  ** ******************************** ***** *** ******* *****

humanAbcc8        GAGTTCGATAAGCCAGAGAAGCTGCTCAGCCGGAAGGACAGCGTCTTCGCCTCCTTCGTC 4857
hamsterabcc8      GAGTTTGACAAGCCAGAGACGCTCCTCAGCCAGAAGGACAGCGTGTTCGCCTCCTTTGTC 4734
                  ***** ** ********** *** ******* ************ *********** ***

humanAbcc8        CGTGCAGACAAGTGACCTGCCAGAGCCCAAGTGCCATCCCACATTCGGACCCTGCCCATA 4917
hamsterabcc8      CGTGCGGACAAGTGA---------------------------------------------- 4749
                  ***** *********

humanAbcc8        CCCCTGCCTGGGTTTTCTAACTGTAAATCACTTGTAAATAAATAGATTTGATTATTTCCT 4977
hamsterabcc8      ------------------------------------------------------------

humanAbcc8        A 4978
hamsterabcc8      -
```

Clinical, Biochemical and Genetic Mechanisms of Hyperinsulinaemic Hypoglycemia.

Consultant Paediatric Endocrinologist: Dr Khalid Hussain (02079052128 or K.Hussain@ich.ucl.ac.uk)
Consultant Molecular Geneticist: Prof S. Ellard (01392-402910 or Sian.Ellard@rdeft.nhs.uk)

Please contact Dr Ved Bhushan Arya, Clinical Research Fellow at the Institute of Child Health (07737672273,
0207 2429789/ Extn 2864, v.arya@ucl.ac.uk) as soon as diagnosis is established.
Please fill in as fully as possible and circle Yes/ No where appropriate.

Patient details
Surname.....
name.....
First name(s).....
.....
Date of birth.....
Address.....
Gender..... .....
report.....
Hospital No.....
.....
Address.....
Tel No.....
Ethnic origin.....

Requestor details
Clinician
Telephone
Email
Address for

Type of Test: Diagnostic ☐
Research ☐

Clinical information
Age at presentation (weeks): ..... Duration of hyperinsulinism:.....
Any suggestion of protein sensitivity (episodes of hypoglycaemia post protein rich meals): Yes/No/Not known
Any syndromic features (e.g. Beckwith Weidemann Syndrome). Please give details:
.....

Any other medical problems? : .....

Neonatal History
Birth weight (g): ..... Gestation (weeks): .....
IUGR: Yes/No Perinatal Asphyxia: Yes/No
Maternal details: Pre-eclampsia Yes/No
Gestational diabetes Yes/No
Other significant maternal history .....
Details of Treatment
Current Treatment and Dose (mg/kg/d): .....
Responsive to current treatment? : Yes/No
Diazoxide responsive? Yes/No/Not tried
Any other medications tried? Please give details (name of drug, duration tried): .....
18F-DOPA/PET CT scan performed? : Yes/No
If yes, focal/diffuse/atypical disease: .....
Pancreatectomy performed? : Yes/No
If yes, focal/diffuse disease: .....

Family history
Are parents related? If yes – how? : .....
Any family history of hypoglycaemia? :
.....
Any family history of diabetes? Please give details of affected family members (age of onset, treatment and duration of diabetes):
.....
.....
.....
(*NB. A pedigree showing clinical details of affected family members would be very helpfu*l).

Biochemical information
Insulin level: …….. (mU/l) C-peptide: ..... (pmols/l) Glucose level: ……. (mmol/l)
Hyperammonaemia? : Yes/No/Not known If Yes,ammonia level …….
Acyl Carnitine profile? : Normal/Abnormal/Not done. If abnormal, result?……
.....
……
Lactate, if done : …….. Pyruvate,if done : ……..
Plasma amino acids : ……
Urine organic acids result: …….

Special Investigations

Oral Glucose Tolerance test done? Yes/No. If yes, result……..

Oral Protein Loading test done? Yes/No. If yes, result……

Oral Leucine Loading test done? Yes/No. If yes, result……..

Any other information?.....
.....
.....
.....
.....
……

Testing required *(If no boxes are ticked, testing will be performed according to the clinical information provided)*
SUR1 sequencing ☐ *KCNJ11* (gene encoding Kir6.2) sequencing ☐ *GCK* (glucokinase) sequencing ☐
GLUD1 sequencing ☐ LOH analysis for 11p15 (paraffin-embedded pancreatic tissue required + blood DNA) ☐

Consent form

Consent by parent or guardian for genetic testing to determine the cause of hypoglycemia in a child less than 16 years old

Date:……..

Child's full name:……..

Date of birth:……..

Parent or guardian's full name:……..

I have given permission for a blood sample to be taken from my child to allow genetic testing to be performed. I understand that this testing will be only for the purpose of determining the cause of hypoglycaemia in my child or a member of my family. The sample will not be used for any other purpose. The testing will be performed in the molecular genetic laboratory, Peninsula Medical School, Exeter UK.

The details of the testing have been explained by …….

Signed ……

Consent for genetic testing to determine the cause of hypoglycemia (patient)

Date:……..

Name of the person:……..

Date of birth:……..

I have given a blood sample to allow genetic testing to be performed on my blood. I understand that this testing will be only for the purpose of determining the cause of hypoglycaemia that affects myself or a member of my family. The sample will not be used for any other purpose. The testing will be performed in the molecular genetic laboratory, Peninsula Medical School, Exeter UK.

The details of the testing have been explained by …….

Signed ……

If samples from other family members have been sent previously please give details:

.....
...……..

Consent for genetic testing to determine the cause of hypoglycemia (family member, if applicable)

I have given a blood sample to allow genetic testing to be performed on my blood. I understand that this testing will be only for the purpose of determining the cause of hypoglycaemia that affects a member of my family. The sample will not be used for any other purpose. The testing will be performed in the molecular genetic laboratory, Peninsula Medical School, Exeter UK.

The details of the testing have been explained by …….

1) Name of the person:……

Date of birth:……

Relationship with the patient:……..

Signed ……Date…….

2) Name of the person:……

Date of birth:……

Relationship with the patient:…….

Signed ……Date…….

3) Name of the person:……

Date of birth:……

Relationship with the patient:…….

Signed ……Date…….

4) Name of the person:……

Date of birth:……

Relationship with the patient:…….

Signed ……Date…….

Samples taken
The samples should be labeled with name and date of birth and can either be:
1. Our preferred option is Blood 3-5 mls: taken in tubes containing EDTA and couriered fresh (not frozen). This should be sent in a package with at least two layers of wrapping and include absorbent material to absorb any blood that leaks out of the tube.
2. Or made into DNA and 2-10 micrograms (to allow repeats) sent at room temperature. Again please make sure the tube is very securely sealed.

Where should samples be sent?
Please discuss with Dr Ved Bhushan Arya (v.arya@ucl.ac.uk/ 07737672273/ 02072429789, Ex 2864) before sending samples.
The samples should be sent to:
Dr. Ved Bhushan Arya
Clinical Research Fellow
Institute of Child Health
Clinical & Molecular Genetics Unit
Developmental Endocrinology Research
30, Guildford Street
London
WC1N 1EH
Email: v.arya@ucl.ac.uk

Other questions
Please do contact me if there are any other questions. We would be very keen to help in any way we can.

Parent/Guardian Information Sheet – January 2012

Project Title: Clinical, Biochemical and Genetic Mechanisms of Hyperinsulinaemic Hypoglycemia.

1. The aim of the study

The aim of this project is to investigate the genetic causes of hypoglycemia (low blood glucose) in newborns, infants and children.

Previous research has already identified a number of abnormalities in certain genes that can cause excessive amounts of insulin (hyperinsulinism) to be made causing hypoglycemia, but we still don't know the cause in the majority of children. Recently, we found a new genetic cause of this condition and the aim of this study is to characterize this novel type of hyperinsulinism along with trying to unravel further genetic causes.

2. Why is the study being done?

A normal blood glucose level is important for brain function. Hypoglycemia (low blood glucose levels) can cause significant brain injury. We currently have very little understanding as to the genetic mechanisms that cause hypoglycemia in childhood. This study will allow us to understand why hypoglycemia develops in some children and the genetic basis of this. This will have important implications for the future treatment of our children.

3. How is the study being done?

If you agree to participate in this study, your child will have an additional blood sample taken when they are having their routine investigations. We will use this blood sample to extract DNA (genetic material). The DNA will then be used to analyze certain genes. The extra blood sample that we take will do no harm to your child, as the amount of blood that we will take is extremely small (a few tea spoonfuls). As a part of the study, we might request blood samples from you or other related family members; especially if there is a family member affected with diabetes mellitus/ hypoglycemia. This blood sample will be used to extract DNA that will be used only for the purpose of establishing a genetic cause for hypoglycemia.

4. What are the risks and discomfort?

No risk to the child can be foreseen. Your child might have a cannula inserted for routine medical treatment and we will then take the blood sample from the cannula. There is discomfort from the insertion of the cannula but we would normally numb the skin anyway with a local anaesthetic cream.

5. Who will have access to the case/research records?

Only the researchers and a representative of the Research Ethics Committee will have access to the data collected during this study.

6. What are the arrangements for compensation?

An independent Research Ethics Committee who believes that it is of minimal risk to your child has approved this research. However, research can carry unforeseen risks and we are required to tell you that *if your child is harmed and this is due to someone's negligence, you may have grounds for legal action for compensation in respect of any harm arising out of participation in the study.*

7. What are the potential benefits?

This study will not bring any immediate benefits to your child. However, if we find the genetic mechanism that is causing the hypoglycemia in your child we will explain this to you and it will give us a better understanding of why some children do develop this condition.

8. Do I have to take part in this study?

If you decide, now or at a later stage, that you do not wish to participate in this research project, that is entirely your right and will not in any way prejudice any present or future treatment.

9. Who do I speak to if problems arise?

If you have any complaints about the way in which this research project has been, or is being conducted, please, in the first instance, discuss them with the researcher (Dr.Ved Bhushan Arya: 07737672273; 02072429789/ Extn 2864; v.arya@ucl.ac.uk).

LIST OF PRESENTATIONS

- **Arya VB**, Alam S, Senniappan S, Flanagan SE, Ellard S, Hussain K. Long-term endocrine and exocrine outcome of medically unresponsive diffuse congenital hyperinsulinism managed with near-total pancreatectomy: 18 years' experience. Poster presentation at 41st Meeting of the British Society of Paediatric Endocrinology and Diabetes in Brighton, 13-15 November 2013.
- **Arya VB,** Heslegrave A, Shah P, Gilbert C, Morgan K, Hinchey L, Flanagan SE, Ellard S, Hussain K. Normoammonaemic Protein Sensitive Hyperinsulinaemic Hypoglycaemia: ? A novel syndrome. Poster presentation at 41st Meeting of the British Society of Paediatric Endocrinology and Diabetes in Brighton, 13-15 November 2013.
- Senniappan S, Alexandrescu S, Tatevian N, Shah P, **Arya V**, Flanagan SE, Ellard S, Rampling D, Ashworth M, Brown R, Hussain K. Successful treatment of four patients with severe hyperinsulinaemic hypoglycaemia with a novel therapy using mTOR inhibitor. Free communication at the 41st Meeting of the British Society of Paediatric Endocrinology and Diabetes in Brighton, 13-15 November 2013.
- Shah P, Gilbert C, Morgan K, Hinchey L, Senniappan S, **Arya V**, Levy H, Hussain K. Successful Use of Long Acting Octreotide in Treatment of Congenital Hyperinsulinism. Free communication at the 41st Meeting of the British Society of Paediatric Endocrinology and Diabetes in Brighton, 13-15 November 2013.
- Sherif MM, Hadeed I, **Arya VB**, Dattani M, Hussain K. Three families with diabetes mellitus and sensorineural deafness. Poster presentation at the 41st Meeting of the British Society of Paediatric Endocrinology and Diabetes in Brighton, 13-15 November 2013.
- **Arya VB**, Alam S, Senniappan S, Flanagan SE, Ellard S, Hussain K. Long-term endocrine and exocrine outcome of medically unresponsive diffuse congenital hyperinsulinism managed with near-total pancreatectomy: 18 years' experience. Poster presentation at the 9th Joint Meeting of Paedriatic Endocrinology in Milan, Italy September 19-22, 2013.
- Nessa A, Thomas A, Aziz QH, Harmer S, Heslegrave A, James C, **Arya VB**, Rahman S, Sherif M, Flanagan SE, Kapoor RR, Ellard S, Tinker A, Hussain K. Understanding the molecular basis of congenital hyperinsulinism due to autosomal dominant ABCC8 and KCNJ11 mutations. Free communication at the 9th Joint Meeting of Paedriatic Endocrinology in Milan, Italy September 19-22, 2013.

- Senniappan S, Shah P, **Arya VB**, Flanagan SE, Ellard S, Rampling D, Ashworth M, Hussain K. Successful treatment of five patients with severe hyperinsulinaemic hypoglycaemia with a novel therapy using mTOR inhibitor. Free communication at the 9th Joint Meeting of Paedriatic Endocrinology in Milan, Italy September 19-22, 2013.
- Sherif MM, Hadeed I, Nessa A, Rahman SA, **Arya VB**, Senniappan S, Dattani M, Hussain K. Two families with diabetes mellitus and sensorineural deafness. Poster presentation at the 9th Joint Meeting of Paedriatic Endocrinology in Milan, Italy September 19-22, 2013.
- **Arya VB**, Senniappan S, Flanagan SE, Ellard S, Hussain K. Assessment of pancreatic exocrine function in children following near total pancreatectomy for diffuse congenital hyperinsulinism. Poster presentation at annual European Society of Paediatric Endocrinology meeting in Leipzig, Germany, 2012
- Senniappan S, **Arya VB**, Hussain K. Prospective follow up of patients with diffuse congenital hyperinsulinism successfully treated with octreotide therapy. Poster presentation at annual European Society of Paediatric Endocrinology meeting in Leipzig, Germany, 2012
- **Arya VB**, Papadopoulou M, Senniappan S, Hussain K. Beckwith-Wiedemann syndrome due to paternally inherited duplication of chromosome 11p and Jacobsen syndrome. Poster presentation at 40th Meeting of British Society of Paediatric Endocrinology and Diabetes, Leeds, 7-9 Nov 2012

LIST OF PUBLICATIONS IN PEER REVIEWED JOURNALS

(PDF of 6 most important publications attached)

1. Senniappan S, Pitt K, Shah P, **Arya V**, Jaiswal S, Haddad M, Hind J, Dhawan A, Davenport M, Hussain K. Postprandial Hyperinsulinaemic Hypoglycaemia Secondary to a Congenital Portosystemic Shunt. *Horm Res Paediatr. 2015 Jan 21*.
2. **Arya VB,** Aziz Q, Nessa A, Tinker A, Hussain K. Congenital hyperinsulinism: clinical and molecular characterisation of compound heterozygous ABCC8 mutation responsive to Diazoxide therapy. *Int J Pediatr Endocrinol. 2014;2014(1):24.*
3. Shah P, **Arya VB**, Flanagan SE, Morgan K, Ellard S, Senniappan S, Hussain K. Sirolimus therapy in a patient with severe hyperinsulinaemic hypoglycaemia due to a compound heterozygous ABCC8 gene mutation. *J Pediatr Endocrinol Metab. 2014 Dec 17.*
4. **Arya, VB**, Guemes, M., Nessa, A., Alam, S., Shah, P., Gilbert, C., Senniappan S., Flanagan S.E., Ellard S., Hussain, K. (2014). Clinical and histological heterogeneity of congenital hyperinsulinism due to paternally inherited heterozygous ABCC8/KCNJ11 mutations.. *Eur J Endocrinol*, *171*(6), 685-695.
5. Kühnen, P., Matthae, R., Blankenstein, O., **Arya, V**., Rothe K, Wächter S, Singer M, Mohnike W, Eberhard T, Raile K, Lauffer LM, Iakoubov R, Hussain K, Blankenstein O. (2014). Occurrence of giant focal forms of congenital hyperinsulinism with incorrect visualization by F DOPA-PET/CT scanning. *Clinical Endocrinology*. *Dec;81(6):847-54.*
6. Khoriati, D., **Arya VB**, Hussain, K., Flanagan, S. E., & Ellard, S. (2013). Prematurity, macrosomia, hyperinsulinaemic hypoglycaemia and a dominant ABCC8 gene mutation. *BMJ Case Reports*.
7. Senniappan, S., Alexandrescu, S., Tatevian, N., Shah, P., **Arya, V.**, Flanagan, S., Ellard S, Rampling D, Ashworth M, Brown RE., Hussain, K. (2014). Sirolimus therapy in infants with severe hyperinsulinemic hypoglycemia.. *N Engl J Med*, *370*(12), 1131-1137.
8. Demirbilek, H., Tahir, S., Baran, R. T., Sherif, M., Shah, P., Ozbek, M. N., Hatipoglu N, Baran A, **Arya VB**, Hussain, K. (2014). Familial isolated growth hormone deficiency due to a novel homozygous missense mutation in the growth hormone releasing hormone receptor gene: clinical presentation with hypoglycemia.. *J Clin*

Endocrinol Metab, *99*(12), E2730-E2734.

9. Kalaivanan, P., **Arya VB**, Shah, P., Datta, V., Flanagan, S. E., Mackay, D. J. G., Ellard S., Senniappan S., Hussain, K. (2014). Chromosome 6q24 transient neonatal diabetes mellitus and protein sensitive hyperinsulinaemic hypoglycaemia. *J Pediatr Endocrinol Metab., 27*(11-12), 1065-1069.
10. Demirbilek, H., Shah, P., **Arya VB**, Hinchey, L., Flanagan, S. E., Ellard, S., Hussain, K. (2014). Long-Term Follow-Up of Children With Congenital Hyperinsulinism on Octreotide Therapy. *J Clin Endocrinol Metab*, *99*(10), 3660-3667.
11. **Arya VB**, Senniappan, S., Demirbilek, H., Alam, S., Flanagan, S. E., Ellard, S., Hussain, K. (2014). Pancreatic endocrine and exocrine function in children following near-total pancreatectomy for diffuse congenital hyperinsulinism.. *PLoS One*, *9*(5), e98054.
12. Demirbilek, H., **Arya VB**, Ozbek, M. N., Akinci, A., Dogan, M., Demirel, F., Houghton J, Kaba S, Guzel F, Baran RT, Unal S, Tekkes S, Flanagan SE, Ellard S,. Hussain, K. (2014). Clinical characteristics and phenotype-genotype analysis in Turkish patients with congenital hyperinsulinism; predominance of recessive KATP channel mutations.. *Eur J Endocrinol*, *170*(6), 885-892.
13. Padidela, R., Fiest, M., **Arya, V.**, Smith, V. V., Ashworth, M., Rampling, D., Newbould M, Batra G, James J, Wright NB, Dunne MJ, Clayton PE, Banerjee I,. Hussain, K. (2014). Insulinoma in childhood: Clinical, radiological, molecular and histological aspects of nine patients. *Eur J Endocrinol*, *170*(5), 741-747
14. **Arya VB**, Flanagan, S. E., Schober, E., Rami-Merhar, B., Ellard, S., & Hussain, K. (2014). Activating AKT2 mutation: hypoinsulinemic hypoketotic hypoglycemia.. *J Clin Endocrinol Metab*, *99*(2), 391-394.
15. **Arya VB**, Mohammed, Z., Blankenstein, O., De Lonlay, P., & Hussain, K. (2014). Hyperinsulinaemic hypoglycaemia.. *Horm Metab Res*, *46*(3), 157-170.
16. **Arya VB**, Rahman, S., Senniappan, S., Flanagan, S. E., Ellard, S., & Hussain, K. (2014). HNF4A mutation: switch from hyperinsulinaemic hypoglycaemia to maturity-onset diabetes of the young, and incretin response.. *Diabet Med*, *31*(3), e11-e15.
17. **Arya VB**, Flanagan, S. E., Kumaran, A., Shield, J. P., Ellard, S., Hussain, K., Kapoor, R. R. (2013). Clinical and molecular characterisation of hyperinsulinaemic hypoglycaemia in infants born small-for-gestational age.. *Arch Dis Child Fetal Neonatal Ed*, *98*(4), F356-F358.
18. Mohamed, Z., **Arya VB**, & Hussain, K. (2012). Hyperinsulinaemic Hypoglycaemia:

Genetic Mechanisms, Diagnosis and Management. *Journal Of Clinical Research In Pediatric Endocrinology*, *4*(4), 169-181.

19. Senniappan, S., **Arya VB**, & Hussain, K. (2013). The molecular mechanisms, diagnosis and management of congenital hyperinsulinism.. *Indian J Endocrinol Metab*, *17*(1), 19-30.
20. **Arya VB**, Senniappan, S., Guemes, M., & Hussain, K. (2013). Neonatal Hypoglycemia. *Indian Journal of Pediatrics*, 1-8.
21. Kapoor, R. R., Flanagan, S. E., **Arya VB**, Shield, J. P., Ellard, S., & Hussain, K. (2013). Clinical and molecular characterisation of 300 patients with congenital hyperinsulinism.. *Eur J Endocrinol*, *168*(4), 557-564.

INTERNATIONAL JOURNAL OF PEDIATRIC ENDOCRINOLOGY

CASE REPORT Open Access

Congenital hyperinsulinism: clinical and molecular characterisation of compound heterozygous *ABCC8* mutation responsive to Diazoxide therapy

Ved Bhushan Arya[1†], Qadeer Aziz[2†], Azizun Nessa[3], Andrew Tinker[2] and Khalid Hussain[1,4*]

Abstract

Background: Mutations in *ABCC8* and *KCNJ11* are the most common cause of congenital hyperinsulinism (CHI). Recessive as well as dominant acting *ABCC8/KCNJ11* mutations have been described. Diazoxide, which is the first line medication for CHI, is usually ineffective in recessive *ABCC8* mutations. We describe the clinical and molecular characterisation of a recessive *ABCC8* mutation in a CHI patient that is diazoxide response.

Clinical case: A term macrosomic female infant presented with symptomatic persistent hypoglycaemia confirmed to be secondary to CHI. She exhibited an excellent response to moderate doses of diazoxide (10 mg/kg/day). Molecular genetic analysis of the proband confirmed a biallelic *ABCC8* mutation – missense R526C inherited from an unaffected mother and a frameshift c.1879delC mutation (H627Mfs*20) inherited from an unaffected father. Follow-up highlighted persistent requirement for diazoxide to control CHI. Functional analysis of mutants confirmed them to result in diazoxide-responsive CHI, consistent with the clinical phenotype.

Conclusion: Biallelic *ABCC8* mutations may result in diazoxide-responsive CHI. Irrespective of the molecular genetic analysis results, accurate assessment of the response to diazoxide should be undertaken before classifying a patient as diazoxide-responsive or unresponsive CHI.

Keywords: Congenital hyperinsulinism, Hypoglycaemia, *ABCC8*, Diazoxide

Background

Congenital hyperinsulinism (CHI) is due to an inappropriate insulin secretion by the β-cells of the islets of Langerhans [1]. It usually presents with severe hypoketotic hypofattyacidaemic hypoglycaemia [2]. The majority of the affected newborns are macrosomic at birth and require high intravenous glucose administration to maintain plasma glucose above 3.5 mmol/l [3].

Mutations in *ABCC8* and *KCNJ11*, which encode the SUR1 and Kir6.2 subunits of pancreatic ATP-sensitive potassium channel (K_{ATP}), are by far the most common cause of CHI and are estimated to account for 36%-69% of all cases [4-6]. K_{ATP} channels are octameric protein complexes composed of four pore-forming Kir6.2 subunits and four sulfonylurea receptor 1 (SUR1) subunits, and form a link between cellular metabolism and membrane excitability [7,8]. It is thought that the β-cells in patients with CHI are persistently depolarized because of abnormally modulated or absent K_{ATP} channels. This depolarisation opens the voltage-gated calcium channels and leads to unregulated insulin exocytosis. Although dominant acting *ABCC8/KCNJ11* mutations have been reported, recessively inherited mutations are more common [4,5,9,10].

Diazoxide, which binds to the SUR1 subunit of the K_{ATP} channel and reduces insulin secretion by hyperpolarisation of the pancreatic β-cell plasma membrane, is the first line of treatment for CHI [1]. However, recessive inactivating mutations in *ABCC8* and *KCNJ11* usually cause severe diazoxide-unresponsive CHI due to defects in channel biogenesis, turnover, trafficking or regulation [11].

* Correspondence: khalid.hussain@ucl.ac.uk
†Equal contributors
[1]London centre for Paediatric Endocrinology, Great Ormond Street Hospital for Children NHS Foundation Trust, London WC1N 3JH and The Institute of Child Health, University College London, London WC1N 1EH, UK
[4]Developmental Endocrinology Research Group, Molecular Genetics Unit, Institute of Child Health, University College London, 30 Guilford Street, London WC1N 1EH, UK
Full list of author information is available at the end of the article

We describe a unique genotype-phenotype correlation with diazoxide responsive CHI in a patient with compound heterozygous *ABCC8* mutation. Functional work on the mutants was consistent with the observed clinical phenotype.

Case presentation

Clinical case

A term large-for-gestational age (birth weight 4500 g at 39 weeks gestation) female infant born to non-consanguineous Caucasian parents presented with symptomatic hypoglycaemia on first day of life. There was no history of gestational diabetes mellitus in the mother. The proband developed tonic clonic seizures associated with laboratory blood glucose of 0.4 mmol/l at 22 hours of age. The infection and metabolic screen was negative. She required infusion of high concentration glucose (glucose infusion rate 16 mg/kg/minute) to maintain blood glucose above 3.5 mmol/l.

A controlled hypoglycaemia screen established the diagnosis of CHI (serum Insulin 44.5 mU/l associated with lab glucose of 2.3 mmol/l and undetectable non-esterified fatty acids and β-hydroxybutyrate). Her serum cortisol was 570 nmol/l during the hypoglycaemia screen. The rest of the hypoglycaemic screen including insulin like growth factor-1 (IGF1), and insulin-like growth factor binding protein-3 (IGFBP3), serum ammonia, lactate, acylcarnitine profile, plasma amino acids and urine organic acids was within normal reference range (results not shown).

Molecular genetic analysis for CHI was performed after informed consent from the parents (see below). She was commenced on diazoxide (5 mg/kg/day in three divided doses) and the dose was gradually increased to 10 mg/kg/day. Chlorothiazide was given along with diazoxide to counteract the side effect of fluid retention. On 10 mg/kg/day of diazoxide, she was successfully weaned off intravenous glucose administration. She demonstrated age appropriate fasting tolerance on diazoxide before discharge.

Blood glucose monitoring performed at home demonstrated satisfactory glycaemic control on diazoxide. No adjustment in diazoxide dose was required with her growth. At 9 months of age, a trial off diazoxide therapy resulted in recurrence of hypoglycaemia with fasting tolerance of only 3½ hours. Diazoxide was recommenced at 5 mg/kg/day, which led to disappearance of hypoglycaemia and age appropriate fasting tolerance.

At the time of writing, the proband is 15 months old and is able to fast for 12 hours without developing hypoglycaemia on a low dose of diazoxide (5 mg/kg/day). Neurodevelopmental assessment did not identify any abnormality.

Genetic analysis

Methods

Genomic DNA was extracted from peripheral blood leukocytes using standard procedures. The single exon of the *KCNJ11* gene was amplified in 3 overlapping fragments and sequenced. When no mutations were identified in *KCNJ11*, the 39 exons of the *ABCC8* gene were amplified by polymerase chain reaction (PCR). The products were sequenced using Big Dye Terminator cycler sequencing Kit v3.1 (Applied Biosystems, Warrington, UK) and sequencing reactions were analysed on an ABI3730 (Applied Biosystems, Warrington, UK). Sequences were compared to the reference sequence (NM_000352.2) using Mutation Surveyor software (SoftGenetics, Pa., USA).

Results

Sequence analysis identified biallelic *ABCC8* mutation in the proband – a missense mutation, R526C, inherited from an unaffected mother and a frameshift mutation, c.1879delC (H627Mfs*20), inherited from an unaffected father. Both R526C and c.1879delC (H627Mfs*20) mutations have previously been reported as recessive acting mutations in patients with focal CHI [5].

Functional analysis of mutant channels

Methods

Single point mutations (R526C and c.1879delC) were introduced into the hamster SUR1 clone by PCR using the Strategene XL Mutagenesis Kit according to the manufacturer's instructions.

Human Embryonic Kidney (HEK) 293 cells were transiently transfected with Kir6.2/SUR1, Kir6.2/SUR1c1879delC, Kir6.2/SUR1R526C or Kir6.2/SUR1c1879C + SUR1R526C (together with a small amount of eGFP (Green Fluorescence Protein) expressing plasmid to enable identification of transfected cells using epifluorescence) using FuGENE HD (Roche Diagnostics, UK) as per the manufacturers' instructions and cells were subjected to whole cell patch-clamp 48 hours after transfection.

Whole-cell patch-clamp recordings were performed as previously described [12]. Capacitance transients and series resistance in whole-cell recordings were compensated electronically by using amplifier circuitry (Multiclamp 700B). Data were filtered at 1 kHz using the filter provided with the Multiclamp 700B (4 pole Bessel) and sampled at 5 kHz using a Digidata 1440 (Axon Instruments). Currents were acquired and analysed using pClamp 10.4 (Axon Instruments). The intracellular (pipette) solution contained (mM); 140 KCl, 1.2 $MgCl_2$, 1 $CaCl_2$, 10 EGTA and 5 HEPES, 0.1 mM Na.ATP and 1 mM Na.ADP, pH 7.2 using KOH. The bath solution contained (mM); 5 KCl, 140 NaCl, 2.6 $CaCl_2$, 1.2 $MgCl_2$ and 5 HEPES (pH 7.4). Pipette resistances were between 2–4 mΩ. Diazoxide and Tolbutamide were obtained from Sigma Aldrich (Poole, UK). Agents were applied to the bath using a gravity-driven perfusion system.

Results

Whole-cell patch-clamp recordings from HEK 293 cells transfected with wild-type (WT) Kir6.2/SUR1 cDNA showed normal K_{ATP} currents which was activated by the K_{ATP} channel opener diazoxide (100 μM) and inhibited by the K_{ATP} blocker tolbutamide (100 μM) (control, 144.77 ± 25.57 pA/pF; diazoxide, 382.7 ± 37.67 pA/pF; diazoxide + tolbutamide, 98.05 ± 28.05 pA/pF, n = 5 cells, $P < 0.05$). Currents from cells transfected with the frameshift mutation SUR1c1879delC were unresponsive to diazoxide and tolbutamide (control, 85.26 ± 12.7 pA/pF; diazoxide, 91.98 ± 14.36 pA/pF; tolbutamide, 79.57 ± 11.57 pA/pF, n = 7 cells, $P > 0.05$). In contrast, currents from cells transfected with the missense mutation, SUR1R526C, activated in the presence of diazoxide albeit to a lesser extent when compared to WT (control, 76.55 ± 8.2 pA/pF; diazoxide, 175.2 ± 16.47 pA/pF; tolbutamide, 64.55 ± 8.88 pA/pF, n = 5 cells, $P < 0.05$).

Interestingly, co-expression of SUR1c1879delC and SUR1R526C (to mimic the compound heterozygous *ABCC8* (R256C/H627Mfs*20) mutation) rescued the diazoxide-sensitive K_{ATP} current which was absent when SUR1c1879-delC was expressed alone (control, 62.9 ± 9.3 pA/pF; diazoxide, 223.11 ± 60.21 pA/pF; tolbutamide, 52.26 ± 11.36 pA/pF, n = 5 cells, $P < 0.05$). These data are shown in Figure 1. The diazoxide-sensitive K_{ATP} current in the double mutant transfected cells was significantly greater as compared to SUR1c1879delC transfected cells (160.2 ± 52.9 vs 8.72 ± 4.41 pA/pF, $P = 0.01$) and equivalent to WT Kir6.2/SUR1 transfected cells (160.2 ± 52.9 vs 237.9 ± 59.1 pA/pF, $P = 0.33$).

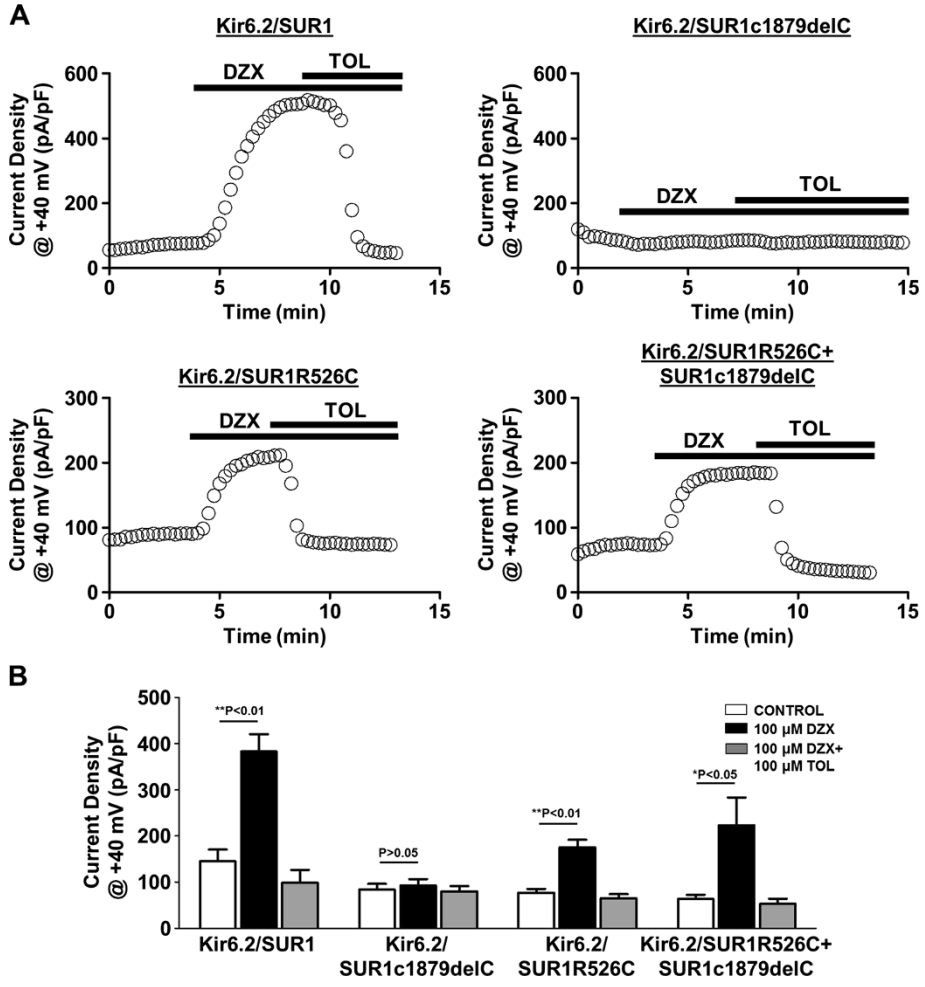

Figure 1 Functional characterisation of K_{ATP} channels with a heterozygous *ABCC8* R526C/H627Mfs*20 compound mutation. A, Representative whole-cell time-current density traces at +40 mV recorded from HEK293 cells expressing Kir6.2/SUR1, Kir6.2/SUR1c1879delC, Kir6.2/SUR1R526C and Kir6.2/SUR1R526C + SUR1C1879delC showing the effects of diazoxide (DZX) and tolbutamide (in the presence of diazoxide) (TOL). Current were recorded using a 1 s ramp protocol (−150 mV to 50 mV). **B**, Summary of the mean current-densities at +40 mV. Values are mean ± S.E.M from 5–7 cells, *$P < 0.05$, **$P < 0.01$ compared to control

There was no statistically significant difference in the K_{ATP} current seen in cells transfected with SUR1R256C alone and cells co-transfected with SUR1R256C and SUR1c1879delC (p = 0.291).

Discussion

We describe a patient with diazoxide responsive CHI due to compound heterozygous *ABCC8* mutation. The proband was macrosomic at birth (consistent with foetal hyperinsulinism) and presented with severe hypoketotic hypoglycaemia requiring high glucose infusion (16 mg/kg/minute). Investigations confirmed CHI and compound heterozygous *ABCC8* (R256C/H627Mfs*20) mutation. Surprisingly, the proband showed an excellent response to moderate doses of diazoxide (10 mg/kg/day). Subsequent follow-up revealed persistent requirement for diazoxide to control CHI. Functional analysis of the mutant K_{ATP} channel subunits confirmed a phenotype of diazoxide-responsive CHI in association with *ABCC8* R526C/H627Mfs*20 compound heterozygous mutation.

Mutations in *ABCC8* and *KCNJ11,* both monoallelic and biallelic, account for the majority of CHI patients [4,5]. Although monoallelic *ABCC8/KCNJ11* mutations can cause both diazoxide-responsive as well as diazoxide-unresponsive CHI, nearly all biallelic *ABCC8/KCNJ11* mutations result in diazoxide unresponsive CHI [9,10,13,14]. In two recent large studies comprising more than 700 patients with CHI, there was no patient reported with diazoxide responsive CHI due to biallelic *ABCC8/KCNJ11* mutation [4,5].

However, Dekel et al. reported a patient with a compound heterozygous *ABCC8* mutation (c.3992-9G > A/F1388del) who responded to diazoxide [15]. However, no functional work was done to correlate with the clinical observations.

Previous functional work on compound heterozygous *ABCC8* mutations has shown that mutations may interact to modify K_{ATP} channel function and influence disease severity. Muzyamba et al. showed that single SUR1 mutants (D1193V or R1436Q) trafficked to the plasma membrane whereas the double mutant (SUR1D1193V/R1436Q) was retained in the endoplasmic reticulum [16].

Both SUR1 R526C and H627Mfs*20 mutations have been described previously as presumed recessive acting mutations in association with CHI. Snider et al. reported one patient each with both these mutations in association with focal CHI [5]. No functional work had been done on either of these mutations. The H627Mfs*20 mutation is a frameshift mutation and is severely damaging to the protein function as shown by our functional work. When the SUR1H627Mfs*20 mutant was co-expressed with Kir6.2, there was no increase in current with the application of diazoxide indicating either absence of K_{ATP} channels on the plasma membrane surface and\or severely dysfunctional K_{ATP} channel. With the SUR1R526C mutant, there was reduced current flow under basal conditions as compared to wild-type. However, importantly, there was an increase in current with the application of diazoxide which persisted when the two mutants (SUR1R526C/H627Mfs*20) were expressed in combination, suggesting this variant to be diazoxide-responsive.

As the frameshift mutation H627Mfs*20 results in a premature termination codon and is likely to be degraded by non-sense mediated decay, it is possible that the K_{ATP} channels in double mutant SUR1R256C/H627Mfs*20 will contain SUR1 subunits produced by allele carrying R526C mutation only and hence the response shown by the SUR1R256C/H627Mfs*20 resembles that of SUR1R256C mutant. However non-sense mediated decay cannot be reproduced in the expression studies as that requires replication of intronic and exonic structure of the gene whereas the plasmids can only accommodate cDNA of the gene.

Although we used 100 μM diazoxide to assess the responsiveness of SUR1 mutants, to our knowledge there is no data in the literature as to what concentration of diazoxide is achieved at the cellular level with the standard doses of diazoxide used for medical management of CHI. However, assuming a distribution volume of ~0.2 L/kg, the dose of diazoxide administered orally to this proband is likely to result in a concentration higher (~2×) than the 100 μM we used for our studies at the cellular level [17].

Our functional data, however, is not consistent with the previous observation of diazoxide-unresponsive focal CHI in association with paternally inherited heterozygous *ABCC8* R526C mutation [5]. Marked intrafamilial clinical heterogeneity in four haploidentical siblings harbouring the identical *ABCC8* homozygous c.3992-9G > A mutation was also highlighted by Kapoor et al. [18]. This difference in clinical expression may be due to background genetic factors and other unknown factors involved in regulating gene expression.

Conclusion

In conclusion, although the majority of biallelic *ABCC8/KCNJ11* mutations result in diazoxide-unresponsive CHI, occasional biallelic and particularly compound heterozygous *ABCC8* mutations may lead to a diazoxide-responsive phenotype. Accurate clinical assessment would avoid the need for near-total pancreatectomy in such cases.

Consent

Written informed consent was obtained from the patient for publication of this Case report and any accompanying images. A copy of the written consent is available for review by the Editor-in-Chief of this journal.

Abbreviations

CHI: Congenital hyperinsulinism; KATP: Potassium sensitive ATP channel; SUR1: Sulfonylurea receptor 1; IGF1: Insulin-like growth factor 1; IGFBP3: IGF binding protein 3; PCR: Polymerase chain reaction; HEK 293 cells: Human Embryonic Kidney 293 cells; GFP: Green Fluorescence Protein; WT: Wild type.

Competing interests

The authors declare that they have no competing interests.

Authors' contributions

VBA contributed to acquisition of data and drafted the manuscript. QA performed the experiments, analyzed and interpreted the data and helped in drafting the manuscript. AN contributed to interpretation of data and revising it critically for important intellectual content. AT contributed to analysis and interpretation of data and revising it critically for important intellectual content. KH contributed to analysis and interpretation of data and revising it critically for important intellectual content. All authors read and approved the final manuscript.

Acknowledgements

The authors would like to acknowledge Dr Sarah E. Flanagan and Prof Sian Ellard from University of Exeter Medical School for contribution towards genetic testing. There is no source of funding for this manuscript preparation.

Author details

[1]London centre for Paediatric Endocrinology, Great Ormond Street Hospital for Children NHS Foundation Trust, London WC1N 3JH and The Institute of Child Health, University College London, London WC1N 1EH, UK. [2]The Heart Centre, William Harvey Research Institute, Barts and the London School of Medicine and Dentistry, Charterhouse Square, London, UK. [3]The Institute of Child Health, University College London, London WC1N 1EH, UK. [4]Developmental Endocrinology Research Group, Molecular Genetics Unit, Institute of Child Health, University College London, 30 Guilford Street, London WC1N 1EH, UK.

Received: 21 August 2014 Accepted: 25 November 2014
Published: 15 December 2014

References

1. Aynsley-Green A, Hussain K, Hall J, Saudubray JM, Nihoul-Fekete C, De Lonlay-Debeney P, Brunelle F, Otonkoski T, Thornton P, Lindley KJ: **Practical management of hyperinsulinism in infancy.** *Arch Dis Child Fetal Neonatal Ed* 2000, **82:**F98–F107.
2. Hussain K, Blankenstein O, De Lonlay P, Christesen HT: **Hyperinsulinaemic hypoglycaemia: biochemical basis and the importance of maintaining normoglycaemia during management.** *Arch Dis Child* 2007, **92:**568–570.
3. Arya VB, Mohammed Z, Blankenstein O, De Lonlay P, Hussain K: **Hyperinsulinaemic hypoglycaemia.** *Horm Metab Res* 2014, **46:**157–170.
4. Kapoor RR, Flanagan SE, Arya VB, Shield JP, Ellard S, Hussain K: **Clinical and molecular characterisation of 300 patients with congenital hyperinsulinism.** *Eur J Endocrinol* 2013, **168:**557–564.
5. Snider KE, Becker S, Boyajian L, Shyng SL, MacMullen C, Hughes N, Ganapathy K, Bhatti T, Stanley CA, Ganguly A: **Genotype and phenotype correlations in 417 children with congenital hyperinsulinism.** *J Clin Endocrinol Metab* 2013, **98:**E355–E363.
6. Demirbilek H, Arya VB, Ozbek MN, Akinci A, Dogan M, Demirel F, Houghton J, Kaba S, Guzel F, Baran RT, Unal S, Tekkes S, Flanagan SE, Ellard S, Hussain K: **Clinical characteristics and phenotype-genotype analysis in Turkish patients with congenital hyperinsulinism; predominance of recessive KATP channel mutations.** *Eur J Endocrinol* 2014, **170**(6):885–892.
7. Shyng S, Nichols CG: **Octameric stoichiometry of the KATP channel complex.** *J Gen Physiol* 1997, **110:**655–664.
8. Ashcroft FM: **ATP-sensitive potassium channelopathies: focus on insulin secretion.** *J Clin Invest* 2005, **115:**2047–2058.
9. Kapoor RR, Flanagan SE, James CT, McKiernan J, Thomas AM, Harmer SC, Shield JP, Tinker A, Ellard S, Hussain K: **Hyperinsulinaemic hypoglycaemia and diabetes mellitus due to dominant ABCC8/KCNJ11 mutations.** *Diabetologia* 2011, **54:**2575–2583.
10. Huopio H, Reimann F, Ashfield R, Komulainen J, Lenko HL, Rahier J, Vauhkonen I, Kere J, Laakso M, Ashcroft F, Otonkoski T: **Dominantly inherited hyperinsulinism caused by a mutation in the sulfonylurea receptor type 1.** *J Clin Invest* 2000, **106:**897–906.
11. James C, Kapoor RR, Ismail D, Hussain K: **The genetic basis of congenital hyperinsulinism.** *J Med Genet* 2009, **46:**289–299.
12. Aziz Q, Thomas AM, Khambra T, Tinker A: **Regulation of the ATP-sensitive potassium channel subunit, Kir6.2, by a Ca2+−dependent protein kinase. C.** *J Biol Chem* 2012, **287:**6196–6207.
13. Pinney SE, MacMullen C, Becker S, Lin YW, Hanna C, Thornton P, Ganguly A, Shyng SL, Stanley CA: **Clinical characteristics and biochemical mechanisms of congenital hyperinsulinism associated with dominant KATP channel mutations.** *J Clin Invest* 2008, **118:**2877–2886.
14. Macmullen CM, Zhou Q, Snider KE, Tewson PH, Becker SA, Aziz AR, Ganguly A, Shyng SL, Stanley CA: **Diazoxide-unresponsive congenital hyperinsulinism in children with dominant mutations of the beta-cell sulfonylurea receptor SUR1.** *Diabetes* 2011, **60:**1797–1804.
15. Dekel B, Lubin D, Modan-Moses D, Quint J, Glaser B, Meyerovitch J: **Compound heterozygosity for the common sulfonylurea receptor mutations can cause mild diazoxide-sensitive hyperinsulinism.** *Clin Pediatr (Phila)* 2002, **41:**183–186.
16. Muzyamba M, Farzaneh T, Behe P, Thomas A, Christesen HB, Brusgaard K, Hussain K, Tinker A: **Complex ABCC8 DNA variations in congenital hyperinsulinism: lessons from functional studies.** *Clin Endocrinol (Oxf)* 2007, **67:**115–124.
17. Ogilvie RI, Nadeau JH, Sitar DS: **Diazoxide concentration-response relation in hypertension.** *Hypertension* 1982, **4:**167–173.
18. Kapoor RR, Flanagan SE, Ellard S, Hussain K: **Congenital hyperinsulinism: marked clinical heterogeneity in siblings with identical mutations in the ABCC8 gene.** *Clin Endocrinol (Oxf)* 2012, **76:**312–313.

doi:10.1186/1687-9856-2014-24
Cite this article as: Arya *et al.*: Congenital hyperinsulinism: clinical and molecular characterisation of compound heterozygous *ABCC8* mutation responsive to Diazoxide therapy. *International Journal of Pediatric Endocrinology* 2014 **2014**:24.

Clinical and histological heterogeneity of congenital hyperinsulinism due to paternally inherited heterozygous *ABCC8/KCNJ11* mutations

Ved Bhushan Arya[1,2,*], Maria Guemes[1,2,*], Azizun Nessa[1], Syeda Alam[2], Pratik Shah[1,2], Clare Gilbert[2], Senthil Senniappan[1,2], Sarah E Flanagan[3], Sian Ellard[3] and **Khalid Hussain[1,2]**

[1]Developmental Endocrinology Research Group, Clinical and Molecular Genetics Unit, Institute of Child Health, University College London, 30 Guilford Street, London WC1N 1EH, UK, [2]London Centre for Paediatric Endocrinology, Great Ormond Street Hospital for Children, London WC1N 3JH, UK and [3]Institute of Biomedical and Clinical Science, University of Exeter Medical School, Exeter EX2 5DW, UK
[*](V B Arya and M Guemes contributed equally to this work)

Correspondence should be addressed to K Hussain
Email
Khalid.Hussain@ucl.ac.uk

European Journal of Endocrinology

Abstract

Context: Congenital hyperinsulinism (CHI) has two main histological types: diffuse and focal. Heterozygous paternally inherited *ABCC8/KCNJ11* mutations (depending upon whether recessive or dominant acting and occurrence of somatic maternal allele loss) can give rise to either phenotype. However, the relative proportion of these two phenotypes in a large cohort of CHI patients due to paternally inherited heterozygous *ABCC8/KCNJ11* mutations has not been reported.
Objective: The purpose of this study is to highlight the variable clinical phenotype and to characterise the distribution of diffuse and focal disease in a large cohort of CHI patients due to paternally inherited heterozygous *ABCC8/KCNJ11* mutations.
Design: A retrospective chart review of the CHI patients due to heterozygous paternally inherited *ABCC8/KCNJ11* mutations from 2000 to 2013 was conducted.
Results: Paternally inherited heterozygous *ABCC8/KCNJ11* mutations were identified in 53 CHI patients. Of these, 18 (34%) either responded to diazoxide or resolved spontaneously. Fluorine-18 L-3, 4-dihydroxyphenylalanine positron emission tomography computerised tomography (^{18}F DOPA–PET CT) scanning in 3/18 children showed diffuse disease. The remaining 35 (66%) diazoxide-unresponsive children either had pancreatic venous sampling ($n=8$) or ^{18}F DOPA–PET CT ($n=27$). Diffuse, indeterminate and focal disease was identified in 13, 1 and 21 patients respectively. Two patients with suspected diffuse disease were identified to have focal disease on histology.
Conclusions: Paternally inherited heterozygous *ABCC8/KCNJ11* mutations can manifest as a wide spectrum of CHI with variable ^{18}F DOPA–PET CT/histological findings and clinical outcomes. Focal disease was histologically confirmed in 24/53 (45%) of CHI patients with paternally inherited heterozygous *ABCC8/KCNJ11* mutations.

European Journal of Endocrinology (2014) **171**, 685–695

Introduction

Congenital hyperinsulinism (CHI) is one of the main causes of hypoglycaemia and is characterised by inappropriate insulin secretion (1). Mutations in nine different genes (*ABCC8*, *KCNJ11*, *GLUD1*, *GCK*, *HADH*, *SLC16A1*, *UCP2*, *HNF4A* and *HNF1A*) have been reported so far as the genetic causes of CHI (1, 2). The pancreatic β-cell ATP-sensitive potassium channel (K_{ATP} channel) regulates glucose-mediated insulin release and is composed of two

www.eje-online.org
DOI: 10.1530/EJE-14-0353

Published by Bioscientifica Ltd.

subunits: Kir6.2 encoded by *KCNJ11* and SUR1 encoded by *ABCC8* gene (2). Both genes are localised in the 11p15.1 region and mutations in these accounts for the majority of CHI patients (3, 4, 5, 6, 7, 8, 9, 10, 11).

There are two main forms of CHI (focal and diffuse) that are clinically identical but differ in histology, underlying genetic mechanism and management. In diffuse CHI, histologically there is an increase in the β-cell nuclear size throughout the pancreas. Diffuse CHI is genetically heterogeneous and most commonly due to mutations in *ABCC8* or *KCNJ11* genes (3, 12, 13, 14, 15). Diazoxide, an agonist that targets the SUR1 subunit, is usually ineffective in patients with autosomal recessive form of *ABCC8* or *KCNJ11* mutations. The management of the medically unresponsive diffuse CHI patients involves near-total pancreatectomy.

The focal lesions are characterised by nodular hyperplasia of islet-like cell clusters with ductuloinsular complexes and scattered giant β-cell nuclei with normal surrounding tissue (16). The focal CHI results from a paternally inherited heterozygous *ABCC8/KCNJ11* mutation together with a somatic loss of the maternal chromosome in the 11p15 region (most likely caused by paternal isodisomy) (16, 17). The resulting loss of heterozygosity (LOH) renders the β-cells biallelic for the abnormal foci, altering the K_{ATP} channel and resulting in dysregulated insulin secretion within the focal lesion (16, 17, 18). The consequent imbalance in the expression of adjacent imprinted genes implicated in cell proliferation (such as *CDKN1C* and *H19* normally expressed from the maternal allele and *IGF2* paternally expressed) within the 11p15.5 region leads to focal islet cell adenomatous hyperplasia (19, 20, 21, 22). Focal CHI is usually medically unresponsive, although diazoxide-responsive focal CHI has been recently described (23). Targeted surgical removal of the lesion will cure the patient.

Fluorine-18 L-3, 4-dihydroxyphenylalanine positron emission tomography computerised tomography (^{18}F DOPA–PET CT) scan can help to differentiate the focal from diffuse forms of CHI and aids in the clinical management of these patients (24). Before the advent of ^{18}F DOPA–PET CT, pancreatic venous sampling (PVS) and selective pancreatic arterial calcium stimulation with hepatic venous sampling (ASVS) were used to differentiate between the two subtypes (25, 26). A recent systematic review and meta-analysis has found ^{18}F DOPA–PET CT to be far superior to PVS and ASVS in diagnosing and localising focal CHI (27).

Patients with CHI associated with heterozygous paternally inherited *ABCC8/KCNJ11* mutations may or may not have the second hit of somatic maternal allele loss in the pancreatic β-cell. Accordingly, these patients can either have focal or diffuse disease. Furthermore, diffuse disease can either be diazoxide-responsive or unresponsive depending on the underlying molecular basis of the mutation and other unclear genetic or environmental influences (28). There are isolated case reports of heterozygous paternally inherited *ABCC8/KCNJ11* mutations leading to diffuse CHI in the literature (3, 10, 29, 30). The proportion of patients with paternally inherited heterozygous *ABCC8/KCNJ11* mutations who develop focal CHI has not been reported in any study so far. Herein, we describe the heterogeneous clinical presentation and the histological basis of a relatively large cohort of patients with heterozygous paternally inherited *ABCC8/KCNJ11* mutations. We also report the proportion of focal and diffuse disease in a large cohort of CHI patients with paternally inherited heterozygous *ABCC8/KCNJ11* mutations.

Subjects and methods

The study was approved by the Ethics Committee of Great Ormond Street Children's Hospital and the Institute of Child Health. Informed written consent was obtained from the parents of children enrolled for molecular genetic testing for CHI (*ABCC8/KCNJ11* sequencing).

This is a descriptive study of the clinical characteristics of children with CHI due to paternally inherited heterozygous *ABCC8/KCNJ11* mutations. Clinical presentation, disease course and outcome for consecutive patients with CHI associated with paternally inherited heterozygous *ABCC8/KCNJ11* mutations between the years 2000 and 2013 were retrospectively reviewed.

CHI was diagnosed by a controlled fasting test that demonstrated an inappropriately detectable serum insulin and/or C-peptide concentration and/or inappropriately low β-hydroxybutyrate and non-esterified fatty acids concentrations in the presence of hypoglycaemia (plasma glucose concentration <3.0 mmol/l). The patients with confirmed diagnosis of CHI underwent molecular genetic analysis after informed consent (see below). Diazoxide (5–15 mg/kg per day in three divided doses) was commenced as the first-line medical treatment. The patients were defined as diazoxide unresponsive if age appropriate fasting tolerance could not be achieved by treatment with 15 mg/kg per day diazoxide for a minimum of 5 days. Diazoxide-unresponsive patients associated with paternally inherited heterozygous *ABCC8/KCNJ11* mutation underwent further investigations (PVS or

^{18}F DOPA–PET CT) to differentiate between focal and diffuse disease. PVS was performed and interpreted as described previously by de Lonlay-Debeney *et al*. (26). The detailed protocol used for ^{18}F DOPA–PET CT and analysis of the images has already been described (31).

Diazoxide-unresponsive diffuse disease was managed by octreotide injections (5–30 μg/kg per day in three to four divided doses) ± near-total pancreatectomy along with carbohydrate-rich feeds. The focal disease was managed with the resection of the focal lesion or partial pancreatectomy. Post-surgery, glycaemic control was periodically assessed by 24-h blood glucose profile and controlled fast to ensure cure of the focal CHI and appropriate control of diffuse CHI.

Genetic testing

Genomic DNA was extracted from peripheral leukocytes using standard procedures. The single-coding exon of the *KCNJ11* gene and the 39 exons of the *ABCC8* gene were amplified using the PCR. Unidirectional sequencing was performed using universal M13 primers and a Big Dye Terminator Cycle Sequencing Kit v3.1 (Applied Biosystems) according to the manufacturer's instructions. The reactions were analysed on an ABI 3730 Capillary Sequencer (Applied Biosystems) and the sequences were compared with the reference sequences (NM_000525 and NM_000352.2) using Mutation Surveyor v3.24 (SoftGenetics, PA, USA). Dosage analyses by multiplex ligation-dependent probe amplification were done in patients with a heterozygous *ABCC8/KCNJ11* mutation and diffuse disease on ^{18}F DOPA–PET scan/PVS (32).

LOH was investigated by microsatellite analysis of DNA extracted from paraffin-embedded pancreatic tissue and peripheral leukocytes, mainly when there was a discrepancy between the histology and ^{18}F DOPA–PET CT/PVS result. Six markers (D11S2071, D11S1964, D11S419, D11S1397, D11S1888 and D11S4138) spanning chromosome 11p15.1–11p15.5 were amplified by PCR and allele peak heights were compared using GeneMarker v1.85 (SoftGenetics).

Results

Over a period of 14 years (2000–2013), more than 300 children with confirmed biochemical and genetic diagnosis of CHI were managed in our centre. Of these, 53 children had paternally inherited heterozygous *ABCC8/KCNJ11* mutation (*ABCC8*, 42 and *KCNJ11*, 11). Of the 35 different *ABCC8* mutations seen in 42 patients, 19 affected a single amino acid (missense or in-frame deletion/insertion). Of the ten different *KCNJ11* mutations seen in 11 patients, eight affected a single amino acid (missense or in-frame deletion/insertion), one was a frame shift mutation and one was a non-stop codon mutation resulting in extension of the Kir6.2 protein sequence by three amino acids (Fig. 1). As shown in Fig. 1, mutations occurred throughout SUR1 and Kir6.2.

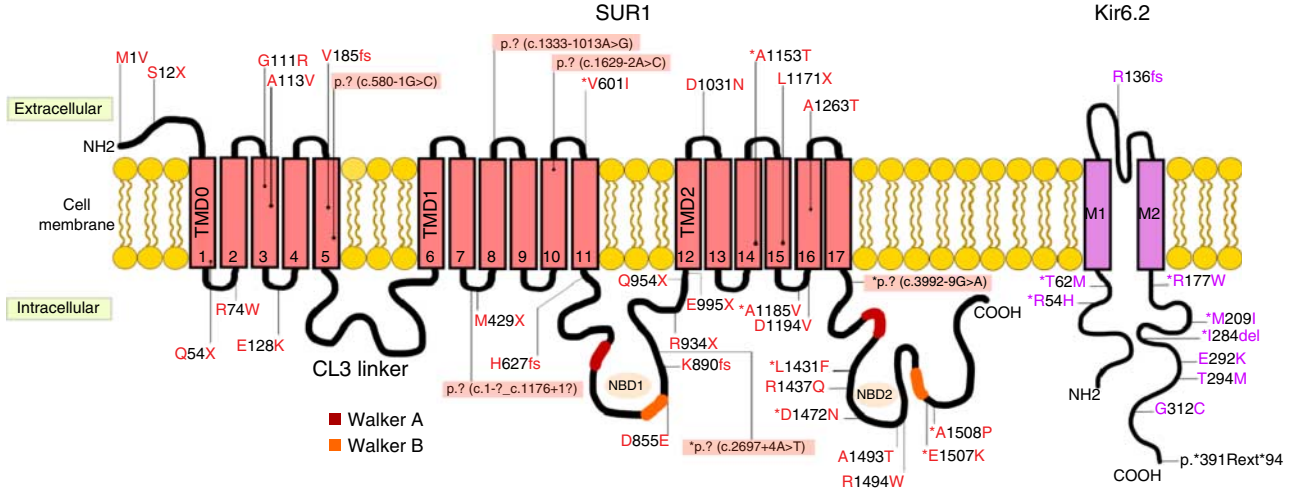

Figure 1

Paternal mutations mapped onto the SUR1 and Kir6.2 protein. All SUR1 intronic splice site mutation mutants have been highlighted in red. All mutants with * are responsive to diazoxide (transmembrane domain (TMD) and nucleotide-binding domain (NBD)). A full colour version of this figure available via http://dx.doi.org/10.1530/EJE-14-0353.

Table 1 Clinical and biochemical characteristics, mutational analysis and clinical outcome of 53 patients with paternally inherited *ABCC8/KCNJ11* mutations.

Patient ID	GA (weeks), birth weight (g)	Gender	Age at presentation (weeks)	Blood glucose (mmol/l)	Serum insulin (mU/l)	Mutation protein description (DNA description)	LOH	Dzx Resp	PET CT/PVS	Outcome
ABCC8										
1	40, 3150	Male	52	2.4	4.3	L1431F/N (c.4291C>T/N)		Yes	–	On Dzx at 6.4 years
2	40, 4000	Male	2	2.4	1.9	p.?/N (c.2697+4A>T/N)		Yes	–	Off Dzx at 2 years
3	40, 5010	Female	<1	2.6	8.6	E1507K/N (c.4519G>A/N)		Yes	–	On Dzx at 2.3 years
4	40, 5600	Male	<1	2.0	7.5	A1508P/N (c.4522G>C/N)		Yes	–	On Dzx at 12 years
5	37, 4820	Male	<1	2.0	9.0	A1153T/N (c.3457G>A/N)		Yes	–	On Dzx at 4 years
6	38, 3630	Female	72	3.1	<2	A1153T/N (c.3457G>A/N)		Yes	–	On Dzx at 2 years
8	35, 2820	Male	<1	1.2	12.9	A1185V/N (c.3554C>T/N)		Yes	–	Off Dzx at 8 months
9	36, 4450	Male	<1	2	28.5	p.?/N (c.3992-9G>A/N)		Yes	–	Off Dzx after 4.5 months
10	41, 2780	Female	<1	1	9.3	D1472N/N (c.4414G>A/N)		Yes	–	Off Dzx after 10 months
11	38, 3750	Male	<1	2.6	5.90	V601I/N (c.1801G>A/N)		Yes	–	Off Dzx after 14 months
13	40, 4160	Female	<1	2.4	14.8	V185fs/N (c.554delT/N)		No	Diffuse	Off octreotide at 5 years
14	37, 3090	Male	<1	0.6	12.4	p.?/N (c.3992-9G>A/N)		No	Focal	On octreotide at 9.5 years
15	40, 3600	Male	<1	2.7	6.7	H627fs/N (c.1879delC/N)		No	Diffuse	Off octreotide at 18 months
16	40, 4700	Female	<1	2.0	<2	E1507K/N (c.4519G>A/N)		NA	–	No treatment required
17	40, 4200	Male	<1	1.0	<2	D1031N/N (c.3091G>A/N)		NA	–	No treatment required
18	41, 4850	Male	<1	1.2	10.1	M1V/N (c.1A>G/N)		No	Diffuse (*PVS*)	Near-total pancreatectomy (95%)
19	38, 2400	Male	<1	2.1	16.3	D1194V; R1437Q/N (c.3581A>T; c.4310G>A/N)	Yes	No	Focal	Hypoglycaemia resolved after removal of focal lesion
20	40, 4580	Female	<1	1.1	103	A1493T/N (c.4477G>A/N)	Yes[a]	No	Diffuse	Near-total pancreatectomy (95%)
21	40, 4600	Male	<1	1.2	22.5	K890fs/N (c.2669_2675del/N)	Yes	No	Focal	Hypoglycaemia resolved after removal of focal lesion
22	40, 4335	Male	<1	2.6	3.4	p.?/N (c.3992-9G>A/N)	Yes	No	Focal	Partial pancreatectomy
23	40, 3030	Male	<1	1.8	15.6	p.?/N (c.3992-9G>A/N)	Yes	No	Focal	Partial pancreatectomy
24	40, 2770	Male	<1	2.2	3.4	p.?/N (c.580-1G>C/N)		No	Indeterminate (PVS)	Partial pancreatectomy – focal lesion on histology
25	41, 4290	Male	2	2.3	4.32	E128K/N (c.382G>A/N)		No	Focal	Hypoglycaemia resolved after removal of focal lesion
27	40, 5095	Male	<1	2.0	10.5	L1171X/N (c.3512delT/N)	Yes	No	Focal	Hypoglycaemia resolved after removal of focal lesion
29	37, 3560	Male	<1	1.6	21.8	p.?/N (c.1629-2A>C/N)		No	Focal	Hypoglycaemia resolved after removal of focal lesion
30	40, 2750	Male	<1	1.5	16.4	G111R/N (c.331G>A/N)	Yes	No	Focal	Hypoglycaemia resolved after removal of focal lesion
31	37, 3340	Male	<1	2.1	15	H627fs/N (c.1879delC/N)	Yes	No	Focal	Hypoglycaemia resolved after removal of focal lesion
32	41, 4950	Male	<1	1.2	11.95	R934X/N (c.2800C>T/N)		No	Focal	Hypoglycaemia resolved after removal of focal lesion
33	40, 3080	Female	12	1.5	4.6	S12X/N (c.35C>A/N)	Yes	No	Focal	Hypoglycaemia resolved after removal of focal lesion
34	39, 3600	Male	<1	2.5	8	R1494W/N (c.4480C>T/N)		No	Diffuse (*PVS*)	Near-total pancreatectomy (95%)
37	36, 3410	Male	<1	0.9	17.42	R1494W/N (c.4480C>T/N)		No	Focal	Partial pancreatectomy

Table 1 *Continued*

Patient ID	GA (weeks), birth weight (g)	Gender	Age at presentation (weeks)	Blood glucose (mmol/l)	Serum insulin (mU/l)	Mutation protein description (DNA description)	LOH	Dzx Resp	PET CT/PVS	Outcome
38	39, 4900	Female	<1	1.4	23.61	A113V/N (c.338C>T/N)		No	Diffuse (*PVS*)	Near-total pancreatectomy (95%)
39	36, 3210	Male	<1	0.6	114	Mosaic Q54X (c.160C>T)		No	Diffuse	Near-total pancreatectomy (95%)
40	41, 4300	Female	<1	2.1	17	Q954X/N (c.2860C>T/N)		No	Diffuse	Near-total pancreatectomy (95%)
41	36, 2730	Male	<1	?	?	p.?/N (c.1333-1013A>G/N)	Yes	No	Focal	Hypoglycaemia resolved after removal of focal lesion
42	37, 4480	Female	<1	1.7	5.6	A1263T/N (c.3787G>A/N)		No	Diffuse (*PVS*)	Near-total pancreatectomy (95%)
45	39, 3960	Male	<1	2.4	23.6	p.?/N (c.1-?_c.1176+1?/N)		No	Focal	Hypoglycaemia resolved after removal of focal lesion
46	34, 3800	Male	<1	0.8	201	D855E/N (c.2565C>A/N)		No	Focal	Hypoglycaemia resolved after removal of focal lesion
47	41, 4780	Male	<1	2.4	15.9	M429X/N (c.1254_1284dup/N)		No	Focal	Hypoglycaemia resolved after removal of focal lesion
48	40, 3800	Female	<1	2.4	5.9	M429X/N (c.1254_1284dup/N)		No	Diffuse	On octreotide at 7 months
49	40, 4100	Male	<1	0.8	9.1	R74W/N (c.220C>T/N)		No	Focal	Hypoglycaemia resolved after removal of focal lesion
51	38, 3730	Female	<1	1.9	21.6	E995X (c.2983G>T)		No	Focal	Hypoglycaemia resolved after removal of focal lesion
KCNJ11										
7	38, 3780	Female	<1	1.7	29.6	M209I/N (c.627G>A/N)		Yes	Diffuse	On Dzx at 2.8 years
12	40, 3450	Male	<1	2	6.7	R54H/N (c.161G>A/N)		Yes	–	Off Dzx after 4 months
26	36, 3880	Male	<1	<1.0	6.1	E292K/N (c.874G>A/N)		No	Diffuse (*PVS*)	Near-total pancreatectomy (95%)
28	40, 4600	Male	<1	1.3	38.87	R136fs/N (c.405dupG/N)		No	Diffuse (*PVS*)	Near-total pancreatectomy (95%)
35	38, 4120	Female	<1	2.2	12.0	T294M/N (c.881C>T/N)		No	Diffuse (*PVS*)	Near-total pancreatectomy (95%)
36	37, 3960	Male	<1	1.9	7.0	G312C/N (c.934G>T/N)		No	Focal	Hypoglycaemia resolved after removal of focal lesion
43	40, 4100	Female	<1	1.0	35	I284del/N (c.850_852delATC/N)		Yes	Diffuse	Off Dzx at 4 years of age
44	40, 4580	Female	32	2.2	7	p.*391Rext*94/N (c.1171T>C/N)		No	Focal	Partial pancreatectomy, currently on Dzx
50	37, 3980	Male	<1	0.5	2.9	T62M/N (c.185C>T/N)		Yes	–	Off Dzx at 1 month
52	40, 5190	Male	<1	2.5	8.4	R177W/N (c.529A>T/N)		Yes	Diffuse	On Dzx at 3 months of age
53	40, 3920	Male	<1	2.1	9.2	E292K/N (c.874G>A/N)		Yes	Diffuse	Off Dzx at 5 months of age

Dzx, diazoxide; PET, positron emission tomography; PVS, pancreatic venous sampling; GA, gestational age; Wt, weight; LOH, loss of heterozygosity; Resp, responsiveness.
[a]This patient had giant focal lesion and virtually occupied the whole of pancreas.

Clinical and biochemical characteristics

The mean (±2 s.d.) gestational age and birth weight of our cohort was 38.9 (±1.8) weeks and 3980 (±760) g respectively. Of these, 19 infants (36%) were macrosomic (birth weight >2 s.d.) at birth. The gender distribution was 37 males and 16 females. The majority of patients in our cohort were of Caucasian descent. Only one proband was a product of the consanguineous marriage. There were two pairs of two siblings and the rest of the cohort was unrelated. The median age of presentation with hypoglycaemia was <1 week (range <1–130 weeks). More than 85% (46/53) patients presented with hypoglycaemia within first week of life. The mean (±s.d.) serum insulin during hypoglycaemia was 21.1 (±34.2) mU/l. In three infants in whom serum insulin was undetectable, C-peptide level was inappropriately elevated for the blood glucose measurement. The serum ammonia was within normal range and β-hydroxybutyrate/non-esterified fatty acids were inappropriately low in all children (Table 1).

Clinical course, ^{18}F DOPA–PET CT and PVS findings and final outcome

Diazoxide-responsive group ▸ In two (4%) patients (Table 1: patients 16 and 17), CHI resolved spontaneously within few weeks before investigations were repeated in our centre (Fig. 2). Previous functional work has established milder disease phenotype with a mutation seen in one of these two patients (*ABCC8* (*E1507K*)) (33). The mutation identified in the second patient (*ABCC8* (*D1031N*)) is not reported in dbSNP and predicted to be disease causing (Table 2).

Sixteen patients (30%) with presumably diffuse CHI responded to diazoxide treatment (Fig. 2). In three patients from diazoxide-responsive group who underwent ^{18}F DOPA–PET CT, diffuse uptake throughout the pancreas was noticed. Nine patients (17%) successfully managed to come off diazoxide treatment after a variable period of time. The remaining seven (13%) patients were on diazoxide for a median duration of 2.8 years (range 3 months–12 years) at the time of writing.

The mutations in this subgroup are predicted to be pathogenic by various mutation prediction programmes (Table 2) (34, 35).

Diazoxide-unresponsive group ▸ The remaining 35 (66%) patients were unresponsive to maximum doses of diazoxide and were investigated either by using PVS (n=8) or ^{18}F DOPA–PET CT scan (n=27).

PVS was suggestive of diffuse disease in seven patients and no differentiation between focal and diffuse was

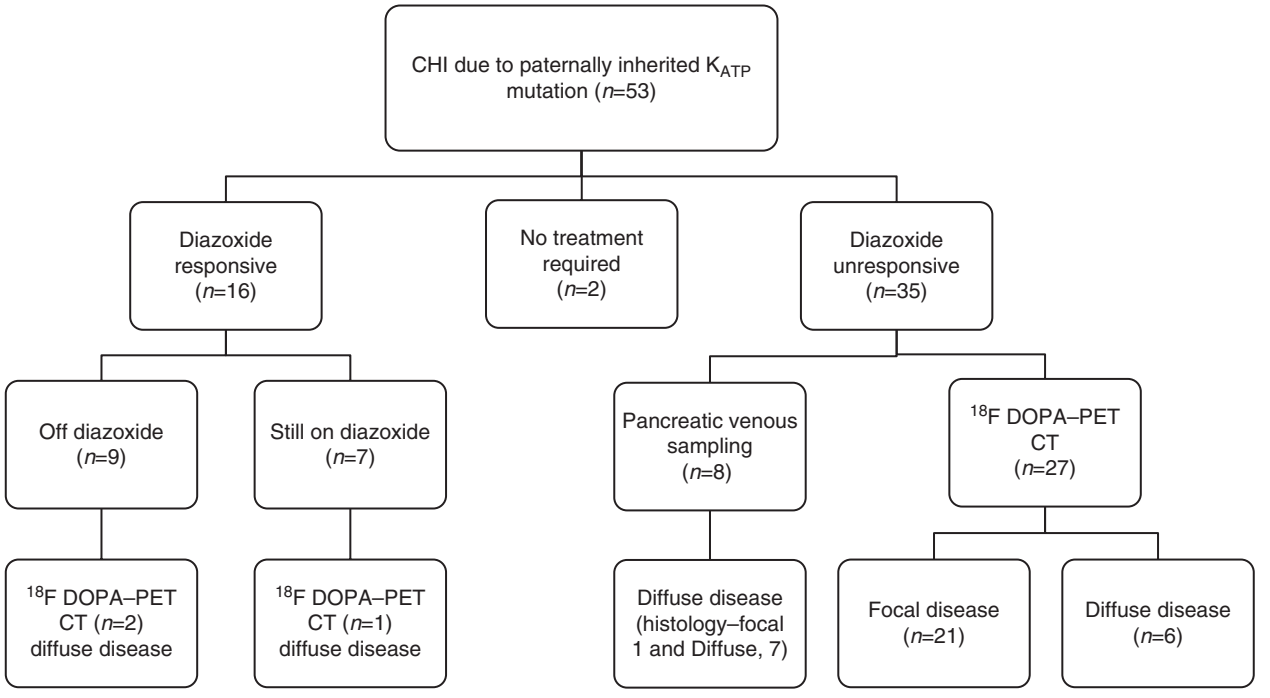

Figure 2
Clinical course, ^{18}F DOPA–PET CT/pancreatic venous sampling findings and outcome.

Table 2 *In silico* pathogenicity prediction of diazoxide-responsive patients' mutations.

Mutation	Prediction				Mutation previously reported
	Found in dbSNP	Provean	SIFT	MutationTaster	
ABCC8					
L1431F (c.4291C>T)	No	Deleterious	Damaging	Disease causing	(38)[a]
p.? (c.2697+4A>T)	No	Not available	Not available	Disease causing	Novel
E1507K (c.4519G>A)	Yes	Deleterious	Damaging	Disease causing	(32)
A1508P (c.4522G>C)	No	Deleterious	Damaging	Disease causing	(38)[a]
A1153T (c.3457G>A)	No	Deleterious	Damaging	Disease causing	Novel
A1185V (c.3554C>T)	No	Neutral	Damaging	Disease causing	Novel
p.? (c.3992-9G>A)	No	Not available	Not available	Disease causing	(5)[a]
D1472N (c.4414G>A)	Yes	Deleterious	Damaging	Disease causing	(24)[a]
V601I (c.1801G>A)	No	Neutral	Tolerated	Disease causing	Novel[a]
V185fs (c.554delT)	Yes	Not available	Not available	Disease causing	Novel
H627fs (c.1879delC)	No	Not available	Not available	Disease causing	(9)[a]
D1031N (c.3091G>A)	No	Neutral	Tolerated	Disease causing	Novel
M1V (c.1A>G)	No	Neutral	Damaging	Disease causing	(6)[a]
A1493T (c.4477G>A)	Yes	Deleterious	Damaging	Disease causing	(14)[a]
R1494W (c.4480C>T)	Yes	Deleterious	Damaging	Disease causing	(25)[a]
KCNJ11					
M209I (c.627G>A)	No	Neutral	Damaging	Disease causing	Novel
R54H (c.161G>A)	No	Deleterious	Damaging	Disease causing	Novel[a]
E292K (c.874G>A)	No	Deleterious	Damaging	Disease causing	Novel
T62M (c.185C>T)	No	Deleterious	Damaging	Disease causing	(4)
R177W (c.529A>T)	No	Deleterious	Damaging	Disease causing	Novel

[a]These patients were included in reference (3).

possible in one patient. The suspected diffuse disease patients were managed with near-total pancreatectomy. Although histology confirmed diffuse disease in six patients, there was one patient who had focal adenomatous hyperplasia which was presumably missed on PVS. The patient with indeterminate PVS underwent partial pancreatectomy and focal lesion was seen on the histology of the resected pancreas.

Of the 27 patients who were investigated with ^{18}F DOPA–PET scan, focal uptake was seen in 21 and diffuse uptake in six patients (Fig. 3). The focal lesion was successfully managed either with lesionectomy ($n=16$) or partial pancreatectomy ($n=4$). One patient was managed successfully with octreotide injections.

The patients with diffuse tracer pancreatic uptake were either managed with near-total pancreatectomy ($n=3$) or octreotide injections ($n=3$). One patient from this subgroup had atypical histology with pancreatic β-cell enlargement in parts of body and head of the pancreas due to mosaic interstitial paternal uniparental isodisomy for chromosome 11p15.1 (36).

Discussion

This study reports the proportion of focal disease in a large cohort of patients with CHI associated with paternally inherited heterozygous *ABCC8/KCNJ11* mutations. In addition, it highlights the clinical and histological heterogeneity of CHI associated with paternally inherited heterozygous *ABCC8/KCNJ11* mutation.

Mutations in the *ABCC8/KCNJ11*, which account for the majority of genetically confirmed CHI cases, can either be biallelic or monoallelic (3, 4, 37). Biallelic *ABCC8/KCNJ11* mutations result in diffuse CHI, whereas monoallelic mutations can either be asymptomatic

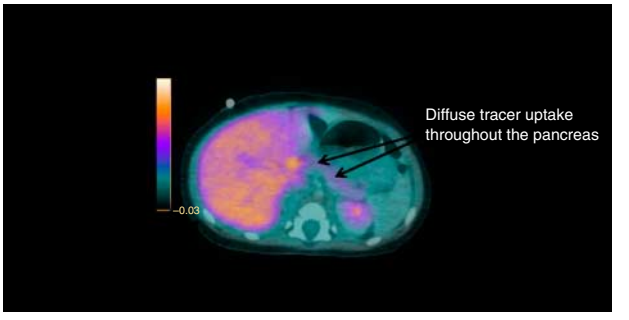

Figure 3
^{18}F DOPA–PET CT image of patient 40 showing diffuse tracer uptake throughout the pancreas in a patient with paternally inherited heterozygous *ABCC8* mutation. Full colour version of this figure available via http://dx.doi.org/10.1530/EJE-14-0353.

(recessive acting), or lead to focal CHI (if paternally inherited and associated with loss of somatic maternal 11p allele) or diffuse CHI (dominant acting). Diazoxide, a K_{ATP} channel opener, which is the first-line management for CHI, is usually ineffective in biallelic disease and monoallelic focal disease (3, 4). However, recently a case of diazoxide-responsive focal CHI was described (23). It may be possible that as more diazoxide-responsive CHI patients are investigated with ^{18}F DOPA–PET CT scan, more diazoxide-responsive focal lesions are identified. However, currently diazoxide responsiveness in our institution is generally considered equivalent to excluding monoallelic focal disease and this group of patients are not usually considered as suitable candidates for further investigations with ^{18}F DOPA–PET CT. On the other hand, diazoxide-unresponsive subgroup, particularly associated with paternally inherited monoallelic *ABCC8/KCNJ11* mutations or no identified *ABCC8/KCNJ11* mutations, is investigated with ^{18}F DOPA–PET CT to identify focal or diffuse subtype before proceeding with definitive treatment as the treatment for focal (limited pancreatectomy) and diffuse CHI (near-total pancreatectomy) is drastically different (38).

In our cohort of 53 CHI patients associated with paternally inherited monoallelic *ABCC8/KCNJ11* mutations, 18 (33%) patients either responded to diazoxide or resolved spontaneously and are likely to have dominant acting CHI. Mutations in these 18 patients are predicted to be pathogenic by different mutation prediction programmes (Table 2). Functional work has already established some of these mutants to be dominant acting and exerting their effect by a dominant-negative mechanism (33, 39, 40). Although there was no history of hypoglycaemia in the fathers of our cohort, formal evaluation with controlled provocation fasting studies has not been done. Other studies also have reported parents to be asymptomatic carriers of dominant acting mutations (41). In view of severe diazoxide side effects and parental request, three patients from this subgroup underwent ^{18}F DOPA–PET CT imaging to avoid long-term treatment with diazoxide. This was in the hope that these patients could be managed with removal of focal lesion if found to be the underlying cause for CHI. However, as suspected from the phenotype of diazoxide-responsiveness, ^{18}F DOPA–PET CT identified diffuse tracer uptake throughout the pancreas.

Evaluation with ^{18}F DOPA–PET CT in 27 diazoxide-unresponsive patients with paternally inherited heterozygous *ABCC8/KCNJ11* mutations identified focal disease in 21 (78%) patients. Majority of these patients presented within the first week of life. There was no difference in the age of presentation between those who were diagnosed with diffuse or focal CHI. Apart from one patient who was managed with octreotide therapy, these patients were either managed with resection of the focal lesion or partial pancreatectomy. Follow-up assessment highlighted age-appropriate fasting tolerance and resolution of hypoglycaemia in all except one (19/20; 95%) after the removal of the focal lesion. Similar to our results, Lord *et al.* (42) recently reported that 94% of their cohort of focal CHI after pancreatectomy remained euglycaemic and required no treatment for blood glucose abnormalities. In the cohort reported by Beltrand *et al.* (43), 91.4% (43/47) patients with focal CHI had complete resolution of hypoglycaemia post-surgery. One patient in whom the evidence of CHI persisted despite the removal of a histologically confirmed focal lesion was managed with diazoxide and regular feeds. A repeat ^{18}F DOPA–PET CT revealed diffuse tracer uptake in the remaining pancreas. Molecular basis for CHI in this particular patient is unclear and further studies are in progress.

In six (21%) diazoxide-unresponsive patients investigated with ^{18}F DOPA–PET CT, diffuse tracer uptake throughout the pancreas was noticed (Fig. 3). Three of these patients were managed with near-total pancreatectomy and in one of these patients, histology and microsatellite analysis was suggestive of giant focal lesion (44). Diffuse uptake in this particular patient was due to the size of the focal lesion, which occupied nearly the whole pancreas. Diffuse CHI has been described in the literature with paternally inherited *ABCC8/KCNJ11* mutations. Fernandez-Marmiesse *et al.* (10) reported five patients with paternally inherited K_{ATP} mutations and whose post pancreatectomy pathology result was not consistent with that of focal lesion. Similar findings have been reported by other studies (1, 21, 27, 30).

There are a number of possible mechanisms as to how a heterozygous *ABCC8/KCNJ11* mutation can lead to diffuse disease. For example there could be a post-zygotic second hit within the pancreas or a maternally inherited mutation may reside within a non-coding regulatory/intronic region of the *ABCC8/KCNJ11* gene. Recently, in a patient with focal CHI but no exonic or splice site *ABCC8/KCNJ11* mutation, next-generation sequencing identified a deep intronic *ABCC8* mutation inherited from the unaffected father, which created a cryptic spice site and an out of frame pseudoexon (32). A third possibility is allelic drop-out due to a rare polymorphism within a primer binding site. In this scenario, a maternally inherited coding mutation could escape detection by Sanger sequencing. Besides, some of the missense mutations may be dominantly acting (dominant negative).

As compared with recessive acting mutations where there is defective biogenesis or trafficking of K_{ATP} channel to the β-cell membrane, the dominant acting mutants traffic normally to the plasma membrane but show impaired responsiveness to the channel agonists, MgADP and diazoxide (45). Diazoxide-unresponsive mutations produce a more severe impairment in the expressed channel response to activation by diazoxide and MgADP as compared with diazoxide-responsive mutations (28).

A novel genetic mechanism of diffuse disease due to mosaic paternal uniparental isodisomy in a patient with heterozygous *ABCC8/KCNJ11* mutations was recently described (36). Lastly, it could also very rarely be due to failure of Sanger sequencing to detect the second *ABCC8/KCNJ11* mutation or a missed histological diagnosis of focal CHI in these patients. Although *ABCC8* and *KCNJ11* are not known to be imprinted genes, they are next to the 11p15.5 imprinted region, so another hypothesis could be the involvement of epigenetic mechanisms.

In summary, of the 53 patients associated with paternally inherited *ABCC8/KCNJ11* mutations, 29 (55%) patients had diffuse CHI (18 (34%) patients – diazoxide-responsive; 11 (21%) patients – diazoxide-unresponsive) and 24 (45%) patients had confirmed focal CHI either based on histology or LOH studies. One patient had giant focal lesion based on histology and LOH studies, confusing the interpretation of ^{18}F DOPA–PET CT. From our results, it is clear that paternally inherited heterozygous *ABCC8/KCNJ11* mutations can manifest as a wide spectrum of CHI with focal disease in 45% patients. This heterogeneous clinical picture could be due to modifying genes or other unknown factors, e.g. environmental, that influence the expression of the phenotype in CHI patients.

Declaration of interest

The authors declare that there is no conflict of interest that could be perceived as prejudicing the impartiality of the research reported.

Funding

This research did not receive any specific grant from any funding agency in the public, commercial or not-for-profit sector.

References

1 Senniappan S, Shanti B, James C & Hussain K. Hyperinsulinaemic hypoglycaemia: genetic mechanisms, diagnosis and management. *Journal of Inherited Metabolic Disease* 2012 **35** 589–601. (doi:10.1007/s10545-011-9441-2)

2 Kapoor RR, Flanagan SE, James C, Shield J, Ellard S & Hussain K. Hyperinsulinaemic hypoglycaemia. *Archives of Disease in Childhood* 2009 **94** 450–457. (doi:10.1136/adc.2008.148171)

3 Kapoor RR, Flanagan SE, Arya VB, Shield JP, Ellard S & Hussain K. Clinical and molecular characterisation of 300 patients with congenital hyperinsulinism. *European Journal of Endocrinology* 2013 **168** 557–564. (doi:10.1530/EJE-12-0673)

4 Snider KE, Becker S, Boyajian L, Shyng SL, MacMullen C, Hughes N, Ganapathy K, Bhatti T, Stanley CA & Ganguly A. Genotype and phenotype correlations in 417 children with congenital hyperinsulinism. *Journal of Clinical Endocrinology and Metabolism* 2013 **98** E355–E363. (doi:10.1210/jc.2012-2169)

5 Nestorowicz A, Wilson BA, Schoor KP, Inoue H, Glaser B, Landau H, Stanley CA, Thornton PS, Clement JP, Bryan J *et al*. Mutations in the sulonylurea receptor gene are associated with familial hyperinsulinism in Ashkenazi Jews. *Human Molecular Genetics* 1996 **5** 1813–1822. (doi:10.1093/hmg/5.11.1813)

6 Greer RM, Shah J, Jeske YW, Brown D, Walker RM, Cowley D, Bowling FG, Liaskou D, Harris M, Thomsett MJ *et al*. Genotype–phenotype associations in patients with severe hyperinsulinism of infancy. *Pediatric and Developmental Pathology* 2007 **10** 25–34. (doi:10.2350/06-04-0083.1)

7 Darendeliler F, Fournet JC, Bas F, Junien C, Gross MS, Bundak R, Saka N & Gunoz H. ABCC8 (SUR1) and KCNJ11 (KIR6.2) mutations in persistent hyperinsulinemic hypoglycemia of infancy and evaluation of different therapeutic measures. *Journal of Pediatric Endocrinology & Metabolism* 2002 **15** 993–1000.

8 Tornovsky S, Crane A, Cosgrove KE, Hussain K, Lavie J, Heyman M, Nesher Y, Kuchinski N, Ben-Shushan E, Shatz O *et al*. Hyperinsulinism of infancy: novel ABCC8 and KCNJ11 mutations and evidence for additional locus heterogeneity. *Journal of Clinical Endocrinology and Metabolism* 2004 **89** 6224–6234. (doi:10.1210/jc.2004-1233)

9 Gloyn AL, Siddiqui J & Ellard S. Mutations in the genes encoding the pancreatic β-cell K_{ATP} channel subunits Kir6.2 (KCNJ11) and SUR1 (ABCC8) in diabetes mellitus and hyperinsulinism. *Human Mutation* 2006 **27** 220–231. (doi:10.1002/humu.20292)

10 Fernandez-Marmiesse A, Salas A, Vega A, Fernandez-Lorenzo JR, Barreiro J & Carracedo A. Mutation spectra of ABCC8 gene in Spanish patients with Hyperinsulinism of Infancy (HI). *Human Mutation* 2006 **27** 214. (doi:10.1002/humu.9401)

11 Shimomura K, Flanagan SE, Zadek B, Lethby M, Zubcevic L, Girard CA, Petz O, Mannikko R, Kapoor RR, Hussain K *et al*. Adjacent mutations in the gating loop of Kir6.2 produce neonatal diabetes and hyperinsulinism. *EMBO Molecular Medicine* 2009 **1** 166–177. (doi:10.1002/emmm.200900018)

12 Muzyamba M, Farzaneh T, Behe P, Thomas A, Christesen HB, Brusgaard K, Hussain K & Tinker A. Complex ABCC8 DNA variations in congenital hyperinsulinism: lessons from functional studies. *Clinical Endocrinology* 2007 **67** 115–124. (doi:10.1111/j.1365-2265.2007.02847.x)

13 Otonkoski T, Nanto-Salonen K, Seppanen M, Veijola R, Huopio H, Hussain K, Tapanainen P, Eskola O, Parkkola R, Ekstrom K *et al*. Noninvasive diagnosis of focal hyperinsulinism of infancy with [^{18}F]-DOPA positron emission tomography. *Diabetes* 2006 **55** 13–18. (doi:10.2337/diabetes.55.01.06.db05-1128)

14 Kassem SA, Ariel I, Thornton PS, Hussain K, Smith V, Lindley KJ, Aynsley-Green A & Glaser B. p57(KIP2) expression in normal islet cells and in hyperinsulinism of infancy. *Diabetes* 2001 **50** 2763–2769. (doi:10.2337/diabetes.50.12.2763)

15 Suchi M, MacMullen C, Thornton PS, Ganguly A, Stanley CA & Ruchelli ED. Histopathology of congenital hyperinsulinism: retrospective study with genotype correlations. *Pediatric and*

Developmental Pathology 2003 **6** 322–333. (doi:10.1007/s10024-002-0026-9)
16 Damaj L, le Lorch M, Verkarre V, Werl C, Hubert L, Nihoul-Fekete C, Aigrain Y, de Keyzer Y, Romana SP, Bellanne-Chantelot C *et al*. Chromosome 11p15 paternal isodisomy in focal forms of neonatal hyperinsulinism. *Journal of Clinical Endocrinology and Metabolism* 2008 **93** 4941–4947. (doi:10.1210/jc.2008-0673)
17 Verkarre V, Fournet JC, de Lonlay P, Gross-Morand MS, Devillers M, Rahier J, Brunelle F, Robert JJ, Nihoul-Fekete C, Saudubray JM *et al*. Paternal mutation of the sulfonylurea receptor (SUR1) gene and maternal loss of 11p15 imprinted genes lead to persistent hyperinsulinism in focal adenomatous hyperplasia. *Journal of Clinical Investigation* 1998 **102** 1286–1291. (doi:10.1172/JCI4495)
18 Calton EA, Temple IK, Mackay DJ, Lever M, Ellard S, Flanagan SE, Davies JH, Hussain K & Gray JC. Hepatoblastoma in a child with a paternally-inherited ABCC8 mutation and mosaic paternal uniparental disomy 11p causing focal congenital hyperinsulinism. *European Journal of Medical Genetics* 2013 **56** 114–117. (doi:10.1016/j.ejmg.2012.12.001)
19 Shuman C, Smith AC, Steele L, Ray PN, Clericuzio C, Zackai E, Parisi MA, Meadows AT, Kelly T, Tichauer D *et al*. Constitutional UPD for chromosome 11p15 in individuals with isolated hemihyperplasia is associated with high tumor risk and occurs following assisted reproductive technologies. *American Journal of Medical Genetics. Part A* 2006 **140** 1497–1503. (doi:10.1002/ajmg.a.31323)
20 Giurgea I, Bellanne-Chantelot C, Ribeiro M, Hubert L, Sempoux C, Robert JJ, Blankenstein O, Hussain K, Brunelle F, Nihoul-Fekete C *et al*. Molecular mechanisms of neonatal hyperinsulinism. *Hormone Research* 2006 **66** 289–296. (doi:10.1159/000095938)
21 Fournet JC, Verkarre V, De Lonlay P, Rahier J, Brunelle F, Robert JJ, Nihoul-Fekete C, Saudubray JM & Junien C. Loss of imprinted genes and paternal SUR1 mutations lead to hyperinsulinism in focal adenomatous hyperplasia. *Annales d'Endocrinologie* 1998 **59** 485–491.
22 de Lonlay P, Fournet JC, Rahier J, Gross-Morand MS, Poggi-Travert F, Foussier V, Bonnefont JP, Brusset MC, Brunelle F, Robert JJ *et al*. Somatic deletion of the imprinted 11p15 region in sporadic persistent hyperinsulinemic hypoglycemia of infancy is specific of focal adenomatous hyperplasia and endorses partial pancreatectomy. *Journal of Clinical Investigation* 1997 **100** 802–807. (doi:10.1172/JCI119594)
23 Maiorana A, Barbetti F, Boiani A, Rufini V, Pizzoferro M, Francalanci P, Faletra F, Nichols CG, Grimaldi C, de Ville de Goyet J *et al*. Focal congenital hyperinsulinism managed by medical treatment: a diagnostic algorithm based on molecular genetic screening. *Clinical Endocrinology* 2014. In press. (doi:10.1111/cen.12400)
24 Hardy OT, Hernandez-Pampaloni M, Saffer JR, Scheuermann JS, Ernst LM, Freifelder R, Zhuang H, MacMullen C, Becker S, Adzick NS *et al*. Accuracy of [^{18}F]fluorodopa positron emission tomography for diagnosing and localizing focal congenital hyperinsulinism. *Journal of Clinical Endocrinology and Metabolism* 2007 **92** 4706–4711. (doi:10.1210/jc.2007-1637)
25 Stanley CA, Thornton PS, Ganguly A, MacMullen C, Underwood P, Bhatia P, Steinkrauss L, Wanner L, Kaye R, Ruchelli E *et al*. Preoperative evaluation of infants with focal or diffuse congenital hyperinsulinism by intravenous acute insulin response tests and selective pancreatic arterial calcium stimulation. *Journal of Clinical Endocrinology and Metabolism* 2004 **89** 288–296. (doi:10.1210/jc.2003-030965)
26 de Lonlay-Debeney P, Poggi-Travert F, Fournet JC, Sempoux C, Vici CD, Brunelle F, Touati G, Rahier J, Junien C, Nihoul-Fekete C *et al*. Clinical features of 52 neonates with hyperinsulinism. *New England Journal of Medicine* 1999 **340** 1169–1175. (doi:10.1056/NEJM199904153401505)
27 Blomberg BA, Moghbel MC, Saboury B, Stanley CA & Alavi A. The value of radiologic interventions and (18)F-DOPA PET in diagnosing and localizing focal congenital hyperinsulinism: systematic review and meta-analysis. *Molecular Imaging and Biology* 2013 **15** 97–105. (doi:10.1007/s11307-012-0572-0)
28 Macmullen CM, Zhou Q, Snider KE, Tewson PH, Becker SA, Aziz AR, Ganguly A, Shyng SL & Stanley CA. Diazoxide-unresponsive congenital hyperinsulinism in children with dominant mutations of the β-cell sulfonylurea receptor SUR1. *Diabetes* 2011 **60** 1797–1804. (doi:10.2337/db10-1631)
29 Bellanne-Chantelot C, Saint-Martin C, Ribeiro MJ, Vaury C, Verkarre V, Arnoux JB, Valayannopoulos V, Gobrecht S, Sempoux C, Rahier J *et al*. ABCC8 and KCNJ11 molecular spectrum of 109 patients with diazoxide-unresponsive congenital hyperinsulinism. *Journal of Medical Genetics* 2010 **47** 752–759. (doi:10.1136/jmg.2009.075416)
30 Mohnike K, Wieland I, Barthlen W, Vogelgesang S, Empting S, Mohnike W, Meissner T & Zenker M. Clinical and genetic evaluation of patients with K channel mutations from the German registry for congenital hyperinsulinism. *Hormone Research in Paediatrics* 2014 **81** 156–168. (doi:10.1159/000356905)
31 Meintjes M, Endozo R, Dickson J, Erlandsson K, Hussain K, Townsend C, Menezes L & Bomanji J. ^{18}F-DOPA PET enhanced CT imaging for congenital hyperinsulinism: initial UK experience from a technologist's perspective. *Nuclear Medicine Communications* 2013 **34** 601–608. (doi:10.1097/MNM.0b013e32836069d0)
32 Flanagan SE, Xie W, Caswell R, Damhuis A, Vianey-Saban C, Akcay T, Darendeliler F, Bas F, Guven A, Siklar Z *et al*. Next-generation sequencing reveals deep intronic cryptic ABCC8 and HADH splicing founder mutations causing hyperinsulinism by pseudoexon activation. *American Journal of Human Genetics* 2013 **92** 131–136. (doi:10.1016/j.ajhg.2012.11.017)
33 Huopio H, Reimann F, Ashfield R, Komulainen J, Lenko HL, Rahier J, Vauhkonen I, Kere J, Laakso M, Ashcroft F *et al*. Dominantly inherited hyperinsulinism caused by a mutation in the sulfonylurea receptor type 1. *Journal of Clinical Investigation* 2000 **106** 897–906. (doi:10.1172/JCI9804)
34 Schwarz JM, Rodelsperger C, Schuelke M & Seelow D. MutationTaster evaluates disease-causing potential of sequence alterations. *Nature Methods* 2010 **7** 575–576. (doi:10.1038/nmeth0810-575)
35 Choi Y, Sims GE, Murphy S, Miller JR & Chan AP. Predicting the functional effect of amino acid substitutions and indels. *PLoS ONE* 2012 **7** e46688. (doi:10.1371/journal.pone.0046688)
36 Hussain K, Flanagan SE, Smith VV, Ashworth M, Day M, Pierro A & Ellard S. An ABCC8 gene mutation and mosaic uniparental isodisomy resulting in atypical diffuse congenital hyperinsulinism. *Diabetes* 2008 **57** 259–263. (doi:10.2337/db07-0998)
37 Flanagan S, Damhuis A, Banerjee I, Rokicki D, Jefferies C, Kapoor R, Hussain K & Ellard S. Partial ABCC8 gene deletion mutations causing diazoxide-unresponsive hyperinsulinaemic hypoglycaemia. *Pediatric Diabetes* 2012 **13** 285–289. (doi:10.1111/j.1399-5448.2011.00821.x)
38 Banerjee I, Skae M, Flanagan SE, Rigby L, Patel L, Didi M, Blair J, Ehtisham S, Ellard S, Cosgrove KE *et al*. The contribution of rapid K_{ATP} channel gene mutation analysis to the clinical management of children with congenital hyperinsulinism. *European Journal of Endocrinology* 2011 **164** 733–740. (doi:10.1530/EJE-10-1136)
39 Kapoor RR, Flanagan SE, James CT, McKiernan J, Thomas AM, Harmer SC, Shield JP, Tinker A, Ellard S & Hussain K. Hyperinsulinaemic hypoglycaemia and diabetes mellitus due to dominant ABCC8/KCNJ11 mutations. *Diabetologia* 2011 **54** 2575–2583. (doi:10.1007/s00125-011-2207-4)
40 Thornton PS, MacMullen C, Ganguly A, Ruchelli E, Steinkrauss L, Crane A, Aguilar-Bryan L & Stanley CA. Clinical and molecular characterization of a dominant form of congenital hyperinsulinism caused by a mutation in the high-affinity sulfonylurea receptor. *Diabetes* 2003 **52** 2403–2410. (doi:10.2337/diabetes.52.9.2403)
41 Pinney SE, MacMullen C, Becker S, Lin YW, Hanna C, Thornton P, Ganguly A, Shyng SL & Stanley CA. Clinical characteristics and biochemical mechanisms of congenital hyperinsulinism associated with dominant K_{ATP} channel mutations. *Journal of Clinical Investigation* 2008 **118** 2877–2886. (doi:10.1172/JCI35414)

42 Lord K, Dzata E, Snider KE, Gallagher PR & De Leon DD. Clinical presentation and management of children with diffuse and focal hyperinsulinism: a review of 223 cases. *Journal of Clinical Endocrinology and Metabolism* 2013 **98** E1786–E1789. (doi:10.1210/jc.2013-2094)

43 Beltrand J, Caquard M, Arnoux JB, Laborde K, Velho G, Verkarre V, Rahier J, Brunelle F, Nihoul-Fekete C, Saudubray JM *et al*. Glucose metabolism in 105 children and adolescents after pancreatectomy for congenital hyperinsulinism. *Diabetes Care* 2012 **35** 198–203. (doi:10.2337/dc11-1296)

44 Ismail D, Kapoor RR, Smith VV, Ashworth M, Blankenstein O, Pierro A, Flanagan SE, Ellard S & Hussain K. The heterogeneity of focal forms of congenital hyperinsulinism. *Journal of Clinical Endocrinology and Metabolism* 2012 **97** E94–E99. (doi:10.1210/jc.2011-1628)

45 Yan FF, Lin YW, MacMullen C, Ganguly A, Stanley CA & Shyng SL. Congenital hyperinsulinism associated ABCC8 mutations that cause defective trafficking of ATP-sensitive K^+ channels: identification and rescue. *Diabetes* 2007 **56** 2339–2348. (doi:10.2337/db07-0150)

Received 1 May 2014
Revised version received 28 July 2014
Accepted 8 September 2014

OPEN ACCESS Freely available online

PLOS ONE

Pancreatic Endocrine and Exocrine Function in Children following Near-Total Pancreatectomy for Diffuse Congenital Hyperinsulinism

Ved Bhushan Arya[1,2], Senthil Senniappan[1,2], Huseyin Demirbilek[1,2,3], Syeda Alam[1], Sarah E. Flanagan[4], Sian Ellard[4], Khalid Hussain[1,2]*

1 Department of Paediatric Endocrinology, Great Ormond Street Hospital for Children NHS Foundation Trust, London, United Kingdom, **2** Institute of Child Health, University College London, London, United Kingdom, **3** Departments of Paediatric Endocrinology, Ankara Pediatric Hematology and Oncology Training Hospital, Ankara, Turkey, **4** Institute of Biomedical and Clinical Science, University of Exeter Medical School, Exeter, United Kingdom

Abstract

Context: Congenital hyperinsulinism (CHI), the commonest cause of persistent hypoglycaemia, has two main histological subtypes: diffuse and focal. Diffuse CHI, if medically unresponsive, is managed with near-total pancreatectomy. Post-pancreatectomy, in addition to persistent hypoglycaemia, there is a very high risk of diabetes mellitus and pancreatic exocrine insufficiency.

Setting: International referral centre for the management of CHI.

Patients: Medically unresponsive diffuse CHI patients managed with near-total pancreatectomy between 1994 and 2012.

Intervention: Near-total pancreatectomy.

Main Outcome Measures: Persistent hypoglycaemia post near-total pancreatectomy, insulin-dependent diabetes mellitus, clinical and biochemical (faecal elastase 1) pancreatic exocrine insufficiency.

Results: Of more than 300 patients with CHI managed during this time period, 45 children had medically unresponsive diffuse disease and were managed with near-total pancreatectomy. After near-total pancreatectomy, 60% of children had persistent hypoglycaemia requiring medical interventions. The incidence of insulin dependent diabetes mellitus was 96% at 11 years after surgery. Thirty-two patients (72%) had biochemical evidence of severe pancreatic exocrine insufficiency (Faecal elastase 1$<$100 μg/g). Clinical exocrine insufficiency was observed in 22 (49%) patients. No statistically significant difference in weight and height standard deviation score (SDS) was found between untreated subclinical pancreatic exocrine insufficiency patients and treated clinical pancreatic exocrine insufficiency patients.

Conclusions: The outcome of diffuse CHI patients after near-total pancreatectomy is very unsatisfactory. The incidence of persistent hypoglycaemia and insulin-dependent diabetes mellitus is very high. The presence of clinical rather than biochemical pancreatic exocrine insufficiency should inform decisions about pancreatic enzyme supplementation.

Citation: Arya VB, Senniappan S, Demirbilek H, Alam S, Flanagan SE, et al. (2014) Pancreatic Endocrine and Exocrine Function in Children following Near-Total Pancreatectomy for Diffuse Congenital Hyperinsulinism. PLoS ONE 9(5): e98054. doi:10.1371/journal.pone.0098054

Editor: Klaus Brusgaard, Odense University hospital, Denmark

Received February 22, 2014; **Accepted** April 28, 2014; **Published** May 19, 2014

Funding: The authors have no support or funding to report.

Competing Interests: The authors have declared that no competing interests exist.

* E-mail: Khalid.Hussain@ucl.ac.uk

Introduction

Congenital hyperinsulinism (CHI) is a major cause of persistent and recurrent hypoglycaemia in the neonatal and infancy periods [1]. It is characterized by inappropriate and unregulated secretion of insulin from pancreatic β-cells in relation to the blood glucose concentration. CHI is a heterogeneous disease in terms of clinical presentation, histological subgroups and underlying molecular genetics. There are 2 main histological subtypes: diffuse (60%–70% of patients) and focal (30%–40% of patients) [2]. Typically children with diffuse CHI have homozygous recessive or compound heterozygous mutations in the *ABCC8* or *KCNJ11* genes (which encode the SUR1 and Kir6.2 proteins respectively – the two components of the ATP-sensitive K^+ (K_{ATP}) channel of the pancreatic β-cell) [3,4].

Focal CHI is sporadic in inheritance and requires two independents events: inheritance of a paternal mutation in the *ABCC8* or *KCNJ11* gene, and somatic loss of maternal 11p allele within the focal lesion [5]. Focal CHI is managed with lesionectomy, whereas first line of treatment for diffuse CHI is medical management (diazoxide, octreotide and continuous feeding). If unresponsive to maximum medical management, children with diffuse CHI are managed with near-total pancreatectomy (with high risk of diabetes mellitus).

A significant percentage of children undergoing near-total pancreatectomy continue to experience recurrent hypoglycaemia as well as develop diabetes mellitus eventually [6,7]. Near-total pancreatectomy is also associated with the risk of pancreatic exocrine insufficiency. Small studies evaluating long term pancreatic exocrine function (using pancreozymin-secretin stimulation test or 72 hour stool collection) following 85–95% or subtotal pancreatectomy for CHI have been done [8,9,10,11]. There are a number of pancreatic function tests available but measurement of faecal elastase-1 is the currently preferred pancreatic function test [12].

There are very few studies reporting the long term glucose metabolism in a large cohort of diffuse CHI patients managed with near-total pancreatectomy and no large studies assessing pancreatic exocrine function after near-total pancreatectomy. We describe the immediate and long term pancreatic exocrine and endocrine function in a large cohort of diffuse CHI patients who underwent near-total pancreatectomy over an 18-years period.

Materials and Methods

The study was approved by the Ethics Committee of Great Ormond Street Hospital for Children and the Institute of Child Health, University College London. Informed written consent was obtained from parents of enrolled children for molecular genetic testing for CHI (*ABCC8/KCNJ11* sequencing).

Among more than 300 patients with CHI managed during this time period, 45 children had medically unresponsive diffuse disease and were included in this study. The detailed data about clinical presentation and management, molecular genetic analysis results, and post-pancreatectomy periodic assessment of glucose homeostasis were retrospectively collected by medical case-notes review.

CHI was diagnosed based on critical blood sample taken during an episode of spontaneous or provoked hypoglycaemia. Before 2000 when our centre started performing trans-hepatic pancreatic venous sampling (PVS) for differentiation between diffuse and focal CHI, all medically unresponsive CHI patients were managed with near-total pancreatectomy (95% pancreatectomy), the resection being identical in all patients. Medically unresponsive diffuse disease was defined as persistent hypoglycaemia with normal feeding schedule on diazoxide 20 mg/kg/d and/or octreotide 30 mcg/kg/d and carbohydrate enriched feeds. After May 2006, we started performing positron emission tomography using isotope Fluroine-18 L-3, 4-dihydroxyphenyalanine [^{18}F-DOPA-PET]) to differentiate between diffuse and focal disease. Biopsies were taken during surgery from various parts of pancreas and analysed contemporaneously to confirm the diffuse disease before resection, if not already suspected by genetic analysis. The diagnosis was subsequently confirmed on histology.

Genetic testing

Genomic DNA was extracted from peripheral leukocytes using standard procedures. The single-coding exon of the *KCNJ11* gene and the 39 exons of the *ABCC8* gene were amplified using the polymerase chain reaction. Unidirectional sequencing was performed using universal M13 primers and a Big Dye Terminator Cycler Sequencing Kit v3.1 (Applied Biosystems, Warrington, UK) according to the manufacturer's instructions. Reactions were analysed on an ABI 3730 Capillary sequencer (Applied Biosystems, Warrington, UK) and sequences were compared to the reference sequences (NM_000525 and NM_000352.2) using Mutation Surveyor v3.24 (SoftGenetics, PA, USA).

Loss of heterozygosity was investigated by microsatellite analysis of DNA extracted from paraffin-embedded pancreatic tissue and peripheral leukocytes. Six markers (D11S2071, D11S1964, D11S419, D11S1397, D11S1888 and D114138) were amplified by PCR and allele peak heights were compared using GeneMarker v1.85 (SoftGenetics, PA, USA).

Pancreatic endocrine assessment

Post-pancreatectomy, periodic 24-hr blood glucose profile, controlled fast and/or oral glucose tolerance tests were performed in our centre to assess glucose homeostasis, starting before hospital discharge after pancreatectomy (immediate outcome). Recurrent or persistent hypoglycaemia (blood glucose <3 mmol/l) post-pancreatectomy was managed with addition of extra carbohydrate in the feeds, continuous feeds and/or medical therapy with diazoxide or octreotide. Second pancreatectomy was undertaken if normoglycaemia could not be achieved with medical management. Controlled fast was used to inform decisions about regular daytime feeds, overnight continuous feeds and extra carbohydrate in the feeds. Multiple readings of hyperglycaemia (blood glucose $>$ 11 mmol/L) on 24-hour profile was investigated with oral glucose tolerance test. Diabetes mellitus was diagnosed according to World Health Organisation criteria. Episodes of postprandial hyperglycaemia were managed with dietary management. Insulin therapy was considered when patient developed pre- and postprandial hyperglycaemia and started in low doses to avoid hypoglycaemia due to residual endogenous insulin production.

Pancreatic exocrine assessment and Anthropometry

Within 3 months of pancreatectomy, faecal elastase 1 was measured by sandwich ELISA method utilizing two monoclonal antibodies highly specific for human pancreatic elastase 1 (ScheBo). A single random stool sample (about 100 mg) was required. The sample was prepared and analysed according to manufacturer's instruction. The detection range was 15 to 500 μg E1/g stool.

In addition to measurement of faecal elastase 1, patients were also monitored for clinical symptoms of pancreatic exocrine insufficiency including pale stools, abdominal discomfort, excessive flatulence, and poor weight gain. Patients manifesting these symptoms were managed with pancreatic enzyme replacement (Creon Micro [Abbott Healthcare, Maidenhead, UK] 100 mg before each feed or equivalent). Resolution of symptoms on pancreatic enzyme supplements was used as criteria for clinical pancreatic exocrine insufficiency.

In patients not requiring pancreatic enzyme supplementation, faecal elastase 1 was measured annually or at the onset of clinical pancreatic exocrine insufficiency. In those patients already commenced on pancreatic enzyme supplementation during previous assessment, only clinical monitoring was performed. Correlation between clinical and biochemical pancreatic exocrine insufficiency was made.

Weight and height from the last clinical assessment was converted to weight and height standard deviation score (SDS).

Statistical analysis

Data analysis was conducted by using SPSS statistics software, version 22.0 (IBM SPSS Statistics 22). The normality of the data was assessed by Shapiro-Wilk test. The medians were compared using Mann-Whitney U test. A P value<0.05 was considered statistically significant. The evolution of diabetes mellitus post-pancreatectomy was estimated using Kaplan-Meier analysis.

Results

From 1994 to 2012, 45 children underwent near-total pancreatectomy for management of medically unresponsive diffuse CHI (table 1). These patients presented with severe hypoketotic, hypofattyacidaemic hypoglycaemia, biochemical hallmark of inappropriate insulin secretion. Five patients presented between 1994 and 2000, and underwent near-total pancreatectomy without undergoing PVS or ^{18}F-DOPA-PET. All five patients had diffuse disease on histology. Later genetic analysis confirmed four patients to have biallelic *ABCC8* mutation, and one patient to have paternally inherited monoallelic *ABCC8* mutation.

Nine patients with medically unresponsive CHI who presented between 2000 and May 2006 were diagnosed to have diffuse CHI on PVS. The remaining medically unresponsive CHI patients who presented after May 2006 were diagnosed as diffuse CHI either on the basis of ^{18}F-DOPA-PET or molecular genetic analysis (biallelic mutations).

Apart from one international patient who developed diabetes mellitus immediately post-pancreatectomy and was lost to follow-up, all patients were regularly followed up in our centre at least until they developed diabetes mellitus.

Pancreatic Endocrine function

Figure 1 shows immediate post-operative pancreatic endocrine function outcome following near-total pancreatectomy.

Hypoglycaemia

Post-pancreatectomy, 27 children (60%) continued to have episodes of hypoglycaemia. Hypoglycaemia was less severe as compared to before pancreatectomy and was successfully managed with octreotide in 15 (33.3%), diazoxide in 3 (6.6%) and regular daytime and overnight feeds in 7 (15.6%). Second pancreatectomy was required in 2 children (4.4%). Over a mean (± S.D.)/median (range) follow up period of 6.71 (±4.75)/6.52 (0.1–17.5) years, episodes of hypoglycaemia resolved in 12 children (27%) and the medical treatments were successfully stopped. Episodes of hypoglycaemia persisted up to the age of 7 years in some children. In the remaining 15 children, the median fasting tolerance was 5 hours (range 3–14 hours) on the current treatment.

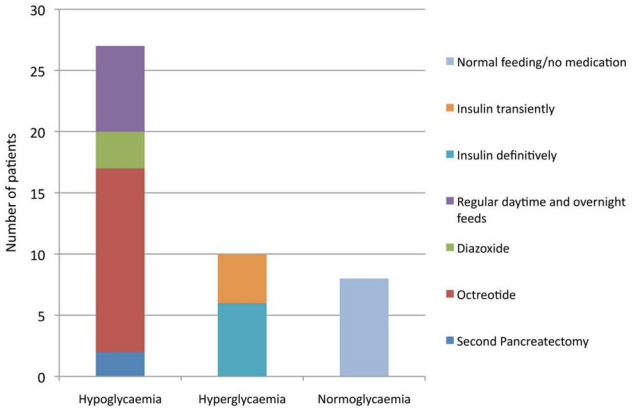

Figure 1. Immediate outcome of 45 children with medically unresponsive diffuse CHI managed with near-total pancreatectomy.
doi:10.1371/journal.pone.0098054.g001

Hyperglycaemia

Over a mean (± S.D.)/median (range) follow up period of 6.71 (±4.75)/6.52 (0.1–17.5) years, twenty-two (49%) children developed hyperglycaemia requiring insulin treatment. Ten children (22%) developed hyperglycaemia requiring insulin therapy immediately after pancreatectomy. Four of these required insulin treatment transiently for a period of 6–12 months. The incidence of hyperglycaemia requiring definitive insulin therapy increased from 13% immediately post-pancreatectomy to 77% at 7 years and then to 96% at 11 years post-surgery (figure 2).

Table 1. Characteristics of 45 children managed with near-total pancreatectomy.

Demographics	Patients (n)	45
	Boys/Girls (n)	20/25
	Birth weight (g)*	4089±805
	Gestational age (weeks)*	38±2
	Age at presentation (days)#	1 (1–56)
Hypoglycaemia screen	Serum glucose (mmol/l)*	1.8±0.7
	Serum Insulin (mU/l)*	34.3±42.9
Age at surgery (n)	0–4 weeks	5
	5–12 weeks	24
	13–52 weeks	12
	>52 weeks	4
ABCC8/KCNJ11 mutation analysis (n)	Homozygous	10
	Compound heterozygous	15
	Dominant heterozygous	12
	Contiguous gene deletion (Usher's syndrome)	3
	No mutation	5

*Mean±S.D.
#Median (Range).
doi:10.1371/journal.pone.0098054.t001

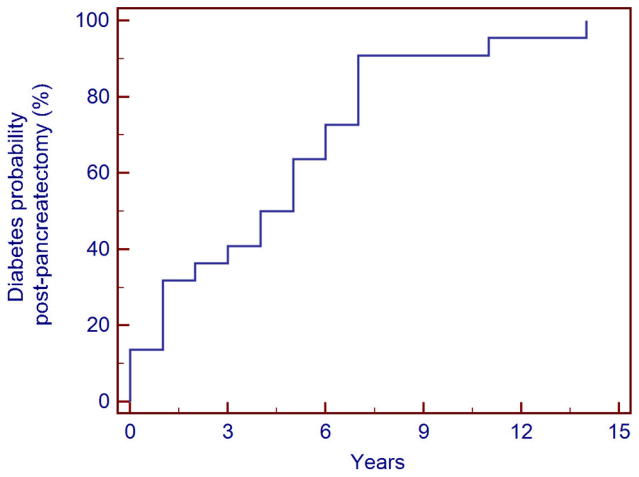

Figure 2. Cumulative incidence of definitive insulin therapy in 45 medically unresponsive diffuse CHI patients managed with near-total pancreatectomy.
doi:10.1371/journal.pone.0098054.g002

Pancreatic Exocrine function and Anthropometry

Of these 45 children, 32 (72%) had faecal elastase 1 either undetectable (<15 μg/g of stools) or suggestive of severe pancreatic exocrine insufficiency (15–100 μg/g of stools). Clinical pancreatic exocrine insufficiency was diagnosed in 22/45 (49%) patients. The sensitivity and specificity of faecal elastase 1 for predicting clinical pancreatic exocrine insufficiency in our series was 95% and 52% respectively.

In the biochemical pancreatic exocrine insufficiency group (n = 32), no statistically significant difference was found in age, weight SDS and height SDS on comparison between subgroups with treated clinical pancreatic exocrine insufficiency (n = 19) and untreated subclinical pancreatic exocrine insufficiency (n = 13) (figure 3).

Discussion

CHI is a heterogeneous disease with regards to responsiveness to medical treatment. A significant proportion of children require surgical resection of the pancreas to control the CHI. Most published series report an unacceptably high incidence of recurrent hyperinsulinemia following <95% pancreatectomy, with need for up to a 98% pancreatectomy in refractory cases [13,14,15]. In addition to persistent hypoglycaemia, these children are also at high risk of developing severe pancreatic exocrine insufficiency and diabetes mellitus.

In our large single centre cohort, 27/45 (60%) children had persistent hypoglycaemia after near-total pancreatectomy. Meissner et al published on long-term follow-up of 114 patients with CHI of all types (focal and diffuse; diazoxide responsive and unresponsive) [16]. More than half patients in this series (63/114; 55%) required pancreatic surgery comprising of partial (3%), subtotal (37%) or near-total (15%) pancreatectomy. Persistent hypoglycaemia was observed in 40% of patients after pancreatic surgery. However as the data was collected by survey of different hospitals, there is likely to be an unknown reporting bias in their study as compared to robust high quality single centre data presented here.

Similar to our study, Beltrand et al. recently published on glucose metabolism in 105 children and adolescents with CHI managed with pancreatectomy, 58 of whom had diffuse CHI and underwent near-total pancreatectomy. Of these 58 children, 59% had persistent but mild hypoglycaemia after surgery [6]. As we report very similar outcome from another large centre, these findings become of heightened clinical interest and highlight the consideration for alternative treatment strategies in this disease such as prolonged intensive medical and nutritional treatment, with high dose medication.

Leibowitz et al. evaluated endocrine pancreatic function in 14 patients with persistent hyperinsulinaemic hypoglycaemia of infancy 6.5–21 years after diagnosis, eight of which have been managed with early subtotal pancreatectomy [17]. In this study, the insulin response to glucose was blunted in all pancreatectomized patients, and six developed overt diabetes mellitus during puberty.

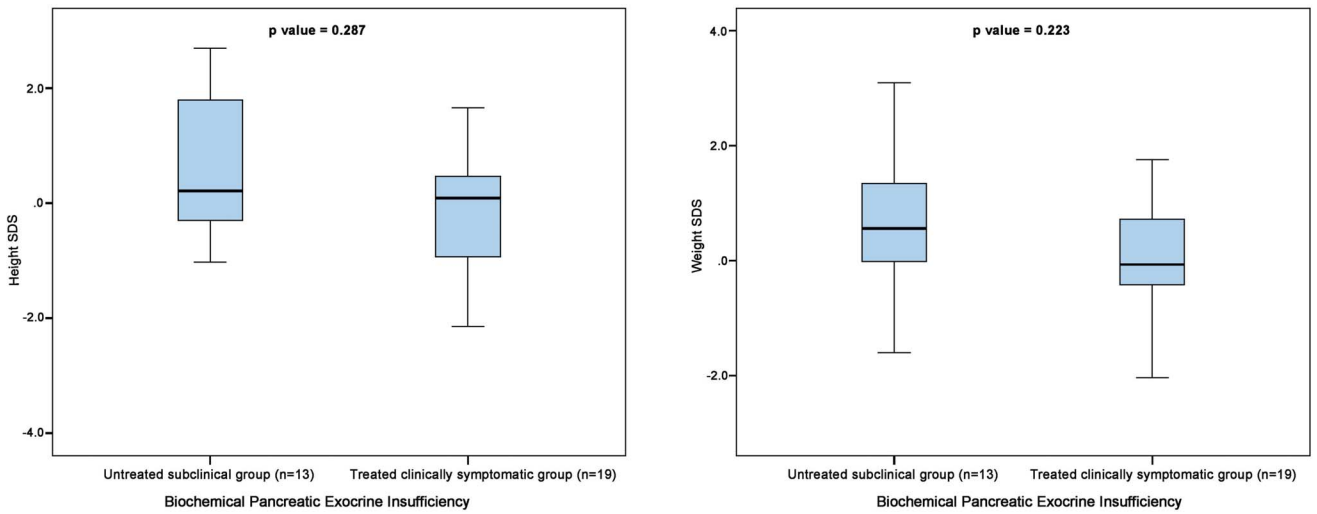

Figure 3. Comparison of weight and height SDS between untreated (no pancreatic enzyme supplementation) subclinical group and treated (appropriate pancreatic enzyme supplementation) clinically symptomatic group using Mann-Whitney U test.
doi:10.1371/journal.pone.0098054.g003

Cade et al. evaluated six children after pancreatectomy for persistent hyperinsulinaemic hypoglycaemia of infancy and reported diabetes mellitus in the only child who had entered puberty [8]. In our cohort, nearly one-quarter of the patients (10/45; 22%) developed hyperglycaemia in the days after surgery. Of these 10 patients with hyperglycaemia after pancreatectomy, 4 (9%) required insulin therapy transiently. The incidence of definitive insulin therapy increased from 13% postoperatively to 80% at 8 years and then 96% at 11 years post pancreatectomy. As compared to the study by Beltrand et al., twice number of patients in our cohort required definitive insulin therapy by 8 years post pancreatectomy (80% vs 42%). Surprisingly, the incidence of insulin-dependent diabetes mellitus in a study by Meissner et al. was only 28% by the mean age of 14 years [16]. This is likely to be due to more patients undergoing sub-total rather than near-total pancreatectomy or perhaps healthy remaining pancreatic β-cells not undergoing apoptosis. The incidence of diabetes mellitus in the study by Meissner et al. rose to 71% after re-operation for persistent HH [16].

Fourteen (31%) patients in our study achieved stable euglycaemia for more than 2 years duration after pancreatectomy without the development of hyperglycaemia. Meissner et al. reported stable long-term euglycaemia after surgery without the need of further surgery or the development of hyperglycaemia in 27% of all operated patients [16]. However for this cohort of patients, surgery was performed without prior investigation for differentiating between focal and diffuse CHI. The authors acknowledged that focal lesions in the head of the pancreas may have been missed by blind pancreatic resections. Although equivalent number of patients achieved stable euglycaemia in our series, the slightly better outcome as compared to the study by Meissner et al. could be because of the exclusion of focal lesions in the head before surgery in our cohort.

Few small studies which have evaluated pancreatic exocrine function using different methods in this clinical setting have reported subclinical deficiency rather than clinical exocrine dysfunction in these patients [8,9,11]. Dunger et al. reported low trypsin, amylase and bicarbonate concentrations with cholecystokinin-secretin test in approximately two-thirds of their patients who had 95% pancreatectomy whereas Rother et al. reported normal pancreatic exocrine function based on clinical history and 72-h stool collection in eight children after subtotal pancreatectomy for CHI [9,11]. Though cholecystokinin-secretion test or one of its modifications are the gold standard for pancreatic exocrine function, they have drawbacks of being time consuming, invasive and not being routinely available in clinical practice. In addition, there are no standardized enzyme cut-off values or agreement between centres as to which parameter is the most specific for the assessment of pancreatic function.

Measurement of faecal elastase 1 is the currently preferred pancreatic function test and is the new gold standard for non-invasive pancreatic function testing. Faecal elastase 1 is a pancreas-specific proteolytic enzyme that binds to bile salts and is not degraded during its passage through the gut, unlike other pancreatic enzymes [18]. Studies have shown that measurement of faecal elastase 1 correlates well with pancreatic output of elastase-1 and other pancreatic enzymes such as amylase, lipase and trypsin [19]. A faecal elastase 1 value of <200 μg/g of stool is the cut-off for pancreatic exocrine insufficiency. To the best of our knowledge, there are no studies assessing pancreatic exocrine function following pancreatectomy utilizing measurement of faecal elastase 1. It is unclear whether subclinical pancreatic exocrine deficient patients will benefit from pancreatic enzyme supplementation.

In our cohort, nearly three-quarter patients (32/45; 72%) had either undetectable faecal elastase 1 or in the severe pancreatic exocrine insufficiency range. Clinical pancreatic exocrine insufficiency was evident in 22/45 (49%) patients requiring pancreatic enzyme supplementation. In nearly one-quarter of the patients (12/45; 27%), no correlation between the biochemical and clinical pancreatic exocrine insufficiency was observed. No statistically significant difference was observed in weight and height SDS between treated subclinical pancreatic exocrine deficient patients and treated clinical pancreatic exocrine insufficiency patients (figures 3).

We acknowledge that faecal elastase 1 is an indirect pancreatic function test and is likely to be more prone to errors than the direct pancreatic function tests but because of its simple technique is used most often in the setting likely to result in pancreatic exocrine insufficiency such as post-pancreatectomy. With the increased awareness of CHI, need for appropriate management to avoid poor neurological outcome (near-total pancreatectomy in medically unresponsive diffuse disease), and advancement in the radiological (^{18}F DOPA-PET CT) and laparoscopic surgical techniques, clinicians are likely to come across post-pancreatectomy biochemical pancreatic exocrine insufficiency scenario. Our results highlight that faecal elastase-1 has poor specificity and should be cautiously interpreted in absence of clinical pancreatic exocrine insufficiency to inform clinical decisions about pancreatic enzyme replacement treatment.

In our cohort, although a number of patients had monoallelic *ABCC8/KCNJ11* mutations which usually results either in mild diazoxide responsive CHI or focal CHI if paternally inherited and associated with somatic loss of maternal 11p allele, detailed evaluation did not show response to medical therapy and histology showed diffuse disease. Diazoxide unresponsive diffuse CHI has been reported in association with dominant heterozygous *ABCC8/KCNJ11* mutations [20]. Another plausible hypothesis is that some of these patients may have a deep intronic mutation on the second allele that was not identified on Sanger sequencing or have a different mechanism of diffuse CHI [21].

A limitation of this study is its retrospective nature. In addition, the data presented here span a period of nearly two decades during which there were a number of significant advances in the management of CHI (introduction of PVS and ^{18}F DOPA-PET CT) and hence changes in the algorithms for the management. Despite these limitations, our robust single centre data on a large cohort of a complex group of CHI patients highlights the need for research for alternative treatment strategies in this disease.

Conclusions

In conclusion, long-term follow up a large cohort of medically unresponsive diffuse CHI patients has shown that milder hypoglycaemia persisted in 60% patients in this CHI subgroup after near-total pancreatectomy. The incidence of insulin dependent diabetes mellitus was nearly 100% after 11 years post-pancreatectomy. There seems to be poor correlation between the biochemical (faecal elastase 1) and clinical evidence of pancreatic exocrine insufficiency. Untreated subclinically pancreatic exocrine deficient children thrive as well as treated clinically pancreatic exocrine deficient children.

Author Contributions

Conceived and designed the experiments: VBA KH. Analyzed the data: VBA. Wrote the paper: VBA. Collection of data: VBA SS SA. Contributed to statistical analysis: HD. Reviewed Manuscript: HD KH. Contributed to genetic analysis: SEF SE. Guarantor of Work: KH.

References

1. Aynsley-Green A, Hussain K, Hall J, Saudubray JM, Nihoul-Fekete C, et al. (2000) Practical management of hyperinsulinism in infancy. Arch Dis Child Fetal Neonatal Ed 82: F98–F107.
2. Rahier J, Guiot Y, Sempoux C (2000) Persistent hyperinsulinaemic hypoglycaemia of infancy: a heterogeneous syndrome unrelated to nesidioblastosis. Arch Dis Child Fetal Neonatal Ed 82: F108–112.
3. Thomas P, Ye Y, Lightner E (1996) Mutation of the pancreatic islet inward rectifier Kir6.2 also leads to familial persistent hyperinsulinemic hypoglycemia of infancy. Hum Mol Genet 5: 1809–1812.
4. Thomas PM, Cote GJ, Wohllk N, Haddad B, Mathew PM, et al. (1995) Mutations in the sulfonylurea receptor gene in familial persistent hyperinsulinemic hypoglycemia of infancy. Science 268: 426–429.
5. Verkarre V, Fournet JC, de Lonlay P, Gross-Morand MS, Devillers M, et al. (1998) Paternal mutation of the sulfonylurea receptor (SUR1) gene and maternal loss of 11p15 imprinted genes lead to persistent hyperinsulinism in focal adenomatous hyperplasia. J Clin Invest 102: 1286–1291. 10.1172/jci4495
6. Beltrand J, Caquard M, Arnoux JB, Laborde K, Velho G, et al. (2012) Glucose metabolism in 105 children and adolescents after pancreatectomy for congenital hyperinsulinism. Diabetes Care 35: 198–203. 10.2337/dc11-1296
7. Ludwig A, Ziegenhorn K, Empting S, Meissner T, Marquard J, et al. (2011) Glucose metabolism and neurological outcome in congenital hyperinsulinism. Seminars in pediatric surgery 20: 45–49. 10.1053/j.sempedsurg.2010.10.005
8. Cade A, Walters M, Puntis JW, Arthur RJ, Stringer MD (1998) Pancreatic exocrine and endocrine function after pancreatectomy for persistent hyperinsulinaemic hypoglycaemia of infancy. Arch Dis Child 79: 435–439.
9. Rother KI, Matsumoto JM, Rasmussen NH, Schwenk WF (2001) Subtotal pancreatectomy for hypoglycemia due to congenital hyperinsulinism: long-term follow-up of neurodevelopmental and pancreatic function. Pediatr Diabetes 2: 115–122. 10.1034/j.1399-5448.2001.002003115.x
10. Cherian MP, Abduljabbar MA (2005) Persistent hyperinsulinemic hypoglycemia of infancy (PHHI): Long-term outcome following 95% pancreatectomy. J Pediatr Endocrinol Metab 18: 1441–1448.
11. Dunger DB, Burns C, Ghale GK, Muller DP, Spitz L, et al. (1988) Pancreatic exocrine and endocrine function after subtotal pancreatectomy for nesidioblastosis. J Pediatr Surg 23: 112–115.
12. Keller J, Aghdassi AA, Lerch MM, Mayerle JV, Layer P (2009) Tests of pancreatic exocrine function - clinical significance in pancreatic and non-pancreatic disorders. Best Pract Res Clin Gastroenterol 23: 425–439. 10.1016/j.bpg.2009.02.013
13. Lovvorn HN 3rd, Nance ML, Ferry RJ Jr, Stolte L, Baker L, et al. (1999) Congenital hyperinsulinism and the surgeon: lessons learned over 35 years. J Pediatr Surg 34: 786–792; discussion 792-783.
14. Shilyansky J, Fisher S, Cutz E, Perlman K, Filler RM (1997) Is 95% pancreatectomy the procedure of choice for treatment of persistent hyperinsulinemic hypoglycemia of the neonate? J Pediatr Surg 32: 342–346.
15. Langer JC, Filler RM, Wesson DE, Sherwood G, Cutz E (1984) Surgical management of persistent neonatal hypoglycemia due to islet cell dysplasia. J Pediatr Surg 19: 786–792.
16. Meissner T, Wendel U, Burgard P, Schaetzle S, Mayatepek E (2003) Long-term follow-up of 114 patients with congenital hyperinsulinism. European journal of endocrinology/European Federation of Endocrine Societies 149: 43–51.
17. Leibowitz G, Glaser B, Higazi AA, Salameh M, Cerasi E, et al. (1995) Hyperinsulinemic hypoglycemia of infancy (nesidioblastosis) in clinical remission: high incidence of diabetes mellitus and persistent beta-cell dysfunction at long-term follow-up. The Journal of clinical endocrinology and metabolism 80: 386–392. 10.1210/jcem.80.2.7852494
18. Stein J, Jung M, Sziegoleit A, Zeuzem S, Caspary WF, et al. (1996) Immunoreactive elastase I: clinical evaluation of a new noninvasive test of pancreatic function. Clin Chem 42: 222–226.
19. Loser C, Mollgaard A, Folsch UR (1996) Faecal elastase 1: a novel, highly sensitive, and specific tubeless pancreatic function test. Gut 39: 580–586.
20. Macmullen CM, Zhou Q, Snider KE, Tewson PH, Becker SA, et al. (2011) Diazoxide-unresponsive congenital hyperinsulinism in children with dominant mutations of the beta-cell sulfonylurea receptor SUR1. Diabetes 60: 1797–1804. 10.2337/db10-1631
21. Flanagan SE, Xie W, Caswell R, Damhuis A, Vianey-Saban C, et al. (2013) Next-generation sequencing reveals deep intronic cryptic ABCC8 and HADH splicing founder mutations causing hyperinsulinism by pseudoexon activation. American journal of human genetics 92: 131–136. 10.1016/j.ajhg.2012.11.017

Clinical characteristics and phenotype–genotype analysis in Turkish patients with congenital hyperinsulinism; predominance of recessive K_{ATP} channel mutations

Huseyin Demirbilek[1,2,3,4], Ved Bhushan Arya[2,3], Mehmet Nuri Ozbek[5], Aysehan Akinci[6], Murat Dogan[7], Fatma Demirel[4], Jayne Houghton[8], Sultan Kaba[6], Fatma Guzel[4], Riza Taner Baran[5], Sevim Unal[4], Selahattin Tekkes[9], Sarah E Flanagan[8], Sian Ellard[8] and **Khalid Hussain[2,3]**

Departments of [1]Neonatology and [2]Paediatric Endocrinology, Great Ormond Street Hospital for Children NHS Trust, London WC1N 3JH, UK, [3]Developmental Endocrinology Research Group, Molecular Genetics Unit, The Institute of Child Health, University College London, 30 Guilford Street, London WC1N 1EH, UK, [4]Departments of Paediatric Endocrinology, Ankara Children's Hematology and Oncology Training Hospital, Ankara, Turkey, [5]Departments of Paediatric Endocrinology, Children State Hospital, Diyarbakır, Turkey, [6]Departments of Paediatric Endocrinology, Inönü University, Malatya, Turkey, [7]Departments of Paediatric Endocrinology, Yüzüncü Yıl University, Van, Turkey, [8]Institute of Biomedical and Clinical Science, University of Exeter Medical School, Exeter EX2 5DW, UK and [9]Department of Medical Biology and Genetics, Dicle University, Diyarbakır, Turkey

Correspondence should be addressed to K Hussain
Email
Khalid.Hussain@ucl.ac.uk

Abstract

Objective: Congenital hyperinsulinism (CHI) is the commonest cause of hyperinsulinaemic hypoglycaemia in the neonatal, infancy and childhood periods. Its clinical presentation, histology and underlying molecular biology are extremely heterogeneous. The aim of this study was to describe the clinical characteristics, analyse the genotype–phenotype correlations and describe the treatment outcome of Turkish CHI patients.

Design and methods: A total of 35 patients with CHI were retrospectively recruited from four large paediatric endocrine centres in Turkey. Detailed clinical, biochemical and genotype information was collected.

Results: Diazoxide unresponsiveness was observed in nearly half of the patients ($n=17$; 48.5%). Among diazoxide-unresponsive patients, mutations in *ABCC8*/*KCNJ11* were identified in 16 (94%) patients. Among diazoxide-responsive patients ($n=18$), mutations were identified in two patients (11%). Genotype–phenotype correlation revealed that mutations in *ABCC8*/*KCNJ11* were associated with an increased birth weight and early age of presentation. Five patients had p.L1171fs (c.3512del) *ABCC8* mutations, suggestive of a founder effect. The rate of detection of a pathogenic mutation was higher in consanguineous families compared with non-consanguineous families (87.5 vs 21%; $P<0.0001$).

Among the diazoxide-unresponsive group, ten patients were medically managed with octreotide therapy and carbohydrate-rich feeds and six patients underwent subtotal pancreatectomy. There was a high incidence of developmental delay and cerebral palsy among diazoxide-unresponsive patients.

Conclusions: This is the largest study to report genotype–phenotype correlations among Turkish patients with CHI. Mutations in *ABCC8* and *KCNJ11* are the commonest causes of CHI in Turkish patients (48.6%). There is a higher likelihood of genetic diagnosis in patients with early age of presentation, higher birth weight and from consanguineous pedigrees.

European Journal of Endocrinology (2014) **170**, 885–892

European Journal of Endocrinology

www.eje-online.org
DOI: 10.1530/EJE-14-0045

Published by Bioscientifica Ltd.

Introduction

Hyperinsulinaemic hypoglycaemia (HH) is the commonest cause of hypoglycaemia in the neonatal, infancy and childhood periods (1, 2, 3). It occurs due to the unregulated secretion of insulin from pancreatic β-cells leading to severe and persistent hypoglycaemia. HH can be congenital (congenital hyperinsulinism, CHI) or transient due to risk factors such as perinatal asphyxia, intrauterine growth restriction (IUGR) and maternal diabetes mellitus (gestational or non-gestational) (1, 2, 3).

CHI refers to a group of conditions that are extremely heterogeneous in terms of clinical presentation, histological subgroups and underlying molecular biology. The molecular basis of CHI involves genetic defects in nine different genes (*ABCC8*, *KCNJ11*, *GLUD1*, *GCK*, *HADH*, *SLC16A1*, *HNF4A*, *HNF1A* and *UCP2*) that are involved in regulating insulin secretion from β-cells (1, 3). Mutations in the *ABCC8* and *KCNJ11* genes that encode the two subunits (SUR1 and Kir6.2) of ATP-sensitive potassium (K_{ATP}) channel are the commonest cause of CHI (4, 5).

At a histological level, two major subtypes of CHI (diffuse and focal) have been described. The differentiation of these two histological subtypes is important from the management point of view (6). The diffuse form may require a near-total pancreatectomy (with the risk of diabetes mellitus and pancreatic exocrine insufficiency), whereas the focal form will only require a limited focal lesionectomy. The frequency of focal disease has been reported to be 30–40% of all CHI patients in different series (7, 8). Genetic analysis and specialised positron emission tomography scan using the isotope Fluorine 18 L-3,4-dihydroxyphenyalanine (^{18}F-DOPA-PET) can be helpful in differentiating focal and diffuse diseases (9, 10). PET scan can also localise the focal lesions within the pancreas. Regarding their underlying genetic basis, the diffuse form is inherited in an autosomal recessive (or dominant) manner, whereas the focal form is sporadic in inheritance.

Besides differentiation of focal and diffuse diseases, documentation of protein sensitivity constitutes another important issue in the management of CHI. Mutations in *GLUD1* and *HADH* are associated with protein-sensitive CHI (11, 12). Protein-restricted diet may increase the success of medical therapy (13).

Although the incidence of CHI in the general population is one in 35 000–40 000, it rises to one in 2500 in the communities with the high rates of consanguinity (14). Turkey also has a high rate of consanguineous marriage (15). Thus, interpretation of clinical characteristics, genetic basis and phenotype–genotype relation of Turkish patients with CHI could bring a new perspective in understanding genetic basis, genotype–phenotype correlation and management of CHI. However, to our knowledge, to date, except for two small studies reporting the clinical and genetic characteristics of five and 13 Turkish patients with CHI, there is no large-scale study reporting clinical and genetic characteristics of Turkish children with CHI (16, 17). In this study, we describe clinical characteristics, genetic results and treatment outcome of a large cohort of CHI patients from Turkey.

Subjects and methods

Patients

Patients presenting with CHI to four large paediatric endocrine centres in Turkey were included in this study. CHI was defined as a detectable insulin level ($\geq$2 mU/l) during an episode of spontaneous or provoked hypoglycaemia (blood glucose $<$3.0 mmol/l). Patients with secondary HH due to IUGR, evidence of perinatal asphyxia and maternal diabetes mellitus were excluded. Detailed clinical and biochemical information was collected from the responsible clinician of these patients.

Written informed consent was obtained from parents of all participants for genetic mutation analysis. Diazoxide (5–15 mg/kg per day) was commenced as first line for the management of CHI. In diazoxide-unresponsive patients, octreotide (5–40 μg/kg per day) was tried. Patients unresponsive to medical therapy were managed with open near-total pancreatectomy. As ^{18}F-DOPA-PET–CT is not currently available in Turkey, a near-total pancreatectomy was performed for all patients who required surgical therapy irrespective of the results of molecular genetic analysis.

Mutation analysis

Genomic DNA was extracted from peripheral leukocytes using standard procedures and the coding regions and intron/exon boundaries of the *ABCC8* and *KCNJ11* genes were amplified by PCR (primers available on request) in all patients. Amplicons were subsequently sequenced using the Big Dye Terminator Cycler Sequencing Kit v3.1 (Applied Biosystems) according to the manufacturer's instruction and reactions were analysed on an ABI 3730 Capillary sequencer (Applied Biosystems). Sequences were compared with the reference sequences (NM_000525.3

and NM_000352.3) using the Mutation Surveyor v3.24 software (SoftGenetics, State College, PA, USA). If no mutations in *ABCC8* and *KCNJ11* were identified, the coding regions of *HADH* (only in diazoxide-responsive patients and those with abnormal acylcarnitine and/or urine organic acid profile) and *HNF4A* were amplified and sequenced as described previously (18, 19).

Statistical analyses

IBM SPSS statistics 21.0 for Windows software package program was used for statistical analyses. The Kolmogorov–Smirnov test was used to test normality for distribution of data. The independent samples *t*-test was used to compare mean of normally distributed data and the Mann–Whitney *U* test for non-normally distributed data. The χ^2-test was used to compare the ratios. A *P* value of <0.05 was considered statistically significant.

Results

A total of 35 patients presented with CHI between April 2002 and October 2013. The clinical and biochemical characteristics at presentation are summarised in Table 1. The median follow-up period for this cohort of patients was 2 years and 3 months (range: 1 month–10.5 years).

Mutation analysis, genotype–phenotype relation and treatment outcome

Mutation analysis ▸ Molecular genetic analysis identified pathogenic mutations in 51.4% of Turkish CHI patients (18/35; *ABCC8* (14 patients), *KCNJ11* (three patients) and *HADH* (one patient)) (Table 2). The K_{ATP} channel mutations included homozygous (13), compound heterozygous (2) and paternally inherited heterozygous (1) mutations. Maternal DNA was unavailable for testing to confirm the inheritance pattern in one patient with heterozygous *ABCC8* mutation.

Table 1 Clinical characteristics of CHI patients.

Clinical characteristics	Results
Number of patients, *n*	35
Males, *n* (%)	20 (57.1)
Gestational age (weeks)[a]	38 (29–40)
Birth weight (g)[b]	3407 ± 789
Large for gestational age (>90th percentile), *n* (%)	14 (40)
Age at presentation (weeks)[a]	1 (1–48)
Presentation within first week of life, *n* (%)	19 (58)
Consanguinity, *n* (%)	16 (45.7)
Family history of CHI, *n* (%)	7 (20)
Hypoglycaemia screen[b]	
Blood glucose (mmol/l)	1.7 ± 0.5
Serum insulin (mU/l)	32.7 ± 35.9
Hyperammonaemia[c]	0

[a]Median (range).
[b]Mean ± s.d.
[c]Serum ammonia more than twice the normal upper limit.

While a mutation was identified in 14 out of 16 patients (87.5%) from consanguineous families, it was identified only in four out of 19 patients (21%) from non-consanguineous families ($P<0.0001$).

In 40% (14/35) of the CHI patients, eight different *ABCC8* mutations were identified. One of the commonest mutations in our cohort was p.L1171fs (c.3512del), a frameshift mutation on exon 28 of *ABCC8* gene (five patients). Four unrelated patients from consanguineous families were homozygous for this mutation and one was heterozygous (inherited from unaffected father). Another common mutation identified was c.3554C>A (p.Ala1185Glu). This was a novel mutation identified in the homozygous state in four first cousins and a second unrelated proband.

The remaining six *ABCC8* mutations, p.R168C, p.N188S, p.L533P, p.W232G, p.R842Q and p.F591L were each identified in a single patient. Among these, p.L533P and p.W232G were novel mutations. These novel variants are not listed in various sequence variant databases (dbSNP, Exome Variant Server and 1000 Genomes) and the nucleotide at this position is conserved across all species. Additionally, *in silico* analysis by SIFT, PolyPhen2, AlignGVGD and Grantham distance predicts these novel variants to be likely pathogenic.

In 8.6% (3/35) of the CHI patients, three different *KCNJ11* mutations were identified. These included two missense (p.E126K, and p.R34H) and one nonsense (p.W91X) mutation. Among these, p.E126K was a novel mutation. The p.E126K mutation was identified in two probands in our cohort. Conservation across species, *in silico* analysis and comparison with various sequence databases predict this variant to be likely pathogenic. The remaining two mutations in *KCNJ11*, p.W91X and p.R34H, were identified *in trans* in a single patient and have been reported previously (20).

A previously described homozygous nonsense mutation in exon 6 of *HADH* (p.R236X) was identified in one patient. A protein-loading test showed protein-sensitive HH in this patient.

Sequencing of *ABCC8*, *KCNJ11*, *HNF4A* and *HADH* did not identify a causative mutation in the remaining 15 patients.

Table 2 Genetic analysis and treatment outcome of 18 patients with mutation-positive CHI.

Gene	Current age (year)	Exon/intron	DNA description	Protein description	Consequence	Transmission	Treatment			Follow-up	Developmental delay	Comments
							Diazoxide responsive	Octreotide responsive	Pancreatectomy (histology)			
ABCC8												
1	3.9	Exon 28	c.3554C>A	p.Ala1185Glu	Missense	Homozygous	−	+	−	Octreotide	+++	Novel mutation
2	0.7	Exon 28	c.3554C>A	p.Ala1185Glu	Missense	Homozygous	−	+	−	Octreotide		Novel mutation
3	9.1	Exon 28	c.3554C>A	p.Ala1185Glu	Missense	Homozygous	−	−	−	Irregular	++++	Novel mutation
4	0.7	Exon 28	c.3554C>A	p.Ala1185Glu	Missense	Homozygous	−	+	−	Octreotide	+	Novel mutation
5	0.2	Exon 28	c.3554C>A	p.Ala1185Glu	Missense	Homozygous	−	+	−	Octreotide		Novel mutation
6	0.7	Exon 28	c.3512delT	p.Leu1171fs	Frameshift	Homozygous	−	−	+ (diffuse)	Remission		
7	0.7	Exon 28	c.3512delT	p.Leu1171fs	Frameshift	Homozygous	−	+	+ (diffuse)	Octreotide		
8	Died	Exon 28	c.3512del	p.Leu1171fs	Frameshift	Heterozygous paternal	−	−	+ (diffuse)	Died		
9	5.8	Exon 28	c.3512delT	p.Leu1171fs	Frameshift	Homozygous	−	+	−	Octreotide	+++	Ectodermal dysplasia
10	9.6	Exon 28	c.3512delT	p.Leu1171fs	Frameshift	Homozygous	−	+	−	Octreotide	+++	
11	0.7	Exon 4	c.502C>T c.563A>G	p.Arg168Cys/ p.Asn188Ser	Missense	Compound heterozygous	−	+	+ (diffuse)	Octreotide	−	
12	Died	Exon 10	c.1598T>C	p.Leu533Pro	Missense	Homozygous	−	+	−	Died		Novel mutation
13	10.6	Exon 5/ exon 21	c.694T>G/ c.2525G>A	p.Trp232Gly/ p.Arg842Gln	Missense/ Missense	Compound heterozygous	−	+	−	Octreotide	++	
14	5.5	Exon 12	c.1771T>C	p.Phe591Leu	Missense	Heterozygous	+		−	Diazoxide	−	
KCNJ11												
15	2.4	Exon 1	c.101G>A/ c.376G>A	p.Arg34His/ p.Glu126Lys	Missense/ Missense	Compound heterozygous	−	+	−	Octreotide	−	
16	3.3	Exon 1	c.272G>A	p.Trp91X	Nonsense	Homozygous	−	+	+ (diffuse)	Octreotide	++	
17	3.2	Exon 1	c.376G>A	p.Glu126Lys	Missense	Homozygous	−	+	+ (diffuse)	Octreotide	++	
HADH												
18	4.4	Exon 6	c.706C>T	p.Arg236X	Nonsense	Homozygous	+			Diazoxide	+	

Table 3 Clinical characteristics of CHI patients with and without mutation at presentation. Data are presented as mean ± S.D.

Characteristics	Mutation positive	Mutation negative	*P* value
Birth weight (g)	3725 ± 664	3070 ± 788	0.012
Gestational age (weeks)	38.6 ± 1.6	37.6 ± 3.1	0.532
Age of presentation (weeks)	3.1 ± 6.8	10.3 ± 13.8	0.032
Serum insulin (mU/l)	36.1 ± 34.4	29.2 ± 38.1	0.355
Blood glucose level (mmol/l)	1.7 ± 0.5	1.8 ± 0.6	0.456

$P<0.05$ was considered statistically significant.

Genotype–phenotype correlation ▸ Comparison between K_{ATP} mutation-positive and K_{ATP} mutation-negative groups highlighted a statistically significant increased birth weight and younger age of presentation in K_{ATP} mutation-positive group as compared with K_{ATP} mutation-negative patients (Table 3).

Rate of detection of a pathogenic mutation in diazoxide-unresponsive patients (16/17; 94.1%) was higher than that of diazoxide-responsive group (2/18, 11.1% ($P<0.0001$) (Fig. 1).

Treatment outcome ▸ Of the total number of patients, 18 (51.4%; median age 22 months (range 3–128 months)) were responsive to diazoxide treatment (Fig. 1). Children were defined as being diazoxide responsive if they demonstrated age-appropriate fasting tolerance or evidence of appropriate hyperketonaemia before developing hypoglycaemia on diazoxide at doses <15 mg/kg per day. Administration of diazoxide could be successfully stopped in four of the diazoxide-responsive CHI patients at a median age of 3.5 months (range, 3–15 months). Of these, a pathogenic mutation was identified in only two patients (monoallelic *ABCC8* – 1 and biallelic *HADH* – 1).

Of the diazoxide-unresponsive group (17), six patients underwent pancreatectomy (five subtotal and one near-total) and ten patients were managed with octreotide treatment. One patient was lost to follow-up and represented at a later age with severe learning disability due to uncontrolled severe hypoglycaemia. A pathogenic mutation was identified in 16 out of 17 patients (94.1%; biallelic K_{ATP} – 15 and paternally inherited K_{ATP} – 1).

The median age at pancreatectomy was 1.5 months (range 1–2 months). Histological examination identified typical diffuse disease (abnormal large β-cell nuclei in pancreatic islets and low nuclear crowding in the whole pancreas) in all of these patients. After pancreatectomy, one patient unfortunately died because of sepsis and four patients required octreotide treatment to maintain euglycaemia. In only one patient who underwent near-total pancreatectomy, normoglycaemia was achieved without the need for additional medical therapy. There was no correlation between the type of mutation and the severity of CHI.

Long-term neurological sequelae such as developmental delay, cerebral palsy and epilepsy were higher in diazoxide-unresponsive patients (9/17) as compared with diazoxide-responsive (3/18) patients (52.9 vs 16.6%; $P=0.035$). This is likely to be due to difficulties in controlling hypoglycaemia in the diazoxide-unresponsive group.

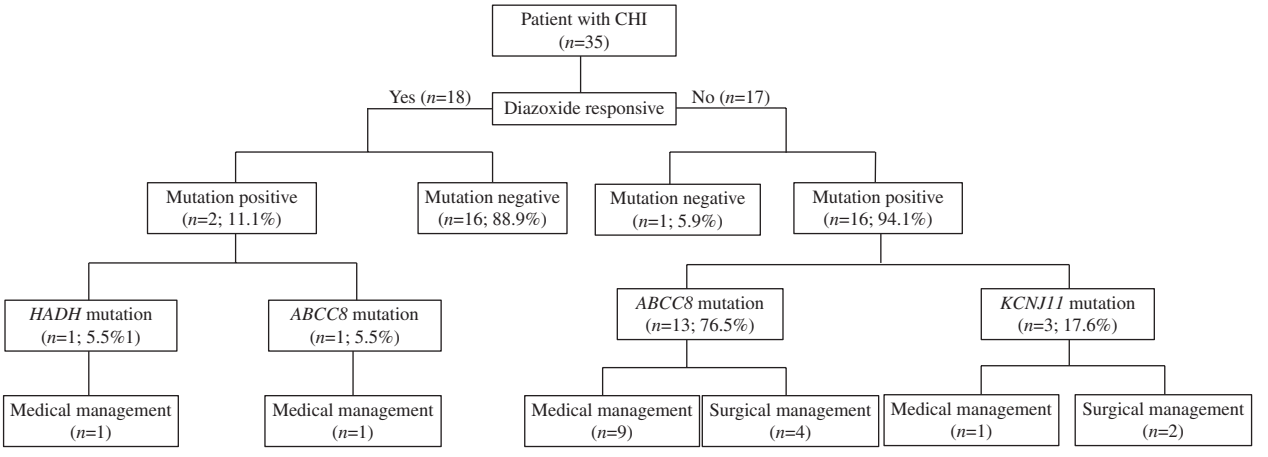

Figure 1
Mutation analysis results and treatment choices for patients with diazoxide-responsive CHI vs diazoxide-unresponsive CHI.

Discussion

In this study, 18 out of 35 patients (51.4%) had a genetically confirmed diagnosis of CHI (biallelic – 15 and monoallelic – 3). In two recent large studies of patients with CHI, genetic mutations were identified in 45.3 and 78.8% (21, 22). Mutations in the K_{ATP} channel genes were the commonest identifiable cause in our cohort (biallelic *ABCC8* – 12, monoallelic *ABCC8* – 2 and biallelic *KCNJ11* – 3).

All patients with biallelic K_{ATP} channel mutations in our cohort ($n=15$; 43%) were unresponsive to diazoxide treatment. Despite high doses of diazoxide for an adequate period of time, these patients could not be weaned off high-concentration dextrose fluids and experienced random episodes of hypoglycaemia. Similar findings have been reported by other investigators (Table 4). In the studies by Kapoor *et al.* (21) and Snider *et al.* (22), all patients with biallelic K_{ATP} mutations (63/300 (21%) and 84/417 (20%)) were unresponsive to diazoxide. The prevalence of homozygous K_{ATP} mutations in these studies (15 and 3.6%) was less when compared with our study (42.8%), possibly due to high consanguinity in our cohort. The studies by Kapoor *et al.* (21) and Snider *et al.* (22) have not mentioned the percentage of patients born of consanguineous marriage in their cohorts.

Five patients with biallelic K_{ATP} mutations were treated with near-total pancreatectomy and the remaining patients were treated with s.c. octreotide injections and carbohydrate-rich feeds. All the patients with biallelic K_{ATP} channel mutations who were pancreatectomised had diffuse disease on histological examination of the pancreatic tissue.

Of the two patients with monoallelic *ABCC8* mutations, the mutation was paternally inherited in one patient (p.Leu1171fs). This patient was medically unresponsive and was treated with near-total pancreatectomy. The histology of the resected pancreatic tissue showed diffuse disease, although it is likely that the focal lesion could have been missed. As this particular *ABCC8* mutation was present in monoallelic state in clinically unaffected parents (although not biochemically evaluated) of four different patients in our cohort and it is a null mutation, it seems likely that this was a recessive *ABCC8* mutation which has been unmasked by paternal uniparental disomy within the pancreas. Although there is no family history of hyperinsulinism or early-onset diabetes mellitus on the maternal side, the milder clinical phenotype (diazoxide responsiveness) of the second patient with monoallelic non-paternal *ABCC8* mutation (maternal DNA unavailable for testing) was suggestive of dominant *ABCC8* mutation.

Table 4 Summary of studies showing mutation detection rate, diazoxide responsiveness and histological subtype of CHI patients.

Reference	Year	*n*	Mutation detection rate *n* (%)			K_{ATP} channel mutations *n* (%)		Other mutations[b]	Histology[a]		Country
			DZ responsive	DZ unresponsive	Overall	Monoallelic	Biallelic		Focal	Diffuse	
This study	2014	35	2/18 (11)	16/17 (94)	18/35 (51)	1 (6)	15 (94)	1	0 (0)	6 (100)	Turkey
(17)	2002	13	0/10 (0)	3/3 (100)	3/13 (23)	0 (0)	3 (100)	–	0 (0)	3 (100)	Turkey
(20)	2011	17	4/5 (80)	7/8 (87)	14/17[c] (82)	10/14 (71)	4/14 (29)	–	0 (0)	6 (100)	Korea
(23)	2011	36	NS	NS	24/36 (67)	17/19 (84)	2/19 (15)	5	1 (10)	9 (90%)	Japan
(25)	2009	26	NS	NS	16/26 (58)	6 (40)	9 (60)	1	3 (33)	6 (67)	Norway
(26)	2013	36	12/25 (48)	9/11 (82)	20/36 (55)	12[d] (92)	1 (8)	8	3 (100)	0 (0)	Italy
(21)	2013	300	41/183 (22)	92/105 (87.6)	136/300[e] (45)	46 (42)	63 (58)	27	NS	NS	UK
(22)	2013	417	56/118 (47)	272/292 (91)	328/417 (79)	200 (69)	88 (31)	40	149 (53)	122[f] (43)	USA

n, number; DZ, diazoxide; NS, not specified.
[a]Mutations detected in other genes (*HADH*, *HNF4A*, *HNF1A*, *GCK*, *UCP2* and *GLUD1*).
[b]Histology proven after surgery.
[c]Diazoxide not tried in three patients.
[d]One patient had monoallelic K_{ATP} as well as *GCK* mutation.
[e]Diazoxide responsiveness not determined in 12 patients.
[f]Histology normal in four patients and atypical diffuse disease in 11 patients.

The other interesting observation in our study was the low prevalence of monoallelic K_{ATP} mutation (2/35; 5.7%). This is in sharp contrast to observations from genetic analysis of patients from Korea and Japan, where the single mutation rate was between 50 and 60% (Table 4) (20, 23). In the study by Kapoor *et al.*, monoallelic K_{ATP} mutation was present in 14.6% of patients, whereas 48% of patients had monoallelic K_{ATP} mutation in the study by Snider *et al.* (21, 22).

In our cohort, about half of the patients were diazoxide responsive ($n=18$). Only two patients from this group had a pathogenic mutation (monoallelic *ABCC8* – 1 and biallelic *HADH* – 1). No mutation could be identified in the remaining 16 out of 18 (88.9%) diazoxide-responsive patients. The mutation detection rate in diazoxide-responsive category in our cohort is less when compared with other studies (21, 22). This may be due to the fact that sequencing of *GLUD1*, *GCK* and *HADH* genes was not performed in these patients unless indicated by the clinical phenotype. Novel genetic mechanisms might be responsible for CHI in these patients.

In our study, the majority of diazoxide-unresponsive patients (16/17; 94.1%) had a K_{ATP} channel mutation. This has been established in large cohort studies by Kapoor *et al.* (21) and Snider *et al.* (22) (87.6 and 91% respectively). Our results are in line with these larger studies.

This study identified a number of novel *ABCC8* and *KCNJ11* mutations (Table 2). One particular novel *ABCC8* missense mutation (p.A1185E, c.3554C>A), co-segregating with disease in the family, was found in four affected cousins from one family and another unrelated patient. In addition to this mutation, another *ABCC8* mutation (p.L1171fs, c.3512delT) was also detected in five patients from four different families, possibly suggesting a founder effect.

In this study, integration of the clinical findings and genetic results suggests the likelihood of K_{ATP} mutations in patients with CHI in the presence of increased birth weight and earlier age of presentation. It was striking that those patients with K_{ATP} channel mutations presented earlier and had a higher birth weight when compared with patients without a K_{ATP} channel mutation. Previous studies have shown that there may be an overlap between birth weight and age of presentation between patients with *HNF4A* and K_{ATP} channel mutations (21). However, our study clearly showed the difference in age of presentation and birth weight between K_{ATP} channel-positive and -negative groups. These observations can be very helpful in the clinical management of patients with CHI, especially if the clinicians do not have access to urgent molecular genetic analysis.

Lastly, in our cohort, 12 out of 35 (34%) patients had long-term neurological sequelae such as developmental delay, cerebral palsy and epilepsy. This is similar to what has been reported in the recent literature from Turkey (24). The likelihood of adverse neurological sequelae was significantly higher in the diazoxide-unresponsive group.

Conclusions

In conclusion, in this largest Turkish cohort with CHI, K_{ATP} channel mutations were detected in 48.6% (17/35) of the patients studied. The likelihood of long-term neurological sequelae was higher in the diazoxide-unresponsive group, highlighting the need for management of these complex patients in highly specialised centres. Additional research to identify novel genetic mechanisms for patients with diazoxide-responsive CHI is required.

Declaration of interest
The authors declare that there is no conflict of interest that could be perceived as prejudicing the impartiality of the research reported.

Funding
H Demirbilek was funded by the European Society for Paediatric Endocrinology (ESPE) and The Scientific and Technological Research Council of Turkey (TUBITAK) during his 1-year clinical fellowship at University College London (UCL) Institute of Child Health, Great Ormond Street Hospital for Children NHS Trust, Department of Paediatric Endocrinology.

Author contribution statement
H Demirbilek contributed to the conceptualisation of the manuscript, collection of data, data analysis and writing of the manuscript; V B Arya, collection of data, data analysis and writing of the manuscript; M N Ozbek, A Akinci, M Dogan, F Demirel, S Kaba, F Guzel, R T Baran, S Unal and S Tekkes, collection of data and review of the manuscript; J Houghton, S E Flanagan and S Ellard, genetic analysis and review of the manuscript and K Hussain, conceptualisation of the manuscript, review of the manuscript and guarantor of the manuscript.

References

1 Mohamed Z, Arya VB & Hussain K. Hyperinsulinaemic hypoglycaemia: genetic mechanisms, diagnosis and management. *Journal of Clinical Research in Pediatric Endocrinology* 2012 **4** 169–181. (doi:10.4274/Jcrpe.821)
2 De Leon DD & Stanley CA. Mechanisms of disease: advances in diagnosis and treatment of hyperinsulinism in neonates. *Nature Clinical Practice. Endocrinology & Metabolism* 2007 **3** 57–68. (doi:10.1038/ncpendmet0368)
3 Senniappan S, Arya VB & Hussain K. The molecular mechanisms, diagnosis and management of congenital hyperinsulinism. *Indian Journal of Endocrinology and Metabolism* 2013 **17** 19–30. (doi:10.4103/2230-8210.107822)

4 Thomas P, Ye Y & Lightner E. Mutation of the pancreatic islet inward rectifier Kir6.2 also leads to familial persistent hyperinsulinemic hypoglycemia of infancy. *Human Molecular Genetics* 1996 **5** 1809–1812. (doi:10.1093/hmg/5.11.1809)
5 Thomas PM, Cote GJ, Wohllk N, Haddad B, Mathew PM, Rabl W, Aguilar-Bryan L, Gagel RF & Bryan J. Mutations in the sulfonylurea receptor gene in familial persistent hyperinsulinemic hypoglycemia of infancy. *Science* 1995 **268** 426–429. (doi:10.1126/science.7716548)
6 Aynsley-Green A, Hussain K, Hall J, Saudubray JM, Nihoul-Fekete C, De Lonlay-Debeney P, Brunelle F, Otonkoski T, Thornton P & Lindley KJ. Practical management of hyperinsulinism in infancy. *Archives of Disease in Childhood. Fetal and Neonatal Edition* 2000 **82** F98–F107. (doi:10.1136/fn.82.2.F98)
7 Sempoux C, Guiot Y, Lefevre A, Nihoul-Fekete C, Jaubert F, Saudubray JM & Rahier J. Neonatal hyperinsulinemic hypoglycemia: heterogeneity of the syndrome and keys for differential diagnosis. *Journal of Clinical Endocrinology and Metabolism* 1998 **83** 1455–1461. (doi:10.1210/jcem.83.5.4768)
8 Goossens A, Gepts W, Saudubray JM, Bonnefont JP, Nihoul F, Heitz PU & Kloppel G. Diffuse and focal nesidioblastosis. A clinicopathological study of 24 patients with persistent neonatal hyperinsulinemic hypoglycemia. *American Journal of Surgical Pathology* 1989 **13** 766–775. (doi:10.1097/00000478-198909000-00006)
9 Hardy OT, Hernandez-Pampaloni M, Saffer JR, Scheuermann JS, Ernst LM, Freifelder R, Zhuang H, MacMullen C, Becker S, Adzick NS *et al*. Accuracy of [18F]fluorodopa positron emission tomography for diagnosing and localizing focal congenital hyperinsulinism. *Journal of Clinical Endocrinology and Metabolism* 2007 **92** 4706–4711. (doi:10.1210/jc.2007-1637)
10 Banerjee I, Skae M, Flanagan SE, Rigby L, Patel L, Didi M, Blair J, Ehtisham S, Ellard S, Cosgrove KE *et al*. The contribution of rapid K_{ATP} channel gene mutation analysis to the clinical management of children with congenital hyperinsulinism. *European Journal of Endocrinology* 2011 **164** 733–740. (doi:10.1530/EJE-10-1136)
11 Kapoor RR, James C, Flanagan SE, Ellard S, Eaton S & Hussain K. 3-Hydroxyacyl-coenzyme A dehydrogenase deficiency and hyperinsulinemic hypoglycemia: characterization of a novel mutation and severe dietary protein sensitivity. *Journal of Clinical Endocrinology and Metabolism* 2009 **94** 2221–2225. (doi:10.1210/jc.2009-0423)
12 Stanley CA, Lieu YK, Hsu BY, Burlina AB, Greenberg CR, Hopwood NJ, Perlman K, Rich BH, Zammarchi E & Poncz M. Hyperinsulinism and hyperammonemia in infants with regulatory mutations of the glutamate dehydrogenase gene. *New England Journal of Medicine* 1998 **338** 1352–1357. (doi:10.1056/NEJM199805073381904)
13 Palladino AA & Stanley CA. The hyperinsulinism/hyperammonemia syndrome. *Reviews in Endocrine and Metabolic Disorders* 2010 **11** 171–178. (doi:10.1007/s11154-010-9146-0)
14 Mathew PM, Young JM, Abu-Osba YK, Mulhern BD, Hammoudi S, Hamdan JA & Sa'di AR. Persistent neonatal hyperinsulinism. *Clinical Pediatrics* 1988 **27** 148–151. (doi:10.1177/000992288802700307)
15 Tuncbilek E & Ulusoy M. Consanguinity in Turkey in 1988. *Turkish Journal of Population Studies* 1989 **11** 35–46.
16 Ocal G, Flanagan SE, Hacihamdioglu B, Berberoglu M, Siklar Z, Ellard S, Savas Erdeve S, Okulu E, Akin IM, Atasay B *et al*. Clinical characteristics of recessive and dominant congenital hyperinsulinism due to mutation(s) in the ABCC8/KCNJ11 genes encoding the ATP-sensitive potasium channel in the pancreatic β cell. *Journal of Pediatric Endocrinology and Metabolism* 2011 **24** 1019–1023. (doi:10.1515/JPEM.2011.347)
17 Darendeliler F, Fournet JC, Bas F, Junien C, Gross MS, Bundak R, Saka N & Gunoz H. ABCC8 (SUR1) and KCNJ11 (KIR6.2) mutations in persistent hyperinsulinemic hypoglycemia of infancy and evaluation of different therapeutic measures. *Journal of Pediatric Endocrinology and Metabolism* 2002 **15** 993–1000. (doi:10.1515/JPEM.2002.15.7.993)
18 Flanagan SE, Kapoor RR, Mali G, Cody D, Murphy N, Schwahn B, Siahanidou T, Banerjee I, Akcay T, Rubio-Cabezas O *et al*. Diazoxide-responsive hyperinsulinemic hypoglycemia caused by HNF4A gene mutations. *European Journal Endocrinology* 2010 **162** 987–992. (doi:10.1530/EJE-09-0861)
19 Flanagan SE, Patch AM, Locke JM, Akcay T, Simsek E, Alaei M, Yekta Z, Desai M, Kapoor RR, Hussain K *et al*. Genome-wide homozygosity analysis reveals HADH mutations as a common cause of diazoxide-responsive hyperinsulinemic-hypoglycemia in consanguineous pedigrees. *Journal of Clinical Endocrinology and Metabolism* 2011 **96** E498–E502. (doi:10.1210/jc.2010-1906)
20 Park SE, Flanagan SE, Hussain K, Ellard S, Shin CH & Yang SW. Characterization of ABCC8 and KCNJ11 gene mutations and phenotypes in Korean patients with congenital hyperinsulinism. *European Journal of Endocrinology* 2011 **164** 919–926. (doi:10.1530/EJE-11-0160)
21 Kapoor RR, Flanagan SE, Arya VB, Shield JP, Ellard S & Hussain K. Clinical and molecular characterisation of 300 patients with congenital hyperinsulinism. *European Journal of Endocrinology* 2013 **168** 557–564. (doi:10.1530/EJE-12-0673)
22 Snider KE, Becker S, Boyajian L, Shyng SL, MacMullen C, Hughes N, Ganapathy K, Bhatti T, Stanley CA & Ganguly A. Genotype and phenotype correlations in 417 children with congenital hyperinsulinism. *Journal of Clinical Endocrinology and Metabolism* 2013 **98** E355–E363. (doi:10.1210/jc.2012-2169)
23 Yorifuji T, Kawakita R, Nagai S, Sugimine A, Doi H, Nomura A, Masue M, Nishibori H, Yoshizawa A, Okamoto S *et al*. Molecular and clinical analysis of Japanese patients with persistent congenital hyperinsulinism: predominance of paternally inherited monoallelic mutations in the K_{ATP} channel genes. *Journal of Clinical Endocrinology and Metabolism* 2011 **96** E141–E145. (doi:10.1210/jc.2010-1281)
24 Agladioglu SY, Savas Erdeve S, Cetinkaya S, Bas VN, Peltek Kendirci HN, Onder A & Aycan Z. Hyperinsulinemic hypoglycemia: experience in a series of 17 cases. *Journal of Clinical Research in Pediatric Endocrinology* 2013 **5** 150–155. (doi:10.4274/Jcrpe.991)
25 Sandal T, Laborie LB, Brusgaard K, Eide SA, Christesen HB, Søvik O, Njølstad PR & Molven A. The spectrum of ABCC8 mutations in Norwegian patients with congenitalhyperinsulinismof infancy. *Clinical Genetics* 2009 **75** 440–448. (doi:10.1111/j.1399-0004.2009.01152.x)
26 Faletra F, Athanasakis E, Morgan A, Biarnés X, Fornasier F, Parini R, Furlan F, Boiani A, Maiorana A, Dionisi-Vici C *et al*. Congenital hyperinsulinism: clinical and molecular analysis of a large Italian cohort. *Gene* 2013 **521** 160–165. (doi:10.1016/j.gene.2013.03.021)

Received 17 January 2014
Revised version received 26 March 2014
Accepted 31 March 2014

DIABETICMedicine

DOI: 10.1111/dme.12369

Case Report

HNF4A mutation: switch from hyperinsulinaemic hypoglycaemia to maturity-onset diabetes of the young, and incretin response

V. B. Arya[1,2]*, S. Rahman[2]*, S. Senniappan[1,2], S. E. Flanagan[3], S. Ellard[3] and K. Hussain[1,2]

[1]Department of Paediatric Endocrinology, Great Ormond Street Hospital for Children NHS, Trust, London, [2]The Institute of Child Health, University College London and [3]Institute of Biomedical and Clinical Science, University of Exeter Medical School, Exeter, UK

Accepted 28 November 2013

Abstract

Background Hepatocyte nuclear factor 4α (HNF4A) is a member of the nuclear receptor family of ligand-activated transcription factors. *HNF4A* mutations cause hyperinsulinaemic hypoglycaemia in early life and maturity-onset diabetes of the young. Regular screening of *HNF4A* mutation carriers using the oral glucose tolerance test has been recommended to diagnose diabetes mellitus at an early stage. Glucagon-like peptide-1 and glucose-dependent insulinotropic polypeptide are incretin hormones, responsible for up to 70% of the secreted insulin after a meal in healthy individuals. We describe, for the first time, gradual alteration of glucose homeostasis in a patient with *HNF4A* mutation after resolution of hyperinsulinaemic hypoglycaemia, on serial oral glucose tolerance testing. We also measured the incretin response to a mixed meal in our patient.

Case report Our patient was born with macrosomia and developed hyperinsulinaemic hypoglycaemia in the neonatal period. Molecular genetic analysis confirmed *HNF4A* mutation (p.M116I, c.317G>A) as an underlying cause of hyperinsulinaemic hypoglycaemia. Serial oral glucose tolerance testing, after the resolution of hyperinsulinaemic hypoglycaemia, confirmed the diagnosis of maturity-onset diabetes of the young at the age of 10 years. Interestingly, the intravenous glucose tolerance test revealed normal glucose disappearance rate and first-phase insulin secretion. Incretin hormones showed a suboptimal rise in response to the mixed meal, potentially explaining the discrepancy between the oral glucose tolerance test and the intravenous glucose tolerance test.

Conclusions Maturity-onset diabetes of the young can develop as early as the first decade of life in persons with an *HNF4A* mutation. Impaired incretin response might be contributory in the early stages of *HNF4A* maturity-onset diabetes of the young.

Diabet. Med. 31, e11–e15 (2014)

Introduction

Hepatocyte nuclear factor 4α (HNF4A) is a member of the steroid/thyroid hormone receptor superfamily and is most highly expressed in the liver, kidney, pancreatic islets and intestine [1,2]. HNF4A is a major activator of hepatocyte nuclear factor 1α (HNF1A), which in turn activates the expression of a large number of liver-specific genes, including those involved in glucose, cholesterol and fatty acid metabolism [3]. Specifically in the pancreatic islets, HNF4A has been shown to control the expression of genes involved in glucose-stimulated insulin secretion [4,5]. *HNF4A* mutations cause hyperinsulinaemic hypoglycaemia and maturity-onset diabetes of the young (MODY) [6–8]. Annual screening of *HNF4A*-mutation carriers with oral glucose tolerance testing was recommended to diagnose diabetes mellitus at an early stage [7].

Glucagon-like peptide-1 (GLP-1) and glucose-dependent insulinotropic polypeptide are incretin hormones, which augment the magnitude of meal-stimulated insulin secretion from islet β-cells in a glucose-dependent manner [9].

We describe, for the first time, the gradual alteration in glucose homeostasis and development of MODY in the *HNF4A*-mutation carrier after resolution of hyperinsulinaemic hypoglycaemia, on prospective follow-up with an annual oral glucose tolerance test. We also report the GLP-1 and glucose-dependent insulinotropic polypeptide response to the mixed-meal test at the onset of diabetes mellitus.

Correspondence to: Khalid Hussain. E-mail: Khalid.Hussain@ucl.ac.uk
*These authors contributed equally to the manuscript.

What's new?

- This study reports the first patient with an *HNF4A* mutation to have been serially monitored from the diagnosis of hyperinsulinaemic hypoglycaemia to maturity-onset diabetes of the young.
- We describe, for the first time, incretin response in a patient with *HNF4A* maturity-onset diabetes of the young, which has the potential to influence the management of these patients.

Research design and methods

KCNJ11, ABCC8 and *HNF4A* sequencing

Genomic DNA was extracted from peripheral leukocytes using standard procedures, and the coding exons and intron/exon boundaries of the *ABCC8*, *KCNJ11* and *HNF4A* genes were amplified by polymerase chain reaction (PCR). *HNF4A* analysis included the coding exons 1d–10 and the P2 pancreatic promoter. PCR products were sequenced using standard methods on an ABI 3730 sequencer (Applied Biosystems, Warrington, UK) and were compared with the published sequence NM_000457.3 (exons 2–10) and AY680697 (exon 1d only) using Mutation Surveyor v3.2 (SoftGenetics, State College, PA, USA) [10].

Oral glucose tolerance test

An oral glucose tolerance test (glucose load 1.75 g/kg) was performed in accordance with standard recommendations and the results were interpreted according to published World Health Organization (WHO) diagnostic criteria [11,12].

Intravenous glucose tolerance test

After an overnight fast of 12 h, 0.5 g/kg of glucose as a 20% solution was infused within 2 min through an intravenous catheter in the antecubital region. Blood samples were obtained at –10, –5, 0, 1, 3, 5, 10, 15, 20, 30, 45 and 60 min through a second intravenous catheter for estimation of blood glucose and serum insulin. The glucose disappearance rate K (%/min) was calculated according to $^{0.693 \times 100}/_{t1/2}$ (in min), where $t_{1/2}$ was the time span (min) required for glucose to fall by 50% from its level at 10 min [12]. The first-phase insulin release was calculated by the area under the insulin stimulation curve between 0 and 10 min [12].

Mixed-meal tolerance test

The mixed-meal tolerance test was performed after an overnight fast of 12 h. A standardized breakfast was ingested over 10 min, calculated by a dietician based on the total caloric needs of the patient (25–30% of their daily caloric intake; 50% of the calories as carbohydrates, 33% lipids and 17% proteins). Blood samples were collected at 0, 15, 30, 45 and 60 min for estimation of blood glucose, serum insulin, total glucose-dependent insulinotropic polypeptide and active GLP-1. The area under curve was estimated by the linear trapezoidal method from the concentration time curve.

Measurement of GLP1 and glucose-dependent insulinotropic polypeptide

Blood was collected in chilled EDTA-treated tubes containing DPP-4 inhibitor (10 μl/ml blood: Millipore, Watford, UK) and aprotonin (trasylol 5000 KIU/ml blood: Bayer, Newbury, UK). Blood was processed according to the manufacturers' instructions for the measurement of hormones using commercially available assays. Total glucose-dependent insulinotropic polypeptide and active GLP-1 were determined using commercially available human ELISA kits according to the manufacturer's guidelines (Millipore). All samples were performed in duplicate.

Case report

We describe a male Caucasian patient, who was born with macrosomia [birthweight 4060 g at 39 weeks of gestation; +1.44 standard deviation score (SDS)] and who developed neonatal hypoglycaemia requiring a high glucose infusion rate (18.5 mg kg^{-1} min^{-1}) to maintain normoglycaemia. There was no family history of diabetes mellitus. Investigations revealed inappropriately elevated serum insulin and inappropriately low β-hydroxybutyrate and non-esterified fatty acids during an episode of hypoglycaemia on three occasions, confirming hyperinsulinaemic hypoglycaemia. Serum cortisol, lactate, ammonia, plasma aminoacids, carnitine profile and urine organic acids were normal. Molecular genetic testing for mutation in *ABCC8/KCNJ11* was negative. Hyperinsulinaemic hypoglycaemia was successfully managed with diazoxide. A 24-h blood glucose profile and controlled fasting studies were carried out at regular intervals until the age of 18 months, at which age his hyperinsulinaemic hypoglycaemia resolved.

At the age of 5 years, after *HNF4A* mutations were first reported as a cause of macrosomia and neonatal hyperinsulinaemic hypoglycaemia, he underwent molecular genetic testing and was identified to have a *de novo* heterozygous *HNF4A* mutation (p.M116I, c.317G>A) [13].

Oral glucose tolerance test

Annual monitoring with an oral glucose tolerance test revealed impaired glucose tolerance and development of diabetes mellitus according to WHO diagnostic criteria (Table 1) [11]. At the diagnosis of diabetes mellitus, he was prepubertal with a bilateral testicular volume of 2 ml. His HbA_{1c} was 40 mmol/mmol (5.8%) and autoantibodies

Table 1 Oral glucose tolerance test

Age BMI, kg/m^2 (SDS)	7 years 15.25 (–0.22)		8 years 15.8 (+0.05)		9 years 17.6 (+0.75)		10 years 19.9 (+1.17)		
Time	Blood glucose (mmol/l)	Serum insulin (mU/l)	Blood glucose (mmol/l)	Serum insulin (mU/l)	Blood glucose (mmol/l)	Serum insulin (mU/l)	Blood glucose (mmol/l)	Serum insulin (mU/l)	C-peptide (pmol/l)
–30 min	4.0	< 2.0	4.0	< 2.0	4.3	< 2.0			
0 min	3.6	< 2.0	3.9	< 2.0	4.2	< 2.0	4.8	5.6	440
30 min	8.8	39.8	8.6	39.6	6.9	23	9.2	47.1	1903
60 min	7.7	39.1	8.5	26.4	9.5	30	11.7	66.7	2522
90 min	6.7	22.5	6.8	17.0	8.5	21	11.5	44.1	2214
120 min	6.8	23.6	8.3	28.9	9.3	26	12.3	35.9	1956
150 min	3.4	6.6	6.2	13.8			13.3	36.3	1926
180 min	3.1	< 2.0	3.2	< 2.0			8.4	17.0	1202

(GAD 65 and islet-cell) were negative. His serial BMI and BMI SDS were normal (Table 1).

Intravenous glucose tolerance test

An intravenous glucose tolerance test (Fig. 1) revealed normal glucose disappearance rate (1.38% per min; normal response > 1.2% per min) and first-phase insulin secretion (2.7 nmol l^{-1} min^{-1} normal 1.4–5.3 nmol l^{-1} min^{-1}), which were not indicative of insulin secretion defect [12].

Mixed-meal tolerance test

To understand the reasons for the discrepancy between diabetic oral glucose tolerance test response and normal intravenous glucose tolerance test response, we measured the incretin hormones in response to the mixed-meal tolerance test (Fig. 2). The 30-min areas under the curve for active GLP-1 and total glucose-dependent insulinotropic polypeptide were 350.9 and 740.2 pmol/l, respectively, which are lower than the sparse data on these hormones in the literature in this age group.

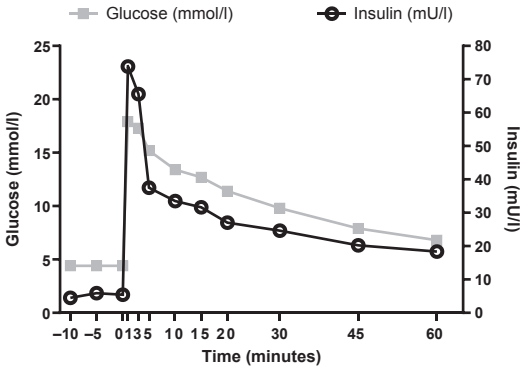

FIGURE 1 Intravenous glucose tolerance test.

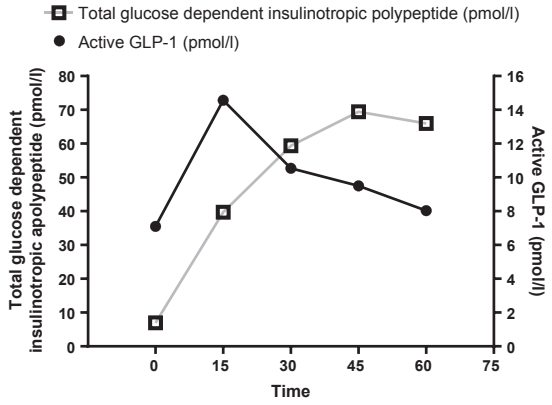

FIGURE 2 Total glucose-dependent insulinotropic polypeptide and active glucagon-like peptide 1 (GLP-1) response to the mixed-meal tolerance test.

Discussion

MODY is a genetically heterogeneous monogenic form of diabetes mellitus, characterized by early onset, usually before 25 years of age and often in adolescence or childhood, and by autosomal dominant inheritance [14]. Heterozygous mutations in the genes encoding the glycolytic enzyme glucokinase and the transcription factors, HNF-1α, HNF-4α and HNF1β have been shown to cause MODY. Clinical studies have shown normal insulin sensitivity, but reduced glucose-stimulated insulin secretion in subjects with pre-diabetes with *HNF-4A* MODY, suggesting that pancreatic β-cell dysfunction rather than insulin resistance is the primary defect in this disorder [15].

Recently, *HNF4A* mutations have been shown to cause macrosomia and hyperinsulinaemic hypoglycaemia (transient and persistent) in early life [7,8]. Hence, in *HNF4A* mutation carriers, there would need to be a switch from increased insulin secretion *in utero* and neonatal life to decreased glucose-stimulated insulin secretion in later

life. The molecular basis for the differential aspects of HNF-4α deficiency on β-cell function and insulin secretion in neonates and later in life and the exact timing of the switch from hyperinsulinaemia to hypoinsulinaemia are unknown.

We describe the first patient with an *HNF4A* mutation to have been serially monitored with oral glucose tolerance testing through to MODY from hyperinsulinaemic hypoglycaemia. The patient was macrosomic at birth and exhibited hyperinsulinaemic hypoglycaemia in the neonatal period and infancy. Annual oral glucose tolerance test monitoring highlighted gradually worsening glucose tolerance (impaired oral glucose tolerance test). At age 10 years, he fulfilled the WHO oral glucose tolerance test criteria for diabetes mellitus [11].

Surprisingly, intravenous glucose tolerance testing demonstrated a normal glucose disappearance rate (*K*) and first-phase insulin secretion, contradictory to what one would expect in MODY (*K* 1.38% per min; normal response > 1.2%, first-phase insulin secretion 2.7 nmol l^{-1} min^{-1}; normal 1.4–5.3 nmol l^{-1} min^{-1}). Similar to our results, when assessed by intravenous glucose tolerance test, Herman *et al.* [15] did not find any significant difference in insulin secretion in *HNF4A* mutation carriers without diabetes as compared with control subjects either. As our patient has been diagnosed at a very early stage of MODY, it is possible that his insulin secretion as assessed by intravenous glucose tolerance test is still preserved.

As our patient had a diabetic response to the oral glucose tolerance test and a relatively normal response to the intravenous glucose tolerance test, we hypothesized a suboptimal glucose-dependent insulinotropic polypeptide and GLP-1 rise in response to oral glucose/meal in *HNF4A* mutation carriers. Glucose-dependent insulinotropic polypeptide and GLP-1 are peptide hormones, responsible for up to 70% of the secreted insulin after a meal in healthy individuals [16].

In response to a mixed-meal tolerance test, the 30-min areas under the curve for GLP-1 and glucose-dependent insulinotropic polypeptide were 350.9 and 740.2 pmol/l, respectively. Rask *et al.* reported a 30-min area under the curve for GLP-1 and glucose-dependent insulinotropic polypeptide after oral glucose as 460 ± 60 and 1491 ± 136 pmol/l, respectively, in subjects with impaired glucose tolerance [17]. Huml *et al.* measured GLP-1 and glucose-dependent insulinotropic polypeptide in healthy children, but at a single time point of 90 min after the standardized breakfast [18]. Unfortunately, there are no normative data on GLP-1 and glucose-dependent insulinotropic polypeptide in healthy control children. Comparing the results, it does seem that our patient mounted a lower GLP-1 and glucose-dependent insulinotropic polypeptide response to the mixed-meal tolerance test, potentially explaining the discrepancy for responses to the oral glucose tolerance test and intravenous glucose tolerance test. However, there are limitations to comparing our results with adult subjects with impaired glucose tolerance from another cause.

From our data, it is plausible that incretin response might be impaired and contributory to glucose intolerance in the preclinical stages in some patients with *HNF4A* MODY. Once glucose intolerance sets in, chronic exposure to supraphysiologic concentrations of glucose over several months can lead to gradual loss of insulin gene expression [19,20].

In conclusion, we report the first patient with *HNF4A* hyperinsulinaemic hypoglycaemia to have switched to maturity-onset diabetes of the young on serial oral glucose tolerance testing. Impaired glucose tolerance can develop within the first decade of life in these patients. Our findings suggest a possibility of impaired incretin response and this is an exciting area to be explored in *HNF4A* maturity-onset diabetes of the young. More *HNF4A*-positive subjects with pre-diabetes and diabetes need to be studied to understand the impact of the *HNF4A* mutation on incretin effect.

Funding sources

The genetic testing was funded by a Medical Council Grant award.

Competing interests

None declared.

Acknowledgements

The authors would like to acknowledge the family. The genetic testing was funded by a Medical Council Grant award to KH and SE. SE is a Wellcome Trust Senior Investigator. KH is the guarantor for the manuscript.

References

1 Xanthopoulos KG, Prezioso VR, Chen WS, Sladek FM, Cortese R, Darnell JE Jr. The different tissue transcription patterns of genes for HNF-1, C/EBP, HNF-3, and HNF-4, protein factors that govern liver-specific transcription. *Proc Natl Acad Sci U S A* 1991; **88**: 3807–3811.

2 Sladek FM, Zhong WM, Lai E, Darnell JE Jr. Liver-enriched transcription factor HNF-4 is a novel member of the steroid hormone receptor superfamily. *Genes Dev* 1990; **4**: 2353–2365.

3 Kuo CJ, Conley PB, Chen L, Sladek FM, Darnell JE Jr, Crabtree GR. A transcriptional hierarchy involved in mammalian cell-type specification. *Nature* 1992; **355**: 457–461.

4 Odom DT, Zizlsperger N, Gordon DB, Bell GW, Rinaldi NJ, Murray HL *et al.* Control of pancreas and liver gene expression by HNF transcription factors. *Science* 2004; **303**: 1378–1381.

5 Wang H, Maechler P, Antinozzi PA, Hagenfeldt KA, Wollheim CB. Hepatocyte nuclear factor 4α regulates the expression of pancreatic β-cell genes implicated in glucose metabolism and nutrient-induced insulin secretion. *J Biol Chem* 2000; **275**: 35953–35959.

6 Yamagata K, Furuta H, Oda N, Kaisaki PJ, Menzel S, Cox NJ *et al.* Mutations in the hepatocyte nuclear factor-4α gene in maturity-onset diabetes of the young (MODY1). *Nature* 1996; **384**: 458–460.

7 Pearson ER, Boj SF, Steele AM, Barrett T, Stals K, Shield JP *et al.* Macrosomia and hyperinsulinaemic hypoglycaemia in patients with heterozygous mutations in the HNF4A gene. *PLoS Med* 2007; **4**: e118.

8 Kapoor RR, Locke J, Colclough K, Wales J, Conn JJ, Hattersley AT *et al.* Persistent hyperinsulinemic hypoglycemia and maturity-onset diabetes of the young due to heterozygous HNF4A mutations. *Diabetes* 2008; **57**: 1659–1663.

9 Drucker DJ. The role of gut hormones in glucose homeostasis. *J Clin Invest* 2007; **117**: 24–32.

10 Colclough K, Bellanne-Chantelot C, Saint-Martin C, Flanagan SE, Ellard S. Mutations in the genes encoding the transcription factors hepatocyte nuclear factor 1 alpha and 4 alpha in maturity-onset diabetes of the young and hyperinsulinemic hypoglycemia. *Hum Mutat* 2013; **34**: 669–685.

11 Alberti KG, Zimmet PZ. Definition, diagnosis and classification of diabetes mellitus and its complications. Part 1: diagnosis and classification of diabetes mellitus provisional report of a WHO consultation. *Diabet Med* 1998; **15**: 539–553.

12 Heinze E, Holl RW. Test of β-cell function in childhood and adolescence. In: Ranke MB ed. *Diagnostics of Endocrine Function in Children and Adolescents*, 3rd ed. Basel: Karger, 2003: 318–338.

13 Flanagan SE, Kapoor RR, Mali G, Cody D, Murphy N, Schwahn B *et al.* Diazoxide-responsive hyperinsulinemic hypoglycemia caused by HNF4A gene mutations. *Eur J Endocrinol* 2010; **162**: 987–992.

14 Fajans SS. Maturity-onset diabetes of the young (MODY). *Diabetes Metab Rev* 1989; **5**: 579–606.

15 Herman WH, Fajans SS, Ortiz FJ, Smith MJ, Sturis J, Bell GI *et al.* Abnormal insulin secretion, not insulin resistance, is the genetic or primary defect of MODY in the RW pedigree. *Diabetes* 1994; **43**: 40–46.

16 Herzberg-Schafer S, Heni M, Stefan N, Haring HU, Fritsche A. Impairment of GLP1-induced insulin secretion: role of genetic background, insulin resistance and hyperglycaemia. *Diabetes Obes Metab* 2012; **14**: S85–90.

17 Rask E, Olsson T, Soderberg S, Holst JJ, Tura A, Pacini G *et al.* Insulin secretion and incretin hormones after oral glucose in non-obese subjects with impaired glucose tolerance. *Metab Clin Exp* 2004; **53**: 624–631.

18 Huml M, Kobr J, Siala K, Varvarovska J, Pomahacova R, Karlikova M *et al.* Gut peptide hormones and pediatric type 1 diabetes mellitus. *Physiol Res* 2011; **60**: 647–658.

19 Robertson RP, Zhang HJ, Pyzdrowski KL, Walseth TF. Preservation of insulin mRNA levels and insulin secretion in HIT cells by avoidance of chronic exposure to high glucose concentrations. *J Clin Invest* 1992; **90**: 320–325.

20 Olson LK, Redmon JB, Towle HC, Robertson RP. Chronic exposure of HIT cells to high glucose concentrations paradoxically decreases insulin gene transcription and alters binding of insulin gene regulatory protein. *J Clin Invest* 1993; **92**: 514–519.

OPEN ACCESS

Clinical and molecular characterisation of hyperinsulinaemic hypoglycaemia in infants born small-for-gestational age

Ved Bhushan Arya,[1] Sarah E Flanagan,[2] Anitha Kumaran,[1] Julian P Shield,[3] Sian Ellard,[2] Khalid Hussain,[1] Ritika R Kapoor[1]

[1]Developmental Endocrinology Research Group, Molecular Genetics Unit, London Centre for Paediatric Endocrinology and Metabolism, Great Ormond Street Hospital for Children NHS Trust, and The Institute of Child Health, University College London, London, UK
[2]Institute of Biomedical and Clinical Science, University of Exeter Medical School, Exeter, UK
[3]Department of Child Health, University of Bristol, and Bristol Royal Hospital for Children, Bristol, UK

Correspondence to
Dr Ritika R Kapoor, Developmental Endocrinology Research Group, Molecular Genetics Unit, Institute of Child Health, University College London, 30 Guilford Street, London WC1N 1EH, UK; sejjrik@ucl.ac.uk

Received 23 August 2012
Revised 3 January 2012
Accepted 4 January 2013
Published Online First 29 January 2013

▶ http://dx.doi.org/10.1136/fetalneonatal-2012-302546

To cite: Arya VB, Flanagan SE, Kumaran A, *et al. Arch Dis Child Fetal Neonatal Ed* 2013;**98**: F356–F358.

ABSTRACT

Objective To characterise the phenotype and genotype of neonates born small-for-gestational age (SGA; birth weight <10th centile) who developed hyperinsulinaemic hypoglycaemia (HH).

Methods Clinical information was prospectively collected on 27 SGA neonates with HH, followed by sequencing of *KCNJ11* and *ABCC8*.

Results There was no correlation between the maximum glucose requirement and serum insulin levels. Serum insulin level was undetectable in five infants (19%) during hypoglycaemia. Six infants (22%) required diazoxide treatment >6 months. Normoglycaemia on diazoxide <5 mg/kg/day was a safe predictor of resolved HH. Sequencing of *KCNJ11/ABCC8* did not identify any mutations.

Conclusions Serum insulin levels during hypoglycaemia taken in isolation can miss the diagnosis of HH. SGA infants may continue to have hypofattyacidaemic hypoketotic HH beyond the first few weeks of life. Recognition and treatment of this group of patients are important and may have important implications for neurodevelopmental outcome of these patients.

What is already known on this topic

- Infants born small-for-gestational age are at an increased risk to develop transient hyperinsulinaemic hypoglycaemia (HH).
- Mutations in *ABCC8/KCNJ11* genes are the commonest cause of congenital HH.

What this study adds

- This largest series of small-for-gestational age infants who developed hyperinsulinaemic hypoglycaemia (HH) highlights that hypofattyacidaemic hypoketotic HH may persist beyond the first few weeks of life.
- HH in these infants is diazoxide responsive and not identified to be due to mutations in *ABCC8/KCNJ11* genes in this series.
- Withdrawal of diazoxide treatment when glycaemic control is maintained at a dose of <5 mg/kg/day can be safely recommended.

INTRODUCTION

Hyperinsulinaemic hypoglycaemia (HH) is characterised by the unregulated secretion of insulin from pancreatic β-cells in relation to the blood glucose concentration. It is the commonest cause of severe and persistent hypoglycaemia in the neonatal and infancy periods.[1] The genetic basis of congenital forms of HH involves defects in key genes (commonest—*ABCC8 and KCNJ11* encoding the two subunits SUR1 and Kir6.2, respectively), which regulate insulin secretion from pancreatic β-cells.[1] HH may be secondary to certain risk factors (such as maternal diabetes mellitus, perinatal asphyxia and small-for-gestational age (SGA)). In 1984, Collins and Leonard first described transient HH in SGA infants.[2] It has not previously been documented whether the HH observed in infants born SGA is due to defects in the *ABCC8/KCNJ11* genes. The phenotype of a large cohort of SGA neonates who developed HH has not been studied previously. The purpose of the present study was to report on the phenotype, clinical course and results of the sequencing of *ABCC8/KCNJ11* in a cohort of infants born SGA who developed HH.

PATIENTS AND METHODS

We prospectively studied the clinical and biochemical features of 27 SGA (defined as birth weight <10th centile) neonates with HH who were admitted to two tertiary paediatric referral centres (Great Ormond Street Hospital and Bristol Royal Hospital for Children). Neonates with history of perinatal asphyxia, Rhesus isoimmunisation and syndromic forms such as Beckwith-Wiedemann syndrome were excluded from the study. All were investigated at the time of clinical and biochemical hypoglycaemia to establish the diagnosis of HH and were commenced on diazoxide (5–20 mg/kg/day). Diazoxide responsiveness was defined as ability to come off intravenous glucose and maintain normoglycaemia during a physiological fast. Following discharge, they were followed up at 3-monthly intervals in outpatient clinic, where glycaemic control and diazoxide dose were reviewed. These infants were readmitted for a 24-h glucose profile and a controlled fast after stopping diazoxide for 3 days, if home glucose monitoring indicated no recurrence of hypoglycaemia on <5 mg/kg/day of diazoxide.[1] If home glucose monitoring revealed hypoglycaemic episodes, the dose of diazoxide was adjusted and the trial off diazoxide was postponed until the dose was <5 mg/kg/day.

Table 1 Clinical characteristics of 27 small-for-gestational age infants with hyperinsulinaemic hypoglycaemia

Age at presentation (days)	
Median (range)	1 (1–14)
Gestational age (weeks)	
Median (range)	37 (32–42)
Birth weight (g)	
Median (range)	2300 (1100–3100)
Male (%)	66.6
Ethnic origin (n)	
Caucasian	17
Afro-Caribbean	6
Asian	2
Mixed	2
Diazoxide responsive (%)	100
Glucose infusion rate (mg/kg/min)	
Median (range)	15.6 (8.0–20.8)

Genetics

Genomic DNA was extracted from peripheral leukocytes using standard procedures and the coding regions and intron/exon boundaries of the *ABCC8* and *KCNJ11* genes were amplified by PCR (primers available on request). Amplicons were subsequently sequenced using the Big Dye Terminator Cycler Sequencing Kit V.3.1 (Applied Biosystems, Warrington, UK) according to manufacturer's instruction and reactions were analysed on an ABI 3730 Capillary sequencer (Applied Biosystems, Warrington, UK). Sequences were compared with the reference sequences (NM_000525.3 and NM_000352.3) using Mutation Surveyor v3.24 software (SoftGenetics, State College, Pennsylvania, USA).

RESULTS

Clinical characteristics and course

The phenotypic details of 27 SGA infants with HH are summarised in table 1.

The plasma insulin levels were inappropriately elevated during hypoglycaemia in 22 infants (81%). The remaining five infants (19%) had inappropriately low β-hydroxybutyrate and non-esterified fatty acids during hypoglycaemia as supportive biochemical evidence of HH. All infants required glucose infusion rate of ≥8 mg/kg/min to maintain normoglycaemia (median 15.6 mg/kg/min). There was no correlation found between maximum glucose infusion rate to maintain normoglycaemia and plasma insulin level during hypoglycaemia (figure 1). Most (89%) responded to mild–moderate doses of diazoxide (5–10 mg/kg/day), with three infants (11%) needing high doses (15–20 mg/kg/day).

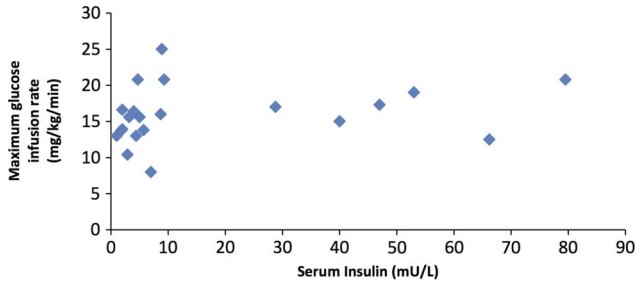

Figure 1 Figure demonstrating the lack of correlation between maximum glucose infusion rate and plasma insulin concentrations.

Glucose profile and fasting responses at resolution of hyperinsulinism

In all, 17 infants (63%) underwent a 24 h glucose profile and controlled fast after stopping diazoxide to demonstrate resolution of hyperinsulinism. None of these infants recorded hypoglycaemia during a 24-h glucose profile. All infants maintained blood glucose concentrations above 3.0 mmol/l at the end of fast appropriate for their age, with 13 infants maintaining blood glucose concentrations >3.5 mmol/l. All infants showed appropriate plasma insulin suppression and elevation of plasma β-hydroxybutyrate/non-esterified fatty acids as evidence of resolution of HH.

Genetic results

Sequencing did not reveal mutations in *ABCC8/KCNJ11* genes in 25/27 DNA samples analysed.

DISCUSSION

This is the largest case series of SGA neonates with HH that reports the clinical characteristics and *ABCC8/KCNJ11* sequencing results in a cohort of 27 subjects. Collins *et al* first described transient HH in three SGA infants and subsequently reported HH in five of 27 SGA neonates studied, suggesting it is common in SGA neonates.[2 3] It is important to recognise this as neonates with HH are especially prone to the complications of hypoglycaemia because of their inability to generate alternative fuels, such as ketone bodies.

In our study, despite other evidence of hyperinsulinism, plasma insulin levels were undetectable during hypoglycaemia in 5/27 SGA neonates. We did not find any correlation between the maximum glucose infusion rate required to maintain normoglycaemia and plasma insulin levels. This is explained by the short half-life of insulin of 4–5 min and rapid clearance by the liver before it reaches peripheral circulation. In a study by Hoe *et al*,[4] plasma insulin was inappropriately elevated in only 11 of 24 neonates who had transient prolonged neonatal hyperinsulinism. Our results corroborate these findings and highlight the value of other parameters (apart from plasma insulin) in the diagnosis of HH.

In this case study of SGA infants referred to two tertiary hospitals with HH, all infants responded to diazoxide, though the dose was variable ranging from 5 to 20 mg/kg/day. Diazoxide was successfully stopped in 21 (78%) patients by 6 months of age. In the remaining six infants, five needed diazoxide until 10 months of age and one infant needed prolonged treatment until 22 months. In a study of 26 neonates with hyperinsulinism which included 7 SGA neonates, HH resolved by a median age of 181 days (range, 18–403 days).[4] Fafoula *et al*[5] also reported prolonged transient HH up to 9 months in SGA infants.

In our cohort, no recurrence of HH was noticed after stopping diazoxide. This highlights that with the management protocol whereby diazoxide was stopped when good glycaemic control was maintained with diazoxide dose <5 mg/kg/day, the risk of recurrence of hypoketotic hypoglycaemia brain injury to these vulnerable infants is avoided.

To our knowledge, no previous study has reported on the genetic results of SGA neonates who developed HH. In our study, no mutations in *ABCC8/KCNJ11* were identified in these SGA infants. However, rarer genetic causes of HH due to mutations in *GLUD1, HADH, GCK* and *HNF4A* were not excluded.

CONCLUSIONS

SGA infants may continue to have hypofattyacidaemic hypoketotic HH beyond the first few weeks of life. Recognition and

treatment of this group of patients are important and may have important implications for neurodevelopmental outcome of these patients. Plasma insulin levels during hypoglycaemia taken in isolation can miss the diagnosis of HH and hence other parameters (such as glucose infusion rates and production of free fatty acids/ketone bodies during hypoglycaemia) must be considered in the diagnosis. Withdrawal of diazoxide treatment when glycaemic control is maintained at a dose of <5 mg/kg/day can be safely recommended.

Finally, the genetic aetiology of HH in SGA infants is not understood and, in this study, mutations in the common genes implicated in the aetiology of congenital hyperinsulinism were not identified. Further studies are required to understand the underlying mechanism of HH in these infants.

Acknowledgements This study was funded by the Wellcome Trust (081188/A/06/Z). VBA was funded by MRC, SEF was the Sir Graham Wilkins Peninsula Medical School Research Fellow, SE was funded by the Royal Devon & Exeter NHS Foundation Trust Research & Development Directorate and RRK was funded by NIHR.

Contributors VBA collected and analysed the data and wrote the manuscript. SEF performed the genetic studies and reviewed the manuscript. AK and JPS collected the data and critically reviewed the manuscript. SE and KH conceptualised the study and critically reviewed the manuscript. RRK conceptualised the study, analysed the data and critically reviewed the manuscript. All authors contributed to the approval of the final version of the manuscript. RRK is the guarantor of this work.

Funding This work was funded by the Wellcome Trust (081188/A/06/Z).

Competing interests None.

Ethics approval Ethics Committee of Great Ormond Street Hospital for Children and the Institute of Child Health, University College London.

Provenance and peer review Not commissioned; externally peer reviewed.

REFERENCES

1 Kapoor RR, Flanagan SE, James C, *et al*. Hyperinsulinaemic hypoglycaemia. *Arch Dis Child* 2009;94:450–7.
2 Collins JE, Leonard JV. Hyperinsulinism in asphyxiated and small-for-dates infants with hypoglycaemia. *Lancet* 1984;2:311–13.
3 Collins JE, Leonard JV, Teale D, *et al*. Hyperinsulinaemic hypoglycaemia in small for dates babies. *Arch Dis Child* 1990;65:1118–20.
4 Hoe FM, Thornton PS, Wanner LA, *et al*. Clinical features and insulin regulation in infants with a syndrome of prolonged neonatal hyperinsulinism. *J Pediatr* 2006;148:207–12.
5 Fafoula O, Alkhayyat H, Hussain K. Prolonged hyperinsulinaemic hypoglycaemia in newborns with intrauterine growth retardation. *Arch Dis Child Fetal Neonatal Ed* 2006;91:F467.